CCSN - Appendix 1a

CVO Groundwater Report 2023
CCSN Comments – 24 April 2024

For the purpose of investigating the potential impact upon the quality of groundwater from CVO, bores have been grouped by geographic location and proximity to the mine. Many of these bores, particularly in the NE of Cadia and S of STSF groups are outside the Mine Licence area. Data provided for 2023 has been grouped accordingly and comparison made to the average of all data over the year for each bore and the range of data points, refer Attachment 1.

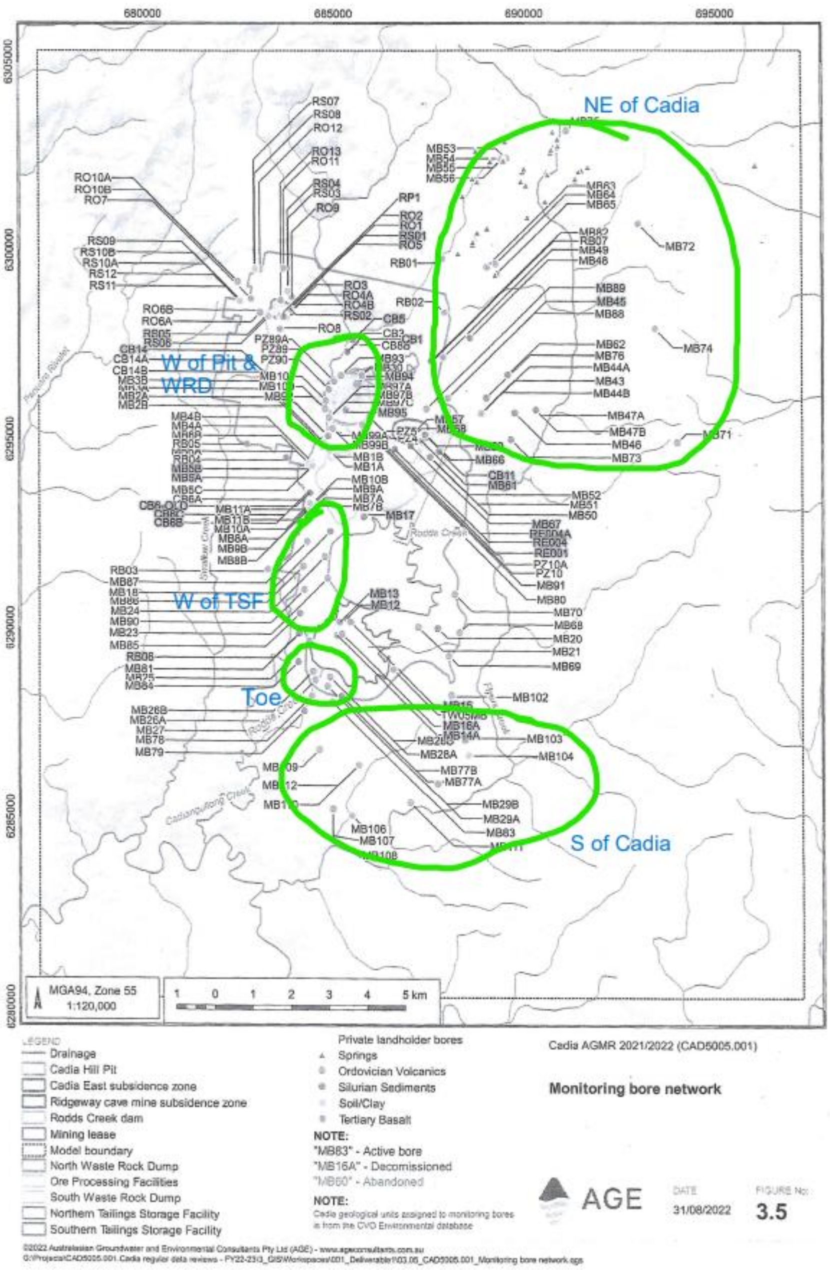

Comparison of CVO bore testing results with prior year data is complicated by the limited data reported by the company, regular changes to the way data is presented and changes to the labelling of bores across the site. However, the 1995 Cadia Gold Mine EIS Vol 3 includes some data for 47 bores across the Mine Licence area, Attachment 2 Location of Monitoring Sites (Ground Water). This data was collected during the period

1993 – 1995. Comparison was also made to the ANZECC guidelines; however, it should be noted the guidelines being used by Cadia are now out of date.

Comparison of Average pH and Sulphates by Area

	NE of Cadia	S of STSF	Toe of STSF	W of TSFs	W of Pit & WRD	CVO 1995	ANZECC
pH	5.69	9.70	7.05	6.67	6.67	7.56	
pH range	4.6-9.0	6.58-12.98	6.05-8.27	6.16 – 7.24	6.23 – 7.41	6.74-9.00	6.5-8.5
Sulphate	4.78	63.45	483	740	1477	325	
Sulphate range	1-30	8-236	201-1150	178-1240	122-2650	5-1424	1000

This comparison has resulted in the following observations:

1995

CVO has published very little base line data, however the 1995 EIS, Cadia Gold Mine Environmental Impact Statement includes data for 47 bores in the Mine Licence area. This data identified that:

- The groundwater was generally of a good quality, fit for livestock and release into the environment.
- pH was within ANZECC guidelines except for ST 38 - pH 9.00, ST 44 – pH 8.90
- sulphates were generally within ANZECC guidelines except for ST 9 – 1010, ST 23 - 1424 and ST28 – 1205

2023

Based upon data published in the Cadia Annual Groundwater Monitoring Review 2023, the ground water is generally ***not*** fit for livestock or release into the environment.

- NE of Cadia, except for MB 53 – pH 6.88 the pH is well below the livestock threshold.
- S of STSF – several bores report very high levels of alkalinity, MB 103, MB 104, MB 105, MB 106.
- Toe of STSF – whilst these bores close to the tailings dams have a pH within guidelines, they contain a cocktail of toxic metals including several with mercury.
- W of TSFs – several bores report low pH, others have high sulphates. Only four bores are within livestock drinking water guidelines for pH and sulphates MB 25,81,84 and 85.
- W of Pit and WRD – most of these bores have extremely high sulphates. Acid Mine Drainage develops as the sulphates combine with oxygen and water to become sulphuric acid, a pre cursor to bacterial AMD. High levels of sulphate may be an indicator of the potential level and volume of acidification yet to develop.

NE of Cadia

This group of bores is to the north and east and downhill from the North Waste Rock Dump and South Waste Rock Dump. Waste rock dumps are considered to be a high-risk source of Acid Mine Discharge (AMD) (often worse than tailings dams) due to the non- homogenous nature of the dump and high levels of ammonium nitrate which triggers production of AMD.

- The lowest pH appears to be in bores closer to CVO and closer to the waste rock dumps. MB54 – 5.29, MB 62 – 4.88, MB 63 4.59, MB 64 – 5.15
- Based upon CVO data there has been a material decrease in pH over the period since 2015.

pH Trends over time

pH	MB 71	MB 72	MB 74
2012	6.70	7.90	7.25
2015	6.91	7.57	7.36
2022 (avg)	5.84	6.23	6.48
2023 (avg)	5.45	5.67	5.41

Source: CVO Annual Groundwater Monitoring Review

S of STSF

There is a cluster of bores between the STSF and the Belubula River reporting very significant levels of alkalinity.

- MB 103, MB 104 and MB 109 are closer to the STSF and show significant fluctuations in pH.

pH	07/22	09/22	10/22	11/22	12/22	01/23	02/23	Avg
MB 103	10.8	11.1	9.99	8.28	8.14	8.29	8.26	9.27
MB104	7.76	7.68	10.81	10.43	10.1	6.58	8.33	8.81
MB109	6.74	11.3	6.68	6.76	6.85	10.26	6.94	8.22

MB 105	8.99	11.89	11.52	10.90	9.51	11.06	8.01	10.27
MB106	12.06	12.47	12.07	11.25	11.2	11.35	12.98	11.91

The tailings dams have been embargoed for 6 years, why would there be a flow of highly alkaline water from the tailings dams? The mine process water is pH 12.

In 2007 CVO commissioned Itasca Australia Pty Ltd to investigate Failure Mechanisms at the Cadia Hill Open Pit (Attachment 3). At that time CVO was concerned by unpredicted failures of the open pit benches. Itasca identified that a series of significant faults run through the pit.

Three-Dimensional Discontinuum Analysis of Structurally Controlled Failure Mechanisms at the Cadia Hill Open Pit — D. Sainsbury, et al.

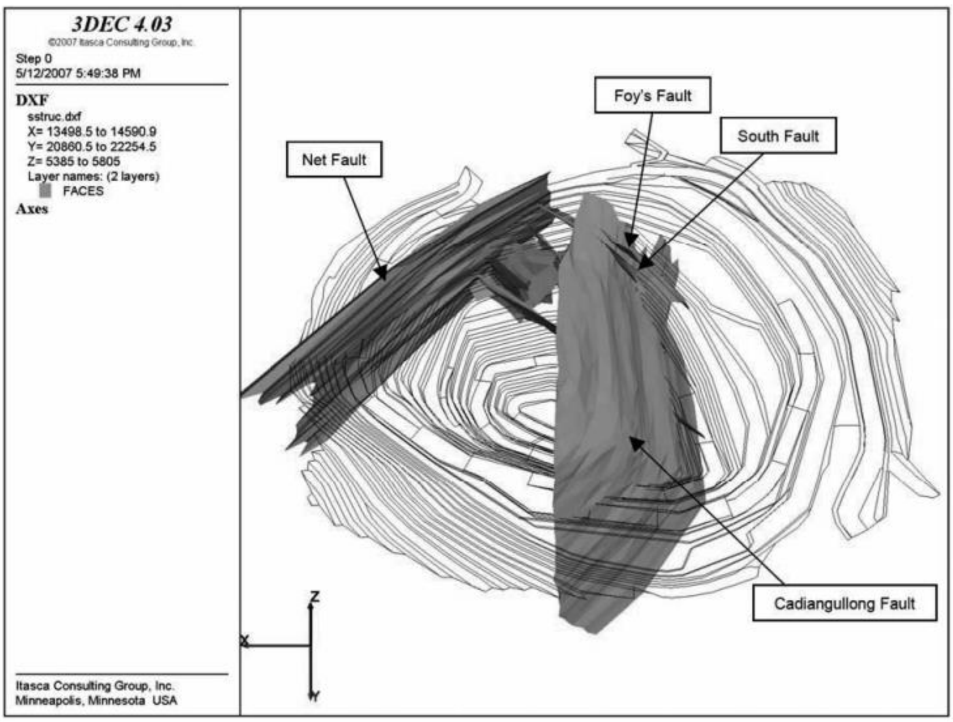

Figure 3 2006 structural model (looking south)

The 2009 EIS for the Cadia East Project identified numerous faults running through the site, including those identified by Itasca as running through the Pit.

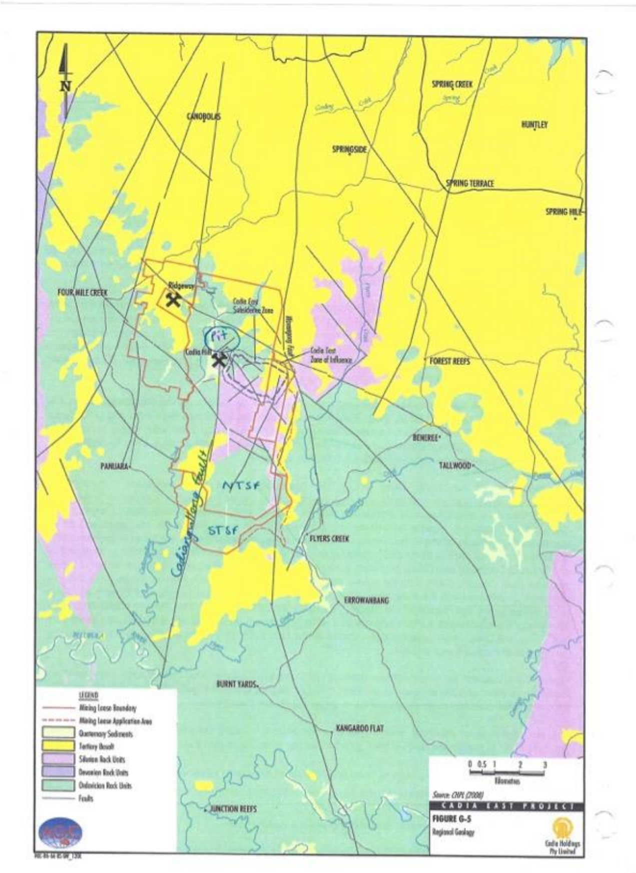

"The Cadiangullong Fault is a 1 m - 10 m wide zone of black cataclasite gouge and intensely fractured wall rocks
The Foys Fault is a 20 m wide zone of intensely fractured siltstone.

The Gibb Fault is a 0.5 m - 2 m wide zone of milled rock-matrix breccia and clay gouge.

The Copper Gully Fault is planar and narrow and has a reddish clay gouge.

The above observations indicate that the faults filled with clay gouge would act as barriers to movement of water, while the faults with breccia fil and fractured wall rocks would likely be conduits for groundwater flow.

The Warrengong Fault is a north-south trending, near vertical structure located approximately 1 km to the east of the Cadia East deposit (Figure G-5). It is considered to be an extensive regional structure"

The Cadiangullong fault which has been identified as "fractured rock" runs through the area to the south of the STSF, possibly bringing with it highly alkaline mine process water.

The 2019 ITRB Report on NTSF Embankment Failure 'Appendix F Hydrogeology' identifies a major fault line as a potential contributor to the failure of the dam. This fault runs north south, close to the slump. If the STSF is used how will CVO prevent the process water from seeping into the fault line and contaminating outside the ML area.

Data for the high alkalinity readings have been included in the Cadia Annual Groundwater Monitoring Review for both 2021/2022 and 2022/2023 water years. However, there has been no comment made in the report on these readings.

Toe of STSF
Although the water seeping at the toe of the STSF is relatively neutral in terms of pH it contains a cocktail of heavy metals including mercury.

West of STSF

It appears that the pit is leaking directly into the bores close to it, The 2023 Groundwater Report S 4.2.2.1. states

"… strong correlation of rising groundwater with pit levels that has been observed in MB94, MB95 and MB 96 is as expected."

4.2.2.2

"groundwater levels at MB 95 started to consistently match the water level in Cadia Hill Pit (from March 2019)"

Similar increases in arsenic concentrations…..at bore MB 94, where groundwater levels also suggest connectivity to the Cadia Hill Pit lake."

"Some risk that ground water may migrate from the pit to Cadiangullong Creek through transmissive fractures and geological structure"

Bores to the West of the mine operations have high levels of multiple elements. Bores are being tested at a level below Cadiangullong Creek. CVO repeatedly concludes that because there is no evidence of contamination in the creek and there is no evidence of contamination moving beyond the mine site, there is no further contamination. A conclusion of no contamination beyond the creek can only be reached if CVO has drilled bores beyond the creek and tested for contamination.

Other Comments

In 2018 CVO tested the sediment in the creeks surrounding CVO for hydrocarbons. ALS identified hydrocarbons in Rodds Creek and Flyers Creek. No comment was made about these test results in the Surface Water Management Report and no further testing of sediments for these materials has been reported.

CCSN Questions

There has been a significant change in the quality of groundwater in the district during the period 1995 – 2023.

Is it possible we are seeing AMD affecting the bores to the NE of the site, was there a trigger event after 2015?

Was the base of the waste rock dumps clay lined to reduce the risk of AMD seeping into one of the many fault lines?

In the Southern area towards the Belubula:

- is it possible that contaminated water is "flushing through" the bores closest to the tailings dam?
- Is the highly alkaline water in these bores coming directly from the pit (as opposed to seepage or discharge from the TSF)?

If contaminated water is moving along the fault line, how far is it going and where does it eventually accumulate? What is the size of the plume and how can this be determined?

Have bores been tested for hydrocarbons and other anthropogenic materials?

Bores NE of Cadia

	2023		
	pH	sulphate	nitrate
MB 43	na		
MB 44A	na		
MB 44b	na		
MB 45	na		
MB 46	na		
MB 47 A	na		
MB 47 B	na		
MB 48	6.21	8	0.01
	6.44	4	0.01
	6.73	1	0.01
avg	6.46	4	0.01
MB 49	5.92	1	0.01
	6.35	1	0.01
	5.86	1	0.01
	6.06	1	0.01
	5.89	1	0.01
	6.02	10	0.01
	6.28	1	0.01
	6.49	1	0.01
	7.01	1	0.01
avg	6.21	2	0.01
MB 53	6.91	7	0.01
	6.97	7	0.01
	6.79	8	0.1
	6.79		
	6.94	7	0.01
avg	6.88	7.25	0.03
MB 54	4.89	1	12.2
	5.33	1	13.2
	5.4	1	13.1
	5.55	2	12.9
avg	5.29	1.25	12.85
MB 55	na		

	2023		
	pH	sulphate	nitrate
MB 65	5.65	1	1.55
	6.05	1	1.68
	5.98	1	1.65
	6.14	1	1.73
avg	5.96	1.00	1.65
MB 71	5.56	17	0.48
	5.46	9	0.48
	5.49	16	0.69
	5.28	25	0.85
avg	5.45	16.75	0.63
MB 72	5.36	1	3.17
	5.32	1	3.8
	5.8	1	1.81
	6.19	1	0.08
avg	5.67	1.00	2.22
MB 73	5.83	1	1.56
	4.83	1	1.58
	5.06	2	1.3
	5.63	4	1.24
	5.04	4	1.23
	5.73	4	1.24
	5.34	2	1.89
	6.04	3	1.8
avg	5.44	2.63	1.48
MB 74	5.44	1	3.19
	5.85	9	0.12
	6.41	7	0.04
	6.52	6	0.01
avg	6.06	5.75	0.84
MB 76	na		

	2023		
	pH	sulphate	nitrate
MB 56	5.15	1	6.88
	5.49	1	7.37
	5.73	1	7.1
	5.83	1	7.27
avg	5.55	1	7.16
MB 62	4.6	1	0.51
	4.56	1	0.86
	4.92	1	0.32
	5	1	0.26
	5.28	1	0.24
	4.93	1	0.24
avg	4.88	1	0.41
MB 63	9	1	1.47
	4.46	1	1.76
	4.6	1	1.52
	4.71	1	1.46
avg	5.69	1	1.55
avg excld "9"	4.59		
MB 64	4.99	1	1.1
	5.15	1	1.52
	5.2	1	1.26
	5.24	1	1.55
avg	5.15	1	1.36
Average all bor	5.69	4.78	2.13
Range			

	2023		
	pH	sulphate	nitrate
MB 88	6.16	4	0.02
	6.53	10	0.01
	6.38		
	6.38	9	0.03
	6.38	15	0.02
	6.19	27	2.29
	6.13	20	2.29
	5.22	30	1.97
	5.82	28	1.59
	6	42	1.37
	6.05	28	1.74
	6	26	1.26
	6.24	24	1.21
avg	6.11	21.92	1.15

Bores West of Pit and WRD

	2023		
	pH	sulphate	nitrate
MB 1A	6.25	2040	0.01
	6.33	2110	0.02
	6.29	2650	0.01
	6.47	2620	0.01
avg	6.34	2355	0.01
MB 1B	na		
MB 2A	6.52	1470	0.01
	6.52	1520	0.02
	6.58	1440	0.01
	6.7	1360	0.01
avg	6.58	1448	0.01
MB 2B	na		
MB 3A	6.34	2130	0.47
	6.38	2110	0.11
	6.43	1970	0.61
	6.58	2090	0.72
avg	6.43	2075	0.48
MB 3B	na		
MB 4A	6.64	829	0.01
	6.69	776	0.06
	6.79	768	0.01
	6.86	734	0.01
avg	6.75	777	0.02
MB 4 B	na		
MB 5A	na		
MB 5B	na		
MB 5C	6.58	1600	0.01
	6.77	1490	0.01
	6.74	1440	0.01
	6.7	1610	0.01
	6.70	1535	0.01

	2023		
	pH	sulphate	nitrate
MB 10B	na		
MB 11A	6.42	2110	0.01
	6.54	1970	0.01
	6.55	1940	0.01
	6.66	1980	0.01
	6.54	2000	0.01
MB 11B	na		
MB 92	6.23	354	0.14
	6.61	390	0.06
	6.51	315	0.53
	6.43	301	0.32
	6.41	253	0.17
	6.56	271	0.13
	6.56	276	0.13
	6.79	272	0.13
	6.53	271	0.06
	6.95	279	0.06
	6.8	279	0.04
avg	6.58	296	0.16
MB 99A	7.03	954	0.19
	7.01	1030	0.16
	6.76	953	0.14
	6.9	932	0.1
	7.25	1160	0.19
	7.13	925	0.17
	7.2	988	0.21
	7.16	895	0.29
	7.15	900	13.3
	7.23	929	0.38
	7.19	908	0.37
	7.3	752	0.01
avg	7.11	944	1.29

	2023		
	pH	sulphate	nitrate
MB XX	6.62	1480	0.83
	6.67	1590	2.7
	6.74	1500	2.46
	6.82	1560	2.27
avg	6.71	1533	2.07
MB 7A	6.72	1500	2.22
	6.88	990	4.42
	6.58	1260	1.24
	6.63	1660	0.59
avg	6.70	1353	2.12
MB 7B na			
MB 8A	6.55		
	6.39	2070	0.01
	6.48	2080	0.06
	6.58	2240	0.01
avg	6.50	2130	0.03
MB 8B NA			
MB 9A	6.54	2500	0.01
	6.49	2270	0.01
	6.6	2100	1.59
	6.68	2180	3
avg	6.58	2263	1.15
MB 9B			
MB 10A	6.55	2200	0.01
	6.7	122	0.01
	6.67	1760	0.01
	6.58	2250	0.01
avg	6.63	1583	0.01
Averag€	**6.67**	**1477**	**1.14**

	2023		
	pH	sulphate	nitrate
MB 99B	6.95	1720	1.23
	6.84	1770	1.32
	6.51	1690	1.7
	6.75	1710	4.86
	6.82	1510	11.8
	6.9	1590	12
	7.07	1570	11.5
	7.21	1590	12.5
	7.21	1540	0.4
	7.35	1640	12
	6.88	1580	15.5
	7.14	1660	26
avg	6.97	1631	9.23
MB 100	7.41		
	7.11	312	0.84
	6.52	238	0.75
	7.14	219	0.34
	6.81	199	0.45
	6.99	335	0.36
	7.07	357	0.24
avg	7.01	237	0.43

Bores West of TSFS

2023				2023		
pH	sulphate	nitrate		pH	sulphate	nitrate
6.26	1190	1.39	MB 87	6.41		
6.39	1100	1.58		6.79	933	7.57
6.28	1020	1.48		6.4	945	4.78
6.45	979	1.64		6.45	877	5.2
6.35	1072	1.52		6.46	863	5.44
				6.51	827	5.5
na				6.48	845	5.28
				6.38	833	5.51
6.69	1120	0.01		6.7	824	5.05
6.8	1080	0.02		6.57	744	5.34
6.5	971	0.5		6.76	782	5.38
6.68	1410	0.48		6.74		
6.67	1145	0.25	avg	6.55	847	5.51
7.24	112	0.01	MB 90	6.58	1260	0.01
7.11	471	0.12		6.83	1100	0.01
6.96	419	16.5		6.33	1500	0.01
7.10	334	5.54		6.5	1200	0.02
				6.52	1230	0.04
6.67	602	0.72		6.41	1150	0.01
6.93	576	0.64		6.51	1010	0.01
6.62	597	0.78		6.46	1240	0.01
6.59	577	0.74		6.62	1170	0.01
6.70	588	0.72		6.57	1190	0.02
				6.72	1180	0.03
6.86	641	4.91		6.82		
6.7	653	5.28		6.57	1203	0.02
6.79	624	3.31				
7	597	5.35				
6.68	632	4.73				
6.59	587	4.9				
6.75	622	5.15				
6.56	605	5.86				
6.69	573	5.52				
6.74	614	5.67				
6.89	551	5.51				
6.91						
6.76	609	5.11				

	2023	
pH	**sulphate**	**nitrate**
6.73	178	7.35
6.99	168	4.44
6.5	160	7.32
6.78	166	7.83
6.74	145	7.56
6.76	140	7.06
6.8	132	6.87
6.77	139	7.01
6.87	134	6.15
6.92	120	6.29
7	116	4.01
7.04		
6.83	145	6.54
6.34	755	5.2
6.81	739	4.16
6.16	773	4.05
6.42	715	5.12
6.39	755	4.15
6.38	751	4.2
6.43	737	4.81
6.29	707	5.34
6.48	660	5.8
6.45	623	6.59
6.67	637	6.97
6.73		
6.46	714	5.13
6.67	**740**	**3.37**

Bores at toe of STSF

	2023		
	pH	sulphate	nitrate
MB 26A	na		
MB 26B	6.05	233	0.32
	6.36	217	0.31
	6.24	222	0.29
	6.46	223	0.31
avg	6.28	224	0.31
MB 27	6.53	610	1.61
	6.76	628	1.8
	6.72	643	1.82
	6.79	614	2.3
	6.6	473	3.49
	6.86	488	3.66
	6.67	469	3.38
	6.69	467	3.02
	6.99	492	3.08
	6.89	484	2.91
	6.83	486	3.11
	6.86		
avg	6.77	532	2.74
MB 28A	na		
MB 28B	6.54	490	2.24
	6.74	506	2.24
	6.71	485	2.59
	6.95	460	2.37
avg	6.74	485	2.36
MB 29A	na		
MB 29B	7.1	12	1.21
	7.37	12	1.8
	7.39	17	2.19
	7.35	16	2.26
avg	7.30	14	1.87

	2023		
	pH	sulphate	nitrate
MB 79	8.04	201	0.01
	7.68	191	0.01
	8.12	197	0.01
	8.27	191	0.01
	7.82	196	0.01
	8.02	102	0.01
	7.85	202	0.01
	7.88	196	0.01
	7.76	193	0.01
	7.95	197	0.01
	7.86	190	0.01
	7.88		
avg	7.93	187	0.01
MB 83	6.97	653	0.01
	6.91	615	0.02
	7.09	600	0.08
	7.77	586	0.05
	6.67	621	0.01
	6.61	571	0.01
	6.77	633	0.01
	6.67	591	0.01
	6.66	547	0.01
	6.91	607	0.01
	6.86	513	0.02
	6.94	528	0.01
avg	6.90	589	0.02

	2023		
	pH	sulphate	nitrate
MB 77A	6.85	1050	1
	6.99	631	1.14
	6.71	671	2.71
	7	741	2.39
avg	6.89	773	1.81
MB 77B	7.06	1150	0.01
	6.84	1090	0.01
	6.96	978	0.24
	7.03	1110	0.04
avg	6.97	1082	0.08
MB 78	7	403	0.09
	7.01	465	0.02
	7.17	538	0.01
	7.36	521	0.1
	6.85	319	2.6
	7.25	406	0.75
	6.95	431	0.22
	6.82	400	0.02
	6.92	358	0.01
	6.99	424	0.01
	7.02	385	0.03
	7.05		
av	7.67	465	0.39
Average all l	7.05	483	1.06

Bores S of STSF

	2023 pH	2023 sulphate	2023 nitrate
MB 103	10.8	89	1.09
	11.1	81	2.38
	9.99	42	0.01
	8.28	18	0.01
	8.14	28	0.02
	8.29	47	0.01
	8.26	59	0.01
		74	0.01
avg	9.27	55	0.44
MB 104	7.76	8	0.07
	7.68	9	0.04
	10.81	25	0.01
	10.43	31	0.01
	10.1	27	0.02
	6.58	23	0.07
	8.33	18	0.17
		14	0.04
avg	8.81	19	0.05
MB 105	8.99	16	2.06
	11.89	23	6.64
	11.52	24	6.6
	10.9	40	6.75
	9.51	26	4.4
	11.06	30	6.6
	8.01	22	1.92
		30	0.81
avg	10.27	26	4.47
MB 106	12.06	78	0.11
	12.47	26	1.37
	12.07	34	1.1
	11.25	30	1.32
	11.2	24	1.31
	11.35	16	0.86
	12.98	28	0.58
		57	0.39
avg	11.91	37	0.88

	2023 pH	2023 sulphate	2023 nitrate
MB 109	6.74	65	0.49
	11.3	227	3.4
	6.68	236	0.06
	6.76	228	0.01
	8.85	58	0.06
	10.26	229	5.96
	6.94	218	0.52
avg	8.22	180	1.50
MB 110	6.92	51	0.92
	7.12	35	1.1
	6.74	27	1.16
	6.91	28	1.18
	7.18	27	1.09
	7.08	39	0.61
	7.12	43	0.44
		34	1.05
avg	7.01	36	0.94
MB 111	6.98	555	4.31
	6.45	623	4.78
	6.33	541	4.91
	6.74	574	4.99
	6.96	500	4.42
	6.22	481	4.51
	6.76	474	4.05
		502	2.2
	6.63	531	4.27

	2023		
	pH	sulphate	nitrate
MB 107	7.95	19	0.01
	7.81	24	0.02
	7.65	18	0.01
	7.7	23	0.01
	7.78	30	0.01
	7.78	41	0.02
	8.12	46	0.01
		58	0.01
avg	7.83	32	0.01
MB 108	7.2	17	0.82
	7.13	18	1.16
	7.08	16	1.5
	7.06	18	1.79
	7.14	16	1.62
	7	16	1.48
	7.06	17	1.81
		16	1.59
avg	7.10	17	1.47
Average all t	**8.56**	**103.68**	**1.56**
Average	**9.70**	**63.45**	**1.47**

CCSN - Appendix 1c

Attachment 2

1995 EIS

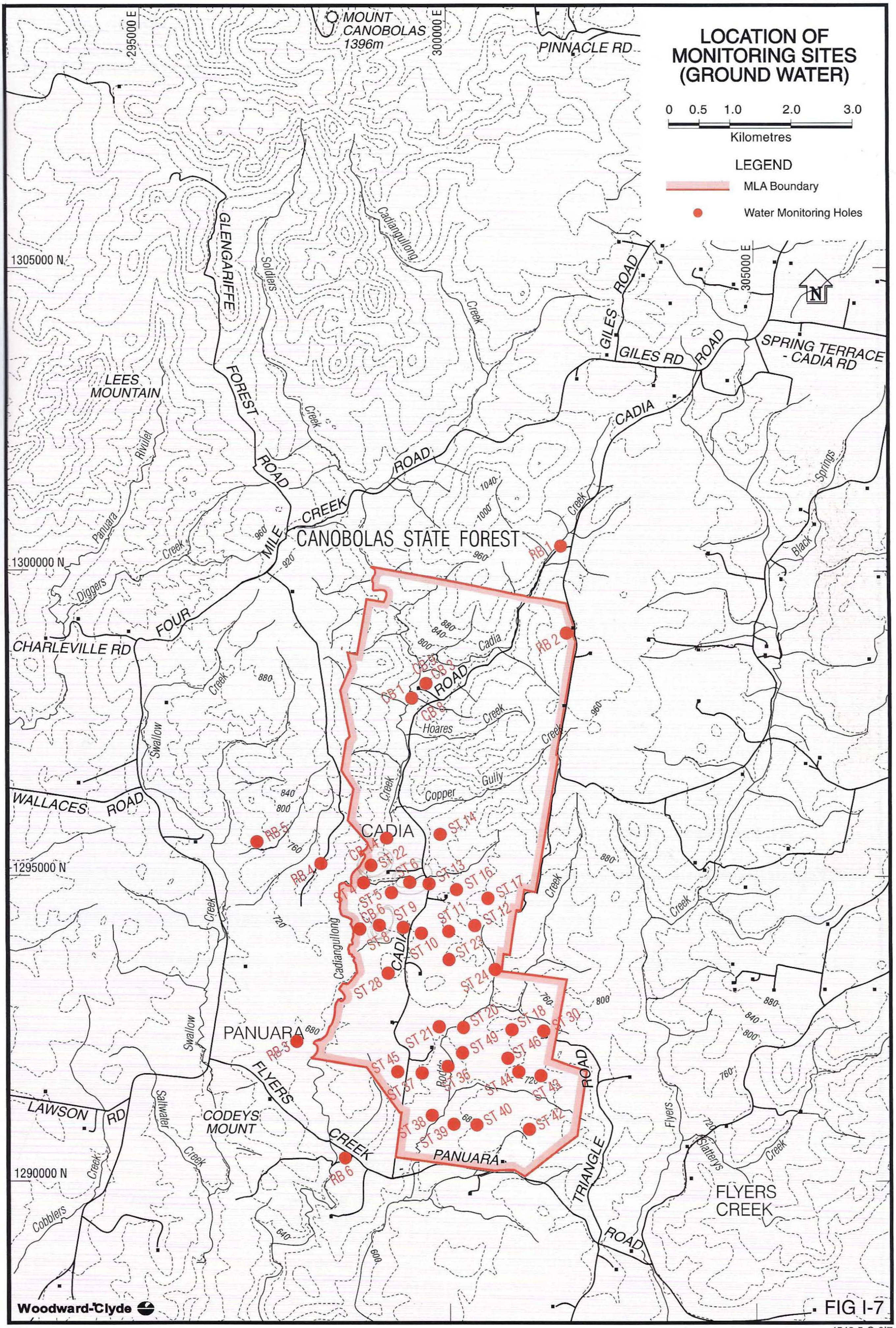

4542-5-G-017

Slope Stability 2007 — Y. Potvin (ed)
©2007 Australian Centre for Geomechanics, Perth, ISBN 978-0-9756756-8-7
https://papers.acg.uwa.edu.au/p/708_18_Sainsbury/

Three-Dimensional Discontinuum Analysis of Structurally Controlled Failure Mechanisms at the Cadia Hill Open Pit

D. Sainsbury *Itasca Australia Pty Ltd, Australia*

F. Pothitos *Ok Tedi Mining Ltd, Papua New Guinea (formerly Newcrest Mining Ltd, Australia)*

D. Finn *Newcrest Mining Ltd, Australia*

R. Silva *Itasca S.A., Chile*

Abstract

The south wall of Newcrest Mining Ltd's Cadia Hill Open Pit experienced a multi-bench (60,000 t) failure during 2006. The observed failure mechanism is a combination of structurally controlled and rock mass failure. The 3DEC code has been developed by Itasca specifically to study complex failure mechanisms involving large numbers of explicit structures (joints, faults) that divide a rock mass into blocks. Slip, separation and rotation along explicit structures can occur, while the individual blocks can also deform and yield.

The following paper details a series of analyses that have been conducted with 3DEC to back-analyse the observed behaviour of the south wall, which happened when mining was at the 505 RL level. The calibrated model has subsequently been used to investigate the behaviour of the south wall after mining has progressed down to the 445 RL level.

1 Introduction

Newcrest Mining Ltd's Cadia Hill Open Pit Mine, near Orange in New South Wales, is located within a complex geological setting. The current pit-slope design is based upon structurally controlled failure mechanisms associated with faults and shear zones that dissect a largely massive rock mass. To date, a number of structurally controlled slope failures have occurred along fault and shear planes with minimal warning. Their scales have ranged from less than one bench height to multiple bench heights.

Routine kinematic, limit equilibrium and two-dimensional numerical modelling analyses are an essential part of any pit-slope design methodology. However, in order to determine accurately the stability of complex wedge-failure mechanisms that involve a combination of rock mass failure in addition to slip along geological structure, a three-dimensional discontinuum analysis is required.

2 Background

Mining commenced at the Cadia Hill Pit during 1997. Figure 1a illustrates Cutback 2, which forms the current pit shell that is being mined. The pit currently measures 1.5 km across, with slope heights ranging from 330 to 490 m. The inter-ramp slope angles range from 35° for the top 100 m in weathered sediments, to 55° for the bottom 135 m of the cutback. The final pit, as illustrated in Figure 1a, currently is designed to be 580 to 720 m deep (Li, 2005).

Following the firing of a trim shot on 9 September 2006, approximately 60,000 t of rock failed in the centre of the south wall from 535 - 656 RL, as illustrated in Figure 1b. There had been 5 mm of rainfall recorded on the day before the failure, and intermittent light rain had occurred during the day of the failure.

A large-scale (trace length > 30 m) shear structure, running sub-parallel to the face at an orientation of 56°/004° formed a basal sliding plane for the failure, as illustrated in Figure 1c. The failure occurred within geological Domain 18, which is comprised of monzonite. The rock mass in this domain is characterised by moderate-to-high RQD values and high intact rock strength (Finn, 2006).

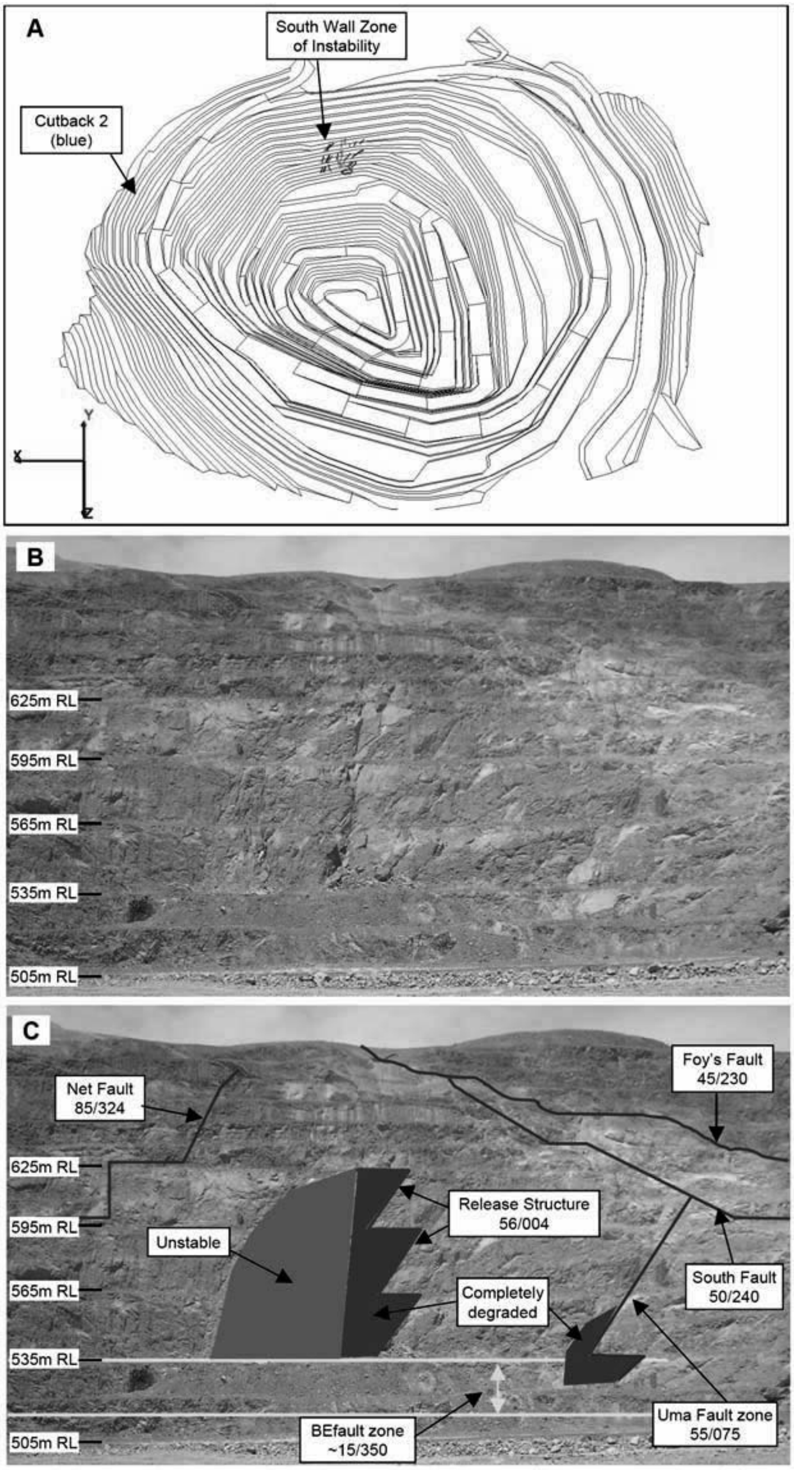

Figure 1 View of the Cadia Hill pit south wall (looking south)

Slope monitoring in the form of survey prisms and radar has been conducted since the beginning of 2006. Prism monitoring identified acceleration in slope displacements during May-June 2006, coincident with mining of the 550 RL level. Increases in slope movements have also been observed to be coincident with blasting and rainfall events.

The south wall failure was a combination of structurally controlled and rock mass failure. The release structure does not form a daylighting wedge that can be analysed using traditional wedge-failure analysis techniques. A conceptual model of the failure mechanism is illustrated in Figure 2, whereby sliding along the shear structure is combined with tensile and shear failure of the rock mass to cause the observed slope failure.

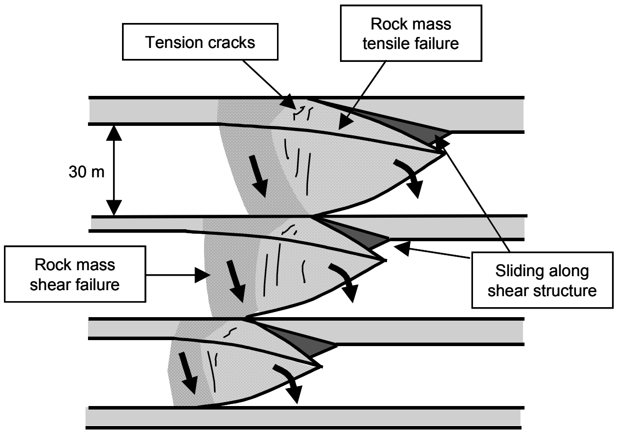

Figure 2 Conceptual model of south wall failure mechanism

Routine two-dimensional limit equilibrium analyses have been conducted for slope design and back-analysis of the multi-bench failure. However, due to the complex nature of the failure mechanism, these traditional methods of pit slope stability analysis have been unable to back-analyse the observed behaviour of the south wall instability.

3 Geotechnical model

The south wall geotechnical model developed for the initial slope design was largely based upon drill hole information with little pit wall exposure data to calibrate the structural model. To manage this uncertainty a large step-in was designed at the 505 RL level. Additional drilling was conducted during late 2005. This additional data was used in conjunction with bench face mapping in order to update the geotechnical model during 2006.

3.1 Geology

The predominant lithology throughout the south wall is monzonite Volcanics and Silurian sediments are also present, associated with faulting.

3.2 Structural geology

The Cadia Hill pit is located on the footwall of several thrust structures. There have been approximately four structural deformation episodes that have contributed to structures having a curvilinear nature, short persistence and varying mechanical properties along the length of the structure. Figure 3 illustrates the structures identified within the 2006 structural model.

Estimates of the shear strength parameters for each south wall structure have been made using field measurements of joint roughness coefficient (JRC) and joint wall compressive strength (JCS). Table 1 presents estimates of the orientation, thickness and shear strength properties for each structure.

Table 1 Estimates of the shear strength parameters for each south wall fault structure

Structure	Dip (deg).	Dip Dir. (deg.)	Thickness (m)	Cohesion (kPa)	Fric. Angle (deg.)
Foy’s Fault	45	230	1.0	20	20
South Fault	50	240	0.2	20	25
Net Fault	85	324	0.1	20	25
Uma Fault Zone	55	75	1.0	50	25
BE Fault Zone	15	330	20.0	0	20

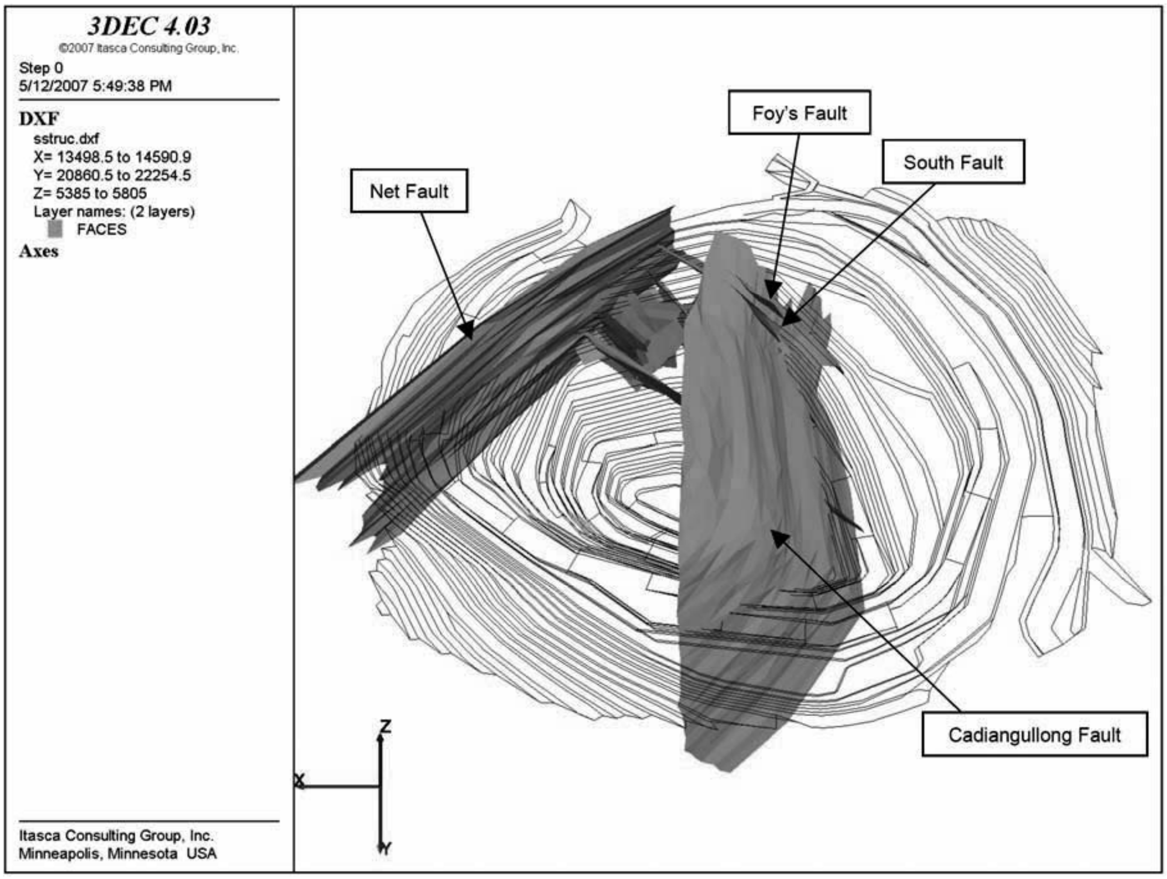

Figure 3 2006 structural model (looking south)

3.3 Rock mass characterisation

The south wall failure occured within monzonite. Laboratory testing of intact samples of this material indicates an unconfined compressive strength (UCS) of 120 MPa. Drillhole and bench face mapping has been conducted to determine the GSI rating for Domain 18. Table 2 presents the rock mass parameters determined for Domain 18 and the BE Fault Zone.

Table 2 Rock mass parameters

Domain/Unit	GSI	σ^{ci} (MPa)	m^i
Domain 18	60–75	120	21
BE Fault Zone	50–60	100	21

For slope stability analysis purposes, it is important to understand that the GSI rating derived at the bench-slope scale needs to be degraded to account for the analysis of inter-ramp and overall pit slopes. This scale-effect phenomenon has been reported by several authors to have a significant impact on rock mass strength, as illustrated in Figure 4. Pothitos (2005) applied a nominal reduction factor of 0.8 to the GSI for analysis of 200 m slopes at the Cadia Hill Pit.

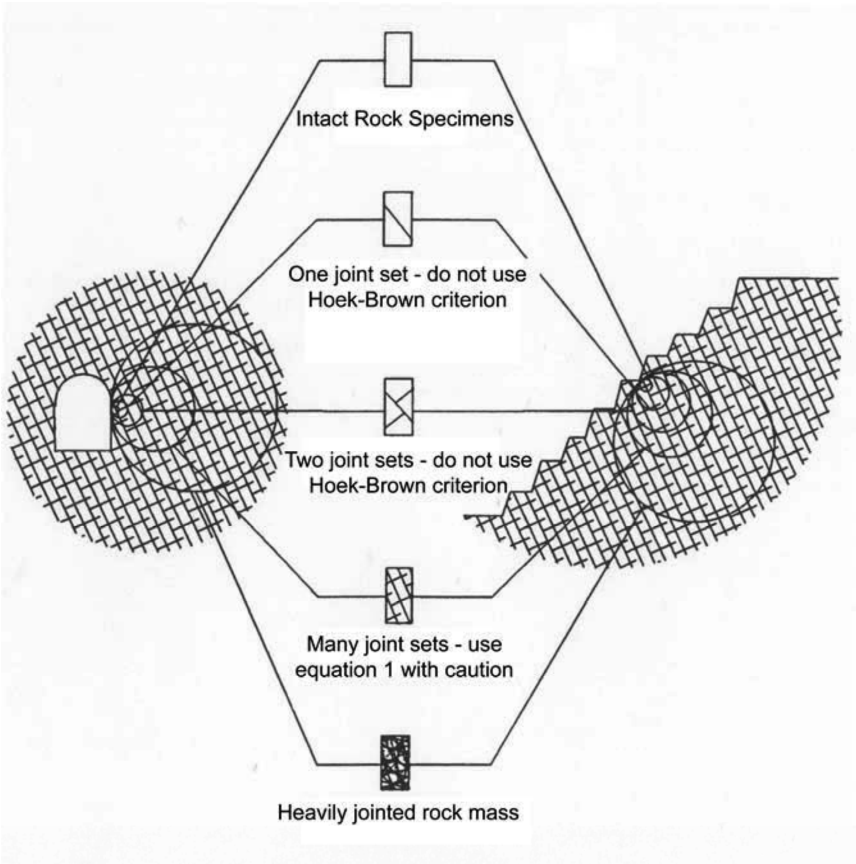

(Hoek et al, 1995)

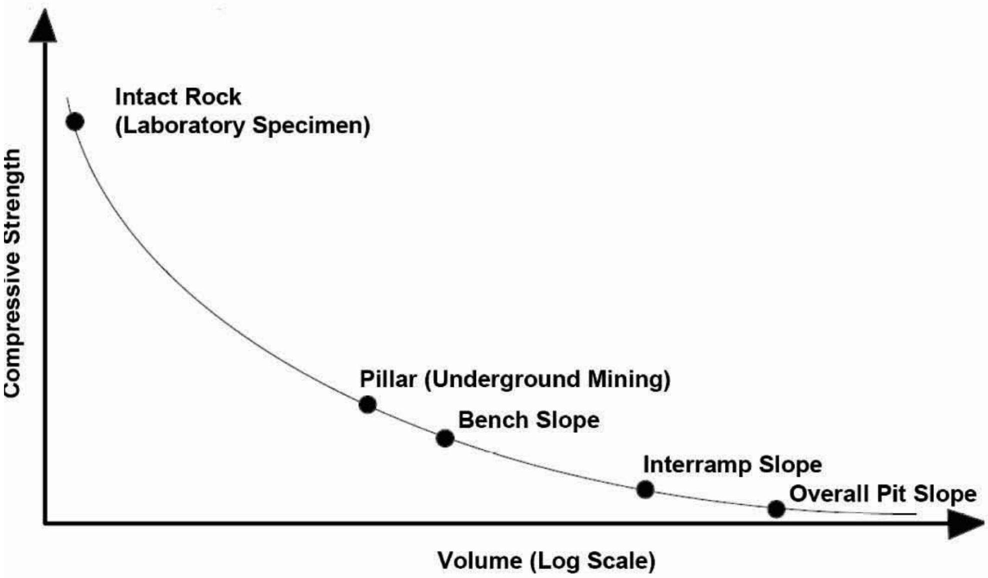

(Sjoberg, 1999)

Figure 4 Rock mass scale effects (after Hoek et al., 1995 and Sjöberg, 1999)

3.4 Hydrogeology

Two vibrating-wire piezometers are located along the crest of the south wall. The phreatic surface interpreted is illustrated in Figure 5. Both piezometers show no reaction to rainfall events. Water seepage has been evident along the south wall at several levels. Along the 610 RL level, several drainholes produced flow rates of approximately 2 l/s.

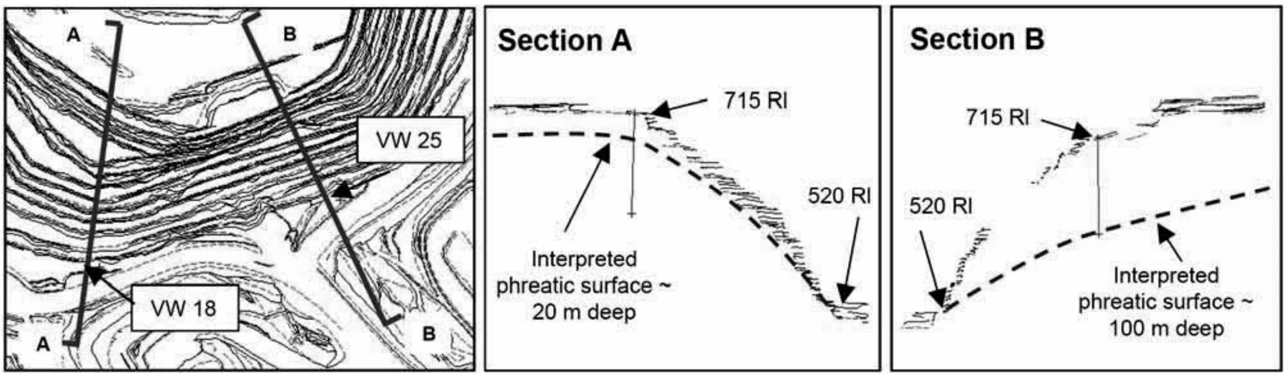

Figure 5 Estimated phreatic surface based upon vibrating wire piezometers

4 Numerical analysis of the Cadia Hill pit south wall

The *3DEC* code (Itasca, 2007) has been developed specifically to study complex failure mechanisms involving large numbers of explicit structures that divide a rock mass into blocks. Slip, separation and rotation along explicit structures can occur, while the individual blocks can deform and yield.

4.1 Model geometry

Figure 6 illustrates the *3DEC* model constructed to simulate the south wall of the Cadia Hill Pit. For the purpose of initial model calibration and investigation of the behaviour of the south wall in the vicinity of the failure, only the south wall to an elevation of 445 RL was constructed. Due to the orientation of the model, displacements at the boundaries were fixed. This limits interpretation of model behaviour close to the boundaries.

The large-scale structures included within the *3DEC* model are illustrated in Figure 6. The BE Fault Zone has been represented as a 20 m thick zone of weaker material bounded by discrete, planar joint surfaces. All other structures have been simplified as discrete planar surfaces.

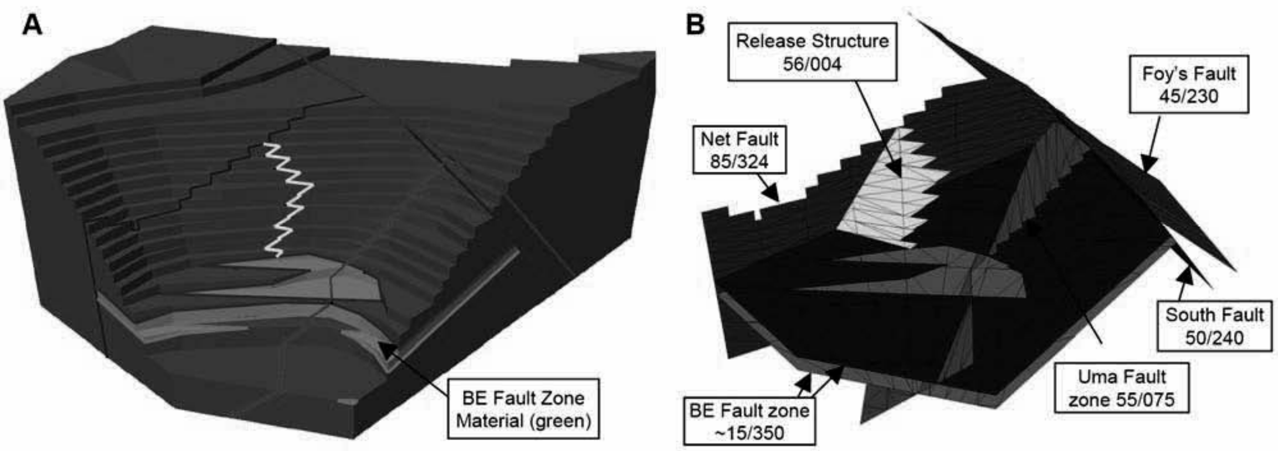

Figure 6 Large-scale structures included within *3DEC* model

4.2 Modelling methodology

A bi-linear Mohr-Coulomb strain-softening constitutive model was used to represent the behaviour of the rock mass. Because the Mohr-Coulomb criterion was used to define the strength of the rock mass, values for cohesion and friction angle were obtained by a least-squares fit to the Hoek-Brown curve. A bi-linear fit was obtained over a range in confining stress from 0 to 1 MPa and 1 to 5 MPa. An example of a bi-linear curve for a material with a GSI of 50, σ_{ci} of 120 MPa and m_i of 21 is illustrated in Figure 7.

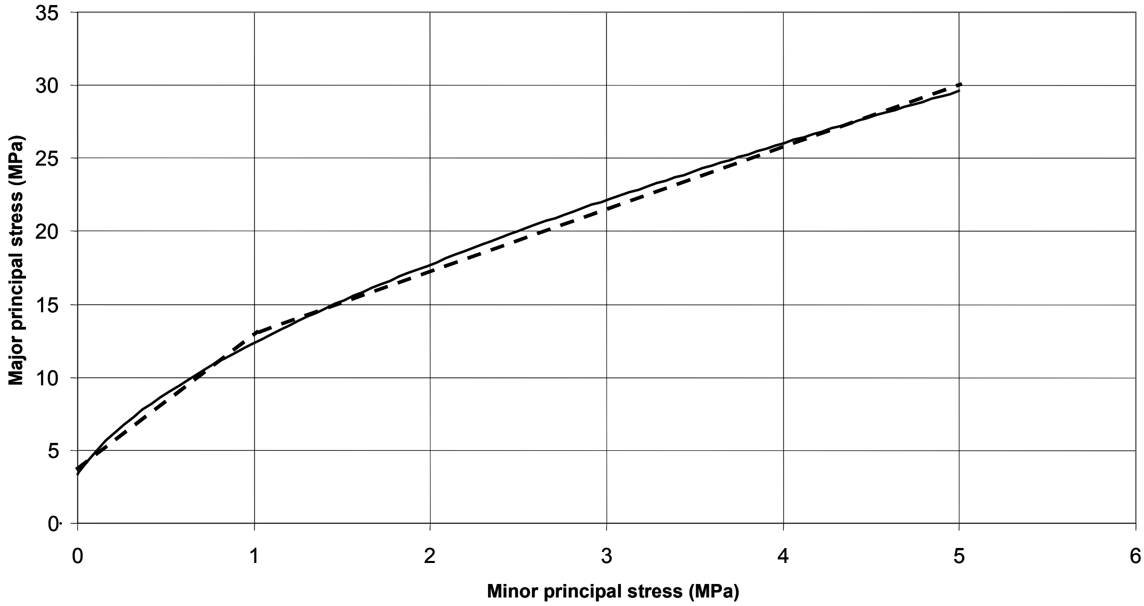

Figure 7 Relation between major and minor principal stresses for Hoek-Brown (solid line) and equivalent bi-linear Mohr-Coulomb (dashed line)

The specification of ductile or brittle behaviour in a numerical model is a very important consideration, as brittle materials tend to undergo progressive collapse much sooner after yielding begins. Ductile materials, on the other hand, are likely to remain stable well after yielding begins. For this reason, a strain-softening model has been used to represent the post-peak strength degradation that accompanies failure of the south wall rock mass.

Sjöberg (1999) states that strain-softening model results are dependent on the model grid used and recommends that strain-softening models should not be used for quantitative rock-slope stability analysis. However, advances in the understanding of strain-softening mesh dependency (Sainsbury and Urie, 2007), together with calibration of the strain-softening parameters to observed slope behaviour allows the use of such models in routine rock-slope stability analysis. Hajiabdolmajid and Kaiser (2002) suggest that a strain-softening material model must be used to simulate accurately the behaviour of rock slopes in which the candidate failure surface is not completely structurally controlled (i.e. failure of intact rock, asperities and rock bridges are involved).

Figure 8 illustrates the results of a simulated *3DEC* UCS test on a 10 × 10 × 10 m rock mass sample with a GSI of 50, σ_{ci} of 120 MPa, m_i of 21 and D of 1.0. The modelling methodology causes localization along shear bands whereby the cohesion and tensile strength have degraded from the intact value to zero. This is the same behaviour observed in physical UCS tests. The strength of the rock mass was degraded by means of gradual reductions in the cohesion and tensile strength with plastic strain (ε^{s}_{crit}). The cohesion and tensile strength parameters were reduced to zero.

There is currently no a priori way to estimate the value for the critical plastic strain of a rock mass. In order to provide a more robust assessment of the rock mass strength, modulus, brittleness and scale effect of the different rock mass domains at the Cadia Hill Pit, it is planned to investigate rock mass behaviour with the Particle Flow Code (PFC) (Itasca, 2005).

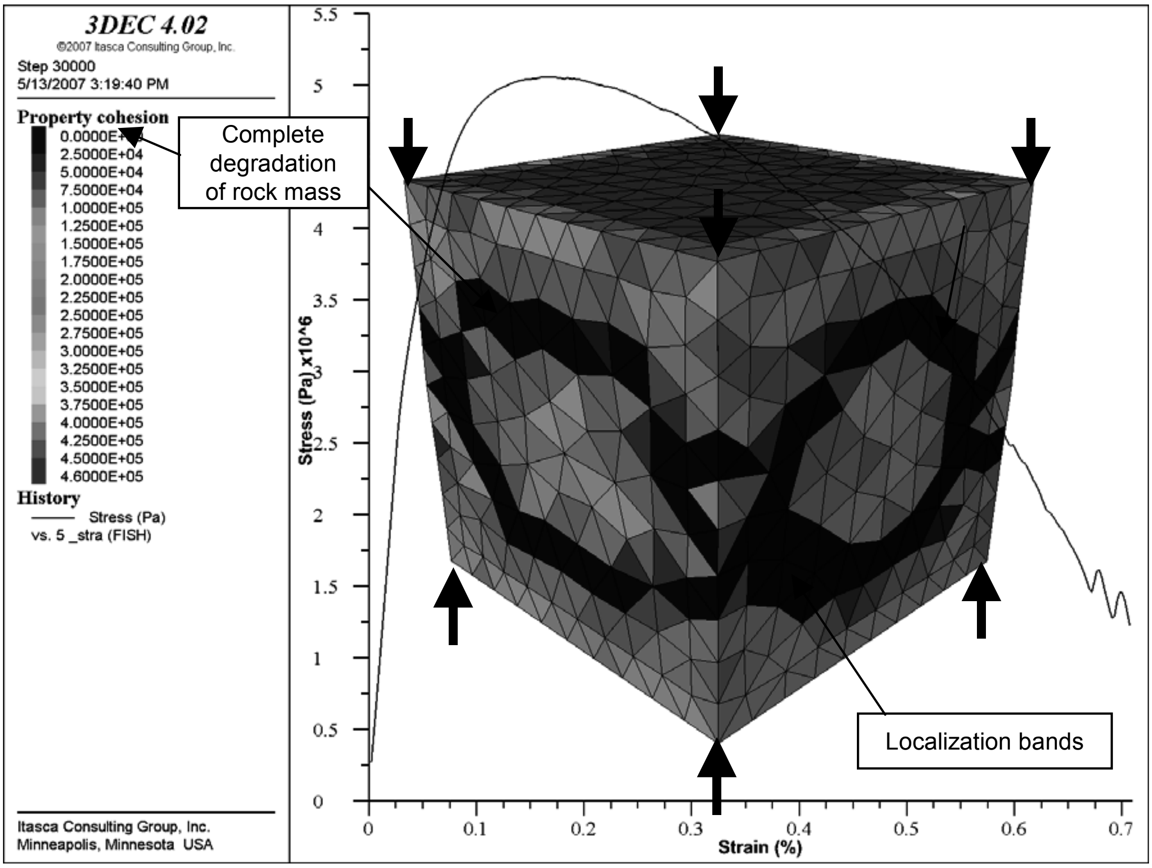

Figure 8 Simulated UCS test on 10-m rock mass sample with GSI of 50, σ_{mi} of 120 and m_i of 21

4.3 Material properties

The rock masses simulated throughout this modelling exercise are assumed to behave as a homogeneous, isotropic material. Table 3 outlines the estimates of the material properties used to simulate the south wall rock mass.

Table 3 Estimates of Mohr-Coulomb parameters for the south wall rock mass

Class	σ_{ci} (MPa)	GSI	m_i	D	Density (kg/m^3)	Young's Modulus (GPa)	Poisson's ratio	Cohesion (MPa)	Friction Angle (deg.)	Cohesion (MPa)	Friction Angle (deg.)	Tension (kPa)
								σ_3 = 0-1 (MPa)		σ_3 = 1-5 (MPa)		
Lower bound	120	50	21	1.0	2700	4.9	0.25	0.46	50	1.26	37	50
Best estimate	120	57.5	21	1.0	2700	9.0	0.25	0.63	54	1.55	41	100
Upper bound	120	70	21	1.0	2700	15.8	0.24	1.27	59	2.36	48	320

The rock mass material within the BE Fault Zone was simulated with separate material properties. Table 4 presents lower-bound and best-estimate properties used to simulate the BE Fault Zone rock mass.

Table 4 Estimates of Mohr-Coulomb parameters for the BE fault zone rock mass

Class	σ_{ci} (MPa)	GSI	m_i	D	Density (kg/m^3)	Young's Modulus (GPa)	Poisson's ratio	Cohe-sion (MPa)	Friction Angle (deg.)	Cohe-sion (MPa)	Friction Angle (deg.)	Tension (kPa)
								σ_3 = 0-1 (MPa)		σ_3 = 1-5 (MPa)		
Lower bound	100	40	21	1.0	2700	5.0#	0.25#	0.30	41	0.88	29	16
Best estimate	100	50	21	1.0	2700	5.0	0.25	0.43	48	1.18	35	41

The Mohr-Coulomb parameters used to simulate each fault structure are presented in Table 5.

Table 5 Estimates of Mohr-Coulomb parameters for fault structures

Class	Fault	Normal stiffness (Pa/m)	Shear stiffness (Pa/m)	Cohesion (kPa)	Friction Angle (deg).	Tension (kPa)
Best estimate	Foy's	1.00E+10	1.00E+09	20	20	0
Best estimate	Net	1.00E+10	1.00E+09	20	25	0
Best estimate	Uma	1.00E+10	1.00E+09	20	25	0
Best estimate	South	1.00E+10	1.00E+09	50	25	0
Best estimate	BE	1.00E+10	1.00E+09	0	20	0

4.4 Pre-mining stresses

A series of HI Cell and acoustic emission (AE) stress measurements have been taken underground at the nearby Ridgeway Mine. Based upon these measurements, the vertical stress at the Cadia Hill Pit was assumed to be lithostatic (assuming a density of 2700 kg/m^3). The pre-mining stresses used throughout the analyses are summarised in Table 6.

Table 6 Pre-mining stresses used in analyses

Principal stress	Stress-depth relation (MPa)	Orientation
σ_v	Overburden (2700 kg/m^3)	Vertical
σ_H	1.72 x σ_v	East-west
σ_h	1.25 x σ_v	North-south

5 Calibration of south wall failure after mining of the 505 RL bench

In order to calibrate the *3DEC* model to the observed behaviour of the south wall failure after mining of the 505 RL bench, a series of analyses was conducted whereby the upper-bound (GSI = 70), best-estimate (GSI = 57.5) and lower-bound (GSI = 50) rock mass properties were simulated. The best-estimate properties for the BE Fault zone (GSI = 50) were simulated, while best-estimate joint properties and phreatic surface conditions also were applied to the models.

The south wall failure mechanism observed throughout the modelling exercise is illustrated in Figure 9. Sliding along the non-daylighting release structure, combined with tensile failure of the rock mass, causes the observed multi-bench slope failure.

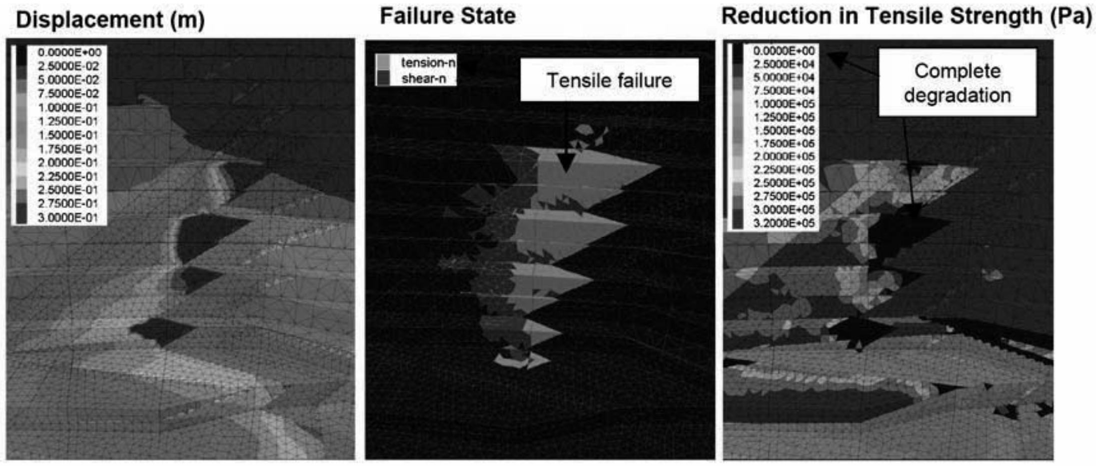

Figure 9 Failure mechanism predicted with *3DEC*

The best-estimate rock mass properties, with a GSI of 57.5, provide a good calibration to the observed behaviour of the south wall failure. Figure 10 illustrates a comparison between the observed and predicted conditions of the south wall after mining of the 505 RL bench. Together with the main multi-bench failure, the bench-scale failure associated with the Uma Fault zone is also predicted within the *3DEC* model.

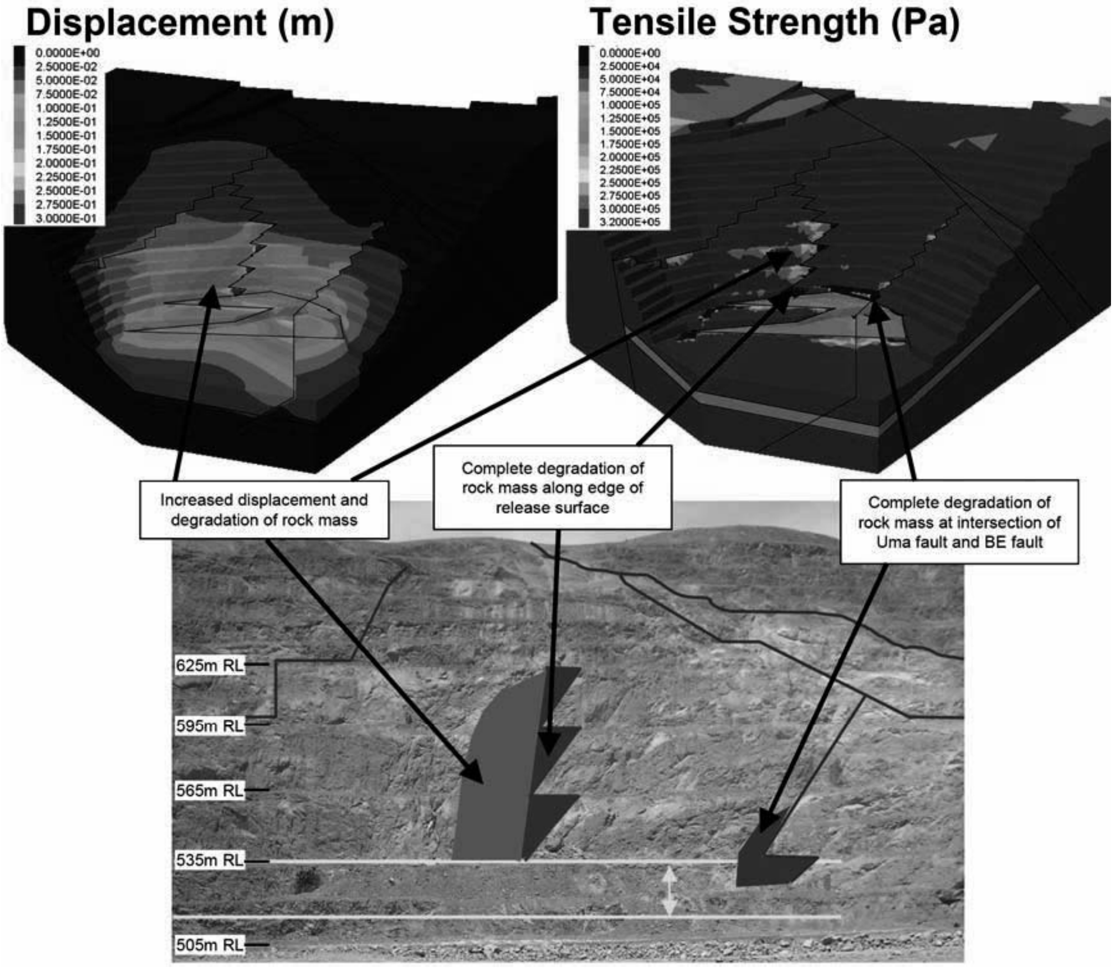

Figure 10 Comparison of observed and predicted behaviour of south wall with a GSI of 57.5

Histories of slope displacements have been measured at the same locations as monitoring prisms with the *3DEC* model. A comparison between the measured and predicted slope displacements is illustrated in Figure 11. Because real time is not simulated within the numerical model, the model displacements have been scaled to the excavation sequence of the south wall. A good correlation has been obtained between the measured and predicted slope displacements.

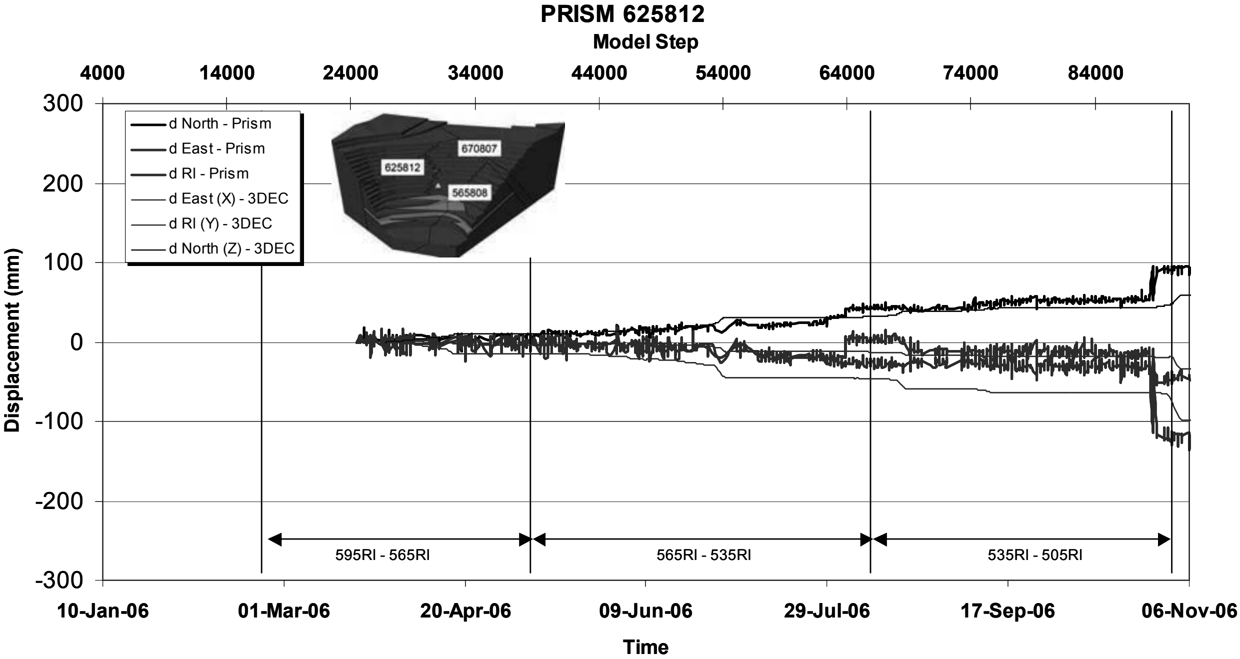

Figure 11 Comparison of actual and predicted slope displacement at prism 625812 location

6 Analysis of south wall behaviour after mining of 445 RL Bench

Due to the good calibration with the observed behaviour of the south wall failure, the best-estimate (GSI = 57.5) rock mass model was used to investigate the likely behaviour of the south wall after mining of the 445 RL bench. Figure 12 illustrates the slope displacement and reduction in tensile strength in the area of the failure. A minor increase in displacement and yielding is observed, but the vertical extent of the failure zone is predicted to remain confined to an approximate 60 m width between 625 RL and 535 RL, bounded by the original release structure.

Figure 13 illustrates the predicted slope displacements as mining progresses from the 505 RL bench to the RL bench. The 625812 prism location is predicted to become unstable during mining between the 475 RL and 445 RL benches.

7 Analysis of 475 RL bench failure

On 23 March 2007, a 35,000 to 40,000 t failure occurred on the 475 RL bench face, in the southwest corner of the Cadia Hill Pit. The failure was triggered by significant rainfall immediately before the time of failure.

Inspection of the failure, reported by Lowther (2007), identified a shallow-dipping shear structure (25º/082º) associated with the BE Fault zone that formed the basal plane of the failure. The failed volume of rock was observed to be intensely jointed.

Although the *3DEC* models analysed do not account for the pore pressures and increased rock-mass density caused by significant rainfall surface runoff, as illustrated in Figure 14, the best-estimate rock mass model indicates a zone of increased displacement and yielding associated with the BE Fault zone on the 475 RL bench face, in the exact location as the observed failure. Analysis of the 475 RL bench failure highlights how a *3DEC* modelling approach can be used as a predictive tool to identify problem areas within the mining sequence.

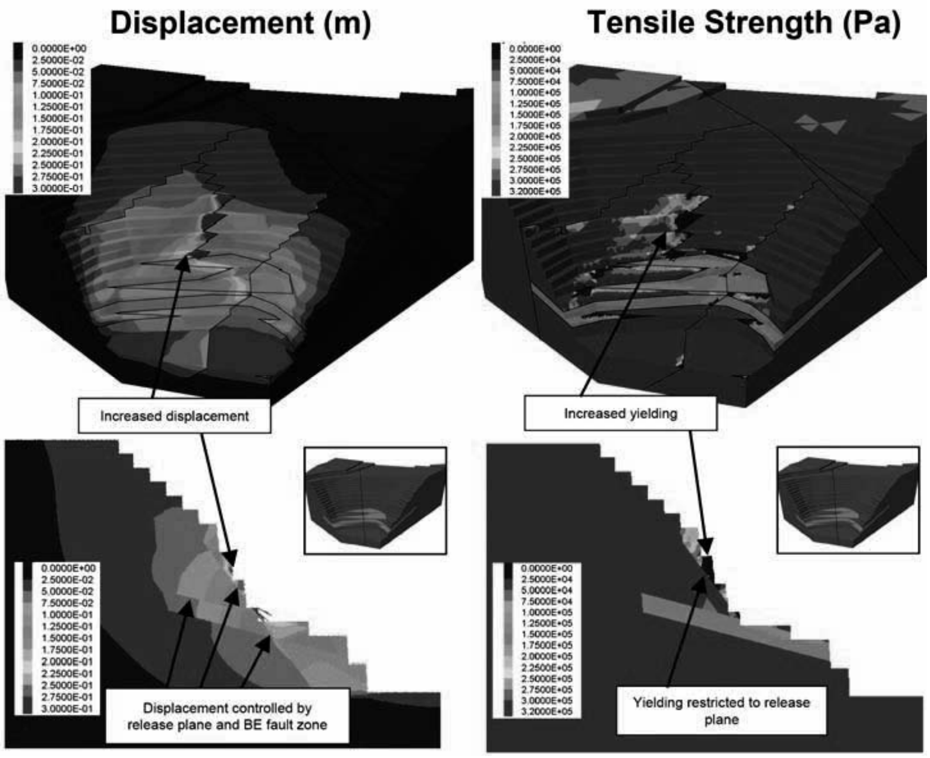

Figure 12 Displacement and reduction in tensile strength after mining of 445 RL bench

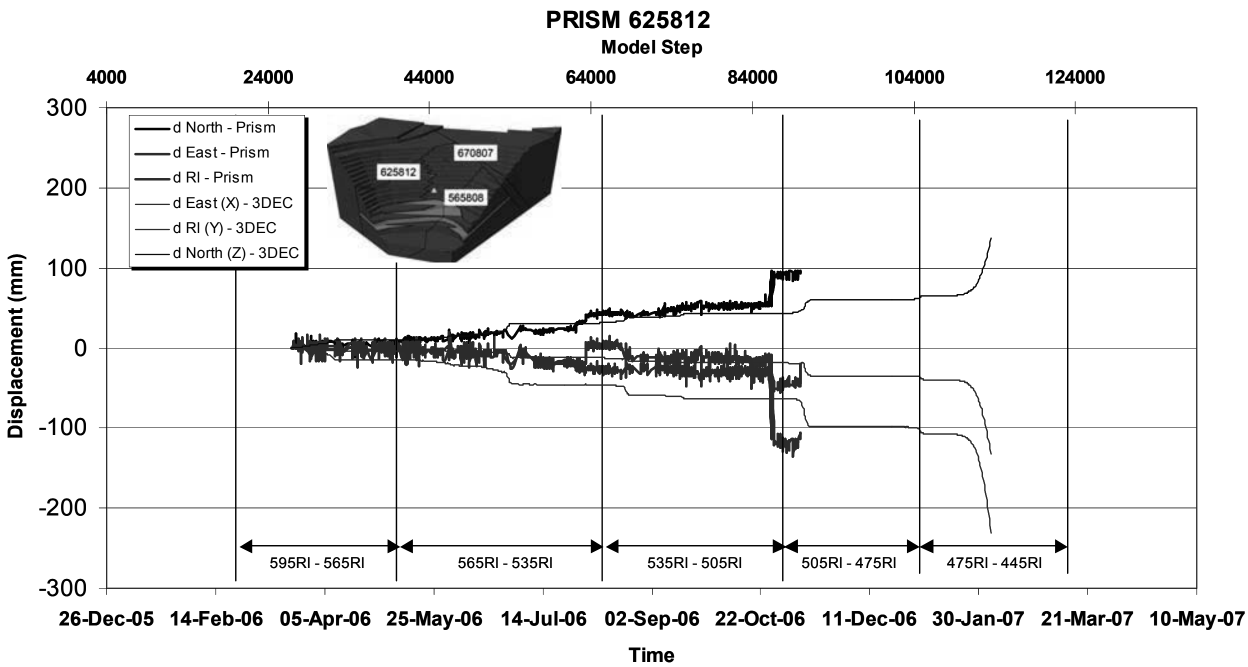

Figure 13 Comparison of actual and predicted slope displacement at prism 625812 location after mining of 445 RL bench

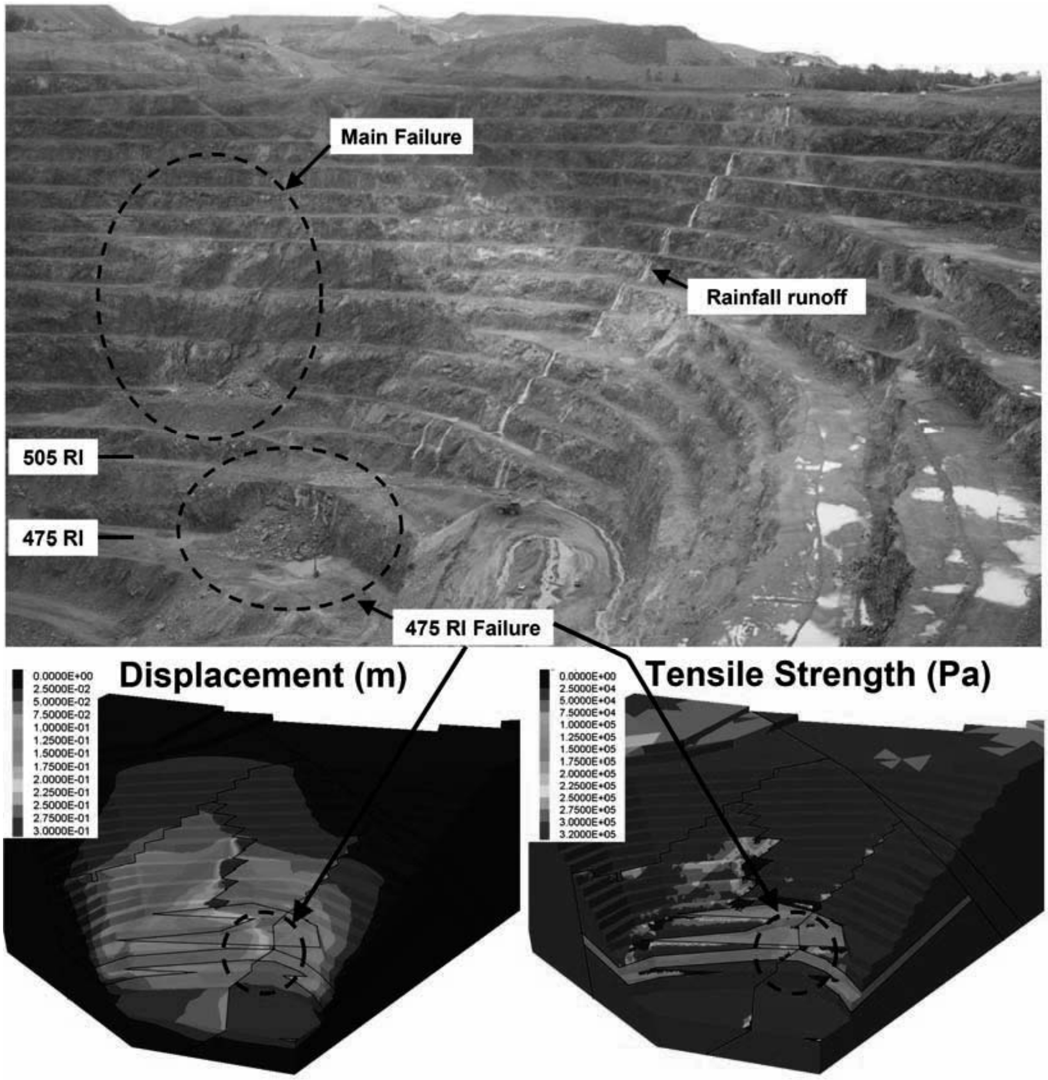

Figure 14 Analysis of 475 RL bench failure

8 Discussion of uncertainties and limitations

In order to understand the sensitivity of the south wall slope behaviour to the different model parameters, a series of analyses was conducted whereby the structure properties, phreatic surface, BE Fault zone material strength and slope angle were varied independently over reasonable upper and lower bound ranges. A single analysis was also conducted in order to investigate the combined effect of the lower-bound model parameters. The combined worst case slope conditions have a significant effect upon the extent of the south wall failure, whereby failure is predicted to propagate to the west, terminating at the Net Fault, as illustrated in Figure 15. Based upon calibration of the observed south wall failure after mining to the 505 RL bench, this condition clearly represents an overly conservative analysis of the slope behaviour.

Analysis of pit slope behaviour with a *3DEC* modelling approach is limited by representation of the explicit structures within the model. Without prior knowledge of the location and orientation of the 56°/004° release structure, modelling would not predict the observed behaviour.

Calibration of the south wall failure indicates that the rock mass strength required to match the measured and observed behaviour of the failure (GSI = 57.5) is less than the rock mass strength derived from drill hole and bench-face mapping (GSI = 60-70). This observation is consistent with the rock-mass scale effects reported by Hoek et al. (1995) and Sjöberg (1999) for the simulation of large-scale rock mass behaviour.

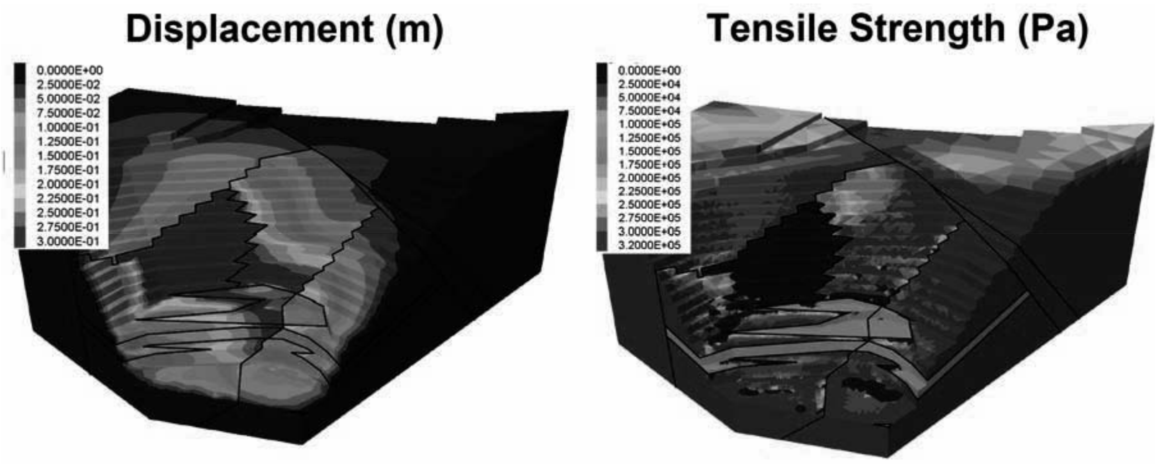

Figure 15 Slope displacement and reduction in tensile strength after mining of 445 RL bench (simulated combined worst-case rock mass, structure and phreatic surface conditions)

9 Conclusions

A calibration exercise has been conducted with the three-dimensional distinct element code *3DEC* to simulate the observed south wall failure at the Cadia Hill Pit. The numerical model provides a good correlation to the behaviour of the failure after mining of the 505 RL bench. Predictive analysis of the behaviour of the south wall after mining of the 445 RL bench indicates a minor increase in displacement and yielding in the area of the failure, but the extent of failure zone is predicted to remain confined to an approximate 60 m width between 625 RL and 535 RL, bounded by the original release structure.

The best-estimate rock mass model indicates a zone of increased displacement and yielding associated with the BE Fault zone on the 475 RL bench face, in the exact location as a 35,000 to 40,000 t failure that was triggered by significant rainfall runoff. Although the *3DEC* models analysed do not account for the pore pressures and increased rock mass density caused by significant rainfall surface runoff, analysis of the 475 RL bench failure highlights how a *3DEC* modelling approach can be used as a predictive tool to identify problem areas within the mining sequence.

Acknowledgements

The management of Newcrest Mining Limited, Cadia Valley Operations is acknowledged for permission to publish this paper.

References

Finn, D. (2006) Instability report south wall of the pit, Cadia Valley Operations Internal Memorandum.

Hajiabdolmajid, V. and Kaiser, P.K. (2002) Modelling slopes in brittle rock. NARMS-TAC 2002: Mining and Tunneling Innovation and Opportunity, Vol. 1, R. Hammah, W. Bawden, J. Curran, and M. Telesnicki (eds). Toronto: University of Toronto Press, pp. 331-338.

Hoek, E., Kaiser, P.K. and Bawden, W.F. (1995) Support of Underground Excavations in Hard Rock. Rotterdam: Balkema.

Itasca Consulting Group, Inc. (2007) 3DEC (Three-Dimensional Distinct Element Code), Version 4.02. Minneapolis.

Itasca Consulting Group, Inc. (2005) PFC2D (Particle Flow Code in Two-Dimensions), Version 3.1. Minneapolis.

Li, T. (2005) Geotechnical Engineering at Newcrest Mining, Australian Centre for Geomechanics Newsletter, Vol. 25.

Lowther, R. (2007) Geomechanical Instability Report – 475 RL Major Rainfall Triggered Rockfall Event, Cadia Valley Operations Internal Memorandum.

Sainsbury, D.P. and Urie, R. (2007) Stability Analysis of Horizontal and Vertical Paste Fill Exposures at the Raleigh Mine, Minefill 2007 – Innovation and Experience. Proceedings of the 9th International Symposium on Mining with Backfill, Montreal, May 2007, CD Proceedings, Paper No. 2527, CIM, Montreal.

Sjöberg, J. (1999) Analysis of Failure Mechanisms in High Rock Slopes, Doctoral Thesis, Department of Civil and Mining Engineering, Division of Rock Mechanics, Luleå University of Technology, 1999:01/ISSN: 1402-1544, January.

Our ref: DW24/214

Frances & Gem
The Cadia Community Sustainability Network

By email:

Dear Frances & Gem

Thank you for your email of 28 May 2024 regarding your concerns about groundwater and surface water impacts from the Cadia Mine operations, I also refer to the meeting on 3 June 2024 with Evie Madden, Director Corporate Affairs, and Steve Beaman, Executive Director Regulatory Practice and Services, to discuss these concerns.

Groundwater and surface water samples have been collected

The NSW Environment Protection Authority (EPA) collected groundwater and surface water samples for laboratory analysis during the week commencing 27 May 2024.

As part of the groundwater analysis, the groundwater bore locations were chosen to enable the investigation of onsite groundwater contamination resulting from mining operations and potential offsite migration. Groundwater levels were measured (dipped) to confirm the direction of groundwater flow.

Surface water samples were collected to provide an initial assessment of surface water quality. At your request, these samples are being tested for per- and polyfluoroalkyl substances (PFAS) and hydrocarbons.

The EPA is developing a comprehensive water quality monitoring program to assess the Cadia Community Sustainability Network’s concerns. We will seek the Cadia Expert Panel’s advice on its design.

Groundwater assessments are technically complex and need to consider local and regional characteristics. An independent groundwater and surface water specialist will review historical groundwater monitoring data. This review will assess potential on and offsite impacts to ground and surface water from the tailings facilities and the waste rock emplacement area at the Cadia Mine, and inform changes to the licence that will ensure the highest operational standards and reduce potential impacts on the surrounding community and environment.

Environmental monitoring is an important aspect of the licence review process

The EPA has identified air quality and groundwater monitoring as priorities for the current review of the environment protection licence. Groundwater monitoring is currently primarily regulated through planning approval.

The EPA is examining how to integrate groundwater monitoring conditions into the licence.

Groundwater monitoring framework is specified in the planning approval

The 1996 planning consent requires a groundwater management plan, which has been updated following consent modifications. The current management plan was last approved by the NSW

Department of Planning, Housing and Infrastructure (DPHI) in September 2023, and Cadia's water management plan is currently being reviewed as part of the Mod 14 submission.

The current groundwater monitoring network includes 149 locations on and around the Cadia mine. Groundwater quality trends over time and site-specific guideline values for water quality have been developed for the monitoring network. They are implemented through a trigger action response plan (TARP) in the water management plan. The TARP includes notification requirements to the EPA if the guideline values are exceeded.

EPA undertook surface water sampling in 2023

The 2023 test results for water samples collected from Oakey Creek Dam, Cadiangullong Creek, Flyers Creek, and Belubula River showed that the water quality on the day of sampling met the criteria described in the Livestock Drinking Water Guidelines (2023).

As always, we will continue to provide you with updates regarding the outcomes of the independent groundwater review and the sampling.

Yours sincerely

TONY CHAPPEL
Chief Executive Officer

27 June 2024

CCSN Comments re
EPA Cadia Region Groundwater Testing Report of August 2024

September 2024

The EPA tested water in groundwater monitoring bores at the Cadia Valley Operations ("CVO") gold and copper mine in May 2024. This testing program was in response to concerns raised by the CCSN relating to changes in the quality of groundwater and high levels of contamination identified in monitoring bores at the CVO mine site.

Relevant Documents and Extracts

CVO has issued multiple reports relating to the quality of the groundwater, a number of them identifying contamination in both the monitoring bores and the Belubula River. Accordingly, the EPA's Cadia Region Groundwater Testing Report issued of August 2024 should be read in conjunction with the following documents.

a) Minutes of the Annual Environmental Monitoring Report Meeting (available online 2010/11 -2017/18) which refer on several occasions to tailings dams seeping into the groundwater. The EPA attended these meetings. The minutes relevantly include the following statements:

AEMR minutes 12 Dec 2017

- *"Groundwater quality changes are attributed to the compression of the system by the bulk mass of the TSF, however there may be some minor contribution from TSF seepage into groundwater*".
- "*Changes from pre-2015 indicate a change in water chemistry that may be attributed to the Southern Tailings Storage Facility(STSF)/Leachate dams*"
- "*Surface water at CAWS 55 and CAWS 41 influenced by tailings water chemistry*"

MOM-AEMR Meeting Minutes 2017

- *"A discharge is occurring from site that is not permitted by EPL5590 (seepage below STSF). [Joint agency audit finding]".*
- *"there may be some minor contribution from TSF seepage into groundwater"*

MEETING MINUTES - AEMR 2013-14 PRESENTATION

- *"aquatic ecosystem monitoring will commence in two locations downstream to monitor stream health."*

MEETING MINUTES - AEMR 2011-12 PRESENTATION

- *"Darryl Clift – asked what Mick was referring to when talking about seepage? Michael Butcher– Confirmed it referred to modelled seepage through the in-situ clay into groundwater from TSF."*

AEMR PRESENTATION MINUTES (2009/2010)

- *"Items / actions arising from 2009/10 AEMR. - 3 Continued investigation and remediation of diesel seep."*

b) Cadia Annual Groundwater Monitoring Review (available online 2010/11 through to 2022/23), which (among other issues):

- identify on multiple occasions that the tailings dams are contaminating the ground water, including:
  - 24 monitoring bores with a total of 159 exceedances in the year ending June 2023.[1]
  - 23 monitoring bores with a total of 122 exceedances in the year ending June 2022.[2]
  - 19 monitoring bores with a total of 106 exceedances in the year ending June 2021.[3]
  - 3 monitoring bores with a total of 3 general exceedances in the year ending June 2016[4]

- Identify notable long-term trends in pH, sulfate, sulfate-chloride mass ratios, and various other exceedances in monitoring bores 20, 21, 23, 24, 25, 26B, 27, 28 b, 68, 69, 70, 77A, 77B, 78, 79, 83, 84, 85, 86, 87, 90[5]

c) CVO Groundwater Report 2023 – CCSN Comments 24 April 2024; and

d) Cadia Surface Water Assessment – Belubula River 24 May 2024 and comments from CCSN by email on 12 June 2024. This report identified 2 significant contamination events in the Belubula:

- April – September 2022 (extreme alkalinity) and;
- November 2022 (significant toxic copper levels).

[1] Cadia Annual Groundwater Monitoring Review (**CAGMR**) 2022/2023 Water Year, Table 4.2
[2] CAGMR 2021/2022 Water Year, Table 4.2
[3] CAGMR 2020/2021 Water Year, Table 4.2
[4] Cadia Valley Operations - Groundwater Data Review Report June 2016, Table 4-2
[5] CAGMR 2022/2023 Water Year, 4.5.2.2 Groundwater quality

Approach Taken - EPA Sampling Locations

The EPA collected samples from 12 monitoring bores on the Cadia site. Multiple reports have been presented to the EPA by CVO and the CCSN which identified contaminated Monitoring Bores.

The EPA did NOT include in its sample set:

- Any bores identified by Cadia in the Annual Groundwater Monitoring Review 2022/23 Water Year as reporting a quality exceedance.

- With one exception, any of the bores identified by CCSN as being heavily contaminated:

    - None of the highly alkaline bores between the STSF and the Belubula River: MB 103, MB 104, MB 105, MB 106, MB 109[6] were tested by the EPA.
    - only one (MB74) of the acidic bores to the NE of Cadia (MB71, MB72, MB74) was included in the sample set.

- Any bores identified in CCSN's Mod 15 response as potentially being contaminated with diesel. This information was provided to DPIE in December 2023, CCSN has been informed investigations of the groundwater contamination are being carried out jointly by DPIE and the EPA, (EPA lead investigator).

CCSN would like to know:

- Which of the bores tested are situated on the multiple fault lines which intersect the site, in particular Cadiangullong and Warrengong faults?

- At what depth in the underground water did the EPA sample the monitoring bores? How did the sample depth consider that some of the contaminants of concern are likely to float on the surface of a water body (eg hydrocarbons and PFAS / PFOS) whilst others may be found throughout the water?

- What is the screen height for all of the bores tested and how did this compare to the level of the surface of the water body at the time of testing?

CCSN believes that the data set collected by the EPA does not represent the actual water quality observed in the monitoring bores and does not consider contamination trends already identified by CVO and its consultants and does not represent the actual risks.

Contrary to the EPA statement on page 3 the locations selected <u>do not</u> "*address specific locations that had raised concerns within the community*."

---

[6] CAGMR 2022/2023 Water Year, Appendix C, as highlighted in CVO Groundwater Report 2023 CCSN Comments – 24 April 2024 "S of STSF"

Relevant Standards

Potable water

The Belubula river and a number of tributaries in the Cadia district are defined by the BoM (2019) GDE Atlas as being high potential aquatic groundwater dependent ecosystems.[7] Such ecosystems are known to contain platypus holes and Murray cod which are essential biotic factors to the ecological health of the region.

Accordingly, the relevant ecological protection water quality standard in the river is 99% species survival in the aquatic system, not 95%.

PFAS

It is notable that the EPA tested for PFAS in the sample bores, because CCSN has not seen any previous groundwater testing for PFAS in or near Cadia by CVO or the EPA.

Assuming that the EPA's only data is the testing of these 12 sample bores, and given that the EPA has tested only bores that appear to be generally uncontaminated, the EPA's conclusion that "*contaminants are not present at levels that would typically pose a risk*" is unsupported. CCSN is very concerned that MB2A showed PFOA and PFOS in excess of the relevant guideline. Given the lack of data, and given the presence of PFOA and PFOS in nearby surface water that is known to the EPA, all of the groundwater bores should be tested for these contaminants as a first step to investigating this risk.

Conclusion

In the circumstances of all of the known problems, and knowing the above issues, it is obvious that the testing regime applied by the EPA is inadequate to properly understand the risk and address the community's very serious concerns.

The EPA has not adequately tested the Monitoring Bores at CVO and is not entitled to draw any conclusions regarding groundwater contamination.

CCSN requests that:

1. The EPA withdraw its Cadia Region Groundwater Testing Report August 2024.

2. The Office of the Chief Scientist and Engineer be appointed to independently investigate the source of pollution in the Belubula.

---

[7] BoM Groundwater Dependent Ecosystems Atlas

CERTIFICATE OF ANALYSIS

Work Order	: **ES2430237**	Page	: 1 of 5
Client	[redacted]	Laboratory	: Environmental Division Sydney
Contact	[redacted]	Contact	: Customer Services ES
Address	[redacted]	Address	: 2
Telephone	: ----	Telephone	:
Project	: ----	Date Samples Received	: 12-Sep-2024 11:20
Order number	: ----	Date Analysis Commenced	: 17-Sep-2024
C-O-C number	: ----	Issue Date	: 23-Sep-2024 15:30
Sampler	: ----		
Site	: ----		
Quote number	: ----		
No. of samples received	: 2		
No. of samples analysed	: 2		

Accreditation No. 825
Accredited for compliance with
ISO/IEC 17025 - Testing

This report supersedes any previous report(s) with this reference. Results apply to the sample(s) as submitted, unless the sampling was conducted by ALS. This document shall not be reproduced, except in full.

This Certificate of Analysis contains the following information:

- General Comments
- Analytical Results
- Surrogate Control Limits

Additional information pertinent to this report will be found in the following separate attachments: Quality Control Report, QA/QC Compliance Assessment to assist with Quality Review and Sample Receipt Notification.

Signatories

This document has been electronically signed by the authorized signatories below. Electronic signing is carried out in compliance with procedures specified in 21 CFR Part 11.

Signatories	*Position*	*Accreditation Category*
Ankit Joshi	Senior Chemist - Inorganics	Sydney Inorganics, Smithfield, NSW
Edwandy Fadjar	Organic Coordinator	Sydney Organics, Smithfield, NSW
Franco Lentini	LCMS Coordinator	Sydney Organics, Smithfield, NSW

General Comments

The analytical procedures used by ALS have been developed from established internationally recognised procedures such as those published by the USEPA, APHA, AS and NEPM. In house developed procedures are fully validated and are often at the client request.

Where moisture determination has been performed, results are reported on a dry weight basis.

Where a reported less than (<) result is higher than the LOR, this may be due to primary sample extract/digestate dilution and/or insufficient sample for analysis.

Where the LOR of a reported result differs from standard LOR, this may be due to high moisture content, insufficient sample (reduced weight employed) or matrix interference.

When sampling time information is not provided by the client, sampling dates are shown without a time component. In these instances, the time component has been assumed by the laboratory for processing purposes.

Where a result is required to meet compliance limits the associated uncertainty must be considered. Refer to the ALS Contract for details.

Key : CAS Number = CAS registry number from database maintained by Chemical Abstracts Services. The Chemical Abstracts Service is a division of the American Chemical Society.
LOR = Limit of reporting
^ = This result is computed from individual analyte detections at or above the level of reporting
ø = ALS is not NATA accredited for these tests.
~ = Indicates an estimated value.

- EP231X - Per- and Polyfluoroalkyl Substances (PFAS): Samples received in 20mL or 125mL bottles have been tested in accordance with the QSM5.4 compliant, NATA accredited method. 60mL or 250mL bottles have been tested to the legacy QSM 5.1 aligned, NATA accredited method.
- EP231: Stable isotope enriched internal standards are added to samples prior to extraction. Target compounds have a direct analogous internal standard with the exception of PFPeS, PFHpA, PFDS, PFTrDA and 10:2 FTS. These compounds use an internal standard that is chemically related and has a retention time close to that of the target compound. The DQO for internal standard response is 50-150% of that established at initial calibration or as per tables in USEPA 1633 where listed. PFOS is quantified using a certified, traceable standard consisting of linear and branched PFOS isomers. These practices are in line with recommendations in the National Environmental Management Plan for PFAS and also conform to QSM 5.4 (US DoD) requirements.

Work Order : ES2430237
Client : [redacted]
Project : ----

Flyers

Analytical Results

Sub-Matrix: WATER
(Matrix: WATER)

Compound	CAS Number	LOR	Unit	[redacted]	CA Creek	----	----	----
			Sampling date / time	09-Sep-2024 00:00	08-Sep-2024 00:00	----	----	----
				ES2430237-001	ES2430237-002	--------	--------	--------
				Result	Result	----	----	----
EG020T: Total Metals by ICP-MS								
Arsenic	7440-38-2	0.001	mg/L	**0.010**	<0.001	----	----	----
Cadmium	7440-43-9	0.0001	mg/L	**0.0001**	<0.0001	----	----	----
Chromium	7440-47-3	0.001	mg/L	**0.003**	<0.001	----	----	----
Copper	7440-50-8	0.001	mg/L	**0.056**	**0.061**	----	----	----
Nickel	7440-02-0	0.001	mg/L	**0.005**	<0.001	----	----	----
Lead	7439-92-1	0.001	mg/L	**0.002**	<0.001	----	----	----
Zinc	7440-66-6	0.005	mg/L	**0.569**	<0.005	----	----	----
Vanadium	7440-62-2	0.01	mg/L	**0.01**	<0.01	----	----	----
EG035T: Total Recoverable Mercury by FIMS								
Mercury	7439-97-6	0.0001	mg/L	<0.0001	<0.0001	----	----	----
EP071: Total Petroleum Hydrocarbons								
C10 - C14 Fraction	----	50	µg/L	<50	<50	----	----	----
C15 - C28 Fraction	----	100	µg/L	**530**	<100	----	----	----
C29 - C36 Fraction	----	50	µg/L	**540**	<50	----	----	----
^ **C10 - C36 Fraction (sum)**	----	50	µg/L	**1070**	<50	----	----	----
EP071: Total Recoverable Hydrocarbons - NEPM 2013 Fractions								
>C10 - C16 Fraction	----	100	µg/L	<100	<100	----	----	----
>C16 - C34 Fraction	----	100	µg/L	**920**	<100	----	----	----
>C34 - C40 Fraction	----	100	µg/L	**180**	<100	----	----	----
^ **>C10 - C40 Fraction (sum)**	----	100	µg/L	**1100**	<100	----	----	----
EP231A: Perfluoroalkyl Sulfonic Acids								
Perfluorobutane sulfonic acid (PFBS)	375-73-5	0.02	µg/L	<0.02	<0.02	----	----	----
Perfluorohexane sulfonic acid (PFHxS)	355-46-4	0.01	µg/L	<0.01	<0.01	----	----	----
Perfluorooctane sulfonic acid (PFOS)	1763-23-1	0.01	µg/L	**0.02**	**0.08**	----	----	----
EP231B: Perfluoroalkyl Carboxylic Acids								
Perfluorobutanoic acid (PFBA)	375-22-4	0.1	µg/L	<0.1	<0.1	----	----	----

Analytical Results

Sub-Matrix: WATER (Matrix: WATER)			Sample ID	Flyers [redacted]	CA Creek	----	----	----
			Sampling date / time	09-Sep-2024 00:00	08-Sep-2024 00:00	----	----	----
Compound	CAS Number	LOR	Unit	ES2430237-001	ES2430237-002	--------	--------	--------
				Result	Result	----	----	----
EP231B: Perfluoroalkyl Carboxylic Acids - Continued								
Perfluoropentanoic acid (PFPeA)	2706-90-3	0.02	µg/L	<0.02	<0.02	----	----	----
Perfluorohexanoic acid (PFHxA)	307-24-4	0.02	µg/L	<0.02	<0.02	----	----	----
Perfluoroheptanoic acid (PFHpA)	375-85-9	0.02	µg/L	<0.02	<0.02	----	----	----
Perfluorooctanoic acid (PFOA)	335-67-1	0.01	µg/L	<0.01	<0.01	----	----	----
EP231D: (n:2) Fluorotelomer Sulfonic Acids								
4:2 Fluorotelomer sulfonic acid (4:2 FTS)	757124-72-4	0.05	µg/L	<0.05	<0.05	----	----	----
6:2 Fluorotelomer sulfonic acid (6:2 FTS)	27619-97-2	0.05	µg/L	<0.05	<0.05	----	----	----
8:2 Fluorotelomer sulfonic acid (8:2 FTS)	39108-34-4	0.05	µg/L	<0.05	<0.05	----	----	----
10:2 Fluorotelomer sulfonic acid (10:2 FTS)	120226-60-0	0.05	µg/L	<0.05	<0.05	----	----	----
EP231P: PFAS Sums								
Sum of PFHxS and PFOS	355-46-4/1763-23-1	0.01	µg/L	**0.02**	**0.08**	----	----	----
Sum of PFAS (WA DER List)	----	0.01	µg/L	**0.02**	**0.08**	----	----	----
EP231S: PFAS Surrogate								
13C4-PFOS	----	0.02	%	**102**	**102**	----	----	----
13C8-PFOA	----	0.02	%	**100**	**101**	----	----	----

Surrogate Control Limits

Sub-Matrix: **WATER**

Compound	CAS Number	Recovery Limits (%) Low	High
EP231S: PFAS Surrogate			
13C4-PFOS	----	60	120
13C8-PFOA	----	60	120

CCSN - Appendix 2c

Cadia region surface water testing report

Acknowledgement of Country

The NSW Environment Protection Authority acknowledges the Traditional Custodians of the land on which we live and work, honours the ancestors and the Elders both past and present and extends that respect to all Aboriginal people.

We recognise Aboriginal peoples' spiritual and cultural connection and inherent right to protect the land, waters, skies and natural resources of NSW. This connection goes deep and has since the Dreaming.

We also acknowledge our Aboriginal and Torres Strait Islander employees who are an integral part of our diverse workforce and recognise the knowledge embedded forever in Aboriginal and Torres Strait Islander custodianship of Country and culture.

Published by:
NSW Environment Protection Authority

6&8 Parramatta Square
10 Darcy Street,
Parramatta NSW 2150
Locked Bag 5022,
Parramatta NSW 2124

Phone: +61 2 9995 5000 (switchboard)
Phone: 131 555
(NSW only – environment information and publications requests)

Fax: +61 2 9995 5999

TTY users: phone 133 677, then ask for 131 555

Speak and listen users: phone 1300 555 727, then ask for 131 555

Email: info@epa.nsw.gov.au
Website: www.epa.nsw.gov.au

Report pollution and environmental incidents
Environment Line: 131 555 (NSW only) or info@epa.nsw.gov.au
See also www.epa.nsw.gov.au

ISBN 978 1 922963 93 2
EPA 2024P4537
August 2024

Contents

On 30 May 2024 the NSW Environment Protection Authority collected water samples from Cadiangullong Creek, Flyers Creek and the Belubula River. This was in response to concerns raised by the community regarding water quality of the creeks surrounding Cadia gold mine and the Belubula River. This report summarises the sampling results.

Background

The Newmont Cadia gold mine is flanked by Cadiangullong Creek to the west and Flyers Creek to the east. They feed into the Belubula River south of the mine.

On 30 May 2024 the EPA undertook surface water sampling in the area in response to community concerns about the health of rivers and creeks near Newmont's Cadia gold mine, including the potential impact on livestock.

This report summarises the results of this sampling. It provides a snapshot of water quality in Cadiangullong Creek, Flyers Creek and the Belubula River at the time of sampling and will help to inform future monitoring requirements for the premises.

Approach taken

On 30 May 2024 the EPA collected surface water samples from nine locations along Cadiangullong Creek, Flyers Creek and Belubula River, both upstream and downstream of the mine (see Figure 1). The sampling sites were selected with consideration for the proximity to the mine, accessibility and previous sampling in the area. We included sampling sites near the confluence of the Cadiangullong Creek and Belubula River, and the confluence of Flyers Creek and the Belubula River, because community members leasing the surrounding land for livestock grazing have raised concerns regarding the potential suitability of the waterways for livestock drinking water.

We collected a water sample from each site for chemical analysis and used a water-quality meter to record pH, electrical conductivity, dissolved oxygen, temperature and turbidity. Samples were sent to the NSW Environmental Forensics laboratory and analysed for metals, total dissolved solids, nutrients, hydrocarbons and per- and polyfluoroalkyl substances (PFAS).

We compared the results to the Australian livestock, irrigation and ecological water quality guidelines, where they were available (ANZECC and ARMCANZ 2000, ANZG 2018, PFAS NEMP 2.0 2020).

The Australian and New Zealand guidelines for fresh and marine water quality (ANZG 2018) recommend deriving site-specific guideline values for physicochemical stressors using reference site data. In the absence of suitable long-term reference site data, we have compared our results to the relevant ANZECC (2000) default guideline values for upland rivers.

The National Chemicals Working Group of the Heads of EPA's Australia and New Zealand have developed a PFAS National Environmental Management Plan (PFAS NEMP 2.0), which provides ecological water quality guideline values for PFOS (perfluorooctanesulfonic acid) and PFOA (perfluorooctanoic acid).

Summary of results

Livestock and irrigation water guidelines

There were no exceedances of any current irrigation or livestock water guideline values. Where the concentration of a pollutant is below or outside the range for the relevant guideline value, the pollutant is unlikely to pose a risk for irrigation or stock water use.

However, it should be noted that the draft livestock drinking water guidelines (in review) provide a more conservative value for total dissolved solids (TDS), which was slightly exceeded in the sample taken from Flyers Creek. At this concentration, it is unlikely there will be any adverse effects experienced by livestock, except a slight impact on taste (ANZG 2023).

Ecological water quality guidelines

Conductivity and pH were outside the default guideline range at all but two sites in Cadiangullong Creek.

Hydrocarbons

Samples were tested for a range of volatile and semi volatile hydrocarbons. None were detected.

PFAS

Samples were tested for a range of per- and polyfluoroalkyl substances (PFAS). There were no PFAS substances detected in Cadiangullong Creek or Flyers Creek; however, PFOS was detected in the Belubula River above the ecological water quality guidelines, with the highest concentration measured in the site furthest upstream (Baker's Shaft Reserve). There are no livestock and irrigation water guidelines for PFAS. The presence of PFOS in water samples does not necessarily mean there is a risk to human health or livestock.

Metals

Copper was above the guideline level set to protect water life in Cadiangullong Creek downstream of the mine, but was below the guideline at all other locations. All other metals were below the levels set to protect water life.

Nutrients

Total nitrogen was above the guideline value for upland river ecosystems in the Belubula River. Oxides of nitrogen (NOx as nitrogen) were above guideline values in Cadiangullong Creek and free reactive phosphorus was above the guideline value in the Cadiangullong Creek sample adjacent to the South-Western end of the mine. All exceedances were minor and typical of nutrient levels found in agricultural use regions such as this. Ammonia and total phosphorus were not detected in any samples.

The EPA is continuing to review and monitor surface water quality in the region.

Sample locations

Table 1 Sample site and location descriptions for surface water samples collected in the Cadia region on 30 May 2024

Sampling site	Waterway	Location description
SW 1	Cadiangullong Creek	Upstream of the mine at a V-notch weir
SW 2	Cadiangullong Creek	Adjacent to the South-Western end of the mine
SW 3	Cadiangullong Creek	Immediately upstream of the Belubula River
SW 4	Belubula River	Immediately downstream of Cadiangullong Creek
SW 5	Belubula River	Immediately upstream of Cadiangullong Creek

Sampling site	Waterway	Location description
SW 6	Belubula River	Upstream of Flyers Creek
SW 7	Flyers Creek	Upstream of the Belubula River
SW 8	Belubula River	Downstream of Flyers Creek
SW 9	Belubula River	At Baker's Shaft Reserve, approximately 12 km upstream from Flyers Creek

Figure 1 Overview of the sampling sites

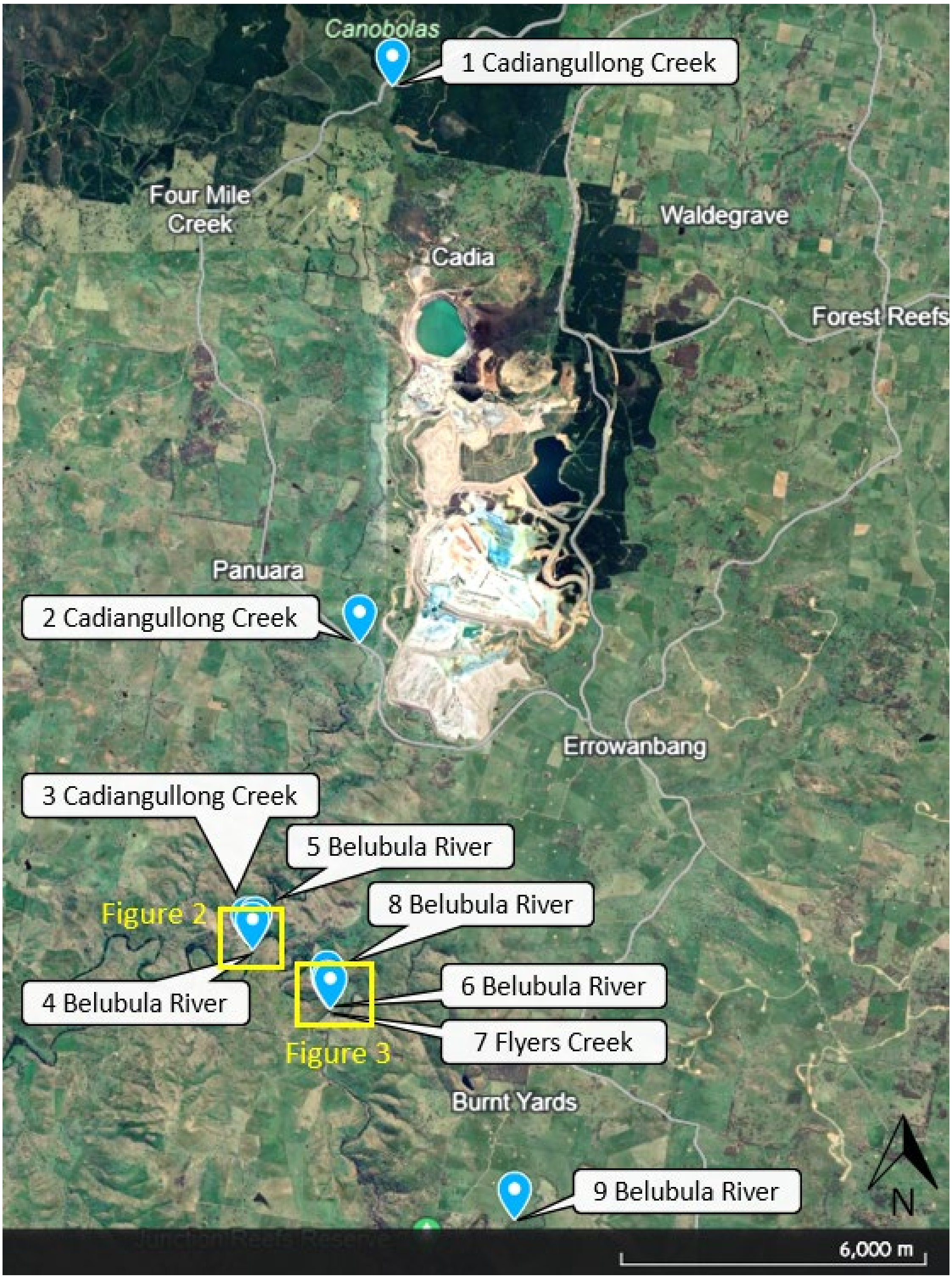

Figure 2 Locations of sampling sites SW3, SW4 and SW5

Figure 3 Locations of sampling sites SW6, SW7 and SW8

Sampling results

Sampling and analysis results for physicochemical parameters, metals, PFAS and hydrocarbons are described below, with data listed in Table 2 and Table 3 below. Any guideline exceedances have been bolded.

Physicochemical stressors

Conductivity and pH were outside the default guideline range at all but two sites in Cadiangullong Creek, those sites being upstream and directly adjacent to the mine.

The total dissolved solids (TDS) concentration slightly exceeded the draft livestock water guideline value (500mg/L) at the Flyers Creek sampling site (SW7; 510mg/L). There were no other exceedances of livestock drinking water or irrigation water quality guideline values.

Total nitrogen was elevated in the Belubula River, ranging between 1.2 and 1.6 times higher than the guideline value for upland river ecosystems in NSW (ANZECC 2000). All samples collected from Cadiangullong Creek and Flyers Creek were below the guideline value. Oxides of nitrogen (NOx as nitrogen) and free reactive phosphorus concentrations were four times above guideline values in the Cadiangullong Creek sample adjacent to the south-western end of the mine. Ammonia and total phosphorus were not detected in any samples.

Metals

Total metals have been compared to the Australian livestock drinking and irrigation water guidelines in Table 2 and dissolved metals have been compared to ecological water quality guidelines in Table 3. Total metals provide a more conservative estimate of exposure for livestock, whereas dissolved metals are used for ecological assessments as this is the bioavailable fraction of the metal (the part that is toxic to organisms).

Copper was above the guideline for slightly to moderately disturbed ecosystems in Cadiangullong Creek but was below the guideline at all other sites. All other metals were below guidelines at all sites.

Per- and polyfluoroalkyl substances (PFAS)

There are no PFAS guidelines for livestock drinking and irrigation water. Exceedances of the ecological guidelines are displayed below in Table 3 in bold. PFOS exceeded the guideline in the Belubula River, however was not detected in Cadiangullong Creek or Flyers Creek. PFOA was not detected in any of the samples.

Hydrocarbons

No hydrocarbons were detected in any samples.

Table 2 TDS, nutrient and metal (total acid-extractable) concentrations compared to the Australian Livestock Drinking Water Guidelines and the Australian Irrigation Guidelines (ANZECC & ARMCANZ 2000)

Parameter	**Guideline for livestock drinking water** mg/L	**Guideline for irrigation water (short-term use)** mg/L	**Site 1 Cadiangullong Creek** mg/L	**Site 2 Cadiangullong Creek** mg/L	**Site 3 Cadiangullong Creek** mg/L	**Site 4 Belubula River** mg/L	**Site 5 Belubula River** mg/L	**Site 6 Belubula River** mg/L	**Site 7 Flyers Creek** mg/L	**Site 8 Belubula River** mg/L	**Site 9 Belubula River** mg/L
TDS	0–2000*	-	75	310	470	490	490	490	510	500	360
Sulfate	1000	-	1	89	130	110	110	100	140	110	32
Nitrate	400	-	<0.9	<0.9	<0.9	<0.9	<0.9	<0.9	<0.9	<0.9	<0.9
Nitrite	30	-	<0.25	<0.25	<0.25	<0.25	<0.25	<0.25	<0.25	<0.25	<0.25
Total nitrogen	-	25–125	<0.1	0.2	0.1	0.3	0.3	0.4	0.1	0.3	0.3
Ammonia	-	-	<0.005	<0.005	<0.005	<0.005	<0.005	<0.005	<0.005	<0.005	<0.005
NOx as N	-	-	0.02	0.06	0.02	0.008	0.007	0.05	0.009	0.06	0.03
Total phosphorus		0.8–12	<0.05	<0.05	<0.05	<0.05	<0.05	<0.05	<0.05	<0.05	<0.05
Free reactive phosphorus	-	-	<0.05	0.06	<0.05	<0.05	<0.05	<0.05	<0.05	<0.05	<0.05
Metals											
Aluminium	5	20	0.08	0.02	<0.01	0.02	0.02	0.03	<0.01	0.01	0.07
Arsenic	0.5	2	<0.001	<0.001	<0.001	0.006	0.006	0.007	0.003	0.006	0.003
Copper	0.5**	5	<0.0005	0.0082	0.0021	0.001	0.0011	0.0011	0.0008	0.001	0.0011
Lead	0.1	5	<0.0001	<0.0001	<0.0001	<0.0001	<0.0001	<0.0001	<0.0001	<0.0001	<0.0001
Manganese	No value	10	0.12	0.043	0.015	0.024	0.027	0.028	0.012	0.021	0.081
Mercury	0.002	0.002	<0.00005	<0.00005	<0.00005	<0.00005	<0.00005	<0.00005	<0.00005	<0.00005	<0.00005

Parameter	Guideline for livestock drinking water mg/L	Guideline for irrigation water (short-term use) mg/L	Site 1 Cadiangullong Creek mg/L	Site 2 Cadiangullong Creek mg/L	Site 3 Cadiangullong Creek mg/L	Site 4 Belubula River mg/L	Site 5 Belubula River mg/L	Site 6 Belubula River mg/L	Site 7 Flyers Creek mg/L	Site 8 Belubula River mg/L	Site 9 Belubula River mg/L
Nickel	1	2	<0.0005	<0.0005	<0.0005	0.0005	0.0006	0.0007	<0.0005	0.0005	0.0007
Zinc	20	5	<0.001	<0.001	<0.001	<0.001	<0.001	<0.001	<0.001	<0.001	<0.001

* Value for poultry, other livestock tolerate higher TDS concentrations. Draft revised livestock drinking guidelines have TDS set to <500mg/L: this is exceeded in the Flyer's Creek site (sample 7).

**Guideline value for sheep. Value is higher for other typical types of livestock.

Table 3 Physicochemical water quality, nutrient and metal concentrations compared to ecological water quality guidelines (ANZG 2018, ANZECC & ARMCANZ 2000 and PFAS NEMP 2.0 2020)

Parameter	Ecological water quality guideline	Site 1 Cadiangullong Creek	Site 2 Cadiangullong Creek	Site 3 Cadiangullong Creek	Site 4 Belubula River	Site 5 Belubula River	Site 6 Belubula River	Site 7 Flyers Creek	Site 8 Belubula River	Site 9 Belubula River
Phys Chem										
Temperature (°C)	-	7.3	8.8	9.5	9.4	9.4	10.3	11.5	10.9	11.8
Dissolved oxygen (mg/L)	-	9.6	9.7	11.8	11.3	11.3	12.5	12.4	12.3	13.5
Conductivity (µS/cm)	30–350	55	333	**503**	**542**	**544**	**560**	**559**	**561**	**454**
pH	6.5–8.0	6.7	7.7	**8.4**	**8.5**	**8.5**	**8.5**	**8.7**	**8.6**	**8.8**
Turbidity (NTU)	25	8.8	1.6	0.3	1.0	1.3	**1.5**	**0.3**	**0.9**	**3.3**
Nutrients										
Total nitrogen (mg/L)	0.25	<0.1	0.2	0.1	**0.3**	**0.3**	**0.4**	0.1	**0.3**	**0.3**
Ammonia (mg/L)	0.013	<0.005	<0.005	<0.005	<0.005	<0.005	<0.005	<0.005	<0.005	<0.005
NOx as N (mg/L)	0.015	**0.02**	**0.06**	**0.02**	0.008	0.007	0.05	0.009	0.06	0.03

Parameter	Ecological water quality guideline	Site 1 Cadiangullong Creek	Site 2 Cadiangullong Creek	Site 3 Cadiangullong Creek	Site 4 Belubula River	Site 5 Belubula River	Site 6 Belubula River	Site 7 Flyers Creek	Site 8 Belubula River	Site 9 Belubula River
Total phosphorus (mg/L)	0.02	<0.05	<0.05	<0.05	<0.05	<0.05	<0.05	<0.05	<0.05	<0.05
Free reactive phosphorus (mg/L)	0.015	<0.05	**0.06**	<0.05	<0.05	<0.05	<0.05	<0.05	<0.05	<0.05
Metals										
Aluminium (mg/L)	0.055	0.02	<0.01	<0.01	<0.01	<0.01	<0.01	<0.01	<0.01	<0.01
Arsenic (mg/L)	0.013	<0.001	<0.001	<0.001	0.006	0.006	0.007	0.003	0.005	0.002
Copper (mg/L)	0.0014	<0.0005	**0.0038**	**0.0016**	0.0008	0.0008	0.0009	0.0006	0.0008	0.0008
Lead (mg/L)	0.0034	<0.0001	<0.0001	<0.0001	<0.0001	<0.0001	<0.0001	<0.0001	<0.0001	<0.0001
Manganese (mg/L)	1.9	0.13	0.039	0.013	0.016	0.015	0.017	0.009	0.013	0.041
Mercury (mg/L)	0.00006	<0.00005	<0.00005	<0.00005	<0.00005	<0.00005	<0.00005	<0.00005	<0.00005	<0.00005
Nickel (mg/L)	0.011	<0.0005	<0.0005	<0.0005	0.0006	0.0005	0.0007	<0.0005	0.0005	0.0007
Zinc (mg/L)	0.008	<0.001	<0.001	<0.001	<0.001	<0.001	<0.001	<0.001	<0.001	<0.001
PFAS										
PFOA (µg/L)	19	<0.01	<0.01	<0.01	<0.01	<0.01	<0.01	<0.01	<0.01	<0.01
PFOS (µg/L)	0.00023	<0.01	<0.01	<0.01	**0.02**	**0.02**	**0.03**	<0.01	**0.02**	**0.06**

References

ANZECC & ARMCANZ (2000), Australian and New Zealand Guidelines for Fresh and Marine Water Quality, Australian and New Zealand Environment and Conservation Council and Agriculture and Resource Management Council of Australia and New Zealand, Canberra.

ANZG (2018), Australian and New Zealand Guidelines for Fresh and Marine Water Quality, Australian and New Zealand Governments and Australian state and territory governments, Canberra ACT, Australia. Available at www.waterquality.gov.au/anz-guidelines

ANZG (2023), Livestock drinking water guidelines (draft). Australian and New Zealand Guidelines for Fresh and Marine Water Quality. Australian and New Zealand Governments and Australian state and territory governments, Canberra. Available at www.waterquality.gov.au/anz-guidelines/guideline-values/default/primary-industries/stock-water-guidance

PFAS NEMP 2.0 (2020), National Environmental Management Plan Version 2.0, Heads of EPA Australia and New Zealand. Available at https://www.dcceew.gov.au/environment/protection/publications/pfas-nemp-2

Environmental Research 225 (2023) 115518

Contents lists available at ScienceDirect

Environmental Research

journal homepage: www.elsevier.com/locate/envres

Spatio-temporal trends in livestock exposure to per- and polyfluoroalkyl substances (PFAS) inform risk assessment and management measures

Antti T. Mikkonen [a,b,*], Jennifer Martin [b,f], Richard N. Upton [a], Andrew O. Barker [c], Carolyn M. Brumley [b,f], Mark P. Taylor [b], Lorraine Mackenzie [a,d], Michael S. Roberts [a,e]

[a] University of South Australia, Clinical and Health Sciences, Adelaide, South Australia, Australia
[b] Environment Protection Authority Victoria, Centre for Applied Sciences, Macleod, Victoria, Australia
[c] Senversa L6, 15 William St, Melbourne, Victoria, Australia
[d] Basil Hetzel Institute for Translational Health Research, The Queen Elizabeth Hospital, Woodville South, South Australia, Australia
[e] University of Queensland, Diamantina Institute, Queensland, Australia
[f] Arcadis L18, Queen & Collins Tower, 376–390 Collins Street, Melbourne, VIC, Australia

ARTICLE INFO

Handling Editor: Jose L Domingo

Keywords:
Perfluorooctane sulfonate (PFOS)
Perfluorohexane sulfonate (PFHxS)
Livestock
Dynamic exposure
Risk assessment
Risk management

ABSTRACT

The migration of per- and polyfluoroalkyl substances (PFAS) onto agricultural properties has resulted in the accumulation of PFAS in livestock. The environmental determinants of PFAS accumulation in livestock from the grazing environment are poorly understood, resulting in limited capacity to manage livestock exposure and subsequent transfer of PFAS through the food chain. Analytical- (n = 978 samples of soil, water, pasture, and serum matrices), farm management/practice- and livestock physiology data were collated and interrogated from environmental PFAS investigations across ten farms, from four agro-ecological regions of Victoria (Australia). Statistical analysis identified perfluorooctane sulfonate (PFOS) and perfluorohexane sulfonate (PFHxS) as key analytes of concern for livestock bioaccumulation. PFOS and PFHxS concentrations in livestock drinking water were positively correlated with serum concentrations while other intake pathways (pasture and soil) had weaker correlations. Seasonal trends in PFAS body burden (serum concentrations) were identified and suggested to be linked to seasonal grazing behaviours and physiological water requirements. The data showed for the first time that livestock exposure to PFAS is dynamic and with relatively short elimination half-lives, there is opportunity for exposure management. Meat from cattle, grazed on PFAS impacted sites, may exceed health-based guideline values for PFAS, especially for markets with low limits (like the European Commission Maximum Limits or EC MLs). This study found that sites with mean livestock drinking water concentrations as low as 0.003 μg PFOS/L may exceed the EC ML for PFOS in cattle meat. Risk assessment can be used to prioritise site cleanup and development of management plans to reduce PFAS body burden by considering timing of stock rotation and/or supplementation of primary exposure sources.

1. Introduction

Per- and polyfluoroalkyl substances (PFAS) are a group of synthetic compounds manufactured since the early 1940s (Buck et al., 2011). They have been used extensively across different industries with hundreds of documented use categories for some 1400 compounds (Glüge et al., 2020). The migration of these compounds onto agricultural properties has resulted in their accumulation of in livestock (Death et al., 2021).

Although the grouping "PFAS" consists of a large number of individual chemicals with distinct physical and chemical properties, most of the information published on health effects pertain to legacy PFAS of the perfluoroalkyl carboxylate- (PFCAs) and perfluoroalkane sulfonate groups (PFSAs) which include perfluorooctanoic acid (PFOA) and perfluorooctane sulfonate (PFOS) respectively (Fenton et al., 2020; ATSDR, 2018; EFSA, 2020). PFOS and PFOA have been the focus of much research due to their prolific historical use, their ubiquitous presence in the environment and rapidly growing associations with health effects (Rogers et al., 2021). One key historical source of PFAS to the environment (especially PFOS) is aqueous film forming foams (AFFF) which have been widely used to contain and control Class B fires (OECD, 2021). Firefighting and training activities with AFFF products have

* Corresponding author. University of South Australia, Clinical and Health Sciences, Adelaide, South Australia, Australia.
E-mail address: antti.mikkonen@epa.vic.gov.au (A.T. Mikkonen).

https://doi.org/10.1016/j.envres.2023.115518
Received 7 September 2022; Received in revised form 26 January 2023; Accepted 15 February 2023
Available online 24 February 2023

Table 1
Summary of data sources and grouping.

Region ID[a]	Site ID	Distance to PFAS source (km)[b]	Environmental and biomonitoring PFAS data (# sampling rounds)						Primary DW source[d]	Stock rotation[e]
			Surface water[c]	Drinking trough	Soil	Grass	Cattle	Sheep		
A	A1	0.50	×	✓(4)	✓(1)	✓(1)	✓(3)	✓(1)	T[f]	Limited
	A2	1.30	✓(2)	×	✓(1)	✓(1)	✓(1)	✓(1)	SW	Extensive
	A3	0.05	✓(3)	×	✓(1)	✓(1)	×	✓(1)	SW	Limited
	A4	2.40	✓(1)	×	×	×	×	✓(1)	SW	Extensive
B	B1	0.07	✓(3)	×	×	✓(1)	✓(4)	✓(1)	SW	Limited
C	C1	2.00	✓(2)	×	✓(1)	×	✓(1)	✓(1)	SW	Moderate
	C2	6.00	✓(1)	✓(1)	✓(1)	×	✓(1)	✓(1)	SW + T	Extensive
	C3	0.05	✓(1)	✓(2)	✓(1)	×	✓(1)	✓(1)	SW + T	Extensive
	C4	onsite	✓(2)	✓(1)	✓(1)	✓(1)	✓(1)	×	SW + T	Moderate
D	D1	0.14	✓(2)	×	×	×	✓(1)	×	SW	Moderate

[a] Agro-ecological regions (Agriculture Victoria): A = Central Victorian Southern Slopes (temperate climate with mean annual rainfall 500–800 mm), B = Victorian Volcanic Plains (temperate climate with mean annual rainfall 500–700 mm), C = Eastern Plains (temperate climate with mean annual rainfall 550–1120 mm), D = Northern Plains (temperate climate with mean annual rainfall 350–550 mm).
[b] Distance from source site to livestock grazing areas in Km approximated using google maps (measure distance) (Google. Google Maps Victoria Australia, 1895).
[c] Surface water made up of dams, drainage ditches and areas of inundation.
[d] T = trough; SW = surface water; DW = drinking water.
[e] Stock rotation refers to the availability of uncontaminated grazing pasture and drinking water sources and rotation between these sources. “Limited” refers to sites without access to unimpacted pastures or drinking sources, “Moderate” refers to sites with access to several paddocks and drinking water sources with varying levels of PFAS and “Extensive” refers to sites with PFAS impacts confined to few paddocks/drinking water sources (≤25%) and/or a structured rotation practice that involves defined periods without exposure.
[f] Stock trough supplied from a surface water collection dam.

resulted in highly-concentrated and sometimes large-scale (volumes in tons) PFAS releases to the environment (Dorrance et al., 2017; Field et al., 2017; EHP, 2014). Due in part to poor controls for AFFF containment and the mobility and persistence of many of the PFAS (many are not susceptible to biotic or abiotic degradation beyond the dead-end perfluoroalkyl acid transformation products) contained in AFFF, these PFAS releases can lead to far-reaching dispersal from the point of contamination and transfer into plants and animals (Death et al., 2021; Bräunig et al., 2017; Dauchy et al., 2019).

As evidence of PFAS transfer from the environment to food has increased, so too has research and environmental investigations into understanding uptake of PFAS into livestock (Death et al., 2021; Bräunig et al., 2017; Kowalczyk et al., 2012; Kowalczyk et al., 2013; Vestergren et al., 2013; Cardno LanePiper, 2014; Parliament of Victoria, 2016; Zafeiraki et al., 2016; Senversa, 2018; Golder, 2020; Drew et al., 2021a). The transfer of PFAS to edible tissues and milk in livestock creates exposure pathways for their consumers (Death et al., 2021; Dauchy, 2019; Costello and Lee, 2020), and in some countries, impacted farms have been subject to risk based interventions (USDA, 2021).

In Victoria, Australia, the major sources of PFAS release which have resulted in site investigations, has been attributed to the use of AFFF in fire training and firefighting scenarios (based on the experience of the Environment Protection Authority, EPA Victoria). It is noted that other sources with potential to impact agriculture exist, however, sites associated with AFFF use have been more widely investigated in Victoria to date and are thus the focus of this paper.

Environmental assessment of AFFF sites across the State, have shown PFAS migration (from the points of release) to neighboring properties, including farm/grazing land, and PFAS have been reported in livestock as a result (Cardno LanePiper, 2014; Parliament of Victoria, 2016; Senversa, 2018; Golder, 2020).

In 2019–20, approximately 1.8 million adult cattle and 300,000 calves, 3.1 million adult sheep and 10.4 million lambs were processed in Victoria (Agriculture Victoria, 2021). Based on the number of known PFAS source sites with proximity to farming land, the number of animals thought to be impacted by PFAS is considered very low, and consequently exposure of the wider community to PFAS through meat produce is expected to be very low. These observations also reflect the findings of the 27th Australian Total Diet Survey which found that the levels of PFAS in the general food supply are low and acceptable from a public health and safety perspective (FSANZ, 2021). The survey found that out of a suite of 30 analytes, PFOS was the only congener detected and from a total of 112 commonly consumed foods and beverages, PFOS was only detectable in 5 foods (the highest level found in mammalian offal at 0.63 μg/kg) (FSANZ, 2021). While the risk to the general population is considered low, the exposure pattern and market share dilution relevant to the general population may result in an underestimate of exposure to population subgroups that may have higher exposure to PFAS contaminated produce, such as subsistence farmers (enHealth, 2012; U.S. Environmental Protection Agency, 2019).

In Australia, there are no regulatory maximum limits for PFAS in food, with the guidance being that PFAS levels should be kept as low as reasonably achievable (FSANZ, 2021). Health-based guideline values, expressed as tolerable daily intakes, have been derived for the sum of PFOS and PFHxS (20 ng/kg bw/d) and for PFOA (160 ng/kg bw/d) to enable risk assessments for PFAS exposed populations and these were used to develop food produce trigger points (TPs) for investigation at localized contaminated sites in 2016 (FSANZ, 2021). More recently the European Commission released an amendment of Regulation (EC) No 1881/2006 which provides maximum levels (MLs) for perfluoroalkyl substances in some specific food groups including livestock meat and offal (EC, 2022). It is noted there are no exceedances of the MLs for livestock meat or offal from the recent Australian Total Diet Survey (FSANZ, 2021) which reinforces that risk to the general population is considered low and the focus of this paper is on management of localized settings.

Internationally, human health risk assessments for PFAS in meat produce have typically relied on a combination of monitoring (serum) and livestock exposure modelling methods to estimate secondary exposure to consumers. Although several authors have described the uptake, distribution and elimination of PFAS in cattle (Van Asselt et al., 2013; Numata et al., 2014; Drew et al., 2021), exposure pathways and how they relate to the levels of environmental contamination are not well understood.

EPA Victoria has observed several settings in which static approaches to modelling livestock exposure and accumulation of PFAS in serum has resulted in significant over-estimation compared to measured serum concentrations, and in at least one case, underestimation. Challenges in estimating PFAS transfer from the environment to livestock can have subsequent implications for the quality of advice to farmers on the management of livestock exposure. This has led to increased interest in developing understanding of PFAS impacts on livestock farms in a

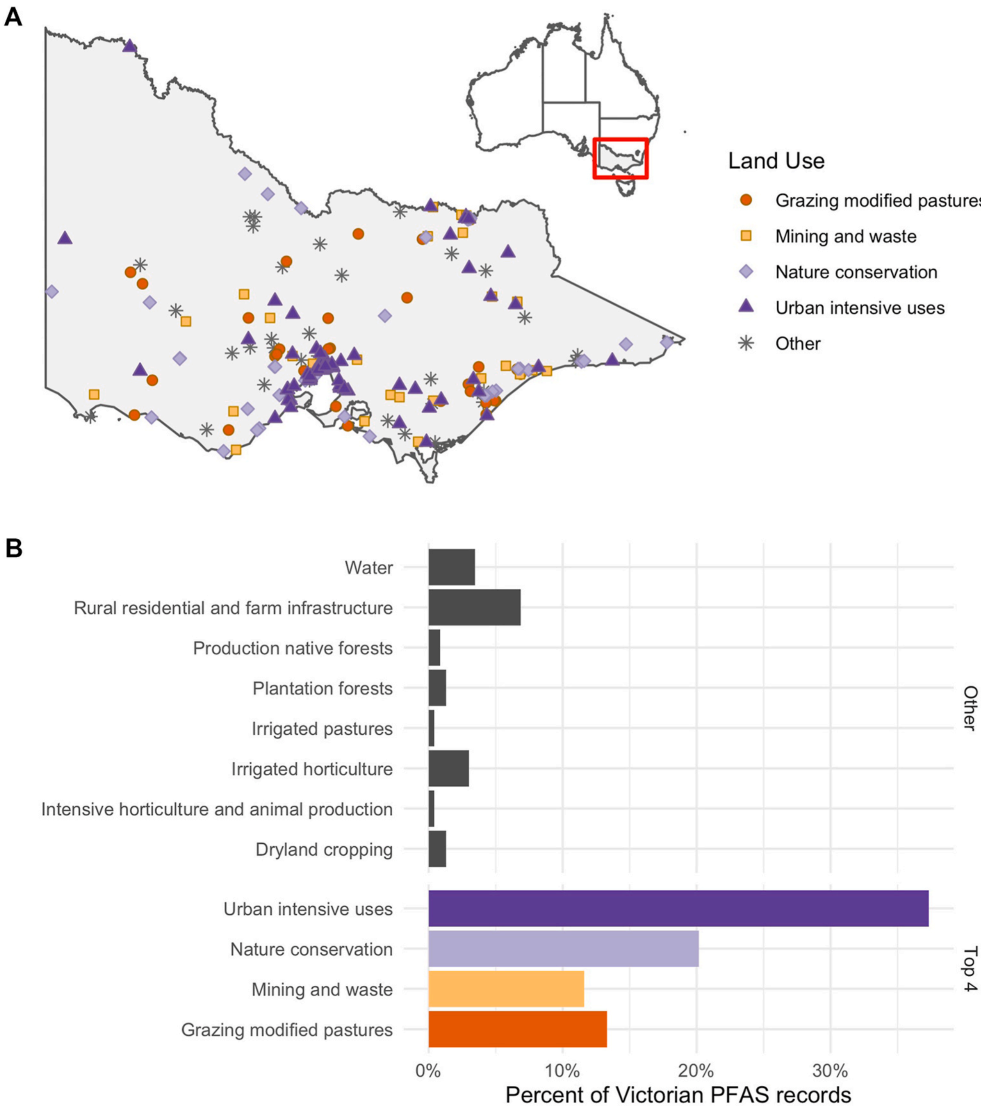

Fig. 1. Representation of known PFAS source sites and surrounding land uses in Victoria (Australia). A) Dots indicate approximate source site locations (Todd, 2021) with colours representing surrounding land-use based on open source datasets (Australian Bureau of Agricultural Resource Economics and Sciences (ABARES), 2021). B) Bar graph representation of surrounding land uses corresponding to each PFAS source site as a percentage of Victorian PFAS records.

wholistic way that can enable proportionate and practical advice to farmers on options to reduce PFAS body burden in their stock, support ongoing farming operations whilst also ensuring exposure to local and home-butchering consumers is kept as low as reasonably practical. The objectives of this study were.

(1) To evaluate which PFAS congeners are of most concern for bioaccumulation in livestock.
(2) To investigate livestock exposure pathways (for grazing livestock) and characterise the determinants of variability in livestock exposure to PFAS to aid risk assessment considerations.
(3) To assess if and how farming practices impact accumulation and what interventions can reduce the body burden of PFAS where livestock have been exposed.

To address these questions, data was compiled and analysed from environmental PFAS investigations undertaken at farms in Victoria, Australia. The anonymized dataset is available for download in supplementary materials. The farms are within four agro-ecological regions of Victoria (Australia) and include PFAS concentrations (for up to 28 analytes) in soil, water, pasture grasses and livestock serum for cattle and sheep, n = 978 all samples, Table 1.

2. Methods

2.1. Study methods

This study involved the following steps: (i) review of environmental investigation reports (for undisclosed agricultural sites) from the study areas to extract PFAS monitoring data for environmental media and livestock; (ii) collation, anonymisation and grouping of data within the study area; (iii) statistical assessment of PFAS concentrations; and (iv) regression analysis to determine the key PFAS exposure pathways for livestock (in the agricultural setting). The methods are further described in the following sections.

2.2. Study area

The study area encompassed PFAS impacted agricultural sites across Victoria, Australia. To keep sites confidential, Fig. 1 provides an overlay of known (reported in public forums) PFAS source sites in Victoria with agricultural land uses, however individual agricultural sites are not

Table 2
Summary of pooled analytical data.

Group[a]	Analyte	Acronym	Serum			Water			Soil			Grass		
			No[b]	Detect[c]	LOR[d]	No	Detect	LOR	No	Detect	LOR	No	Detect	LOR
		Units	#	%	ng/ml	#	%	ng/ml	#	%	ng/g	#	%	ng/g
PFSAs	Perfluorobutanesulfonic acid	PFBS	220	2.7	0.5–10	173	68.2	0.002–0.02	428	13.3	0.1–5	66	48.5	0.2–5
	Perfluoropentane sulfonic acid	PFPeS	117	3.4	1–10	147	69.4	0.002–0.02	315	11.1	0.1–5	57	35.1	0.2–1
	Perfluorohexane sulfonic acid	PFHxS	246	85	1–1	173	73.4	0.002–0.02	426	69.2	0.1–5	59	50.8	0.2–5
	Perfluoroheptane sulfonic acid	PFHpS	136	76	1–10	147	68	0.002–0.02	315	21.6	0.1–5	57	3.5	0–1
	Perfluorooctane sulfonic acid	PFOS	253	92.5	1–6	184	83.7	0.002–0.02	460	78	0.1–5	81	43.2	0.2–5
	Perfluorononane sulfonic acid	PFNS	117	0	1–10	127	11.8	0.0005–0.02	426	5.4	0.1–5	59	0	0.2–5
	Perfluorodecane sulfonic acid	PFDS	156	0	0.5–10	122	30.3	0.002–0.1	315	6	0.2–5	59	10.2	0–5
PFCAs	Perfluorobutanoic acid	PFBA	116	0	1–1	140	68.6	0.0005–0.02	317	18.9	0.1–5	59	42.4	0.2–5
	Perfluoropentanoic acid	PFPeA	145	0	1–10	173	67.1	0.002–0.02	428	36.7	0.1–5	81	38.3	0.2–20
	Perfluorohexanoic acid	PFHxA	184	0.5	0.5–10	143	73.4	0.002–0.02	428	26.6	0.1–5	81	16	0.2–10
	Perfluoroheptanoic acid	PFHpA	184	0.5	0.5–10	184	68.5	0.002–0.02	460	17.2	0.2–5	81	4.9	0.2–5
	Perfluorooctanoic acid	PFOA	184	0	0.5–50	146	51.4	0.0005–0.02	408	12.7	0.1–5	81	2.5	0.2–5
	Perfluorononanoic acid	PFNA	203	21.7	1–10	135	18.5	0.0005–0.05	408	4.2	0.1–5	81	0	0.2–5
	Perfluorodecanoic acid	PFDA	203	0	0.5–10	119	9.2	0.0005–0.05	408	1.7	0.1–5	81	0	0.2–5
	Perfluoroundecanoic acid	PFUnDA	184	0	0.5–10	119	8.4	0.0005–0.05	408	0.7	0.1–5	81	0	0.2–5
	Perfluorododecanoic acid	PFDoDA	184	0	0.5–10	119	8.4	0.0005–0.05	408	0.7	0.1–5	59	0	0.2–5
	Perfluorotridecanoic acid	PFTrDA	156	0	1–10	118	8.5	0.0005–0.5	408	0	0.1–5	59	0	0.5–5
	Perfluorotetradecanoic acid	PFTeDA	139	0	1–10	116	12.9	0.001–0.05	317	0.6	0.1–5	59	0	0.2–5
PFTSs	4:2 Fluorotelomer sulfonic acid	4:2 FTS	156	0	1–10	174	50.6	0.001–0.1	460	5.4	0.2–10	81	3.7	0.5–10
	6:2 Fluorotelomer sulfonic acid	6:2 FTS	184	0	1–20	122	9	0.001–0.5	324	2.5	0.1–5	66	0	0.5–5
	8:2 Fluorotelomer sulfonic acid	8:2 FTS	184	0	1–10	106	0	0.001–0.05	194	0	0.1–5	57	1.8	0.2–2
FASA	Perfluorooctane sulfonamide	PFOSA	156	0	0.5–10	121	21.5	0.0005–0.02	408	6.9	0.2–5	59	0	0.2–10
	N-Methyl perfluorooctane sulfonamide	N-MeFOSA	156	0	1–10	119	8.4	0.001–0.5	408	0	0.2–5	59	0	0.5–10
	N-Ethyl perfluorooctane sulfonamide	N-EtFOSA	110	0	1–10	106	0	0.0005–0.05	295	0.7	0.2–5	57	0	0–1
	N-Methyl perfluorooctane sulfonamidoacetic acid	N-MeFOSAA	156	0	1–10	117	8.5	0.001–0.5	406	0	0.2–5	57	5.3	0.5–2
	N-Ethyl perfluorooctane sulfonamidoacetic acid	N-EtFOSAA	156	0	1–10	119	8.4	0.001–0.05	347	0	0.2–5	59	0	0.5–10
	N-Methyl perfluorooctane sulfonamidoethanol	N-MeFOSE	156	0	1–10	121	1.7	0.0005–0.5	301	0.7	0.2–5	57	0	0.2–2
	N-Ethyl perfluorooctane sulfonamidoethanol	N-EtFOSE	156	0	1–10	119	8.4	0.001–0.5	406	0	0.2–5	57	0	0.5–2

[a] Analyte grouping: PFSAs = Perfluoroalkyl sulfonates, PFCAs = Perfluoroalkyl carboxylates, PFTSs = Fluorotelomer sulfonates, FASA = Perfluoroalkane sulfonamides and perfluoroalkane sulfonamido substances.
[b] No = number (#) of samples refers to the total number of results reported (>LOR and <LOR).
[c] Detect (%) refers to number of results above the LOR.
[d] LOR column displays the range in reported LORs for each analyte.

identified. All sites were impacted due to migration of PFAS from soils and water bodies at source sites through surface water migration and, surface run-off and erosion of sediments, into farm dams and water ways used to support stockwater. No farms in the study applied biosolids or used PFAS impacted water for irrigation of pasture.

2.3. Data collation

Ten agricultural sites with existing investigation reports that covered a number of land uses were identified from environmental investigations. These reports are available on EPA Victoria's website under environmental audits online tool and on the Australian Department of Defence website. Data were anonymized and collated. Victoria has varied agro-ecological zones (AEZ) with differing climate and agricultural systems (Williams et al., 2002) which can lead to differences in livestock rearing conditions and practices. As such, the sites were grouped by AEZ (A-D) and proximity to contaminant source sites. Table 1 provides an overview of data availability, grouping and livestock rearing practices relevant to contaminant exposure on livestock farms. The livestock in this assessment, were grazed on primarily non-irrigated and non-biosolids amended pastures. This meant that stockwater was the primary exposure pathway for livestock, with smaller contributions from soil and pasture, particularly in areas prone to inundation. At some sites livestock had access to drainage ditches, dams, and areas of inundation with vegetation, which made up varying proportions of accessible grazing land. Stock rotation was also considered, as this practice may provide information on the duration and continuity of exposure. Stock rotation potential was noted based on the availability of uncontaminated pasture and water resources within the operation (from limited to extensive), with only one farm with a structured rotation practice.

Data were collated from individual monitoring reports (for each site and sometimes over multiple monitoring periods) spanning approximately 5 years. All analytical work was undertaken by commercial laboratories with acceptable quality assurance and control measures (analysis of surrogate and matrix spike recoveries, blanks and duplicates provided with each analytical report). Throughout this period there were advances in analytical methods, changes in the limits of reporting (LOR) and chemicals added to the analytical suites. As such the number analytes monitored varies between reports as do LORs (LOR ranges provided). It is noted that there are significant differences in LORs for different matrices which reflect differences in guidelines for these matrices as well as difficulties with achieving ultra-low level reporting limits.

Differences in analytical and analyte extraction methods from different matrices exist between different laboratories, however, a proficiency study (NMI, 2018) demonstrated an acceptable interlaboratory consensus for results measuring spiked PFAS concentrations from soil, water and biological samples. In the proficiency study, laboratory performance (accuracy) was compared using standard (z) scores (how

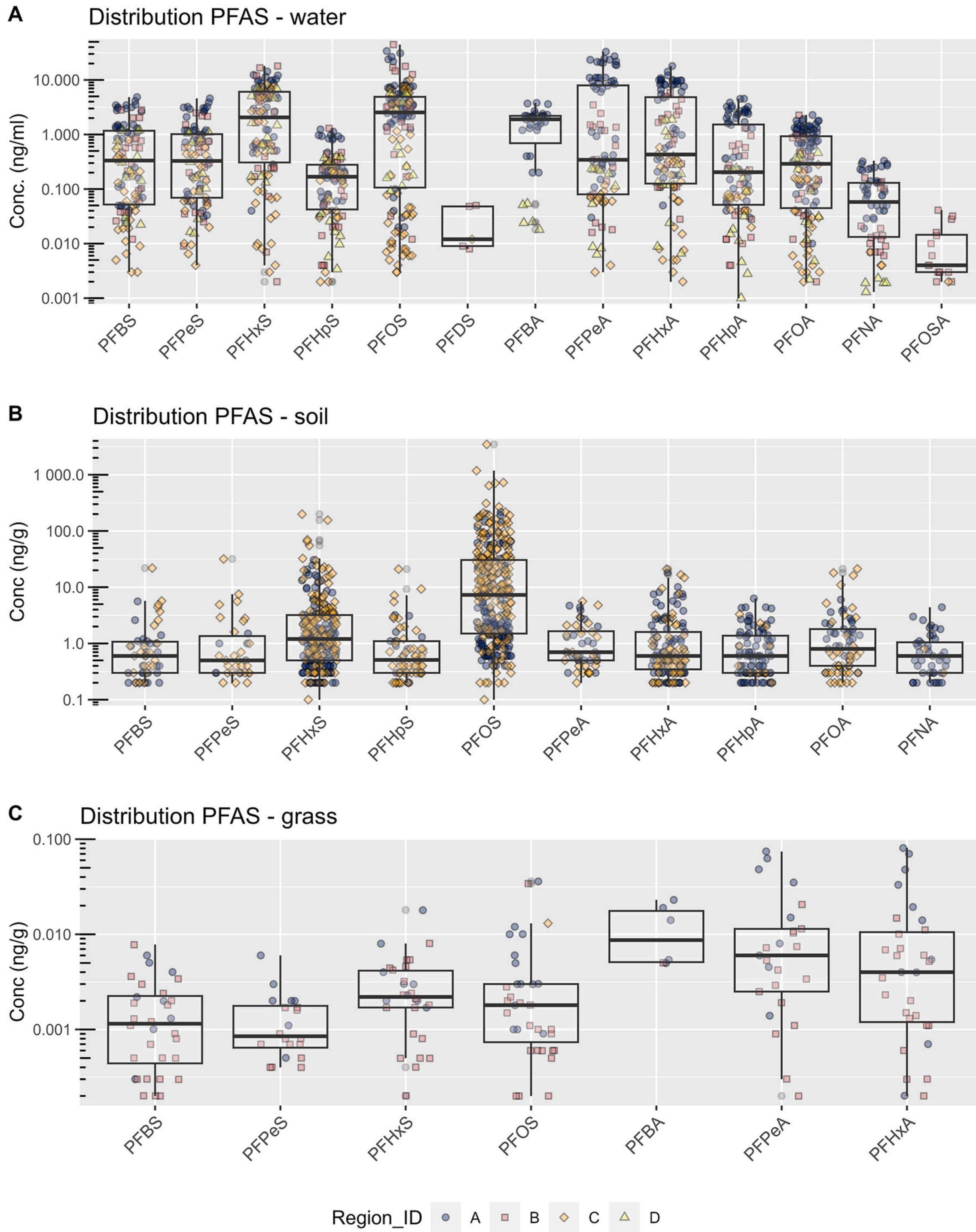

Fig. 2. Box plots (ggplot2 package in R) displaying environmental PFAS distribution in A: water; B: soil; C: pasture grasses for pooled data from 10 PFAS impacted sites across 4 agro-ecological regions in Victoria (A–D).

much the result differs from the assigned value) and En-scores (how closely the result agrees with the assigned value with consideration of uncertainty) which showed that 82% of the results were satisfactory allowing the data to be pooled (NMI, 2018).

The pooled dataset is comprised of a total of 142 cattle serum samples (from a mix of beef cattle breeds, age, and sex), 111 sheep serum samples (from a mix of breeds, age, and sex), 184 water samples (from dams, drainage ditches and areas of inundation and stock troughs), 81 pasture samples and 460 soil samples. It is noted that at most sites targeted environmental sampling was undertaken as the sites were too large for gridded random sampling; and the sampling was typically targeted to areas which livestock accessed. An overview of pooled analytical data, rates of detection and LOR ranges reported for each medium are shown in Table 2.

All analytes are reported as the sum (or total) of its isomers (i.e. sum of linear and branched isomers for each PFAS). Individual isomer reporting is not common in environmental site assessment reports as the individual isomers do not have any bearing on regulation, the perceived risk or how a site may be managed.

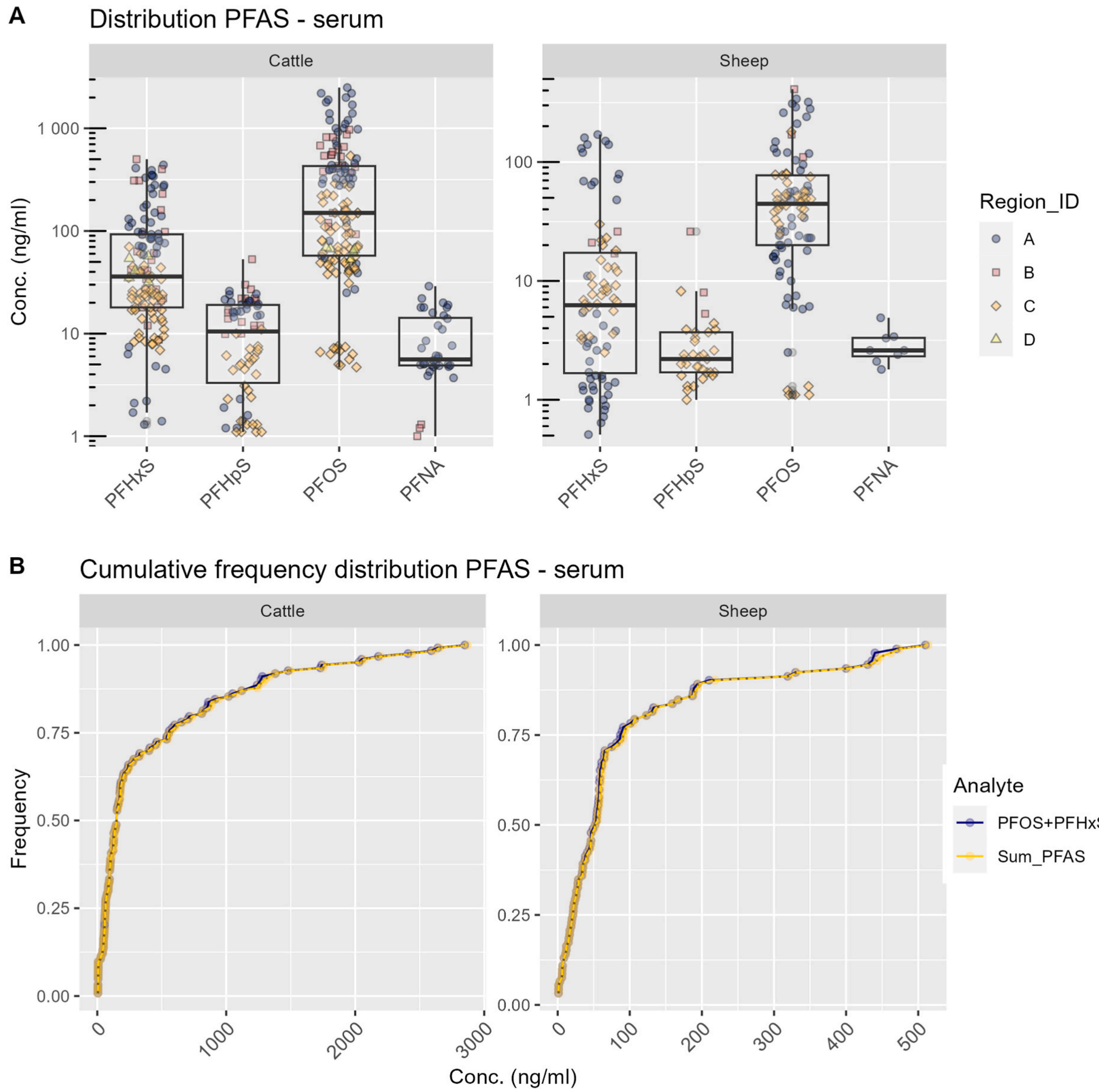

Fig. 3. PFAS distributions plotted (ggplot2 package) for cattle and sheep serum samples. A) Serum PFAS distribution shown for analytes detected in >10% of pooled samples; B) Cumulative frequency distributions shown for total PFAS and the sum of PFOS + PFHxS indicating that the predominant composition of total PFAS was made up of PFOS + PFHxS in both cattle and sheep.

2.4. Data analysis

Censored (or non-detect) results were managed using a substitution method which replaced censored results with a value equal to half-the-limit of reporting (LOR x 0.5). Based on previous studies, this substitution method is comparable to or more accurate than alternative censored data management methods when describing environmental data (Mikkonen et al., 2018). Spearman rank coefficients were then used (psych package (Revelle, 2021)) to test the strength of possible correlations between PFAS concentrations (median) in different environmental matrices and serum samples from each site.

For matrices that showed significant correlations ($p < 0.01$) sample pairing was undertaken to generate relevant spatio-temporal datasets for regression analysis. Surface water PFAS concentrations may be influenced by a number of variables and show temporal variability (Gallen et al., 2014; Lanza et al., 2017; Abunada et al., 2020). As such median annual PFAS concentrations in stock water were paired with median annual serum samples (for the same sampling year). In addition, the dataset used for regression analysis only included cattle with a minimum of 12 months exposure and sheep with a minimum of 6 months exposure (measured as time on-site and based on elimination half-lives for PFOS) to avoid biasing the dataset with serum levels resulting from short-term exposures. PFOS half-lives have been reported to vary depending on the physiological status of the animal and range between 74 and 120 days for cattle (Lupton et al., 2015; Drew et al., 2021b) and 17–74 days for sheep (Hagen et al., 2019). We determined that steady state could be achieved after regular exposure for more than four half-lives which is approximately 12–18 months for cattle (Ito, 2011; Gupta, 2016) and 1–6 months for sheep (Hagen et al., 2019).

The Shapiro-Wilk test, used to check for data distribution normality, indicated that serum PFAS concentrations were skewed to the right so the data were log transformed (log base 10) prior to performing linear regression analyses (ggplot2 (Wickham, 2016)). All analyses were conducted in R Core Team. R, 2019.

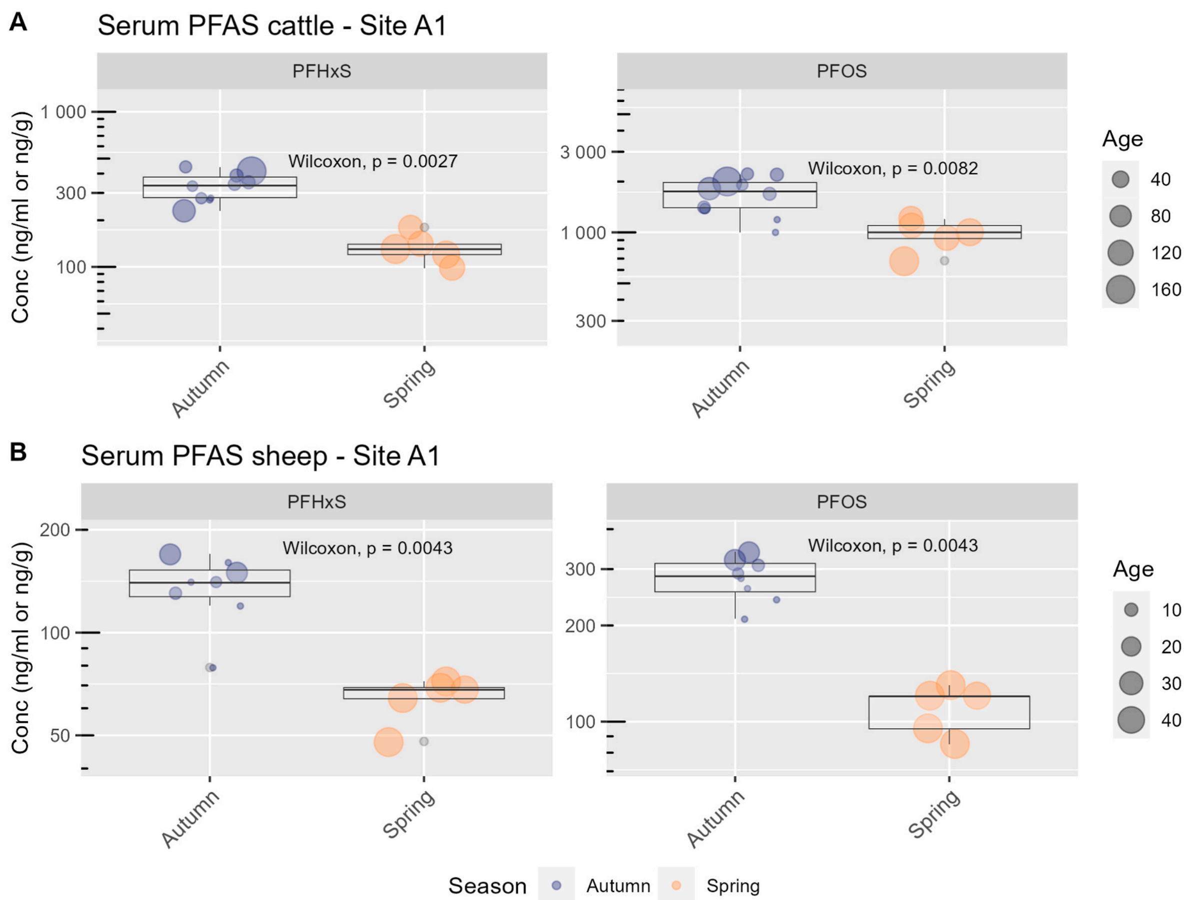

Fig. 4. Boxplots displaying seasonal distribution (ggplot2) of serum PFHxS and PFOS at Site A1 for A) cattle; and B) sheep. Size of the marker conveys age of the animals in months and the Wilcoxon signed-rank test was used to compare the serum concentration means.

3. Results and discussion

3.1. PFAS distribution

The number of PFAS compounds detected (at a rate >10% of samples) were greatest in water samples (16), > soil (10), > pasture (8) and > serum (4). The higher detection rate for PFAS in water is likely influenced by having significantly lower reporting limits while soil, grass and serum had comparable reporting limits. Four-to eight-carbon perfluoroalkyl sulfonates (PFSAs) and -carboxylates (PFCAs) were detected most frequently across environmental media (pasture-, water-, and soil samples) while detections for fluorotelomer sulfonates (PFTSs) and perfluoroalkane sulfonamides and perfluoroalkane sulfonamido substances (FASAs) were most commonly detected in water samples. The predominantly detected compounds (from each group PFSA, PFCA, PFTS and FASA) are consistent with our understanding from the environmental investigations and site histories therein, with AFFF being the primary source. Although the composition of PFAS within historic AFFF formulations varies (depending on manufacturer and the year of manufacture), a significant percentage of these products were made up of PFOS and related perfluoroalkyl sulfonates (PFSAs) like PFHxS (Field et al., 2017; Leeson et al., 2021). Another class of compounds used extensively in AFFF formulations were polyfluorinated fluorotelomer thioamido sulfonates (otherwise known as FtTAoS or the trade name Lodyne) which can be biodegraded (under aerobic conditions) to PFTSs and PFCAs (Field et al., 2017; Yi et al., 2018). Of the FASA compounds only PFOSA was detected at a rate >10% (in any media tested), which may also be found in AFFF foams (Harding-Marjanovic et al., 2016) and is a PFOS precursor (i.e. has potential to biotransform to PFOS (Mejia Avendaño and Liu, 2015; Kowalczyk et al., 2020)).

Individual PFAS from each group typically increased relative to one another with respect to region and matrix; for example, the presence of PFOS typically correlated with the presence of other sulfonate group compounds for a given matrix and region. PFAS concentrations (median) in water and soil showed similar trends with elevated PFTSs and PFSAs in comparison to PFCAs while this trend was reversed in pasture grasses, possibly due to biotransformation processes reported elsewhere (Costello and Lee, 2020; Zhao et al., 2019) and/or the PFAS physicochemical characteristics (like chain length, head group functionality and water solubility) affecting transfer from soil to plants (Wang et al., 2020). Overall soil and pasture grass PFAS concentrations showed high variability which is thought to be due to PFAS migration being driven by surface water flow and variation in sampling programs from site to site (Cardno LanePiper, 2014; Senversa, 2018; Golder, 2020). In most cases the highest soil and pasture PFAS concentrations were found along drainage lines, areas of inundation or proximity to surface water. Fig. 2 provides a summary of environmental PFAS distributions observed for each region (for analytes detected at a rate >10% of samples).

The number of PFAS compounds reported above detection limits in livestock serum was lower than the number detected in environmental samples. In environmental samples (water, soil, pasture grass), 27 of the 28 analytes were detected whereas in serum only 8 analytes were detected (Table 2). This is partly due to differences in LORs and partly due to toxicokinetic factors like excretion rate (or half-life). Where a compound is present in environmental media at a concentration below the serum LOR it will only be detected in serum when the excretion rate < intake rate. This has also been observed in other livestock studies where concentrations of perflouoroalkyl carboxylic acids and

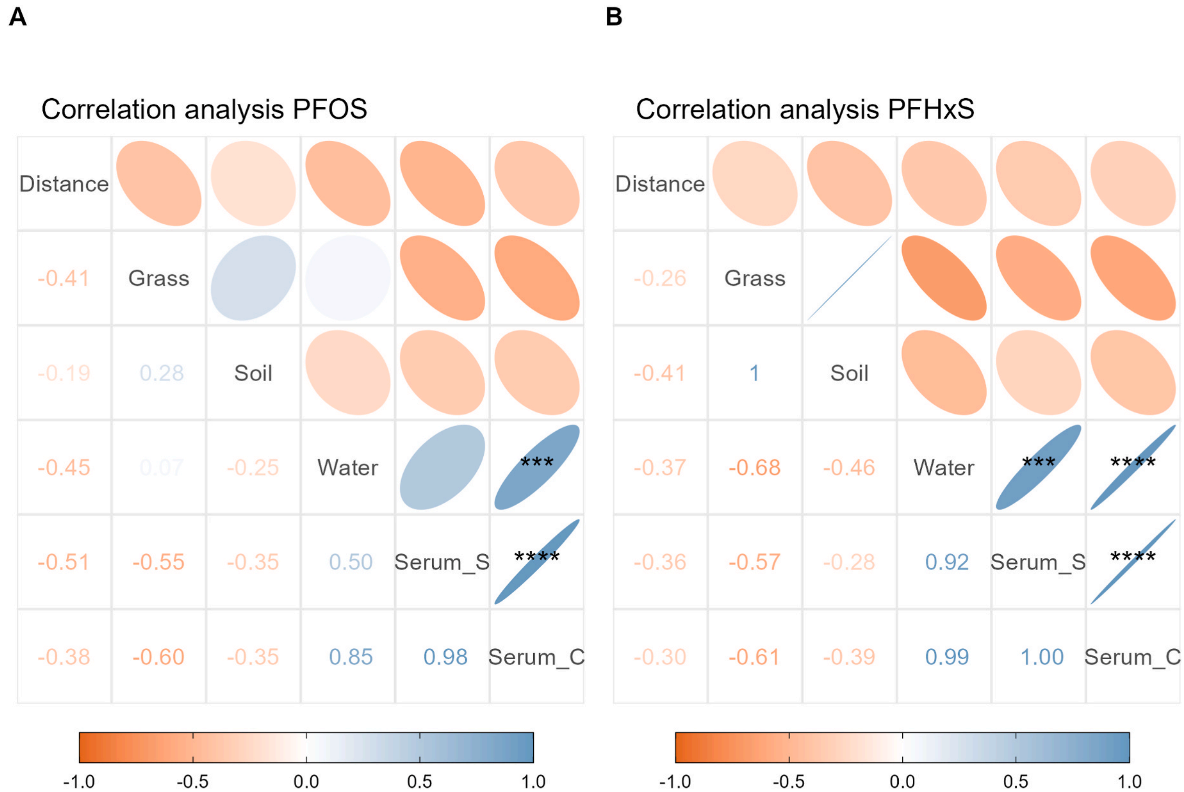

Fig. 5. Correlation analysis (using psych and ggplot2 packages) showing associations between environmental- and serum levels for A) PFOS; and B) PFHxS. The shape, angle and color signify the type (positive = blue, 45°; negative = orange, 135°) and strength of association, with flat elliptoid shape and intensity of color representing a strong correlation (R^2 values displayed on bottom half of plot). Significance denoted by * (* for $p < 0.1$, **for $p < 0.05$, *** for $p < 0.01$ and **** for $p < 0.001$). Serum_S denotes sheep serum samples and Serum_C denotes cattle serum.

perfluoroalkyl sulfonic acids with four or less carbons, were either not detected or detected in very low concentrations (Kowalczyk et al., 2013; Lupton et al., 2022). It is thus likely other PFAS are present in serum (to reflect intake media) however at levels < LOR in this case. Although fewer PFAS were found in serum, they were present more consistently with an overall detection rate >90% of samples (in sheep and cattle combined and 100% in cattle alone). PFASs are known to bioaccumulate to varying degrees (i.e. bioaccumulation increases with the carbon chain length (Xu, 2020) and similar trends have been reported previously for livestock exposed to contaminated feed or water sources (Bräunig et al., 2017; Kowalczyk et al., 2012; Drew et al., 2021a; Van Asselt et al., 2013). Four of the PFAS detected in serum (PFHxS, PFHpS, PFOS and PFNA) had levels higher than those reported in corresponding environmental samples. As shown in Fig. 3 (Panel B), on average PFOS and PFHxS made up >98% of total PFAS detected in serum and as such the lines appear overlaid. Further PFOS was found to account for on average > 70% of the total PFAS detected. PFNA was the only carboxylate compound found in serum while PFTS and FASA were not observed in any animal. This is despite higher overall concentrations of PFAS such as 6:2FTS, PFHxA, PFPeA compared to PFOS and PFHxS in water, indicating elimination half-lives are a driver behind the type and concentration of PFAS detected in serum, rather than the concentration in water itself. Although the precursor PFOSA was not detected in serum, it is considered unlikely that it would have been metabolized and contribute significantly to serum PFOS levels due to low environmental concentrations. Fig. 3 provides an overview of PFAS distribution in serum of cattle and sheep for analytes with >10% detection rate across pooled samples.

Livestock serum levels may also be influenced by season. Fig. 4 presents box plots of serum PFOS and PFHxS levels based on the time of year samples were collected (spring and autumn). The box plots are limited to one site as only site A1 had multiple rounds of serum collected at different times of the year for livestock comprising 52 serum samples total. After the second round of sampling mitigation measures were taken and as such the third round of samples are not comparable which left two years of (single point in time) serum results for cattle aged >6 months (n = 6 for spring and 10 autumn) and two years serum results for sheep aged >6 months (n = 6 spring) and n = 8 autumn)).

Fig. 4 shows that serum concentrations for PFOS and PFHxS, in both cattle and sheep, were significantly higher in autumn than in spring (approximately 6 months apart). Although the dataset is limited, this is not an unexpected result due to livestock consumption patterns. Previous publications have shown that as pasture moisture levels decrease throughout summer and autumn, livestock require more water to meet their daily water requirements (NRC, 2000; Lukas et al., 2008; Olkowski, 2009), which in turn increases the PFAS intake of the animals when the available stock water is contaminated with PFAS. Conversely, in winter and spring, when pasture moisture levels are typically higher, livestock require less drinking water often reaching very low to negligible water intake (NRC, 2000; Lukas et al., 2008) and subsequently serum levels are correspondingly lower as elimination rate exceeds intake during this time. Seasonal differences appear more pronounced in sheep likely due to the comparatively shorter half-lives and their capacity to meet daily water requirements from green pasture alone (NSW DPI, 2014).

3.2. *Correlation analysis*

Considering PFOS and PFHxS account for >98% of PFAS body burden in cattle and sheep, correlation analysis was undertaken for these compounds only. Fig. 5 provides a summary of associations between median environmental PFOS and PFHxS concentrations and serum concentrations.

The correlation plots showed a strong positive correlation between

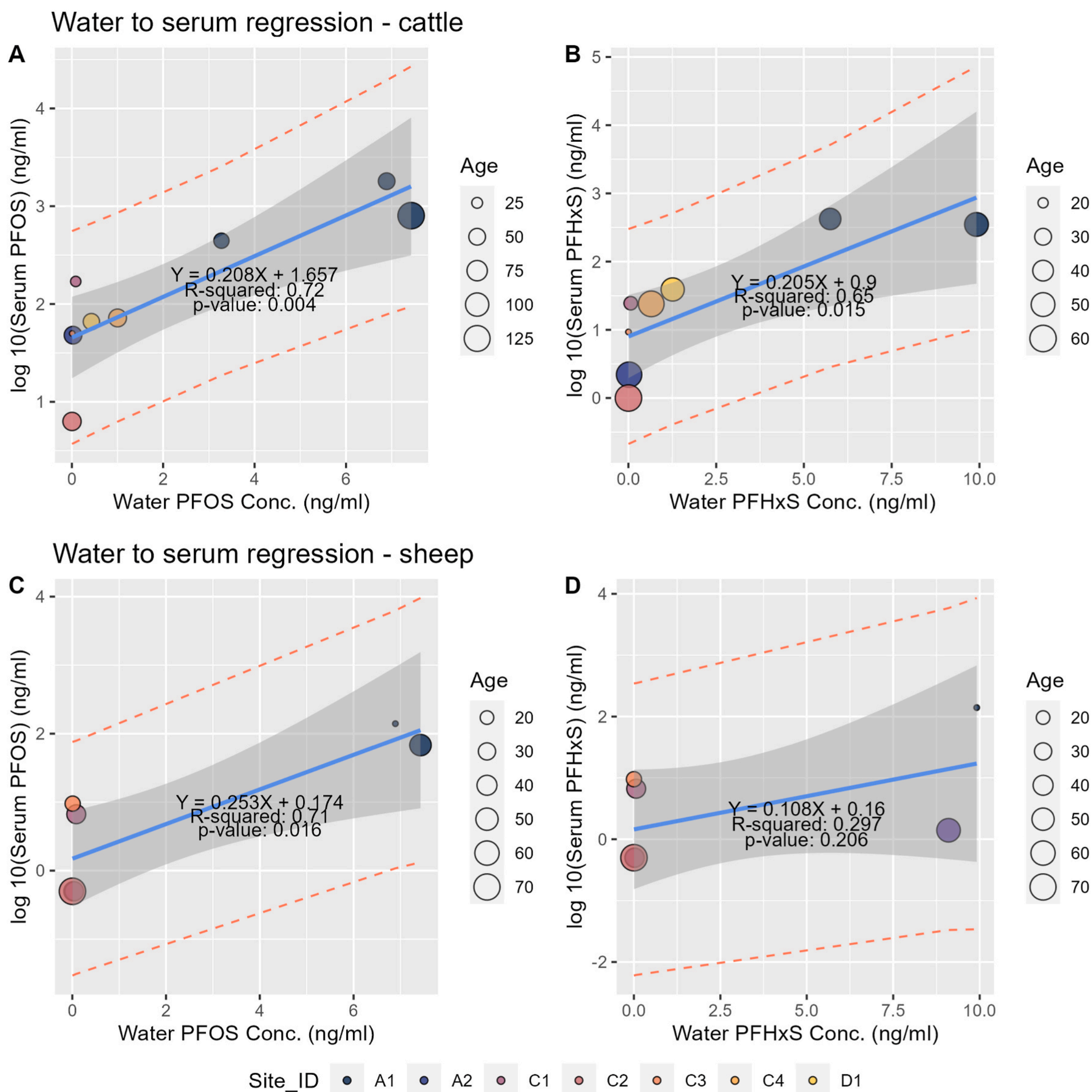

Fig. 6. Summary of PFAS-water to PFAS-serum regression analysis (plotted using ggplot2) for A) PFOS and B) PFHxS in cattle and C) PFOS and D) PFHxS in sheep. 95% confidence intervals (CI) presented using grey shading and the prediction intervals (for future observations) shown using dashed red lines. Size of the marker conveys median age of the animals in months. Statistical summary included in figure provides the slope, R^2 and p-value for the regression line.

water and serum PFHxS concentrations for both cattle (R^2 0.99, $p < 0.001$) and sheep (R^2 0.92, $p < 0.01$) and a moderately strong positive correlation for PFOS between water and cattle (R^2 0.85, $p < 0.01$). While sheep serum and water did show a positive correlation for PFOS this was not statistically significant. Interestingly serum PFOS and PFHxS concentrations showed an inverse correlation with pasture grass and soil concentrations. This is likely because the contributions of PFOS and PFHxS from soil and grass, when drinking water is elevated, are relatively small. Similar conclusions, regarding the relative exposure contributions, were made in a recent publication in which water to serum (cattle and sheep) transfer factors were estimated for PFAS (Drew et al., 2021a).

3.3. Regression analysis

Regression analysis was performed to investigate whether environmental data, gathered from multiple sites (with differing levels of contamination), could provide an adequate regression relationship for the extrapolation of serum concentrations for a given water concentration. Fig. 6 summarises the PFAS-water to PFAS-serum regression results for cattle and sheep.

Overall, the water to serum regression plots for cattle and sheep indicate a positive relationship between increasing serum- and stock water concentrations for both PFOS and PFHxS. Based on the R-squared values, the goodness-of-fit was better for PFOS, and the p-values indicate that the relationships are significant (assuming a 0.05 significance level) in cattle for both PFOS and PFHxS, and for PFOS in sheep. The 95% confidence intervals are wider for sheep, likely to be influenced by the relatively small number of paired water-serum samples as well as the range in serum concentrations observed, especially for PFHxS. In general, the regression relationships and reported concentrations indicate that PFOS and PFHxS bioaccumulation (from water) is lower in sheep than in cattle. This result is not unexpected, given the differences in half-lives between sheep and cattle and perhaps also their water consumption patterns. At very low PFAS water concentrations serum predictions are less reliable due to the influence of other pathways like soil and pasture intake that may contribute more to total exposure as exposure from water decreases. The reported regression relationships may also differ for sites with historical biosolids application/irrigation which could lead to accumulation of PFAS in soils and pastures and therefore

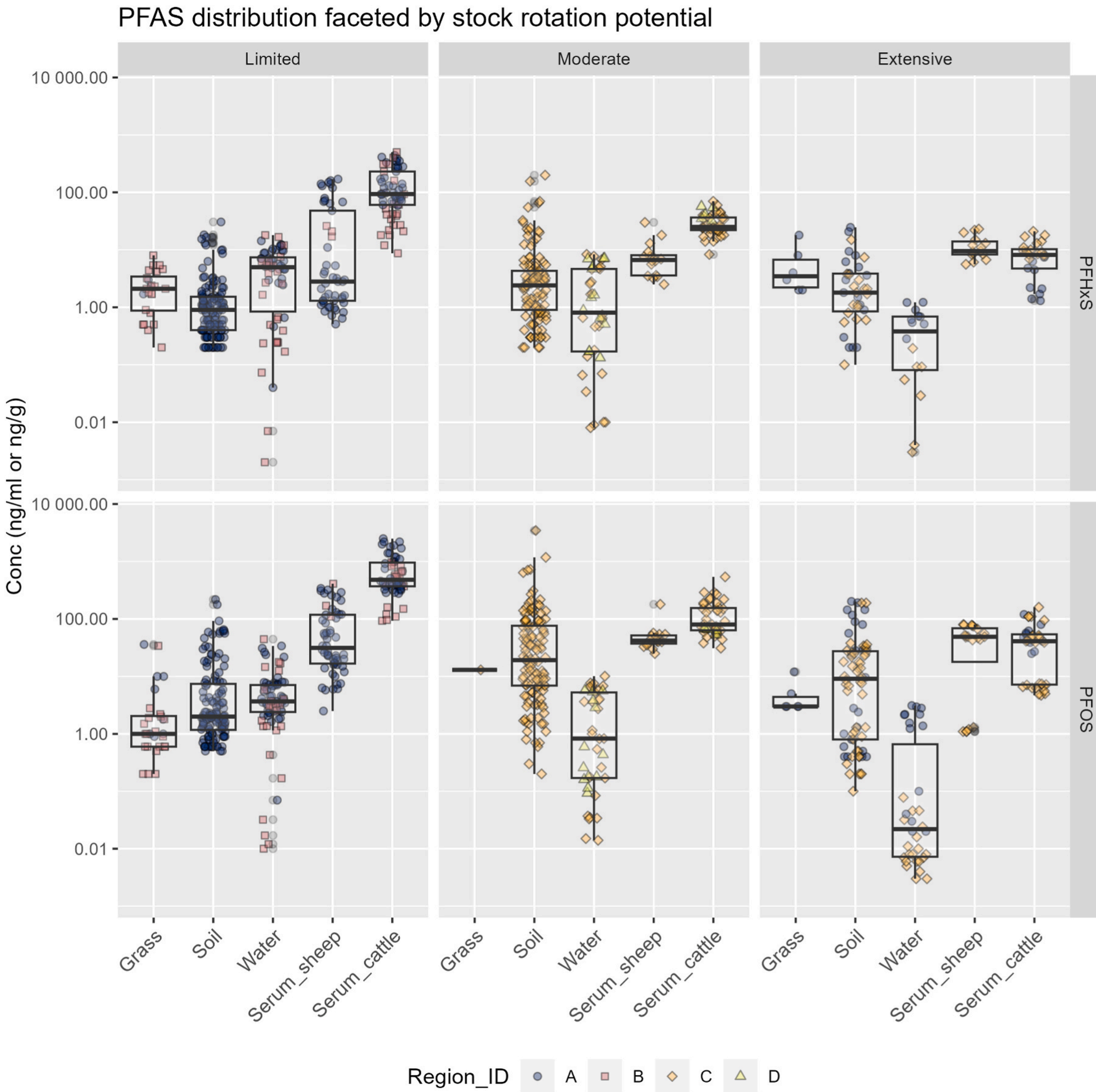

Fig. 7. Boxplots displaying concentration distribution of PFHxS and PFOS in the environment and livestock serum for all sites (faceted by limited, moderate or extensive stock rotation potential).

higher relative contributions. It is also possible that these regression relationships may not be relevant to sites with elevated concentrations of PFOS precursors where precursor biotransformation could lead to higher serum levels of PFOS than otherwise expected (Martin et al., 2010; Glaser et al., 2021).

3.4. Observations on variable livestock exposure

Understanding exposure pathways and trends can provide insights for risk assessment and livestock management. Based on this work, the primary exposure pathway for grazing livestock downgradient from AFFF contaminated sites (on pastures without history of biosolids treatment or irrigation with contaminated water) has been stock water. The role of stock rotation on accumulation of PFAS was assessed by comparing environmental and serum data from farms with “limited,” “moderate” or “extensive” stock rotation potential. Stock rotation refers to the availability of uncontaminated grazing pasture and drinking water sources and rotation between these sources. Sites with “Limited” stock rotation opportunities comprised farms with no unimpacted pasture or drinking sources. Sites with “Moderate” stock rotation opportunities were those with access to several paddocks and drinking water sources with varying levels of PFAS. Sites with “Extensive” stock rotation potential were those where PFAS impacts were confined to a few paddocks/drinking water sources ($\leq$25%) and/or a structured rotation practice was in place that involved defined periods without exposure. Fig. 7 provides a summary of environmental and livestock PFAS distributions based on the level of stock rotation potential identified for each site.

Sites with limited stock rotation (or access to unimpacted water or pasture sources) typically had higher sample densities around the median for water than those with higher stock rotation potential which may be due to limited sources. In general, soil samples showed wider distribution ranges (spanning up to three orders of magnitude for PFHxS and four orders of magnitude for PFOS) than water which may be due to the heterogeneous nature of the contaminant distribution in soil (Zhang et al., 2019). As noted previously soil concentrations appear to have less influence, relative to water, on livestock serum levels. Overall, increasing stock rotation or availability of alternate water sources resulted in lower serum PFOS and PFHxS levels in both cattle and sheep. It was also observed that livestock distance from the source site does not correlate strongly with PFAS serum levels and may not be a good indicator of risk. This may be because overland flows (and their solutes and

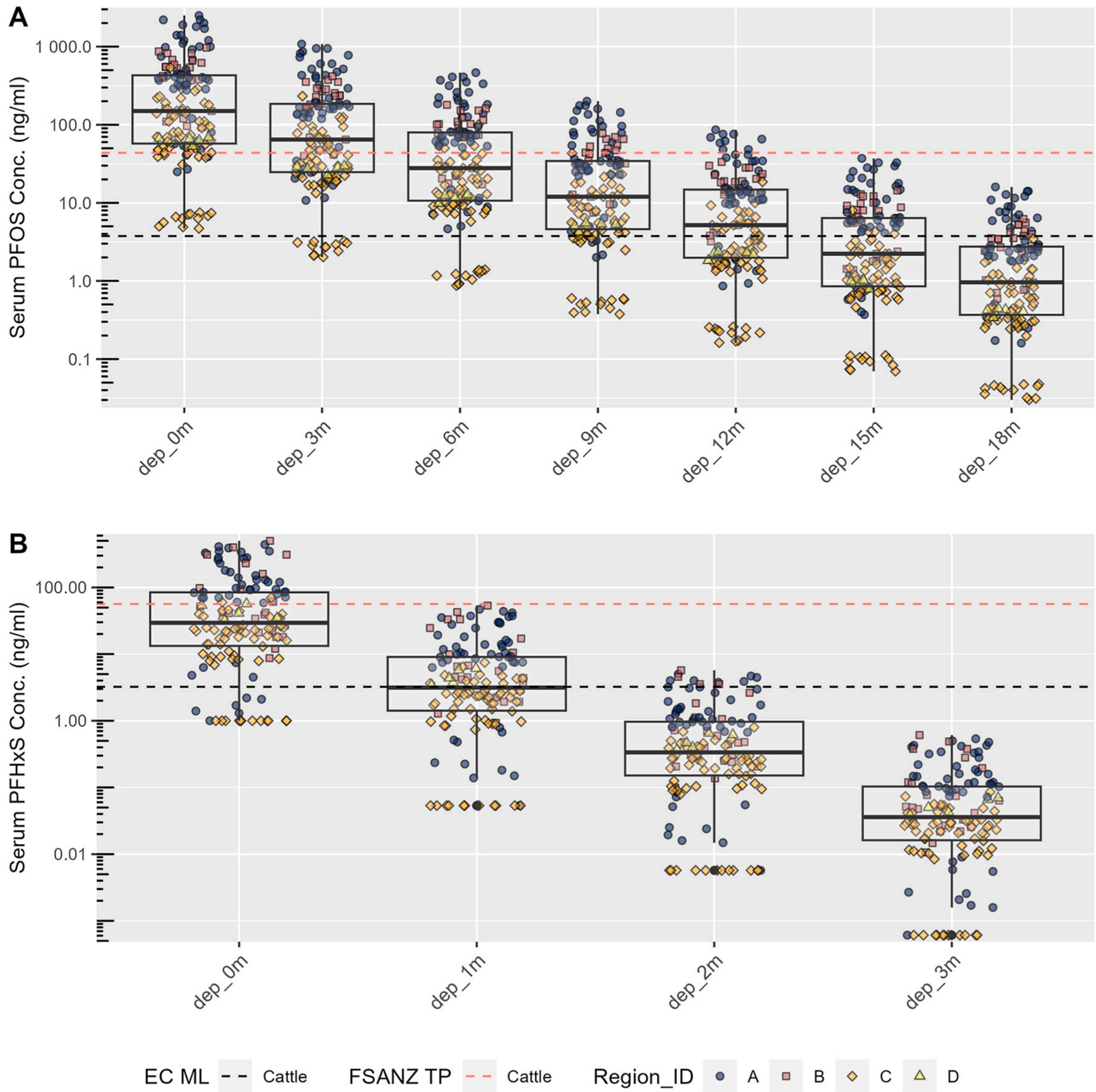

Fig. 8. Boxplots displaying measured and modelled serum A) PFOS; and B) PFHxS levels in cattle from PFAS impacted sites compared to acceptable serum concentrations over time. Time zero (dep_0 m) are measured serum concentrations and dep_1 m – dep_18 m are modelled serum estimates for cattle where exposure to PFAS has been prevented and depuration is occurring.

or suspended particle load) tend to follow topographic gradients or drainage lines (Hu et al., 2020) and proximity to the source is not related to how farm operations capture overland runoff and to what extent it may be utilised for livestock drinking. As such the availability of alternative water sources or stock rotation potential may be a more important determinant of body burden (serum conc.) than distance to a source site.

3.5. *Implications for risk assessment and livestock management*

A key outcome demonstrated by the analyses conducted within this study is that farm practices can have a significant influence on the level and extent of PFAS accumulation and may also support exposure reduction. To that end farm information coupled with environmental investigation data for PFAS, can provide a greater understanding of the need and level of detail required for risk assessment and management. While several PFAS may be identified in environmental media, the number and concentration of PFAS identified in livestock was significantly lower. While detection limits may preclude identification of certain PFAS (i.e. very low environmental concentrations and/or short half-life), they are unlikely to contribute significantly to the risk assessment or management measures for a contaminated site (given that the LORs are below relevant health-based criteria). The importance of livestock management is highlighted in Fig. 8 which provides a comparison of livestock serum levels from impacted sites to health-based criteria in the form of acceptable (or target) serum concentrations estimated based on the FSANZ TPs and the EC MLs over a depuration timeframe of 18 months (where dep_0 m is time zero). Depuration or clearance was modelled using an exponential decay function (Eq (1).) where C is the concentration at a given time, C0 is the concentration at time zero, Ke is the elimination rate (ln (2)/half-life) and t is time. The half-lives (PFOS 74 days; PFHxS 9.4 days) used in the decay estimates are based on cattle field trials conducted in Australia (Drew et al., 2021b, 2021c).

$$C\left(\frac{ng}{ml}\right) = C_0\left(\frac{ng}{ml}\right) \times \exp\hat{(}-Ke\left(d^{-1}\right) \times t(d)) \tag{1}$$

The acceptable serum concentrations were determined by converting tissue levels to serum levels using partition coefficients for meat (ML or TP/serum:tissue partition coefficient). The acceptable serum

Table 3
Risk assessment considerations for problem formulation.

Questions to consider	Example information	Purpose
What type of farm/ operation in question?	Intensive, large, artisan, hobby	Scale of operation may be important for exposure considerations, management measures and market share.
What livestock and purpose?	Cattle for food production	Sets the context for human health risk assessment.
What breed, age, sex?	Angus steers (3–4 months)	Age and sex may be an important consideration for physiological parameters (and exposure considerations).
Production systems	Pasture based grazing, supplementation, stock rotation	Gives context on stock exposure and any potential natural depuration times associated with the farming practice
Discharge intention	(weaners, yearlings, cull for age), selling for growing out, fattening, slaughter, breeding?	Gives context on the likely duration of time between exposure and end market.
Time of year of discharge?	Spring	Time of year influences exposure and should be considered especially when designing monitoring programs.
What is the expected finishing age for market?	12–18 months (yearlings)	Body burden is related to the exposure period.
Home consumption?	One animal per year	Gives indication of amount of produce realistically consumed in home setting.
What is the destination market?	Large abattoir or small-town market or home consumption	Market dilution considerations may apply for large markets, noting this informs risk management rather than risk assessment.
What are the surrounding land uses (and history) and pathways for PFAS contamination?	Former fire fighter training ground	Important for identifying contaminants of interest and contextualising migration pathways. Firefighting activities are linked to the use of AFFF which contain certain classes of PFAS depending on the products used. Some products also contain higher levels of precursors which may biodegrade to PFOS.
Are biosolids used onsite? If so, how many years?	Yes, between 1990 and 2000	PFAS composition and concentrations have changed over time which may be important for identifying chemicals of interest as well as an additional uptake pathway.
What is/are the source(s) of livestock drinking water?	Dams fed by surface water runoff	The number of sources and level of contamination and time spent at each is informative for livestock exposure as well as management options (rotation).
What levels of PFAS found in each drinking source?	PFOS at conc. ranging < LOR to 10 ng/ml	
How long do animals spend in the vicinity of each drinking source?	Weeks to months	
What are the dominant production systems in place?	Pasture based grazing (80% of intake) and supplementation with hay or silage from unimpacted source (20%)	Information about production systems is relevant for exposure estimation.
What levels of PFAS detected in soils and pasture?	PFOS at conc. ranging < LOR to 100 ng/g	

concentrations for the FSANZ TP of 3.5 ng PFOS + PFHxS/g (wet weight) were estimated as 43.75 ng/ml for PFOS and 56.5 ng/ml for PFHxS using serum:tissue partition coefficients of 0.08 [45] for PFOS and 0.062 for PFHxS (Drew et al., 2021c). The acceptable serum concentrations based on the EC MLs for cattle meat (0.3 ng/g for PFOS and 0.2 ng/g for PFHxS) were estimated to be 3.75 ng/ml for PFOS and 3.2 ng/ml for PFHxS.

This figure shows that without management, cattle grazed on PFAS impacted sites may exceed acceptable serum levels, especially for export markets with lower limits (like the EC MLs), however, most cattle can achieve acceptable serum levels (depending on the serum target) between 6 and 18 months for PFOS and within 1–3 months for PFHxS, following prevention of exposure. This is particularly relevant for livestock practices where animals go to feedlots prior to market. Depending on market specifications, some cattle spend a minimum of 100 days in a feedlot to be classed as grain fed, while feeder steers (long fed) and Wagyu can spend up to 300 days in a feedlot (DPI NSW, 2015). The estimated depuration timeframes can aid in prioritising sites for remedial intervention where the depuration timeframes are impracticable or exposure management is not possible.

It is noted that the livestock discussed here were either acquired for further research (Drew et al., 2021b) or managed by either moving to another site or by limiting access to PFAS contaminated resources such that serum levels reduced to acceptable levels (based on FSANZ non-regulatory trigger points for meat in Australia).

With regard to risk assessment and management, this work has highlighted environmental, seasonal and resource factors that have significant impact on the bioaccumulation of PFAS in animals. Although the trends highlighted in this work pertain to surface water contamination, the same principles apply for managing exposure via other sources like biosolids or contaminated groundwater. To develop a robust conceptual site model for site specific livestock risk assessment, certain parameters require consideration, presented here as a series of questions that should be considered during the problem formulation of the risk assessment (Table 3).

4. Conclusions

This study investigated trends in PFAS monitoring- and farm operational data with a focus on furthering our understanding of exposure pathways, determinants of variability in livestock PFAS body burdens and how these relate to risk assessment and management. The PFAS of most concern for risk assessment and management were PFOS and PFHxS. This study showed that PFOS and PFHxS body burden are positively correlated with water intake which, in turn, is influenced by climate, timing and season of sampling. Water intake levels can be as low as 1–8% of bodyweight (non-lactating cattle and sheep) in winter and spring months when pasture moisture is high and evaporative losses low compared to 10–20% of bodyweight (non-lactating cattle and sheep) in summer (NRC, 2000; Olkowski, 2009). These seasonal variables in water and feed intake can also influence PFAS body burden and result in seasonal body burden fluctuations. Due to this, estimates of PFAS body burden currently based on steady state kinetics may result in large discrepancies between actual measured and estimated concentrations depending on the timing of sampling. As such, dynamic exposure models are likely more suitable for modelling PFAS exposure in grazing livestock.

In addition, farming practices such as livestock rotation and timing (of rotation) may be critical for management of livestock on sites with PFAS contamination in order to reduce PFAS body burden prior to finishing livestock. For sites with limited cattle rotation potential supplementation of feed and water sources may also need to be considered whilst remediation options are devised. Biomonitoring data, along with estimated elimination timeframes (to meet health-based guidelines), can assist in prioritising remediation options where the timeframes are impracticable, or exposure management is not feasible or possible.

Author contribution statement

The manuscript was written through contributions of all authors. **Antti T. Mikkonen:** Conceptualization, Methodology, Formal analysis, Visualization, Writing – Original Draft **Jennifer Martin:** Investigation, Resources, Data Curation, Writing – Original Draft **Richard N. Upton:** Methodology, Validation, Supervision **Andrew O. Barker:** Software, Validation, Visualization **Carolyn M. Brumley:** Writing – Review and Editing **Mark P. Taylor:** Writing – Review and Editing **Lorraine Mackenzie:** Writing – Review and Editing, Supervision **Michael S. Roberts:** Writing – Review and Editing, Supervision.

Funding

This research did not receive any specific grant from funding agencies in the public, commercial, or not-for-profit sectors.

Declaration of competing interest

The authors declare the following financial interests/personal relationships which may be considered as potential competing interests: Antti Mikkonen reports a relationship with Nation Partners Pty Ltd that includes: employment. Carolyn Brumley reports a relationship with Nation Partners Pty Ltd that includes: employment. Jennifer Martin reports a relationship with Arcadis Australia Pacific that includes: employment. Antti Mikkonen reports a relationship with CDM Smith Pty Ltd that includes: employment.

Data availability

Attached as supplementary material

Acknowledgments

The authors would like to acknowledge Dr. David Champness from Agriculture Victoria and Effi Liden from the Victorian Department of Health for their comments on the manuscript. The authors thank the Environment Protection Authority Victoria for supporting this work through access to their facilities, administrative- and in-kind support. AM acknowledges the Australian Government, Department of Education, Skills and Employment Research Training Program scholarship that supported his PhD studies at UniSA, which includes this study. MSR was supported by an Australian National Health & Medical Research Council Research Fellowship (#1107356).

Appendix A. Supplementary data

Supplementary data to this article can be found online at https://doi.org/10.1016/j.envres.2023.115518.

References

Abunada, Z., Alazaiza, M.Y.D., Bashir, M.J.K., 2020. An overview of per- and polyfluoroalkyl substances (PFAS) in the environment: source, fate, risk and regulations. Water 12 (12), 3590. https://doi.org/10.3390/w12123590.

Agriculture Victoria, 2019. Prim. Prod. Landsc. Victoria. http://vro.agriculture.vic.gov.au/dpi/vro/vrosite.nsf/pages/prim_prod_lscapes.

Agriculture Victoria, 2021. Victorian Beef Industry Fast Facts. https://agriculture.vic.gov.au/__data/assets/pdf_file/0009/657126/Beef_Fast-Facts_March-2021.pdf.

ATSDR, 2018. Toxicological Profile for Perfluoroalkyls, Draft for Public Comment. U.S. Department of Health and Human Services, Public Health Service, Atlanta, GA.

Australian Bureau of Agricultural Resource Economics and Sciences (ABARES), 2021. In: Catchment Scale Land Use of Australia – Update December 2020. https://doi.org/10.25814/AQJW-RQ15.

Bräunig, J., Baduel, C., Heffernan, A., Rotander, A., Donaldson, E., Mueller, J.F., 2017. Fate and redistribution of perfluoroalkyl acids through AFFF-impacted groundwater. Sci. Total Environ. 596–597, 360–368. https://doi.org/10.1016/j.scitotenv.2017.04.095.

Buck, R.C., Franklin, J., Berger, U., Conder, J.M., Cousins, I.T., de Voogt, P., Jensen, A.A., Kannan, K., Mabury, S.A., van Leeuwen, S.P., 2011. Perfluoroalkyl and polyfluoroalkyl substances in the environment: terminology, classification, and origins. Integrated Environ. Assess. Manag. 7 (4), 513–541. https://doi.org/10.1002/ieam.258.

Cardno LanePiper, 2014. Human Health Risk Assessment - Fiskville Community Fiskville Training College 4549 Geelong-Ballan Rd. Fiskville Victoria. https://www.parliament.vic.gov.au/images/stories/committees/enrc/Fiskville_training_college/other_docs/05_-_2014_CPL_Human_Health_Risk_Assessment_-_Fiskville_Community.pdf.

Costello, M.C.S., Lee, L.S., 2020. Sources, fate, and plant uptake in agricultural systems of per- and polyfluoroalkyl substances. Curr. Pollut. Rep. https://doi.org/10.1007/s40726-020-00168-y.

Dauchy, X., 2019. Per- and polyfluoroalkyl substances (PFASs) in drinking water: current state of the science. Curr. Opin. Environ. Sci. Health 7, 8–12. https://doi.org/10.1016/j.coesh.2018.07.004.

Dauchy, X., Boiteux, V., Colin, A., Bach, C., Rosin, C., Munoz, J.-F., 2019. Poly- and perfluoroalkyl substances in runoff water and wastewater sampled at a firefighter training area. Arch. Environ. Contam. Toxicol. 76 (2), 206–215. https://doi.org/10.1007/s00244-018-0585-z.

Death, C., Bell, C., Champness, D., Milne, C., Reichman, S., Hagen, T., 2021. Per- and polyfluoroalkyl substances (PFAS) in livestock and game species: a review. Sci. Total Environ. 774, 144795 https://doi.org/10.1016/j.scitotenv.2020.144795.

Dorrance, L.R., Kellogg, S., Love, A.H., 2017. What you should know about per- and polyfluoroalkyl substances (PFAS) for environmental claims. Environ. Claims J. 29 (4), 290–304. https://doi.org/10.1080/10406026.2017.1377015.

DPI NSW, 2015. Market specifications for cattle. Primefact 621. https://www.dpi.nsw.gov.au/__data/assets/pdf_file/0005/148415/Market-specifications-for-cattle.pdf.

Drew, R., Hagen, T.G., Champness, D., 2021a. Accumulation of PFAS by livestock – determination of transfer factors from water to serum for cattle and sheep in Australia. Food Addit. Contam. 1–17. https://doi.org/10.1080/19440049.2021.1942562.

Drew, R., Hagen, T.G., Champness, D., Sellier, A., 2021b. Half-lives of several polyfluoroalkyl substances (PFAS) in cattle serum and tissues. Food Addit. Contam. 1–21 https://doi.org/10.1080/19440049.2021.1991004.

Drew, R., Hagen, T., Champness, D., Sellier, A., 2021c. PFAS Tissue Distribution in Cattle. Poster Presentation at IUTOX 15th International Congress of Toxicology.

EC, 2022. ANNEX to the Commission Regulation (EU) .../... Amending Regulation (EC) No 1881/2006 as Regards Maximum Levels of Perfluoroalkyl Substances in Certain Foodstuffs. https://members.wto.org/crnattachments/2022/SPS/EEC/22_4494_00_e.pdf.

EFSA, 2020. Risk to human health related to the presence of perfluoroalkyl substances in food. EFS2 18 (9). https://doi.org/10.2903/j.efsa.2020.6223.

EHP, 2014. Managing Firefighting Foam Policy Explanatory Notes accessed 2022-08-30. https://environment.des.qld.gov.au/__data/assets/pdf_file/0022/89140/firefighting-foam-policy-notes.pdf.

enHealth, 2012. Environmental Health Risk Assessment: Guidelines for Assessing Human Health Risks from Environmental Hazards.

Fenton, S.E., Ducatman, A., Boobis, A., DeWitt, J.C., Lau, C., Ng, C., Smith, J.S., Roberts, S.M., 2020. Per- and polyfluoroalkyl substance toxicity and human health review: current state of knowledge and strategies for informing future research. Environ. Toxicol. Chem. https://doi.org/10.1002/etc.4890 etc.4890.

Field, J.A., Higgins, C.P., Deeb, R., Conder, J.M., 2017. FAQs regarding PFASs associated with 15 AFFF use at U.S. Military sites. Catalyzing Rapid Information Transfer among Key 16 Stakeholders on Per- and Polyfluoroalkyl Substances (PFASs) at Contaminated Military 17 Sites. https://apps.dtic.mil/dtic/tr/fulltext/u2/1044126.pdf.

FSANZ, 2021. In: 27th Australian Total Diet Study Per- and Poly-Fluoroalkyl Substances accessed 2022-01-25). https://www.foodstandards.gov.au/publications/Documents/27th%20ATDS%20report.pdf.

Gallen, C., Baduel, C., Lai, F.Y., Thompson, K., Thompson, J., Warne, M., Mueller, J.F., 2014. Spatio-temporal assessment of perfluorinated compounds in the Brisbane river system, Australia: impact of a major flood event. Mar. Pollut. Bull. 85 (2), 597–605. https://doi.org/10.1016/j.marpolbul.2014.02.014.

Glaser, D., Lamoureux, E., Opdyke, D., LaRoe, S., Reidy, D., Connolly, J., 2021. The impact of precursors on aquatic exposure assessment for PFAS: insights from bioaccumulation modeling. Integrated Environ. Assess. Manag. 17 (4), 705–715. https://doi.org/10.1002/ieam.4414.

Glüge, J., Scheringer, M., Cousins, I.T., DeWitt, J.C., Goldenman, G., Herzke, D., Lohmann, R., Ng, C.A., Trier, X., Wang, Z., 2020. An overview of the uses of per- and polyfluoroalkyl substances (PFAS). Environ. Sci.: Process. Impacts 22 (12), 2345–2373. https://doi.org/10.1039/D0EM00291G.

Golder, 2020. Human Health and Ecological Risk Assessment Bandiana Military Area. https://www.defence.gov.au/Environment/PFAS/docs/Bandiana/Reports/202011BandianaHHERAMainReportFiguresTables.pdf.

Google. Google Maps Victoria Australia. https://www.google.com/maps/place/Victoria/@-36.4856423,140.9779425,6z/data=!3m1!4b1!4m5!3m4!1s0x6ad4314b7e18954f:0x5a4efce2be829534!8m2!3d-36.9847807!4d143.3906074.

Gupta, P.K., 2016. Principles and basic concepts of toxicokinetics. In: Fundamentals of Toxicology. Elsevier, pp. 87–107. https://doi.org/10.1016/B978-0-12-805426-0.00009-3.

Hagen, T., Drew, R., Champness, D., Ryan, J., 2019. PFAS clearance and distribution in sheep. Honolulu, Hawaii. In: IUTOX 15th International Congress of Toxicology; July 15-18. P366–0932.

Harding-Marjanovic, K.C., Yi, S., Weathers, T.S., Sharp, J.O., Sedlak, D.L., Alvarez-Cohen, L., 2016. Effects of aqueous film-forming foams (AFFFs) on trichloroethene (TCE) dechlorination by a dehalococcoides mccartyi -containing microbial community. Environ. Sci. Technol. 50 (7), 3352–3361. https://doi.org/10.1021/acs.est.5b04773.

Hu, L., Bao, W., Shi, P., Wang, J., Lu, M., 2020. Simulation of overland flow considering the influence of topographic depressions. Sci. Rep. 10 (1), 6128. https://doi.org/10.1038/s41598-020-63001-y.

Ito, S., 2011. Pharmacokinetics 101. Paediatr. Child Health 16 (9), 535–536. https://doi.org/10.1093/pch/16.9.535.

Kowalczyk, J., Ehlers, S., Fürst, P., Schafft, H., Lahrssen-Wiederholt, M., 2012. Transfer of perfluorooctanoic acid (PFOA) and perfluorooctane sulfonate (PFOS) from contaminated feed into milk and meat of sheep: pilot study. Arch. Environ. Contam. Toxicol. 63 (2), 288–298. https://doi.org/10.1007/s00244-012-9759-2.

Kowalczyk, J., Ehlers, S., Oberhausen, A., Tischer, M., Fürst, P., Schafft, H., Lahrssen-Wiederholt, M., 2013. Absorption, distribution, and milk secretion of the perfluoroalkyl acids PFBS, PFHxS, PFOS, and PFOA by dairy cows fed naturally contaminated feed. J. Agric. Food Chem. 61 (12), 2903–2912. https://doi.org/10.1021/jf304680j.

Kowalczyk, J., Göckener, B., Eichhorn, M., Kotthoff, M., Bücking, M., Schafft, H., Lahrssen-Wiederholt, M., Numata, J., 2020. Transfer of per- and polyfluoroalkyl substances (PFAS) from feed into the eggs of laying hens. Part 2: toxicokinetic results including the role of precursors. J. Agric. Food Chem. 68 (45), 12539–12548. https://doi.org/10.1021/acs.jafc.0c04485.

Lanza, H.A., Cochran, R.S., Mudge, J.F., Olson, A.D., Blackwell, B.R., Maul, J.D., Salice, C.J., Anderson, T.A., 2017. Temporal monitoring of perfluorooctane sulfonate accumulation in aquatic biota downstream of historical aqueous film forming foam use areas: variability of PFOS downstream of historic AFFF application. Environ. Toxicol. Chem. 36 (8), 2022–2029. https://doi.org/10.1002/etc.3726.

Leeson, A., Thompson, T., Stroo, H.F., Anderson, R.H., Speicher, J., Mills, M.A., Willey, J., Coyle, C., Ghosh, R., Lebrón, C., Patton, C., 2021. Identifying and managing aqueous film-forming foam-derived per- and polyfluoroalkyl substances in the environment. Environ. Toxicol. Chem. 40 (1), 24–36. https://doi.org/10.1002/etc.4894.

Lukas, J.M., Reneau, J.K., Linn, J.G., 2008. Water intake and dry matter intake changes as a feeding management tool and indicator of health and estrus status in dairy cows. J. Dairy Sci. 91 (9), 3385–3394. https://doi.org/10.3168/jds.2007-0926.

Lupton, S.J., Dearfield, K.L., Johnston, J.J., Wagner, S., Huwe, J.K., 2015. Perfluorooctane sulfonate plasma half-life determination and long-term tissue distribution in beef cattle (Bos taurus). J. Agric. Food Chem. 63 (51), 10988–10994. https://doi.org/10.1021/acs.jafc.5b04565.

Lupton, S.J., Smith, D.J., Scholljegerdes, E., Ivey, S., Young, W., Genualdi, S., DeJager, L., Snyder, A., Esteban, E., Johnston, J.J., 2022. Plasma and skin per- and polyfluoroalkyl substance (PFAS) levels in dairy cattle with lifetime exposures to PFAS-contaminated drinking water and feed. J. Agric. Food Chem. 70 (50), 15945–15954. https://doi.org/10.1021/acs.jafc.2c06620.

Martin, J.W., Asher, B.J., Beesoon, S., Benskin, J.P., Ross, M.S., 2010. PFOS or PreFOS? Are perfluorooctane sulfonate precursors (PreFOS) important determinants of human and environmental perfluorooctane sulfonate (PFOS) exposure? J. Environ. Monit. 12 (11), 1979. https://doi.org/10.1039/c0em00295j.

Mejia Avendaño, S., Liu, J., 2015. Production of PFOS from aerobic soil biotransformation of two perfluoroalkyl sulfonamide derivatives. Chemosphere 119, 1084–1090. https://doi.org/10.1016/j.chemosphere.2014.09.059.

Mikkonen, H.G., Clarke, B.O., Dasika, R., Wallis, C.J., Reichman, S.M., 2018. Evaluation of methods for managing censored results when calculating the geometric mean. Chemosphere 191, 412–416. https://doi.org/10.1016/j.chemosphere.2017.10.038.

NMI, 2018. Proficiency Test Report AQA 18-09 PFAS in Soil, Water, Fish and Prawn. https://www.industry.gov.au/sites/default/files/2019-06/aqa-18-09-pfas-in-water-soil-biota-proficiency-test-final-report.pdf.

NRC, 2000. Nutrient Requirements of Beef Cattle: Seventh Revised Edition: Update 2000. National Academies Press, Washington, D.C., p. 9791. https://doi.org/10.17226/9791

NSW DPI, 2014. Water requirements for sheep and cattle. In: Primefact, , third ed.vol. 326

Numata, J., Kowalczyk, J., Adolphs, J., Ehlers, S., Schafft, H., Fuerst, P., Müller-Graf, C., Lahrssen-Wiederholt, M., Greiner, M., 2014. Toxicokinetics of seven perfluoroalkyl sulfonic and carboxylic acids in pigs fed a contaminated Diet. J. Agric. Food Chem. 62 (28), 6861–6870. https://doi.org/10.1021/jf405827u.

OECD, 2021. Emission scenario document on the use of aqueous film-forming foams in firefighting. Ser. Emiss. Scenario Doc. 40 accessed 2022-08-30. https://www.oecd.org/officialdocuments/publicdisplaydocumentpdf/?cote=ENV/CBC/MONO(2021)5&doclanguage=en.

Olkowski, A.A., 2009. Canada; agriculture and agri-food Canada. In: University of Saskatchewan; Saskatchewan; Ministry of Agriculture. Livestock Water Quality: A Field Guide for Cattle, Horses, Poultry and Swine. Agriculture and Agri-Food Canada, Ottawa.

Parliament of Victoria, 2016. Inquiry into the CFA Training College at Fiskville, Final Report. https://www.parliament.vic.gov.au/file_uploads/ENRRDC_Fiskville_Inquiry_Final_Report_myHbwdGN.pdf.

R Core Team. R, 2019. A Language and Environment for Statistical Computing. https://www.R-project.org/.

Revelle, W., 2021. Psych: Procedures for Psychological, Psychometric, and Personality Research. Northwestern University, Evanston, Illinois.

Rogers, R.D., Reh, C.M., Breysse, P., 2021. Advancing per- and polyfluoroalkyl substances (PFAS) research: an overview of ATSDR and NCEH activities and recommendations. J. Expo. Sci. Environ. Epidemiol. 31 (6), 961–971. https://doi.org/10.1038/s41370-021-00316-6.

Senversa, 2018. Human Health and Ecological Risk Assessment RAAF Base East Sale – Per- and Poly-Fluoroalkyl Substances (PFAS) Investigations. https://www.defence.gov.au/Environment/PFAS/docs/EastSale/Reports/RAAFEastSaleFinalHHERAReportBody.pdf.

Todd, G., 2018. Aust. PFAS Chem. Map accessed 2021-05-16. https://pfas.australianmap.net/.

U.S. Environmental Protection Agency, 2019. Guidelines for Human Exposure Assessment. EPA/100/B-19/001.

USDA. Dairy Indemnity Payment Program Expanded to Assist with Livestock Losses Due to Contamination. U.S. Deaprtment of Agriculture News Releases. https://www.fsa.usda.gov/state-offices/Maine/news-releases/2021/dairy-indemnity-payment-program-expanded-to-assist-with-livestock-losses-due-to-contamination.

Van Asselt, E.D., Kowalczyk, J., Van Eijkeren, J.C.H., Zeilmaker, M.J., Ehlers, S., Fürst, P., Lahrssen-Wiederholt, M., Van Der Fels-Klerx, H.J., 2013. Transfer of perfluorooctane sulfonic acid (PFOS) from contaminated feed to dairy milk. Food Chem. 141 (2), 1489–1495.

Vestergren, R., Orata, F., Berger, U., Cousins, I.T., 2013. Bioaccumulation of perfluoroalkyl acids in dairy cows in a naturally contaminated environment. Environ. Sci. Pollut. Control Ser. 20 (11), 7959–7969. https://doi.org/10.1007/s11356-013-1722-x.

Wang, W., Rhodes, G., Ge, J., Yu, X., Li, H., 2020. Uptake and accumulation of per- and polyfluoroalkyl substances in plants. Chemosphere 261, 127584. https://doi.org/10.1016/j.chemosphere.2020.127584.

Wickham, H., 2016. Ggplot2: elegant graphics for data analysis. In: 2016.; Use R!, second ed. Springer International Publishing, Cham. https://doi.org/10.1007/978-3-319-24277-4. Imprint: Springer.

Williams, J., Hamblin, A.P., Hook, R.A., 2002. CSIRO (Australia); Division of Land and Water. Methodologies for Their Derivation and Key Issues in Resource Management. CSIRO Land and Water, Canberra.

Xu, Y., 2020. Serum half-lives for short- and long-chain perfluoroalkyl acids after ceasing exposure from drinking water contaminated by firefighting foam. Environ. Health Perspect. 12.

Yi, S., Harding-Marjanovic, K.C., Houtz, E.F., Gao, Y., Lawrence, J.E., Nichiporuk, R.V., Iavarone, A.T., Zhuang, W.-Q., Hansen, M., Field, J.A., Sedlak, D.L., Alvarez-Cohen, L., 2018. Biotransformation of AFFF component 6:2 fluorotelomer thioether amido sulfonate generates 6:2 fluorotelomer thioether carboxylate under sulfate-reducing conditions. Environ. Sci. Technol. Lett. 5 (5), 283–288. https://doi.org/10.1021/acs.estlett.8b00148.

Zafeiraki, E., Vassiliadou, I., Costopoulou, D., Leondiadis, L., Schafft, H.A., Hoogenboom, R.L.A.P., van Leeuwen, S.P.J., 2016. Perfluoroalkylated substances in edible livers of farm animals, including depuration behaviour in young sheep fed with contaminated grass. Chemosphere 156, 280–285. https://doi.org/10.1016/j.chemosphere.2016.05.003.

Zhang, Q., Yu, R., Fu, S., Wu, Z., Chen, H.Y.H., Liu, H., 2019. Spatial heterogeneity of heavy metal contamination in soils and plants in Hefei, China. Sci. Rep. 9 (1), 1049. https://doi.org/10.1038/s41598-018-36582-y.

Zhao, S., Liang, T., Zhu, L., Yang, L., Liu, T., Fu, J., Wang, B., Zhan, J., Liu, L., 2019. Fate of 6:2 fluorotelomer sulfonic acid in pumpkin (cucurbita maxima L.) based on hydroponic culture: uptake, translocation and biotransformation. Environ. Pollut. 252, 804–812. https://doi.org/10.1016/j.envpol.2019.06.020.

CCSN Comments re:
EPA Report Cadia Region Surface Water Testing
–20 to 21 August Sampling

4 October 2024

The EPA tested water samples collected on 20 and 21 August from 16 locations on the Belubula River and surrounding streams. The report by the EPA was released on 30 September 2024.

CCSN would like to provide the following comments and additional information.

Table 1
Additional Potential Contamination Sources
Table 1 "Potential Contamination Sources" should include reference to Cadia's Dewatering Plant adjacent to Abattoir Creek and the current Dewatering Plant off Newbridge Rd near the Goose Park. CCSN has previously tested the sediment in Abattoir Creek at the culvert close to the site of the old dewatering plant, those tests identified PFOS at 0.0017 mg/kg. Refer to ALS Report ES2423065 reference "Blayney Creek" attached.

Figure 1
Potential Source Locations
A number of locations are identified on the map by a pink pentagon. The following locations should also be included:

- Cadia Valley Operations
- Cadia dewatering plant on Abattoir Creek
- Cadia dewatering plant on Newbridge Rd

Volume of water flow at each location
Comparison of contamination across sites considers only the concentration per litre of water collected. This presents a misleading picture of the magnitude of contamination from each potential source.

The volume of water in the Belubula at say Millamolong is greater by several orders of magnitude than the volume of water in Cowriga Creek and Mackenzies Waterholes Creek.

Full consideration of environmental impacts must take into account the total amount of contamination. Although dilution cannot be accepted as a solution, EPA data to date suggests, for example, that contamination from Cowriga Creek may be diluted to a "safe level" in a relatively short stretch of the Belubula. This is not the case downstream after Ashburtons Bridge. There appears to be a significantly greater quantity of PFOS in the Belubula in absolute terms downstream.

 

Belubula River at Millamolong 25 September 2024. Cowriga Creek 2 October 2024

Visible Changes in the Belubula

Between Ashburtons Bridge and Burnt Yards Rd Bridge there are two visible changes in the Belubula River.

- Bubbles flowing down the river and foam accumulating on the river bank
- White sediment depositing on the river banks and rocks

These changes coincide with an increase in PFOS in the Belubula as identified by the EPA and continue to the most western test point at Boonderoo, off Malongulli Road.

- **Foam**

  The EPA has taken very few samples of the foam and does not appear to have tested it for its full composition and concentration of elements. This investigation should consider all potential data and patterns of contamination. This contamination event does not appear to be "normal" and the usual protocols for sampling and assumptions which might be made may not be appropriate.

  For example, the concentration of calcium identified in foam samples collected on 31 August and 1 September by Assoc Professor Dr. Ian Wright on Flyers Creek.

These results are summarised as follows:

Belubula East – West	
Carcoar	880 mg/kg
Burnt Yards Rd Bridge	2,200 mg/kg
Flyers Creek North – South	
Panuara Rd Bridge	6,100 mg/kg
Old Errowanbang Weir (approx. 11 km north of Belubula)	5,800 mg/kg
Errowanbang	8,200 mg/kg
Braeburn rock pools (approx. 5 .5 km north of Belubula)	44,000mg/kg

Does the dramatic increase in calcium at Braeburn indicate a source of contamination into Flyers Creek close to that part of the Creek?

Did the calcium enter the creek as part of a group of contaminants?

Is this mix of contamination responsible for the significant increase in foam between Errowanbang Weir and the Braeburn rock Pools?

Above - Braeburn Rock Pool

Below – Jann Harries Weir upstream of Braeburn on Flyers Creek

White Stripe
There is a visible white stripe formed by sediment depositing along the edge of the Belubula river on rocks, branches and river banks. This stripe seems to start between Ashburtons Bridge and Burnt Yards Road bridge.

CCSN has collected samples and given them to Assoc Professor Ian Wright for testing. These results will be provided to the EPA when we received. The sediment appears to be exceptionally fine with a texture similar to talcum powder.

Is this stripe from the foam and is it concentrating contaminants along the river bank?

Is it possible the white stripe is the elevated calcium identified in the foam?

Should investigations be looking for large volumes of calcium in the form of a fine powder?

24 & 25 September Belubula River at Millamolong

Hydrocarbons

CCSN and Assoc. Professor Ian Wright have collected multiple samples which have been tested and confirmed as Petroleum Hydrocarbons. By example refer to Attached ALS report ES 2423065 “River Gloucester”.

These elements appear to be forming a film on the surface of still water and contaminating the river, ponds and aquatic environment.

Are these elements part of the foam which has blanketed parts of the river and adjacent ponds for almost 2 months?

Above - rock thrown in black pond on Belubula

Below – film on pond has pulled back together within 15 sec

CCSN has been testing the film by throwing a rock into the pond and observing if the film reconnects (as suggested by the EPA water testing team as a quick way to determine if hydrocarbons are present).

The EPA has not recorded any hydrocarbons, could this be because the EPA is following a protocol to test the river below the surface? Does this protocol mean that the EPA's test results under report contaminants such as PFOS and hydrocarbons which are likely to be on the surface of any water body?

In order to determine the source of pollution it is necessary to identify the cocktail of elements, causing the pollution. CCSN has focused its testing on identifying *what* is in the water, foam and sediments.

The CCSN believes investigation of contamination should consider:

- the "cocktail" of contaminants;
- patterns of distribution for this cocktail and other observations such as the pH;
- the scale of pollution required from a source to change the chemistry of the water flowing in the Belubula west of Ashburtons Bridge
- potential sources of the cocktail of contaminants identified
- extreme episodic events such as those identified in the CVO / GHD report on the Belubula River as well as the ongoing pollution.

CCSN Comments re:
EPA Report Cadia Region Surface Water Testing
–20 to 21 August Sampling
Version 2 – 31 October 2024

18 October 2024

The EPA tested water samples collected on 20 and 21 August from 16 locations on the Belubula River and surrounding streams. The report by the EPA was released on 30 September 2024.

CCSN would like to provide the following comments and additional information.

Table 1
Additional Potential Contamination Sources
Table 1 "Potential Contamination Sources" should include reference to:

- Orange wastewater treatment plant – Cadia has received an average of 9ML / day since 1998.
- Cadia's original dewatering plant adjacent to Abattoir Creek and CCSN has previously tested the sediment in Abattoir Creek at the culvert close to the site of the old dewatering plant, those tests identified PFOS at 1.7 µg/kg. Refer to ALS Report ES2423065 reference "Blayney Creek" attached. A sediment sample collected in the same location by Dr Ian Wright on 13 October 2024 recorded PFOS of 9.4µg/kg.
- The current dewatering plant off Newbridge Rd near the Goose Park.

Figure 1
Potential Source Locations
A number of locations are identified on the map by a pink pentagon. The following locations should also be included:

- Cadia Valley Operations. Since operations began Cadia has received the following PFOS contaminated material:
    - Orange waste water 9ML/day 1998 – to date
    - Blayney waste water 1 ML/day 1998 – late 2019
    - Biosolids stockpiled for future rehabilitation since 1998
    - PFOS fire fighting foam 1998 - 2015
- Cadia Dewatering Plant on Abattoir Creek
- Cadia Dewatering Plant on Newbridge Rd
- Orange waste treatment facility

Volume of water flow at each location
Comparison of contamination across sites considers only the concentration per litre of water collected. This presents a misleading picture of the magnitude of contamination from each potential source.

The volume of water in the Belubula at Millamolong for example, is greater by several orders of magnitude than the volume of water in Cowriga Creek and Mackenzies Waterholes Creek.

Full consideration of environmental impacts must take into account the total amount of contamination. Although dilution cannot be accepted as a solution, EPA data to date suggests, for example, that contamination from Cowriga Creek may be diluted to a "safe level" in a relatively short stretch of the Belubula. This is not the case downstream after Ashburtons Bridge. There appears to be a significantly greater quantity of PFOS in the Belubula in absolute terms downstream.

Belubula River at Millamolong 25 September 2024. Cowriga Creek 2 October 2024

Visible Changes in the Belubula

Between Ashburtons Bridge and Burnt Yards Rd Bridge there are two visible changes in the Belubula River.

- Bubbles flowing down the river and foam accumulating on the river bank
- White sediment depositing on the river banks and rocks

These changes coincide with an increase in PFOS in the Belubula as identified by the EPA and continue to the most western test point at Boonderoo, off Malongulli Road.

- **Foam**

The EPA has taken very few samples of the foam and does not appear to have tested it for its full composition and concentration of elements. This investigation should consider all potential data and patterns of contamination. This contamination event does not appear to be "normal" and the usual protocols for sampling and assumptions which might be made may not be appropriate.

For example, the concentration of calcium identified in foam samples collected on 31 August and 1 September by Assoc Professor Ian Wright on Flyers Creek.

These results are summarised as follows:

Belubula East – West	
Carcoar	880 mg/kg
Burnt Yards Rd Bridge	2,200 mg/kg
Flyers Creek North – South	
Panuara Rd Bridge	6,100 mg/kg
Old Errowanbang Weir (approx 11 km north of Belubula)	5,800 mg/kg
Errowanbang	8,200 mg/kg
Braeburn rock pools (approx 5 .5 km north of Belubula)	44,000mg/kg

Does the dramatic increase in calcium at Braeburn indicate a source of contamination into Flyers Creek close to that part of the Creek?

Did the calcium enter the creek as part of a group of contaminants?

Is this mix of contamination responsible for the significant increase in foam between Errowanbang Weir and the Braeburn rock Pools?

Above - Braeburn Rock Pool

Below – Jann Harries Weir upstream of Braeburn on Flyers Creek

White Stripe
There is a visible white stripe formed by sediment depositing along the edge of the Belubula river on rocks, branches and river banks. This stripe seems to start between Ashburtons Bridge and Burnt Yards Road bridge.

CCSN has collected samples and given them to Assoc Professor Ian Wright for testing. These results will be provided to the EPA when received. The sediment appears to be exceptionally fine with a texture similar to talcum powder. EPA Staff also collected white rocks whilst visiting the area Sept 9 2024.

Is this stripe from the foam and is it concentrating contaminants along the river bank?

Is it possible the white stripe is the elevated calcium identified in the foam?

Should investigations be looking for large volumes of calcium in the form of a fine powder?

 

24 & 25 September Belubula River at Millamolong

Hydrocarbons

CCSN and Assoc. Professor Ian Wright have collected multiple samples which have been tested and confirmed as Petroleum Hydrocarbons. By example refer to Attached ALS report ES 2423065 “River Gloucester”.

These elements appear to be forming a film on the surface of still water and contaminating the river, ponds and aquatic environment.

Are these elements part of the foam which has blanketed parts of the river and adjacent ponds for almost 2 months?

Above - rock thrown in black pond on Belubula

Below – film on pond has pulled back together within 15 sec

CCSN has been testing the film by throwing a rock into the pond and observing if the film reconnects (as suggested by the EPA Water Testing team as a quick way to determine if hydrocarbons are present).

The EPA has not recorded any hydrocarbons, could this be because the EPA is following a protocol to test the river below the surface? Does this protocol mean that the EPA's test results under report contaminants such as PFOS and hydrocarbons which are likely to be on the surface of any water body?

In order to determine the source of pollution it is necessary to identify the cocktail of elements, causing the pollution. CCSN has focused its testing on identifying *what* is in the water, foam and sediments.

The CCSN believes investigation of contamination should consider:

- the "cocktail" of contaminants;
- patterns of distribution for this cocktail and other observations such as the pH;
- the scale of pollution required from a source to change the chemistry of the water flowing in the Belubula west of Ashburtons Bridge
- potential sources of the cocktail of contaminants identified
- extreme episodic events such as those identified in the CVO / GHD report on the Belubula River as well as the ongoing pollution.

CCSN Comments re:
Pollution in the Belubula south of CVO and
EPA Cadia Region Surface Water PFAS testing
22 and 23 October 2024

The EPA on 22 and 23 October 2024 conducted sampling in the Belubula River to investigate potential sources of per and polyfluoroalkyl substances (PFAS) contamination. Samples were collected between the headwaters and early tributaries of the Belubula in the Blayney district and across to the West at Limestone Creek.

Our contamination is a cocktail of chemicals

The contamination measured in water, foam and sediment in the Belubula and creeks in the Cadia valley is a mixture of PFOS, heavy metals and hydrocarbons (C10-C40). Many samples have been collected and tested by ALS and Envirolab with consistent results. CCSN has been told C10-C40 is diesel.

The diesel is forming a film on the ponds adjacent to the Belubula and provides a clear visual marker as the contamination in the water concentrates with evaporation. Refer to CCSN Comments Re: EPA Report Cadia Region Surface Water Testing – 20 to 21 August Sampling dated 4 October 2024

CVO uses diesel as a flotation agent in the ore separation process (Attachment 1).

CVO uses calcium to balance the pH of the tailings.

Why is the EPA not looking for a source for this cocktail of contamination?

Why has the EPA not tested the surface of clearly contaminated ponds for diesel despite repeated requests?

Multiple Fault Lines through the Cadia Valley

There are multiple expert reports and maps which identify an extensive fault system through the Cadia Valley district. These reports have also identified that water could flow down some of these fault lines.

Three-Dimensional Discontinuum Analysis of Structurally Controlled Failure Mechanisms at the Cadia Hill Open Pit
D. Sainsbury, et al.

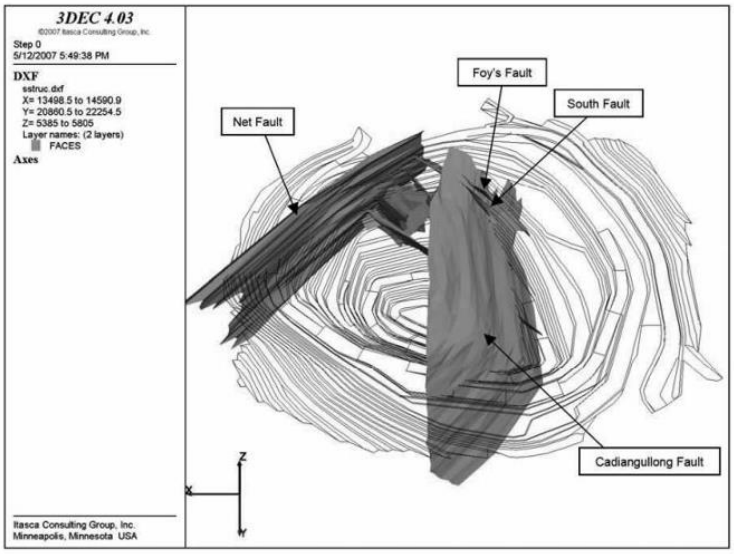

Figure 3 **2006 structural model (looking south)**

From Sainsbury et al – Attachment 2

The map below is taken from CCSN – Groundwater comments to DPE dated 24.04.2024 (Attachment 3).

The 2009 EIS for the Cadia East Project identified numerous faults running through the site, including those identified by Itasca as running through the Pit.

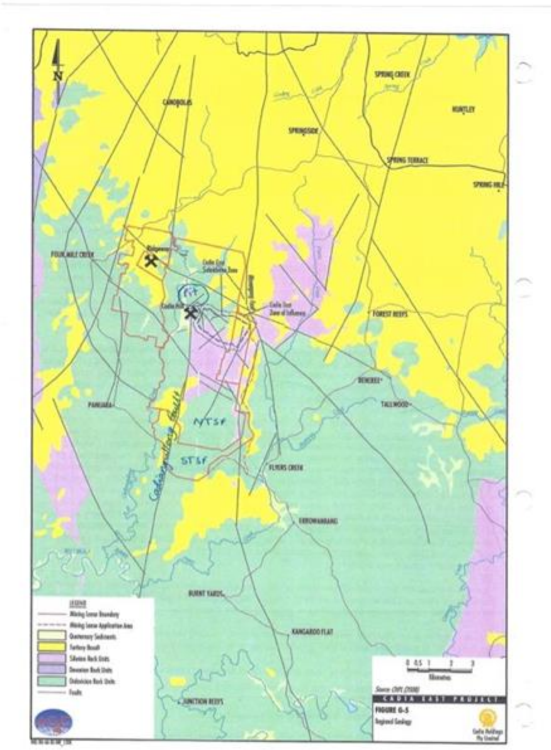

"The Cadiangullong Fault is a 1 m - 10 m wide zone of black cataclasite gouge and intensely fractured wall rocks
The Foys Fault is a 20 m wide zone of intensely fractured siltstone.

The Gibb Fault is a 0.5 m - 2 m wide zone of milled rock-matrix breccia and clay gouge.

The Copper Gully Fault is planar and narrow and has a reddish clay gouge.

The above observations indicate that the faults filled with clay gouge would act as barriers to movement of water, while the faults with breccia fil and fractured wall rocks would likely be conduits for groundwater flow.

The Warrengong Fault is a north-south trending, near vertical structure located approximately 1 km to the east of the Cadia East deposit (Figure G-5). It is considered to be an extensive regional structure"

CCSN has been advised by an Expert Hydrogeologist that:

- "Based on the topography and drainage direction of groundwater flow, it is plausible that contaminated groundwater from Cadia is reporting to Belubula River – in fact we know it does – that's the direction in moves – it just takes a long time to do so."

- "I would expect it plausible that water samples taken from BCA Con and BCA (both on Millamolong close to the Belubula confluence with Cadiangullong creek) and WONF (Wongalong) may reflect general groundwater inflow from Cadia"

- "Samples at B Bridge (Burnt Yards Rd Bridge) may also reflect groundwater from cadia if, for example, for geological structure marked below acted as a conduit for flow.   I do not know the geology of this feature to know this, but it can be reviewed."

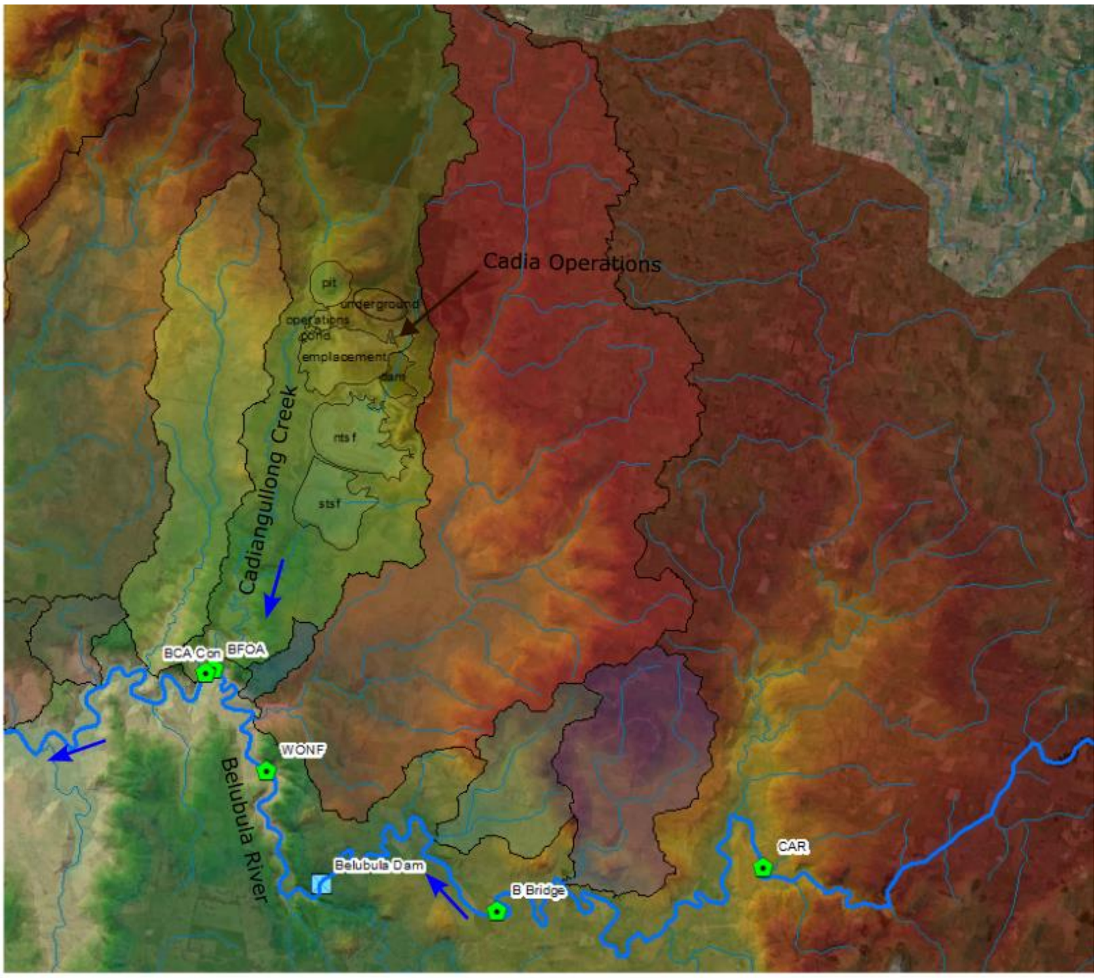

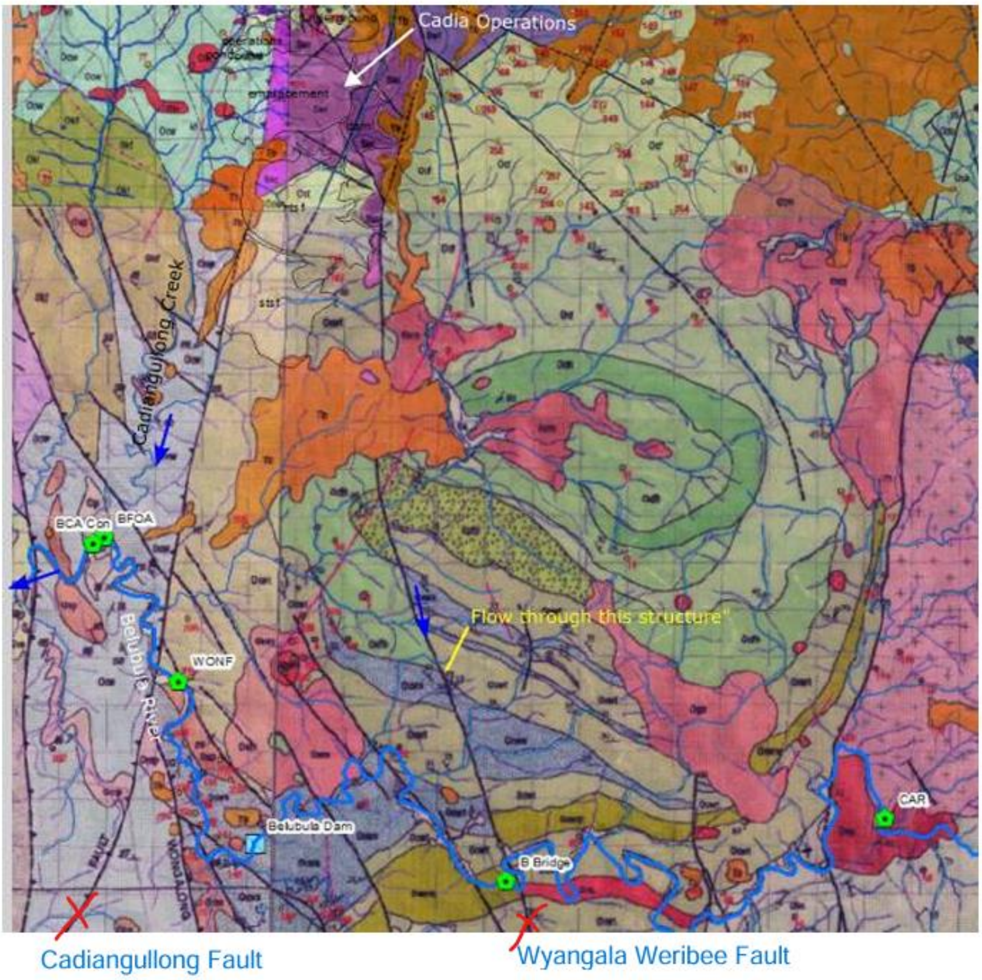

Potential Groundwater Movement in the Cadia Valley

There are several expert reports, including the Independent Expert Scientific Committee (IESC), which identify a clear risk that contaminated water may seep into the groundwater, the creeks and springs and potentially the highly productive Orange Basalt Aquifer.

1. Report on NTSF Embankment Failure by the Independent Technical Review Board (ITRB) April 2019 in particular Appendix F Hydrogeology Klohn Crippen Berger (Attachment 4), which identifies amongst other points;
    - buried paleo channels beneath valley fill tertiary basalt,
    - SW corner of NTSF, an underlying paleo-alluvium of up to 4m thickness,
    - a high permeability aquifer beneath the western NTSF embankment; and
    - multiple faults including the Wyangala – Werribee Fault System which has a strike length of about 30km, a damage zone approximately 200-400m wide, and tertiary basalt flows covering most of the fault

2. IESC 2023 – 14 August 2023 (Attachment 5)

Pg 3 … compaction and loading arising from the modified embankment may change the volume, rate and/or flow paths of seepage currently occurring beneath the TSFs via Rodds Creek and the Cadiangullong Fault and its associated weathered and damage zone

Pg 3 Sections of Flyers Creek to the east of CVO are perennial, receiving discharges from groundwater-fed springs (AGE 2021, p. 5).

Pg 3 Groundwater discharge is also likely to enter Shallow, Cadiangullong and Rodds creeks (AGE 2021, p. 36). Low-flow discharges from CVO occur to Cadiangullong Creek (AGE 2021, p. 5).

Pg 3 The extent of the Orange Basalt aquifer, and the fracture networks which are key for groundwater flow, are not well understood at CVO (AGE 2023, p. 6).

Pg 3 The IESC notes that there are indications of leakage from the TSFs into the shallow groundwater system due to currently approved activities, with potential for discharge to local surface waters and GDEs.

3. IESC 2024 – 15 October 2024 (Attachment 6)

   Pg 5 Potential leakage pathways from the STSFx could occur through fractures in the underlying bedrock, affecting groundwater flow paths, increasing or decreasing groundwater levels, and impacting quality of groundwater that may be used by nearby GDEs.

   How has the EPAs testing program taken into account the recognised risk of contamination to the creeks and Belubula via the many faults and seepage into the groundwater system?

   Has the EPA tested any bores identified to be positioned on a fault line?

Comparison of Total PFOS in Each Water Course

The EPA has sampled the Belubula and its tributaries in multiple locations and made a simple comparison of the concentration (g/L) of PFAS at each location. There has been no consideration of the volume of flow in each water course to determine the actual measured volume of PFAS at that point in time.

CVO recently published its draft 2024 Annual Review; Table 32 identifies the following average daily flow rates:

Belubula River at the needles (downstream of CVO)	79 ML/day
Flyers Creek	5.5 ML / day
Cadiangullong Creek (at southern lease boundary)	4.96 ML / day

Clearly the volume of flow in local creeks and the Belubula in the Blayney township is dramatically different to the flow in the Belubula at say Bakers Shaft and properties to the west.

Cowriga Creek – 11/12/2024

Below: Belubula at BCACon 10/12/2024

A straight comparison of the concentration of PFAS, as presented in the EPA report, without consideration of the volume of flow in each water course to determine the amount of PFAS in total is **misleading**.

Why has the EPA not taken into consideration the volume of stream flow in each sampling location and the actual amount of PFOS flowing in that water course?

Why does the EPA continue to present a misleading picture of the source of contamination?

No Consideration of Chemical Changes in Flyers Creek Running Past Cadia Mine

CVO and the Regulators have assumed contamination from the site will flow in a westerly direction towards Cadiangullong Creek.

The GHD report – Belubula River Surface Water Assessment (May 2024) (Attachment 7) identified 2 significant contamination events which "flushed" through the Belubula:

- July 2022 alkalinity peaked at pH 10.80
- October 2022 copper peaked at 0.010mg/L

Cadia's groundwater Monitoring Reports 2022 and 2023 identified very significant alkalinity with several bores south of the STSF reporting pH in the range 10 / 11 and MB 106 spiking at 12.98, refer to CCSN Comments on Groundwater Report 2023, dated 24/4/2024.

The following EC and pH results are summarised from tests conducted on 11 & 12 October 2024. These tests were conducted at multiple locations on Flyers Creek, starting so far as possible, in the most northern headwaters for each creek and testing at intervals, subject to access, heading south to a point just before the confluence with the Belubula.

The test results are currently being analysed and compared to tests taken earlier this year. Full analysis will be available in due course.

The sample locations are shown on the map below:

Flyers Creek

		EC	pH
FC 1 avg	Springside	41.3	6.38
FC 2	W'grove		
FC 3	W'grove Bridge	106.0	7.62
FC 4	Cottage	397.4	8.71
FC 5	Panuara Rd Bridge	442.0	8.91
FC 6	Old E'bang Weir	568.0	8.96
FC 7	Harrisville	650.0	8.37
FC 8	Braeburn	605.0	8.87
FC 9	Oakey South	553.0	8.44

Sediment Sample locations FC1- FC9 collected on 11 & 12 October 2024

There is a very clear and consistent pattern emerging of contamination in Flyers Creek.

This contamination is consistent with the IESC, the ITRB and Expert Hydrogeologist reports which all identified the risk of groundwater seepage:

"The IESC notes that there are indications of leakage from the TSFs into the shallow groundwater system due to currently approved activities, with potential for discharge to local surface waters and GDEs." IESC 2023-143

Sources of PFOS at CVO

Since operations began Cadia has received the following PFOS contaminated material:

o Orange waste water 9ML/day 1998 – to date

o Blayney waste water 1 ML/day 1998 – late 2019, confirmed by EPA to be contaminated.

o Biosolids stockpiled for future rehabilitation since 1998 and ongoing

- CVO has received all of Orange treated biosolids since 2007. Orange Council has been testing this material since 2020 (GIPA received from OCC) and has confirmed it is contaminated with PFOS, it is reasonable to assume the waste water will also be contaminated.

o PFOS firefighting foam

- CCSN has been informed that a recent site audit identified 2 drums of PFOS
- Separately CCSN has been told CVO has continued to use up "the stockpile" in recent years

- Information received from the Resource Regulator identified on average a fire underground every 6 weeks between May 2018 – March 2024.

Has the EPA conducted an audit of PFOS use in firefighting at the site?

How have PFOS drums been disposed of, have certificates of proper disposal been provided by CVO and audited by the Regulators?

How are bio solids stock piled on site, is there a sealed and bunded storage area to prevent seepage of contaminants into surrounding water courses?

Cadia Dewatering Plant

CCSN has tested the sediment in Abattoir creek at the following locations.

It is known that PFOS is entering the Cadia site in significant quantities AND as demonstrated by the tests at the dewatering plant that the Cadia slurry is contaminated with PFOS. B1 location sediment result of 1.0 µg/kg is in stark contrast to B2 downstream of 9.4 µg/kg for PFOS.

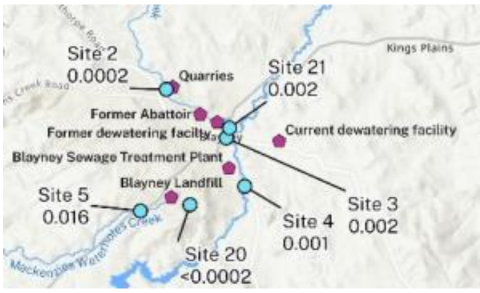

EPA test locations

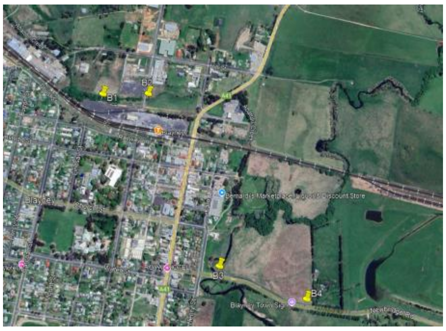

CCSN test locations

Why has the EPA focussed its testing near the old dewatering plant, substantially upstream and well after the site?

What testing has the EPA done of the old dewatering plant site itself?

Livestock Risk

The EPA states in the report relating to testing on 22 and 23 October that:

> "The results to date indicate the risk to livestock is low, but as a precaution, the EPA will be taking soil samples for testing at select properties where livestock graze adjacent to impacted waterways. "

However, the research paper 'Spatio-temporal trends in livestock exposure to per and polyfluoralkyl substances (PFAS) inform risk assessment and management measures' Mikkonen and others 2023 (Attachment 8) found that:

> "sites with mean livestock drinking water concentrations as low as 0.003 µg PFOS/L may exceed the EC ML for PFOS in cattle meat."

The EPA in Victoria co-authored this report.

The requirement for cattle to drink water with a PFOS concentration below 0.003 µg PFOS/L potentially means several producers in the district are at risk of supplying cattle with elevated PFOS levels. There is a meaningful risk of harm to the export cattle industry and contamination of the food chain.

The CCSN has recently tested carp caught at Wongalong and Millamolong, directly south and downstream of the CVO site. These results are summarised as follows:

	Belubula at Wongalong (WONF)	Belubula at Millamolong (East of BFOA)	Millamolong dark pond (West of BCA CON)
PFOS µg/kg	260	250	320

The CCSN believes the presence of contaminated carp in the Belubula and the repeated identification of PFOS in the Belubula at levels above the Victorian EPA threshold for EU export cattle demonstrates there is a very real risk that PFOS is entering the food chain in this district.

Why has the EPA issued no health warnings to users of the Belubula?

On what basis has the EPA determined the risk to livestock is low?

Foam

CCSN notified the EPA of significant foam in the Belubula in July 2024. The EPA collected samples at 2 locations and performed limited testing.

CCSN has now tested multiple samples collected on the Belubula between Bunt Yards Rd bridge and Boonderoo and on Flyers Creek between Errowanbang and the Belubula confluence. This foam is hyper accumulating toxins.

Flyers Creek Sept 2024

Belubula River – August 2024

https://www.abc.net.au/news/2024-08-14/farmers-pull-pfos-chemical-from-belubula-river-nsw-pfas/104193746?utm_campaign=abc_news_web&utm_content=link&utm_medium=content_shared&utm_source=abc_news_web

In true citizen science style, the CCSN has determined that a mix of quick lime (calcium) with diesel and water will form a very persistent foam. Calcium and diesel are present in the tailings in significant quantities (refer Attachment 1).

Is it possible that:

i. the combination of diesel and calcium in the tailings when mixed with water is creating a foam which hyper accumulates the heavy metals and PFOS; ***or***
ii. the PFOS is creating the foam which accumulates the heavy metals, calcium and diesel?

Would alternative (i) above explain why the foam is seen only in an area close to the CVO site and not in the other locations the EPA has identified PFOS in the water.

Would alternative (i) explain why the white stripe is seen only where we have witnessed significant foam events?

Why has the EPA not tested the foam more extensively?

Why has there been no investigation of the chemical reaction that is happening in this section of the Belubula?

White stripe

As stated previously by CCSN (4/10/2024) several landholders have identified a clearly visible white stripe in a localised area, as shown on the map below.

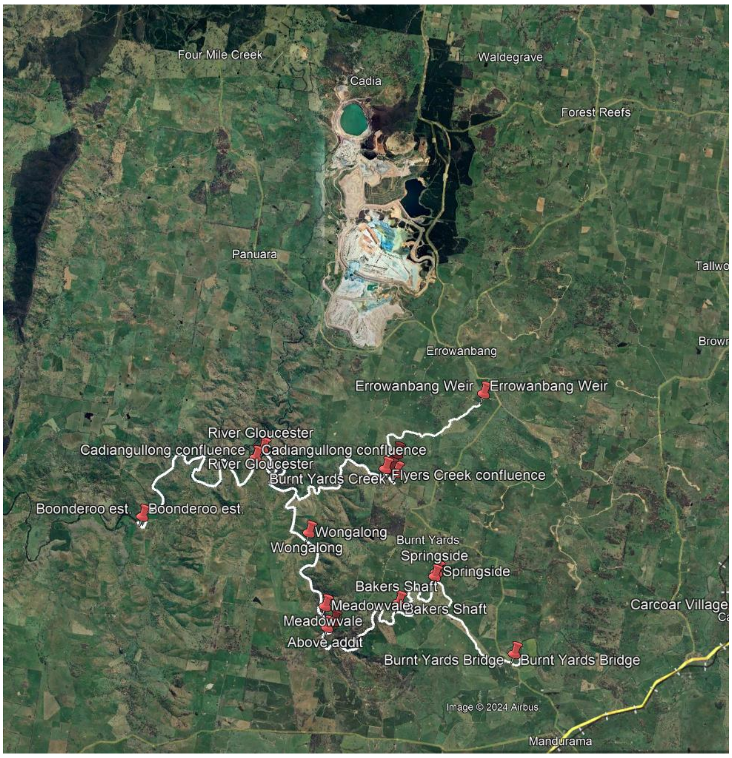

CCSN notes that the EPA identifies this sediment as being from dead diatoms. CCSN believes:

- it is not normal for diatoms to die on mass and leave a visible trail, and
- diatoms can be sensitive to water conditions, such as a flush of contamination.

Is it possible that this white stripe, which appears in the same area as the community has witnessed significant foam events during 2024, is indicative of a contamination event in this section of the river.

There is a visible white stripe formed by sediment depositing along the edge of the Belubula river on rocks, branches and river banks. This stripe seems to start between Ashburtons Bridge (Errowanbang Rd) and Burnt Yards Road bridge (Burnt Yards Rd).

Where has the EPA considered why the diatoms died on mass?

The EPA has focussed on PFAS in the river water. There has been which ignores the foam bergs floating past which we know are hyperaccumulated with contaminants and would be extremely toxic to humans and livestock. Why isn't the EPA developing a testing protocol for the foam?

Where has the EPA taken a multi-factored approach to determine the source of contamination in the Belubula south of CVO?

A multi – factored analysis should include consideration of:

- ***all contaminants including diesel & PFAS, pH, visual observations such as extreme foam levels and white stripe as identified in the field.***
- ***ground water and surface water interaction***
- ***the impact of the alluvial channel and multiple fault lines identified by the ITRB, IESC and CVO's own experts.***
- ***the amount of water flow in each water course.***
- ***the repeated flushing of contaminants in the Belubula as identified by GHD (May 2024).***
- ***the potential toxicity of the foam which is hyperaccumulating toxic chemicals and depositing contaminants on the river bank.***
- ***The impact upon livestock and wildlife in this section of the Belubula which is identified being of high ecological value. Water quality in this area should be suitable for 99% species survival.***

Belubula River at Millamolong February 2022

Reagents used at CVO Concentrator

Reagent	Name	Composition	Use
Lime	Hydrated Lime	>88% $Ca(OH)_2$	pH control
Quicklime	Quicklime	>88% CaO	pH control
Frother	Interfloat F236	10-30% 2-(2-(2-Butoxyethoxy) ethoxy) ethanol & <10% Cyclohexanol	Frothing agent
Collector	CMS2620	>60% Alkyl thiocarbamic acid ester	Collecting agent
Collector2	Aerophine 3418A	50% Sodium diisobutyl-dithiophosphinate	Promoter
Antiscalant	Zalta MA 1143	80 – 90% blended anionic polymers and 10 - 20% mixed caustics (KOH & NaOH)	Antiscalant in process water
Flocculant	FLOPAAM AN 113 SH	89-100% Anionic Polyacrylamide	Conc & tails thickener
PAX	Potassium Amyl Xanthate	60-90% Potassium amyl xanthate	Collector at COF (coarse ore flotation)
Diesel	Diesel HD	Fuels, Diesel 60 – 100% and Fatty acid methyl esters (FAME) 5 – 20%	Collector at COF (coarse ore flotation)

Slope Stability 2007 — Y. Potvin (ed)
©2007 Australian Centre for Geomechanics, Perth, ISBN 978-0-9756756-8-7
https://papers.acg.uwa.edu.au/p/708_18_Sainsbury/

Three-Dimensional Discontinuum Analysis of Structurally Controlled Failure Mechanisms at the Cadia Hill Open Pit

D. Sainsbury *Itasca Australia Pty Ltd, Australia*

F. Pothitos *Ok Tedi Mining Ltd, Papua New Guinea (formerly Newcrest Mining Ltd, Australia)*

D. Finn *Newcrest Mining Ltd, Australia*

R. Silva *Itasca S.A., Chile*

Abstract

The south wall of Newcrest Mining Ltd's Cadia Hill Open Pit experienced a multi-bench (60,000 t) failure during 2006. The observed failure mechanism is a combination of structurally controlled and rock mass failure. The 3DEC code has been developed by Itasca specifically to study complex failure mechanisms involving large numbers of explicit structures (joints, faults) that divide a rock mass into blocks. Slip, separation and rotation along explicit structures can occur, while the individual blocks can also deform and yield.

The following paper details a series of analyses that have been conducted with 3DEC to back-analyse the observed behaviour of the south wall, which happened when mining was at the 505 RL level. The calibrated model has subsequently been used to investigate the behaviour of the south wall after mining has progressed down to the 445 RL level.

1 Introduction

Newcrest Mining Ltd's Cadia Hill Open Pit Mine, near Orange in New South Wales, is located within a complex geological setting. The current pit-slope design is based upon structurally controlled failure mechanisms associated with faults and shear zones that dissect a largely massive rock mass. To date, a number of structurally controlled slope failures have occurred along fault and shear planes with minimal warning. Their scales have ranged from less than one bench height to multiple bench heights.

Routine kinematic, limit equilibrium and two-dimensional numerical modelling analyses are an essential part of any pit-slope design methodology. However, in order to determine accurately the stability of complex wedge-failure mechanisms that involve a combination of rock mass failure in addition to slip along geological structure, a three-dimensional discontinuum analysis is required.

2 Background

Mining commenced at the Cadia Hill Pit during 1997. Figure 1a illustrates Cutback 2, which forms the current pit shell that is being mined. The pit currently measures 1.5 km across, with slope heights ranging from 330 to 490 m. The inter-ramp slope angles range from 35° for the top 100 m in weathered sediments, to 55° for the bottom 135 m of the cutback. The final pit, as illustrated in Figure 1a, currently is designed to be 580 to 720 m deep (Li, 2005).

Following the firing of a trim shot on 9 September 2006, approximately 60,000 t of rock failed in the centre of the south wall from 535 - 656 RL, as illustrated in Figure 1b. There had been 5 mm of rainfall recorded on the day before the failure, and intermittent light rain had occurred during the day of the failure.

A large-scale (trace length > 30 m) shear structure, running sub-parallel to the face at an orientation of 56°/004° formed a basal sliding plane for the failure, as illustrated in Figure 1c. The failure occurred within geological Domain 18, which is comprised of monzonite. The rock mass in this domain is characterised by moderate-to-high RQD values and high intact rock strength (Finn, 2006).

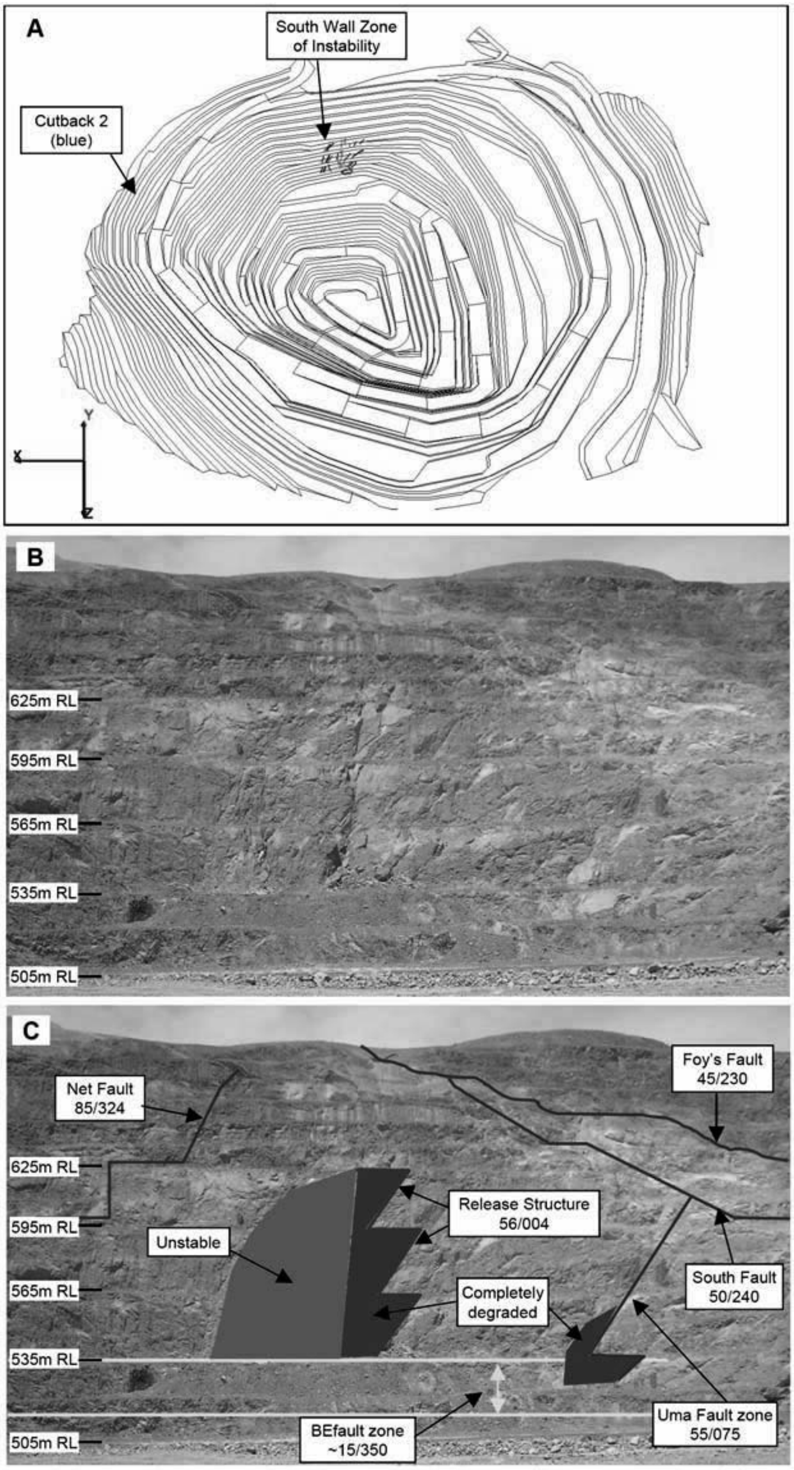

Figure 1 View of the Cadia Hill pit south wall (looking south)

Slope monitoring in the form of survey prisms and radar has been conducted since the beginning of 2006. Prism monitoring identified acceleration in slope displacements during May-June 2006, coincident with mining of the 550 RL level. Increases in slope movements have also been observed to be coincident with blasting and rainfall events.

The south wall failure was a combination of structurally controlled and rock mass failure. The release structure does not form a daylighting wedge that can be analysed using traditional wedge-failure analysis techniques. A conceptual model of the failure mechanism is illustrated in Figure 2, whereby sliding along the shear structure is combined with tensile and shear failure of the rock mass to cause the observed slope failure.

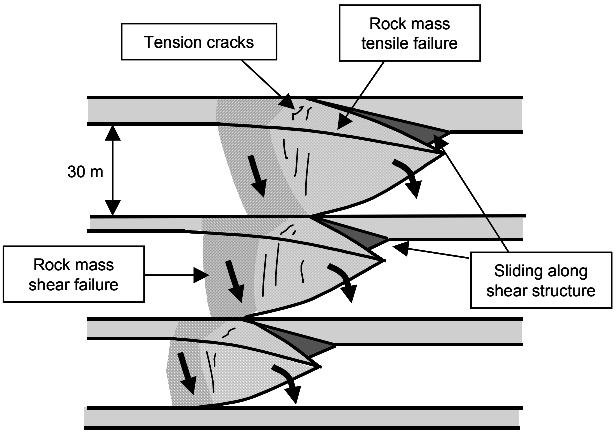

Figure 2 Conceptual model of south wall failure mechanism

Routine two-dimensional limit equilibrium analyses have been conducted for slope design and back-analysis of the multi-bench failure. However, due to the complex nature of the failure mechanism, these traditional methods of pit slope stability analysis have been unable to back-analyse the observed behaviour of the south wall instability.

3 Geotechnical model

The south wall geotechnical model developed for the initial slope design was largely based upon drill hole information with little pit wall exposure data to calibrate the structural model. To manage this uncertainty a large step-in was designed at the 505 RL level. Additional drilling was conducted during late 2005. This additional data was used in conjunction with bench face mapping in order to update the geotechnical model during 2006.

3.1 Geology

The predominant lithology throughout the south wall is monzonite Volcanics and Silurian sediments are also present, associated with faulting.

3.2 Structural geology

The Cadia Hill pit is located on the footwall of several thrust structures. There have been approximately four structural deformation episodes that have contributed to structures having a curvilinear nature, short persistence and varying mechanical properties along the length of the structure. Figure 3 illustrates the structures identified within the 2006 structural model.

Estimates of the shear strength parameters for each south wall structure have been made using field measurements of joint roughness coefficient (JRC) and joint wall compressive strength (JCS). Table 1 presents estimates of the orientation, thickness and shear strength properties for each structure.

Table 1 Estimates of the shear strength parameters for each south wall fault structure

Structure	Dip (deg).	Dip Dir. (deg.)	Thickness (m)	Cohesion (kPa)	Fric. Angle (deg.)
Foy's Fault	45	230	1.0	20	20
South Fault	50	240	0.2	20	25
Net Fault	85	324	0.1	20	25
Uma Fault Zone	55	75	1.0	50	25
BE Fault Zone	15	330	20.0	0	20

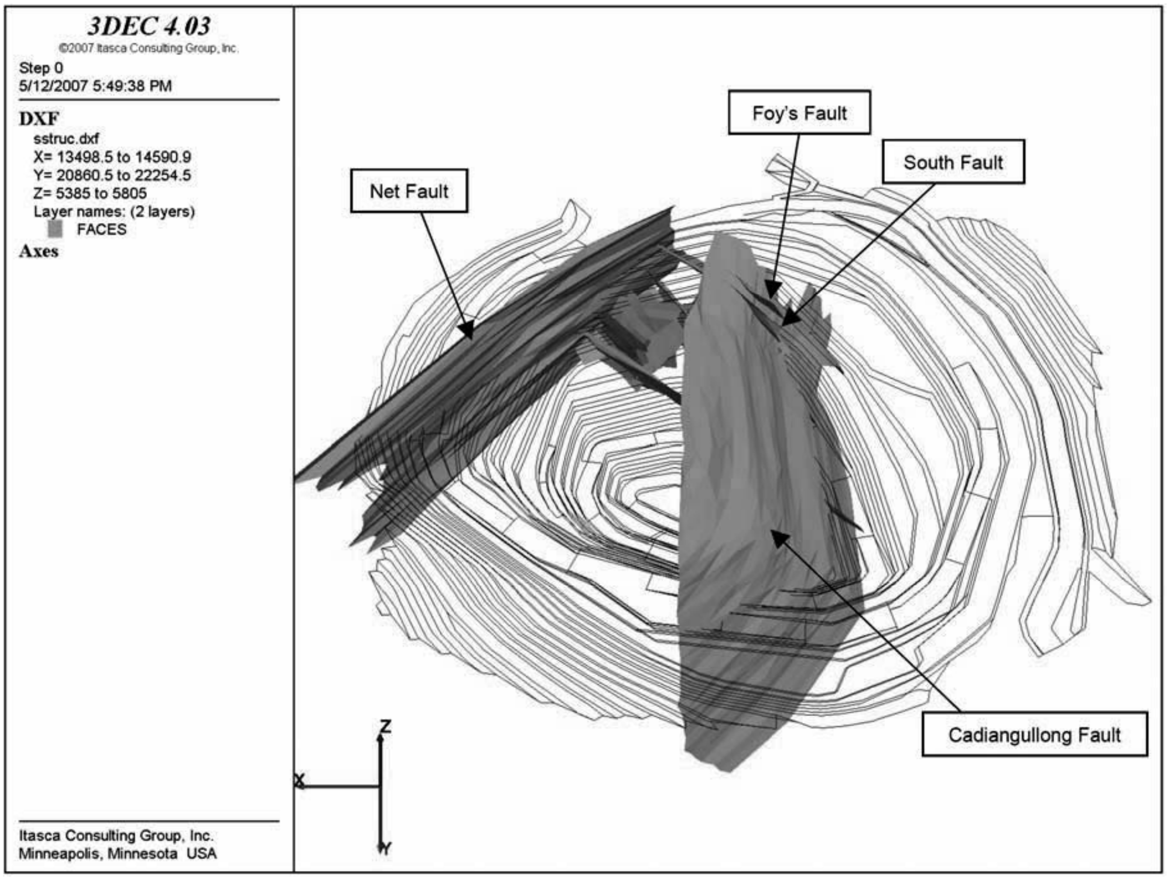

Figure 3 2006 structural model (looking south)

3.3 Rock mass characterisation

The south wall failure occured within monzonite. Laboratory testing of intact samples of this material indicates an unconfined compressive strength (UCS) of 120 MPa. Drillhole and bench face mapping has been conducted to determine the GSI rating for Domain 18. Table 2 presents the rock mass parameters determined for Domain 18 and the BE Fault Zone.

Table 2 Rock mass parameters

Domain/Unit	GSI	σ^{ci} (MPa)	m^i
Domain 18	60–75	120	21
BE Fault Zone	50–60	100	21

For slope stability analysis purposes, it is important to understand that the GSI rating derived at the bench-slope scale needs to be degraded to account for the analysis of inter-ramp and overall pit slopes. This scale-effect phenomenon has been reported by several authors to have a significant impact on rock mass strength, as illustrated in Figure 4. Pothitos (2005) applied a nominal reduction factor of 0.8 to the GSI for analysis of 200 m slopes at the Cadia Hill Pit.

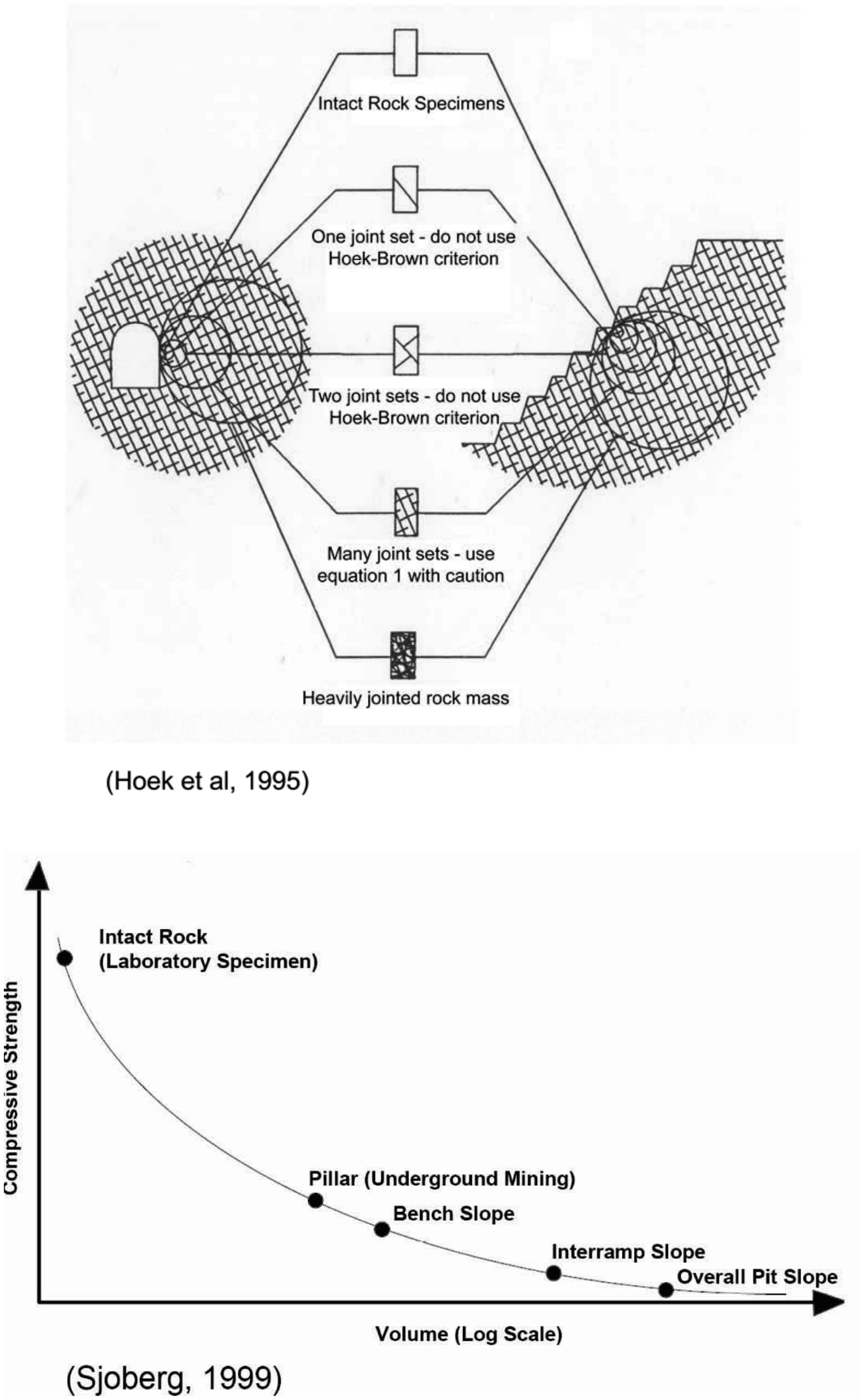

Figure 4 **Rock mass scale effects (after Hoek et al., 1995 and Sjöberg, 1999)**

3.4 Hydrogeology

Two vibrating-wire piezometers are located along the crest of the south wall. The phreatic surface interpreted is illustrated in Figure 5. Both piezometers show no reaction to rainfall events. Water seepage has been evident along the south wall at several levels. Along the 610 RL level, several drainholes produced flow rates of approximately 2 l/s.

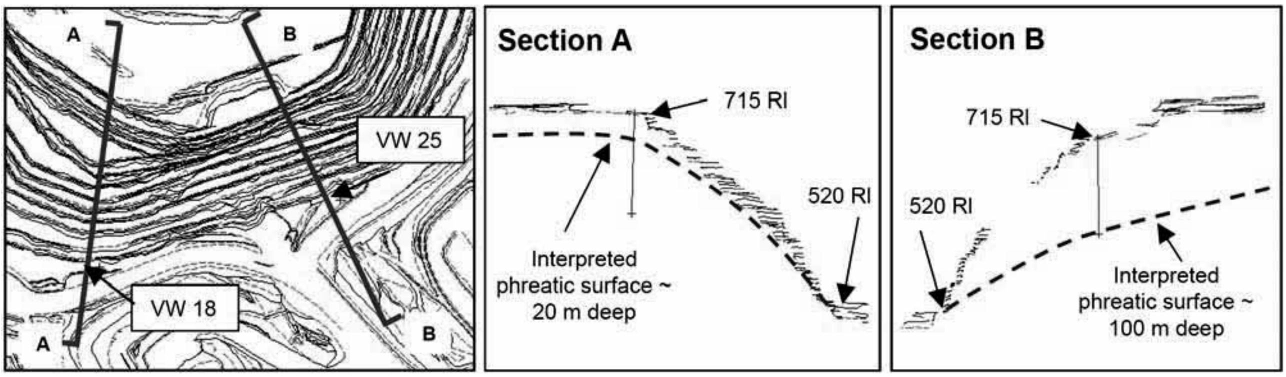

Figure 5 Estimated phreatic surface based upon vibrating wire piezometers

4 Numerical analysis of the Cadia Hill pit south wall

The *3DEC* code (Itasca, 2007) has been developed specifically to study complex failure mechanisms involving large numbers of explicit structures that divide a rock mass into blocks. Slip, separation and rotation along explicit structures can occur, while the individual blocks can deform and yield.

4.1 Model geometry

Figure 6 illustrates the *3DEC* model constructed to simulate the south wall of the Cadia Hill Pit. For the purpose of initial model calibration and investigation of the behaviour of the south wall in the vicinity of the failure, only the south wall to an elevation of 445 RL was constructed. Due to the orientation of the model, displacements at the boundaries were fixed. This limits interpretation of model behaviour close to the boundaries.

The large-scale structures included within the *3DEC* model are illustrated in Figure 6. The BE Fault Zone has been represented as a 20 m thick zone of weaker material bounded by discrete, planar joint surfaces. All other structures have been simplified as discrete planar surfaces.

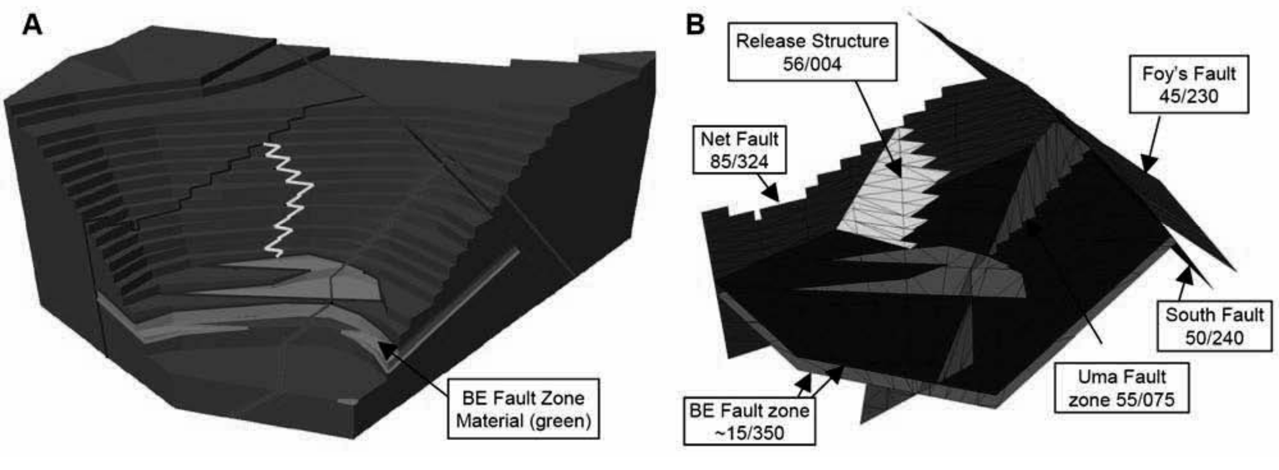

Figure 6 Large-scale structures included within *3DEC* model

4.2 Modelling methodology

A bi-linear Mohr-Coulomb strain-softening constitutive model was used to represent the behaviour of the rock mass. Because the Mohr-Coulomb criterion was used to define the strength of the rock mass, values for cohesion and friction angle were obtained by a least-squares fit to the Hoek-Brown curve. A bi-linear fit was obtained over a range in confining stress from 0 to 1 MPa and 1 to 5 MPa. An example of a bi-linear curve for a material with a GSI of 50, σ_{ci} of 120 MPa and m_i of 21 is illustrated in Figure 7.

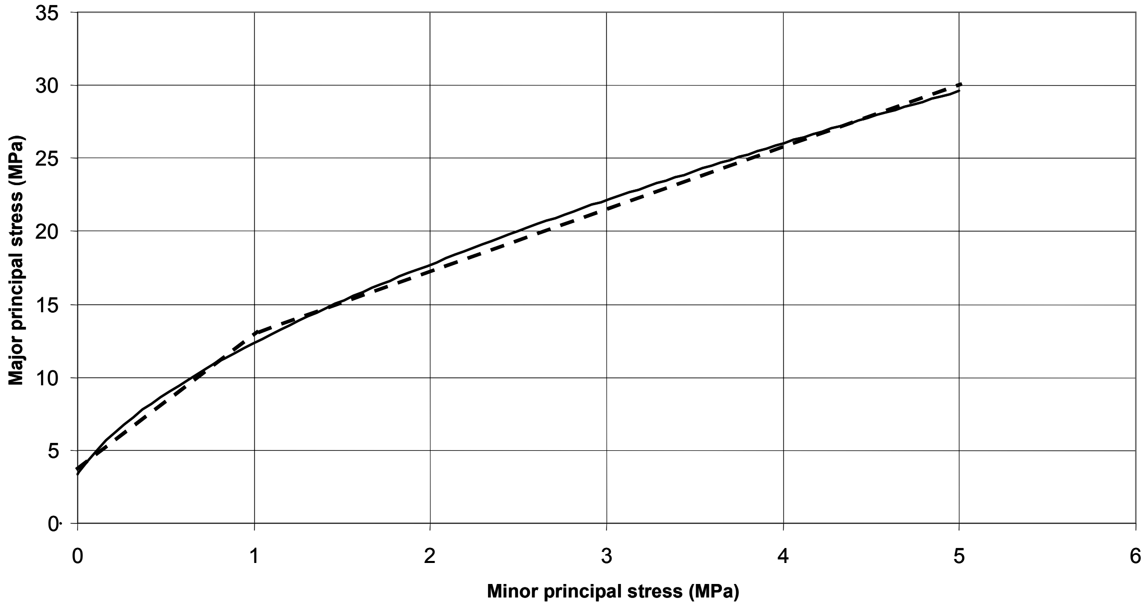

Figure 7 Relation between major and minor principal stresses for Hoek-Brown (solid line) and equivalent bi-linear Mohr-Coulomb (dashed line)

The specification of ductile or brittle behaviour in a numerical model is a very important consideration, as brittle materials tend to undergo progressive collapse much sooner after yielding begins. Ductile materials, on the other hand, are likely to remain stable well after yielding begins. For this reason, a strain-softening model has been used to represent the post-peak strength degradation that accompanies failure of the south wall rock mass.

Sjöberg (1999) states that strain-softening model results are dependent on the model grid used and recommends that strain-softening models should not be used for quantitative rock-slope stability analysis. However, advances in the understanding of strain-softening mesh dependency (Sainsbury and Urie, 2007), together with calibration of the strain-softening parameters to observed slope behaviour allows the use of such models in routine rock-slope stability analysis. Hajiabdolmajid and Kaiser (2002) suggest that a strain-softening material model must be used to simulate accurately the behaviour of rock slopes in which the candidate failure surface is not completely structurally controlled (i.e. failure of intact rock, asperities and rock bridges are involved).

Figure 8 illustrates the results of a simulated *3DEC* UCS test on a 10 × 10 × 10 m rock mass sample with a GSI of 50, σ_{ci} of 120 MPa, m_i of 21 and D of 1.0. The modelling methodology causes localization along shear bands whereby the cohesion and tensile strength have degraded from the intact value to zero. This is the same behaviour observed in physical UCS tests. The strength of the rock mass was degraded by means of gradual reductions in the cohesion and tensile strength with plastic strain (ε^{s}_{crit}). The cohesion and tensile strength parameters were reduced to zero.

There is currently no a priori way to estimate the value for the critical plastic strain of a rock mass. In order to provide a more robust assessment of the rock mass strength, modulus, brittleness and scale effect of the different rock mass domains at the Cadia Hill Pit, it is planned to investigate rock mass behaviour with the Particle Flow Code (PFC) (Itasca, 2005).

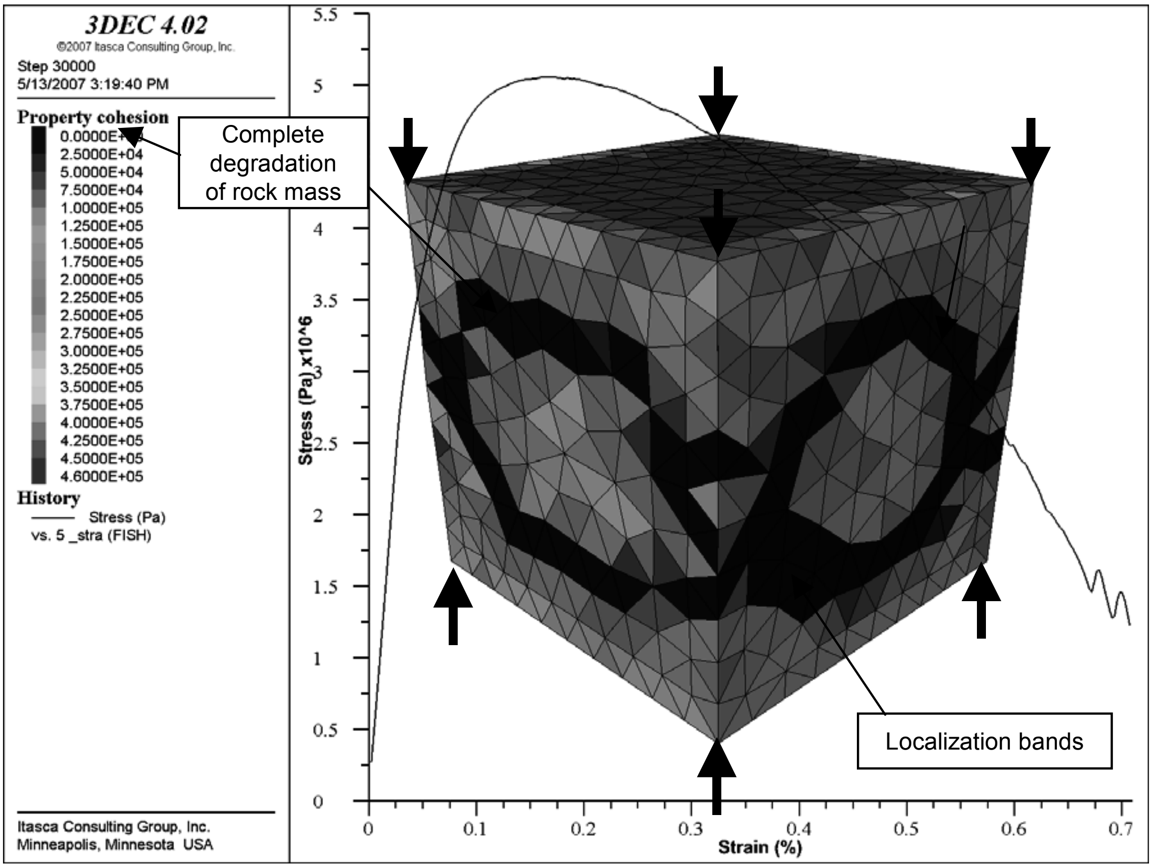

Figure 8 Simulated UCS test on 10-m rock mass sample with GSI of 50, σ_{mi} of 120 and m_i of 21

4.3 Material properties

The rock masses simulated throughout this modelling exercise are assumed to behave as a homogeneous, isotropic material. Table 3 outlines the estimates of the material properties used to simulate the south wall rock mass.

Table 3 Estimates of Mohr-Coulomb parameters for the south wall rock mass

Class	σ_{ci} (MPa)	GSI	m_i	D	Density (kg/m^3)	Young's Modulus (GPa)	Poisson's ratio	Cohesion (MPa)	Friction Angle (deg.)	Cohesion (MPa)	Friction Angle (deg.)	Tension (kPa)
								σ_3 = 0-1 (MPa)		σ_3 = 1-5 (MPa)		
Lower bound	120	50	21	1.0	2700	4.9	0.25	0.46	50	1.26	37	50
Best estimate	120	57.5	21	1.0	2700	9.0	0.25	0.63	54	1.55	41	100
Upper bound	120	70	21	1.0	2700	15.8	0.24	1.27	59	2.36	48	320

The rock mass material within the BE Fault Zone was simulated with separate material properties. Table 4 presents lower-bound and best-estimate properties used to simulate the BE Fault Zone rock mass.

Table 4 Estimates of Mohr-Coulomb parameters for the BE fault zone rock mass

Class	σ_{ci} (MPa)	GSI	m_i	D	Density (kg/m^3)	Young's Modulus (GPa)	Poisson's ratio	Cohesion (MPa)	Friction Angle (deg.)	Cohesion (MPa)	Friction Angle (deg.)	Tension (kPa)
								σ_3 = 0-1 (MPa)		σ_3 = 1-5 (MPa)		
Lower bound	100	40	21	1.0	2700	5.0#	0.25#	0.30	41	0.88	29	16
Best estimate	100	50	21	1.0	2700	5.0	0.25	0.43	48	1.18	35	41

The Mohr-Coulomb parameters used to simulate each fault structure are presented in Table 5.

Table 5 Estimates of Mohr-Coulomb parameters for fault structures

Class	Fault	Normal stiffness (Pa/m)	Shear stiffness (Pa/m)	Cohesion (kPa)	Friction Angle (deg).	Tension (kPa)
Best estimate	Foy's	1.00E+10	1.00E+09	20	20	0
Best estimate	Net	1.00E+10	1.00E+09	20	25	0
Best estimate	Uma	1.00E+10	1.00E+09	20	25	0
Best estimate	South	1.00E+10	1.00E+09	50	25	0
Best estimate	BE	1.00E+10	1.00E+09	0	20	0

4.4 Pre-mining stresses

A series of HI Cell and acoustic emission (AE) stress measurements have been taken underground at the nearby Ridgeway Mine. Based upon these measurements, the vertical stress at the Cadia Hill Pit was assumed to be lithostatic (assuming a density of 2700 kg/m^3). The pre-mining stresses used throughout the analyses are summarised in Table 6.

Table 6 Pre-mining stresses used in analyses

Principal stress	Stress-depth relation (MPa)	Orientation
σ_v	Overburden (2700 kg/m^3)	Vertical
σ_H	1.72 x σ_v	East-west
σ_h	1.25 x σ_v	North-south

5 Calibration of south wall failure after mining of the 505 RL bench

In order to calibrate the *3DEC* model to the observed behaviour of the south wall failure after mining of the 505 RL bench, a series of analyses was conducted whereby the upper-bound (GSI = 70), best-estimate (GSI = 57.5) and lower-bound (GSI = 50) rock mass properties were simulated. The best-estimate properties for the BE Fault zone (GSI = 50) were simulated, while best-estimate joint properties and phreatic surface conditions also were applied to the models.

The south wall failure mechanism observed throughout the modelling exercise is illustrated in Figure 9. Sliding along the non-daylighting release structure, combined with tensile failure of the rock mass, causes the observed multi-bench slope failure.

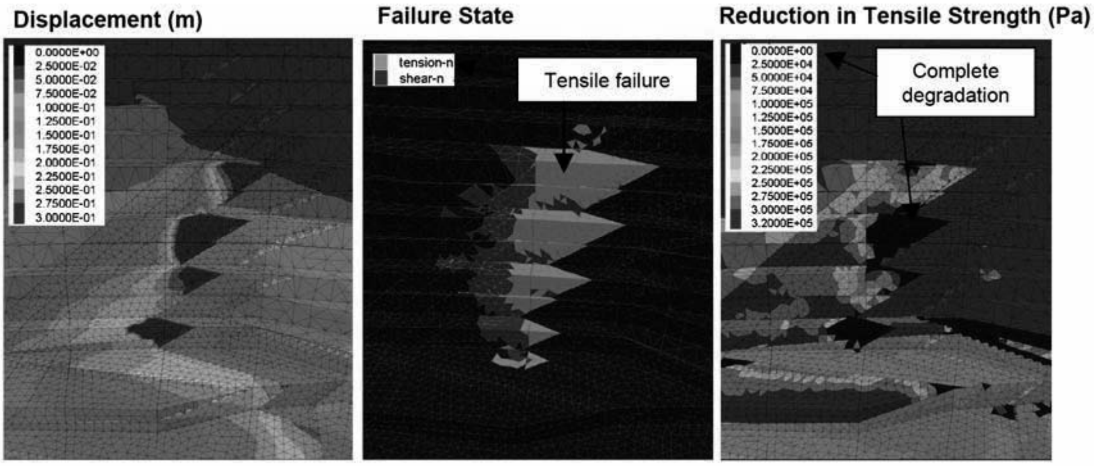

Figure 9 Failure mechanism predicted with *3DEC*

The best-estimate rock mass properties, with a GSI of 57.5, provide a good calibration to the observed behaviour of the south wall failure. Figure 10 illustrates a comparison between the observed and predicted conditions of the south wall after mining of the 505 RL bench. Together with the main multi-bench failure, the bench-scale failure associated with the Uma Fault zone is also predicted within the *3DEC* model.

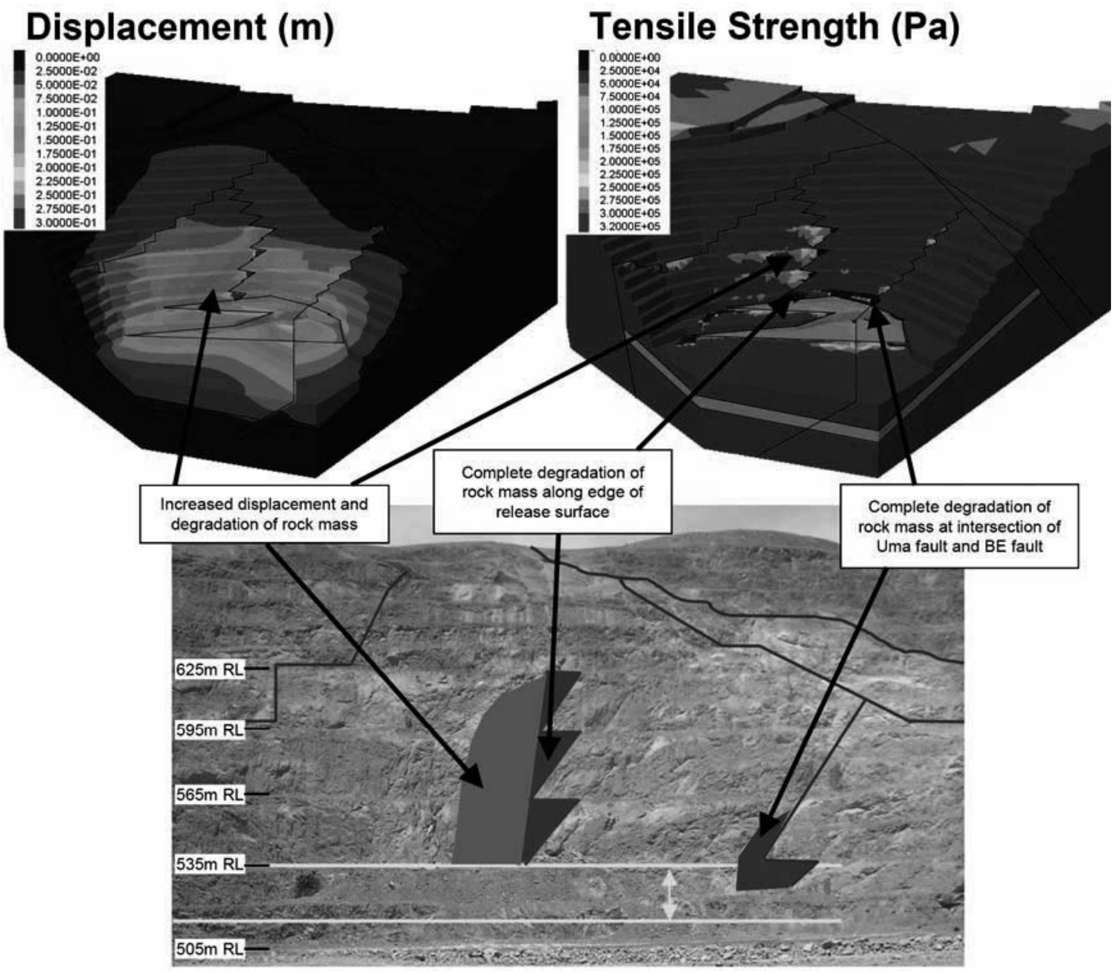

Figure 10 Comparison of observed and predicted behaviour of south wall with a GSI of 57.5

Histories of slope displacements have been measured at the same locations as monitoring prisms with the *3DEC* model. A comparison between the measured and predicted slope displacements is illustrated in Figure 11. Because real time is not simulated within the numerical model, the model displacements have been scaled to the excavation sequence of the south wall. A good correlation has been obtained between the measured and predicted slope displacements.

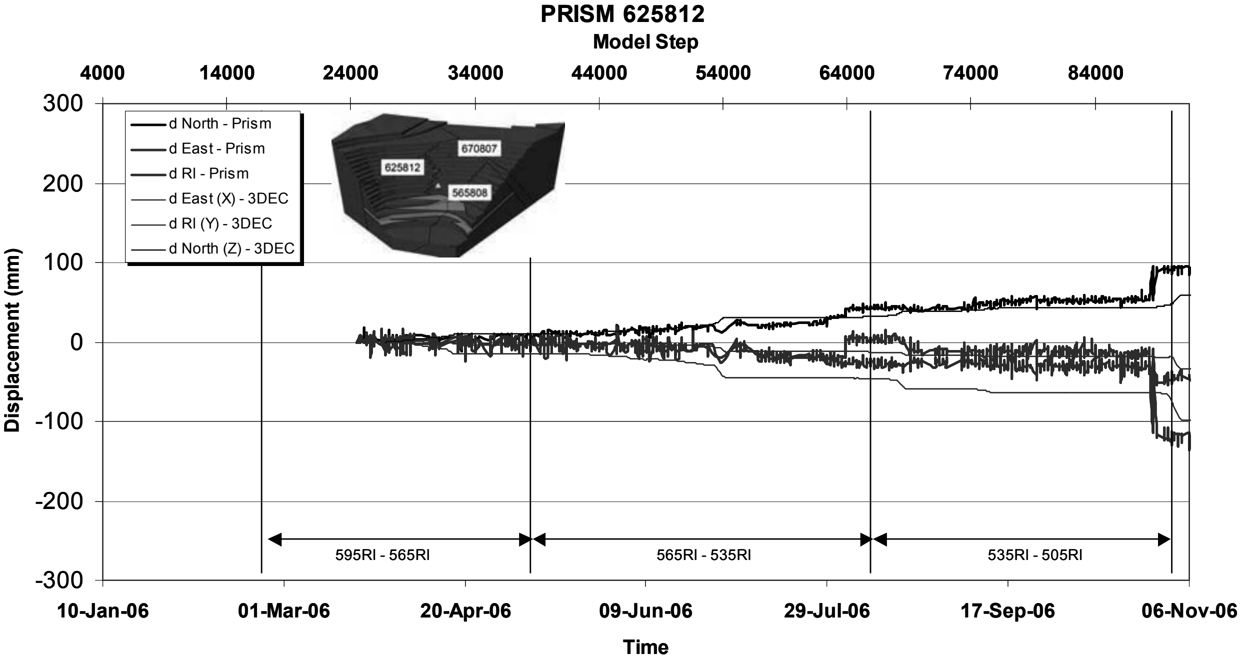

Figure 11 Comparison of actual and predicted slope displacement at prism 625812 location

6 Analysis of south wall behaviour after mining of 445 RL Bench

Due to the good calibration with the observed behaviour of the south wall failure, the best-estimate (GSI = 57.5) rock mass model was used to investigate the likely behaviour of the south wall after mining of the 445 RL bench. Figure 12 illustrates the slope displacement and reduction in tensile strength in the area of the failure. A minor increase in displacement and yielding is observed, but the vertical extent of the failure zone is predicted to remain confined to an approximate 60 m width between 625 RL and 535 RL, bounded by the original release structure.

Figure 13 illustrates the predicted slope displacements as mining progresses from the 505 RL bench to the RL bench. The 625812 prism location is predicted to become unstable during mining between the 475 RL and 445 RL benches.

7 Analysis of 475 RL bench failure

On 23 March 2007, a 35,000 to 40,000 t failure occurred on the 475 RL bench face, in the southwest corner of the Cadia Hill Pit. The failure was triggered by significant rainfall immediately before the time of failure.

Inspection of the failure, reported by Lowther (2007), identified a shallow-dipping shear structure (25º/082º) associated with the BE Fault zone that formed the basal plane of the failure. The failed volume of rock was observed to be intensely jointed.

Although the *3DEC* models analysed do not account for the pore pressures and increased rock-mass density caused by significant rainfall surface runoff, as illustrated in Figure 14, the best-estimate rock mass model indicates a zone of increased displacement and yielding associated with the BE Fault zone on the 475 RL bench face, in the exact location as the observed failure. Analysis of the 475 RL bench failure highlights how a *3DEC* modelling approach can be used as a predictive tool to identify problem areas within the mining sequence.

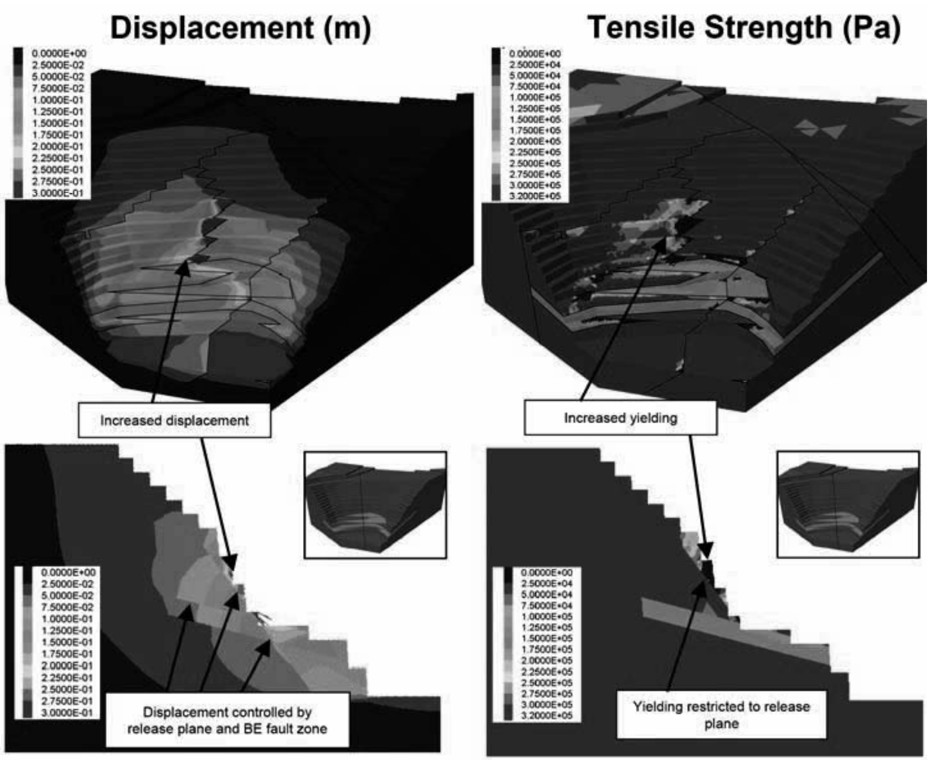

Figure 12 Displacement and reduction in tensile strength after mining of 445 RL bench

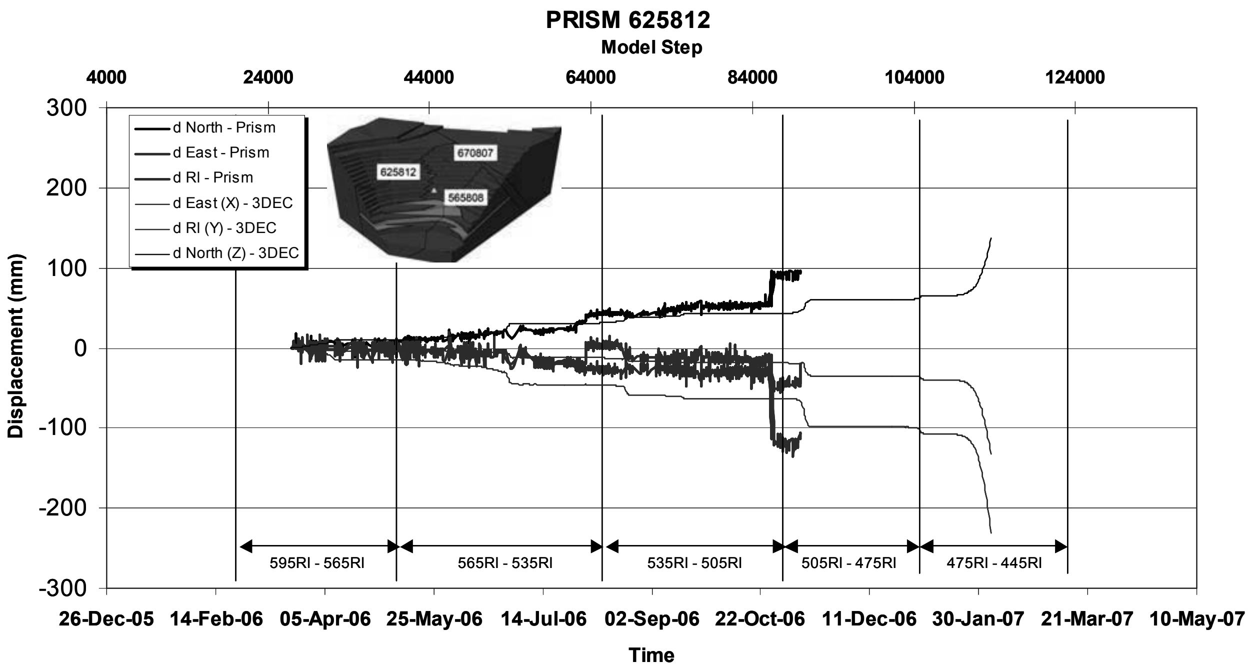

Figure 13 Comparison of actual and predicted slope displacement at prism 625812 location after mining of 445 RL bench

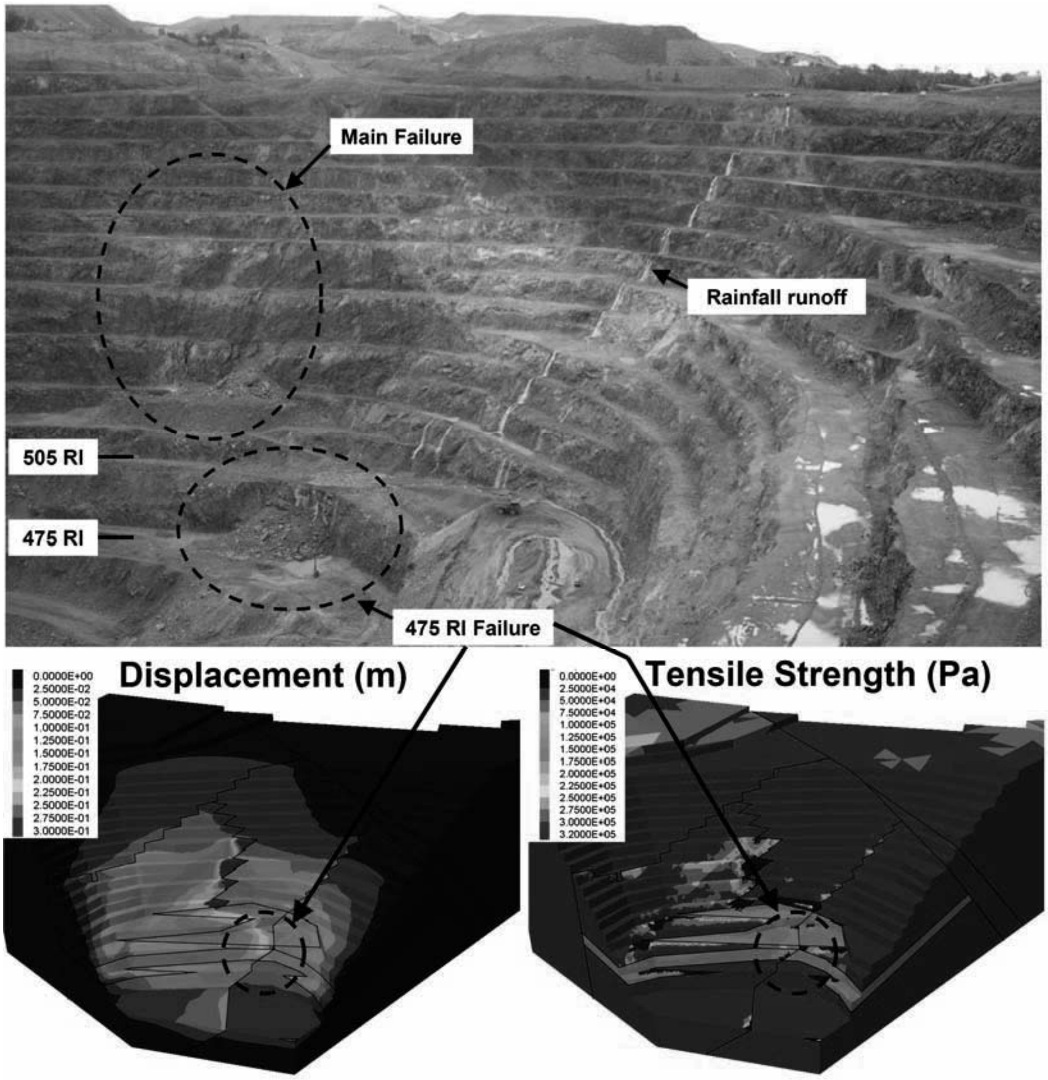

Figure 14 Analysis of 475 RL bench failure

8 Discussion of uncertainties and limitations

In order to understand the sensitivity of the south wall slope behaviour to the different model parameters, a series of analyses was conducted whereby the structure properties, phreatic surface, BE Fault zone material strength and slope angle were varied independently over reasonable upper and lower bound ranges. A single analysis was also conducted in order to investigate the combined effect of the lower-bound model parameters. The combined worst case slope conditions have a significant effect upon the extent of the south wall failure, whereby failure is predicted to propagate to the west, terminating at the Net Fault, as illustrated in Figure 15. Based upon calibration of the observed south wall failure after mining to the 505 RL bench, this condition clearly represents an overly conservative analysis of the slope behaviour.

Analysis of pit slope behaviour with a *3DEC* modelling approach is limited by representation of the explicit structures within the model. Without prior knowledge of the location and orientation of the 56°/004° release structure, modelling would not predict the observed behaviour.

Calibration of the south wall failure indicates that the rock mass strength required to match the measured and observed behaviour of the failure (GSI = 57.5) is less than the rock mass strength derived from drill hole and bench-face mapping (GSI = 60-70). This observation is consistent with the rock-mass scale effects reported by Hoek et al. (1995) and Sjöberg (1999) for the simulation of large-scale rock mass behaviour.

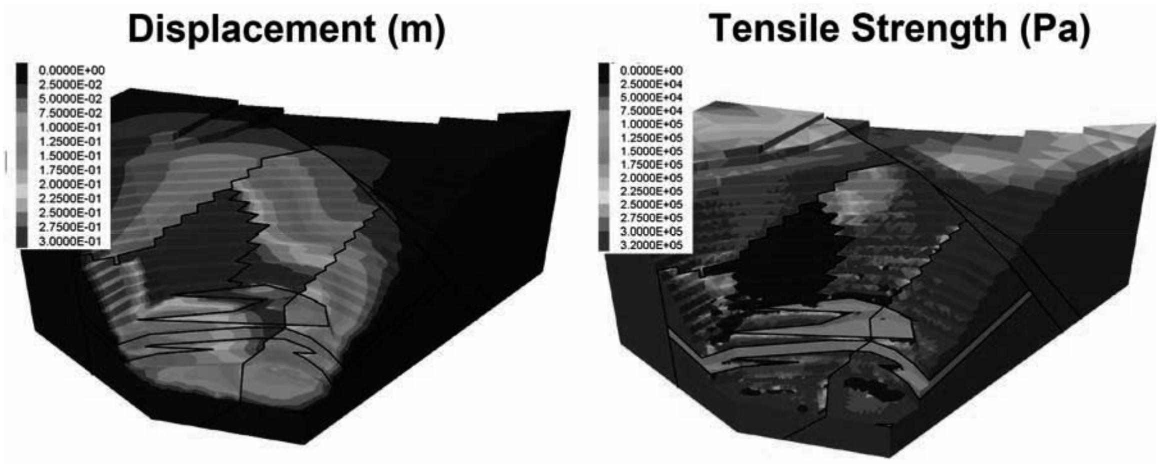

Figure 15 Slope displacement and reduction in tensile strength after mining of 445 RL bench (simulated combined worst-case rock mass, structure and phreatic surface conditions)

9 Conclusions

A calibration exercise has been conducted with the three-dimensional distinct element code *3DEC* to simulate the observed south wall failure at the Cadia Hill Pit. The numerical model provides a good correlation to the behaviour of the failure after mining of the 505 RL bench. Predictive analysis of the behaviour of the south wall after mining of the 445 RL bench indicates a minor increase in displacement and yielding in the area of the failure, but the extent of failure zone is predicted to remain confined to an approximate 60 m width between 625 RL and 535 RL, bounded by the original release structure.

The best-estimate rock mass model indicates a zone of increased displacement and yielding associated with the BE Fault zone on the 475 RL bench face, in the exact location as a 35,000 to 40,000 t failure that was triggered by significant rainfall runoff. Although the *3DEC* models analysed do not account for the pore pressures and increased rock mass density caused by significant rainfall surface runoff, analysis of the 475 RL bench failure highlights how a *3DEC* modelling approach can be used as a predictive tool to identify problem areas within the mining sequence.

Acknowledgements

The management of Newcrest Mining Limited, Cadia Valley Operations is acknowledged for permission to publish this paper.

References

Finn, D. (2006) Instability report south wall of the pit, Cadia Valley Operations Internal Memorandum.

Hajiabdolmajid, V. and Kaiser, P.K. (2002) Modelling slopes in brittle rock. NARMS-TAC 2002: Mining and Tunneling Innovation and Opportunity, Vol. 1, R. Hammah, W. Bawden, J. Curran, and M. Telesnicki (eds). Toronto: University of Toronto Press, pp. 331-338.

Hoek, E., Kaiser, P.K. and Bawden, W.F. (1995) Support of Underground Excavations in Hard Rock. Rotterdam: Balkema.

Itasca Consulting Group, Inc. (2007) 3DEC (Three-Dimensional Distinct Element Code), Version 4.02. Minneapolis.

Itasca Consulting Group, Inc. (2005) PFC2D (Particle Flow Code in Two-Dimensions), Version 3.1. Minneapolis.

Li, T. (2005) Geotechnical Engineering at Newcrest Mining, Australian Centre for Geomechanics Newsletter, Vol. 25.

Lowther, R. (2007) Geomechanical Instability Report – 475 RL Major Rainfall Triggered Rockfall Event, Cadia Valley Operations Internal Memorandum.

Sainsbury, D.P. and Urie, R. (2007) Stability Analysis of Horizontal and Vertical Paste Fill Exposures at the Raleigh Mine, Minefill 2007 – Innovation and Experience. Proceedings of the 9th International Symposium on Mining with Backfill, Montreal, May 2007, CD Proceedings, Paper No. 2527, CIM, Montreal.

Sjöberg, J. (1999) Analysis of Failure Mechanisms in High Rock Slopes, Doctoral Thesis, Department of Civil and Mining Engineering, Division of Rock Mechanics, Luleå University of Technology, 1999:01/ISSN: 1402-1544, January.

CCSN - Appendix 5d

CVO Groundwater Report 2023
CCSN Comments – 24 April 2024

For the purpose of investigating the potential impact upon the quality of groundwater from CVO, bores have been grouped by geographic location and proximity to the mine. Many of these bores, particularly in the NE of Cadia and S of STSF groups are outside the Mine Licence area. Data provided for 2023 has been grouped accordingly and comparison made to the average of all data over the year for each bore and the range of data points, refer Attachment 1.

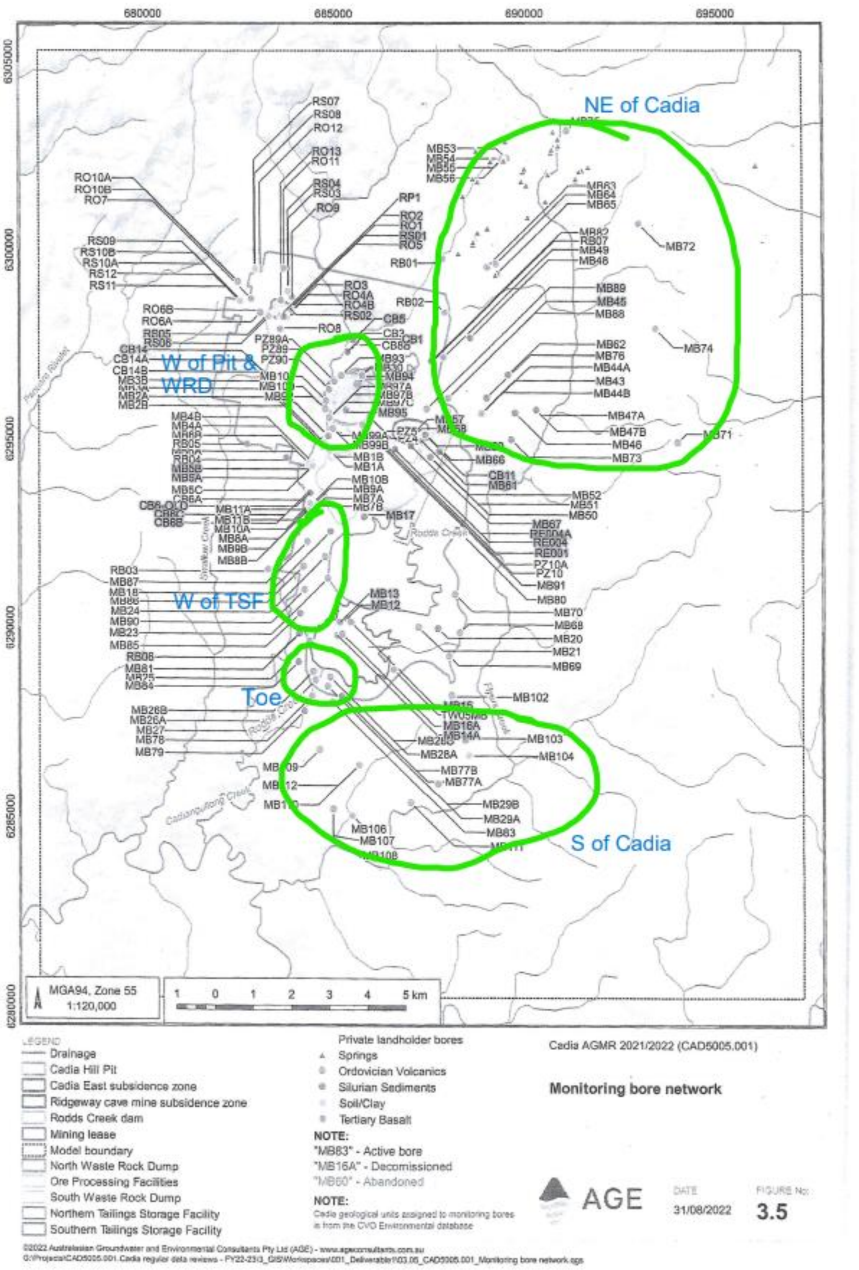

Comparison of CVO bore testing results with prior year data is complicated by the limited data reported by the company, regular changes to the way data is presented and changes to the labelling of bores across the site. However, the 1995 Cadia Gold Mine EIS Vol 3 includes some data for 47 bores across the Mine Licence area, Attachment 2 Location of Monitoring Sites (Ground Water). This data was collected during the period

1993 – 1995. Comparison was also made to the ANZECC guidelines; however, it should be noted the guidelines being used by Cadia are now out of date.

Comparison of Average pH and Sulphates by Area

	NE of Cadia	S of STSF	Toe of STSF	W of TSFs	W of Pit & WRD	CVO 1995	ANZECC
pH	5.69	9.70	7.05	6.67	6.67	7.56	
pH range	4.6-9.0	6.58-12.98	6.05-8.27	6.16 – 7.24	6.23 – 7.41	6.74-9.00	6.5-8.5
Sulphate	4.78	63.45	483	740	1477	325	
Sulphate range	1-30	8-236	201-1150	178-1240	122-2650	5-1424	1000

This comparison has resulted in the following observations:

1995

CVO has published very little base line data, however the 1995 EIS, Cadia Gold Mine Environmental Impact Statement includes data for 47 bores in the Mine Licence area. This data identified that:

- The groundwater was generally of a good quality, fit for livestock and release into the environment.
- pH was within ANZECC guidelines except for ST 38 - pH 9.00, ST 44 – pH 8.90
- sulphates were generally within ANZECC guidelines except for ST 9 – 1010, ST 23 - 1424 and ST28 – 1205

2023

Based upon data published in the Cadia Annual Groundwater Monitoring Review 2023, the ground water is generally ***not*** fit for livestock or release into the environment.

- NE of Cadia, except for MB 53 – pH 6.88 the pH is well below the livestock threshold.
- S of STSF – several bores report very high levels of alkalinity, MB 103, MB 104, MB 105, MB 106.
- Toe of STSF – whilst these bores close to the tailings dams have a pH within guidelines, they contain a cocktail of toxic metals including several with mercury.
- W of TSFs – several bores report low pH, others have high sulphates. Only four bores are within livestock drinking water guidelines for pH and sulphates MB 25,81,84 and 85.
- W of Pit and WRD – most of these bores have extremely high sulphates. Acid Mine Drainage develops as the sulphates combine with oxygen and water to become sulphuric acid, a pre cursor to bacterial AMD. High levels of sulphate may be an indicator of the potential level and volume of acidification yet to develop.

NE of Cadia

This group of bores is to the north and east and downhill from the North Waste Rock Dump and South Waste Rock Dump. Waste rock dumps are considered to be a high-risk source of Acid Mine Discharge (AMD) (often worse than tailings dams) due to the non- homogenous nature of the dump and high levels of ammonium nitrate which triggers production of AMD.

- The lowest pH appears to be in bores closer to CVO and closer to the waste rock dumps. MB54 – 5.29, MB 62 – 4.88, MB 63 4.59, MB 64 – 5.15
- Based upon CVO data there has been a material decrease in pH over the period since 2015.

pH Trends over time

pH	MB 71	MB 72	MB 74
2012	6.70	7.90	7.25
2015	6.91	7.57	7.36
2022 (avg)	5.84	6.23	6.48
2023 (avg)	5.45	5.67	5.41

Source: CVO Annual Groundwater Monitoring Review

S of STSF

There is a cluster of bores between the STSF and the Belubula River reporting very significant levels of alkalinity.

- MB 103, MB 104 and MB 109 are closer to the STSF and show significant fluctuations in pH.

pH	07/22	09/22	10/22	11/22	12/22	01/23	02/23	Avg
MB 103	10.8	11.1	9.99	8.28	8.14	8.29	8.26	9.27
MB104	7.76	7.68	10.81	10.43	10.1	6.58	8.33	8.81
MB109	6.74	11.3	6.68	6.76	6.85	10.26	6.94	8.22

MB 105	8.99	11.89	11.52	10.90	9.51	11.06	8.01	10.27
MB106	12.06	12.47	12.07	11.25	11.2	11.35	12.98	11.91

The tailings dams have been embargoed for 6 years, why would there be a flow of highly alkaline water from the tailings dams? The mine process water is pH 12.

In 2007 CVO commissioned Itasca Australia Pty Ltd to investigate Failure Mechanisms at the Cadia Hill Open Pit (Attachment 3). At that time CVO was concerned by unpredicted failures of the open pit benches. Itasca identified that a series of significant faults run through the pit.

Three-Dimensional Discontinuum Analysis of Structurally Controlled Failure Mechanisms at the Cadia Hill Open Pit — D. Sainsbury, et al.

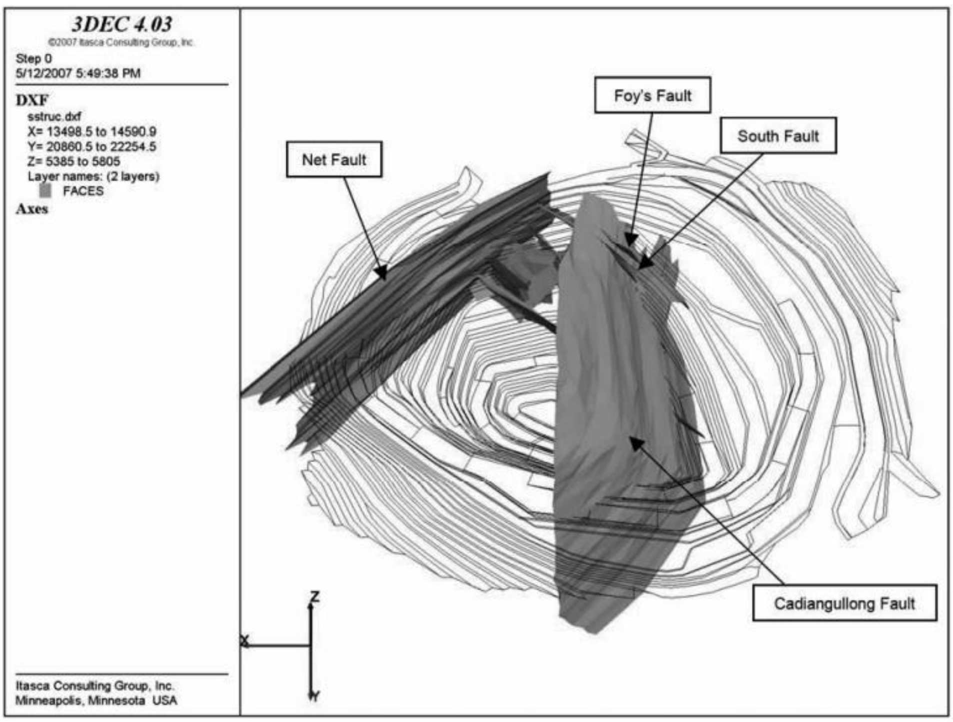

Figure 3 2006 structural model (looking south)

The 2009 EIS for the Cadia East Project identified numerous faults running through the site, including those identified by Itasca as running through the Pit.

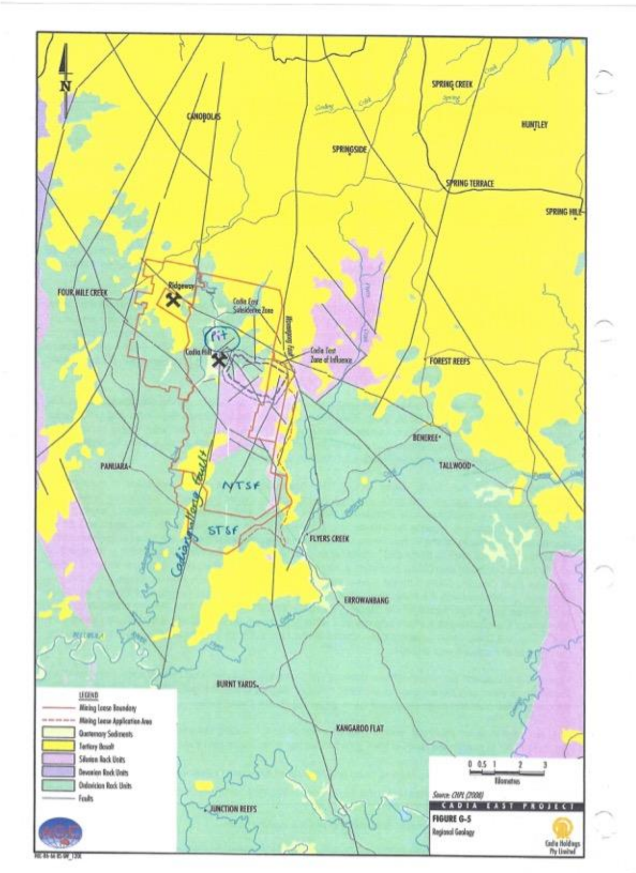

"The Cadiangullong Fault is a 1 m - 10 m wide zone of black cataclasite gouge and intensely fractured wall rocks
The Foys Fault is a 20 m wide zone of intensely fractured siltstone.

The Gibb Fault is a 0.5 m - 2 m wide zone of milled rock-matrix breccia and clay gouge.

The Copper Gully Fault is planar and narrow and has a reddish clay gouge.

The above observations indicate that the faults filled with clay gouge would act as barriers to movement of water, while the faults with breccia fil and fractured wall rocks would likely be conduits for groundwater flow.

The Warrengong Fault is a north-south trending, near vertical structure located approximately 1 km to the east of the Cadia East deposit (Figure G-5). It is considered to be an extensive regional structure"

The Cadiangullong fault which has been identified as "fractured rock" runs through the area to the south of the STSF, possibly bringing with it highly alkaline mine process water.

The 2019 ITRB Report on NTSF Embankment Failure 'Appendix F Hydrogeology' identifies a major fault line as a potential contributor to the failure of the dam. This fault runs north south, close to the slump. If the STSF is used how will CVO prevent the process water from seeping into the fault line and contaminating outside the ML area.

Data for the high alkalinity readings have been included in the Cadia Annual Groundwater Monitoring Review for both 2021/2022 and 2022/2023 water years. However, there has been no comment made in the report on these readings.

Toe of STSF
Although the water seeping at the toe of the STSF is relatively neutral in terms of pH it contains a cocktail of heavy metals including mercury.

West of STSF
It appears that the pit is leaking directly into the bores close to it, The 2023 Groundwater Report S 4.2.2.1. states
"… strong correlation of rising groundwater with pit levels that has been observed in MB94, MB95 and MB 96 is as expected."
4.2.2.2
"groundwater levels at MB 95 started to consistently match the water level in Cadia Hill Pit (from March 2019)"
Similar increases in arsenic concentrations…..at bore MB 94, where groundwater levels also suggest connectivity to the Cadia Hill Pit lake."
"Some risk that ground water may migrate from the pit to Cadiangullong Creek through transmissive fractures and geological structure"

Bores to the West of the mine operations have high levels of multiple elements. Bores are being tested at a level below Cadiangullong Creek. CVO repeatedly concludes that because there is no evidence of contamination in the creek and there is no evidence of contamination moving beyond the mine site, there is no further contamination. A conclusion of no contamination beyond the creek can only be reached if CVO has drilled bores beyond the creek and tested for contamination.

Other Comments
In 2018 CVO tested the sediment in the creeks surrounding CVO for hydrocarbons. ALS identified hydrocarbons in Rodds Creek and Flyers Creek. No comment was made about these test results in the Surface Water Management Report and no further testing of sediments for these materials has been reported.

CCSN Questions
There has been a significant change in the quality of groundwater in the district during the period 1995 – 2023.

Is it possible we are seeing AMD affecting the bores to the NE of the site, was there a trigger event after 2015?

Was the base of the waste rock dumps clay lined to reduce the risk of AMD seeping into one of the many fault lines?

In the Southern area towards the Belubula:
- is it possible that contaminated water is "flushing through" the bores closest to the tailings dam?
- Is the highly alkaline water in these bores coming directly from the pit (as opposed to seepage or discharge from the TSF)?

If contaminated water is moving along the fault line, how far is it going and where does it eventually accumulate? What is the size of the plume and how can this be determined?

Have bores been tested for hydrocarbons and other anthropogenic materials?

Appendix F
Hydrogeology

Klohn Crippen Berger

Ashurst Australia

ITRB Report on NTSF Embankment Failure

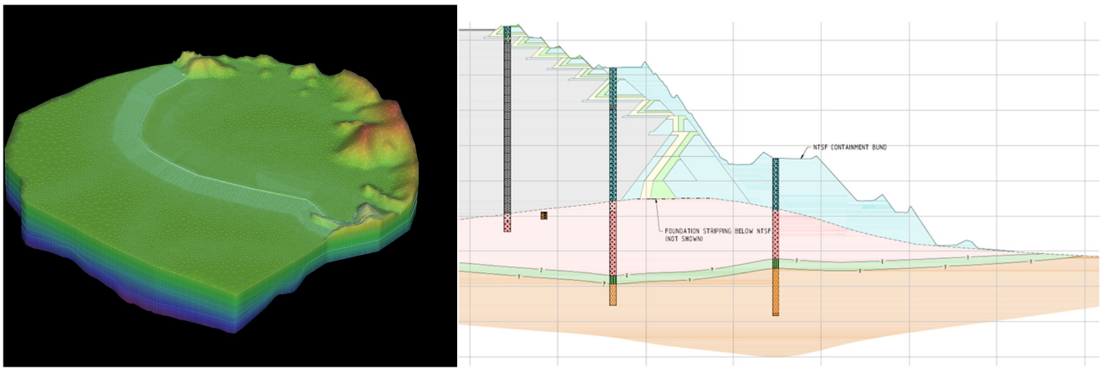

Hydrogeology Assessment Report

CANADA'S BEST MANAGED COMPANIES
Platinum member

ISO 9001
ISO 14001
OHSAS 18001

D03353A02

March 2019

EXECUTIVE SUMMARY

A three-dimensional groundwater flow model has been constructed to replicate performance of the NTSF in the period leading up to the slump event that occurred in March of 2018. The model was constructed based on the conceptual understanding of the site, and the construction detail of the NTSF as it relates to internal management of seepage and phreatic conditions. There are four broad groundwater systems beneath the NTSF, being:

- Low permeability Ordovician volcanics;
- Low permeability Silurian sediments;
- Moderate to high permeability Tertiary basalt, which may include a buried palaeo channel;
- Quaternary alluvium, which in the immediate study area is poorly developed.

Structurally, the Werribee Fault underlies the NTSF and is a regionally mapped N to NNE- trending, westerly dipping thrust with a strike-slip component. Groundwater recharge of the basalt is most likely through rainfall recharge. Recharge of alluvium will be a combination of rainfall, creek flow and spring / seep contributions. Recharge into the Silurian / Ordovician will be via rainfall recharge and will also occur where saturated Tertiary basalt overlies these systems. Springs are noted throughout the area although do not appear to be deep seated in the area of the NTSF.

The NTSF design recognised, and construction had accounted for, the presence of springs and the potential impacts of a high permeability aquifer beneath the western embankment. Performance monitoring has indicated the underdrain installed during Stage 3 construction has performed as intended. Phreatic conditions within the tailings indicate downward drainage, and unsaturated tailings conditions of up to 8m below tailings elevation at the upstream of the embankment. Foundation seepage loss appears to be low and does not appear to have pressurised the contrastingly permeable underlying basalt.

The 3D model construction process was based on this conceptual and construction understanding and was also informed through 2D modelling to assess prominent hydraulic concepts of greatest relevance to prediction of conditions inside the NTSF. Model calibration was to three primary criteria determined to be most influential to NTSF seepage conditions:

- piezometric conditions of the tailings;
- vertical gradients within the tailings derived from CPtu testing; and,
- estimation of drain flow emerging from the Stage 3 underdrain.

Model calibration was able to replicate each of these criteria, and the model was set up to simulate Stage 10 construction to the time of the slump event under transient conditions. During the period of simulation, no significant rainfall was noted, pressure conditions within the tailings did not exhibit abnormal trends compared with prior or recent data, and the decant pond elevation was not substantially increased.

Model simulated conditions for the time of failure do not indicate occurrence of new or abnormal seepage emergence on the dam face, and the effect of the Stage 3 underdrain maintained phreatic conditions upstream of the dam lifts.

TABLE OF CONTENTS

TABLE OF CONTENTS
(continued)

List of Tables

List of Figures

TABLE OF CONTENTS
(continued)

TABLE OF CONTENTS
(continued)

1 INTRODUCTION

1.1 Project Background

1.1.1 Cadia Mine

Cadia Valley Operations (CVO) is a gold/copper mining and processing complex 25 km south of Orange in NSW (Figure 1). Cadia Holdings Pty Ltd (CHPL), a wholly owned subsidiary of Newcrest Mining Limited (NML), is the owner and operator of CVO. The CVO complex comprises the Cadia Hill, Ridgeway and Cadia East mines, minerals processing facilities and associated infrastructure. Mining commenced in 1998, with current approvals taking the project to 2031 (Hatch, 2018).

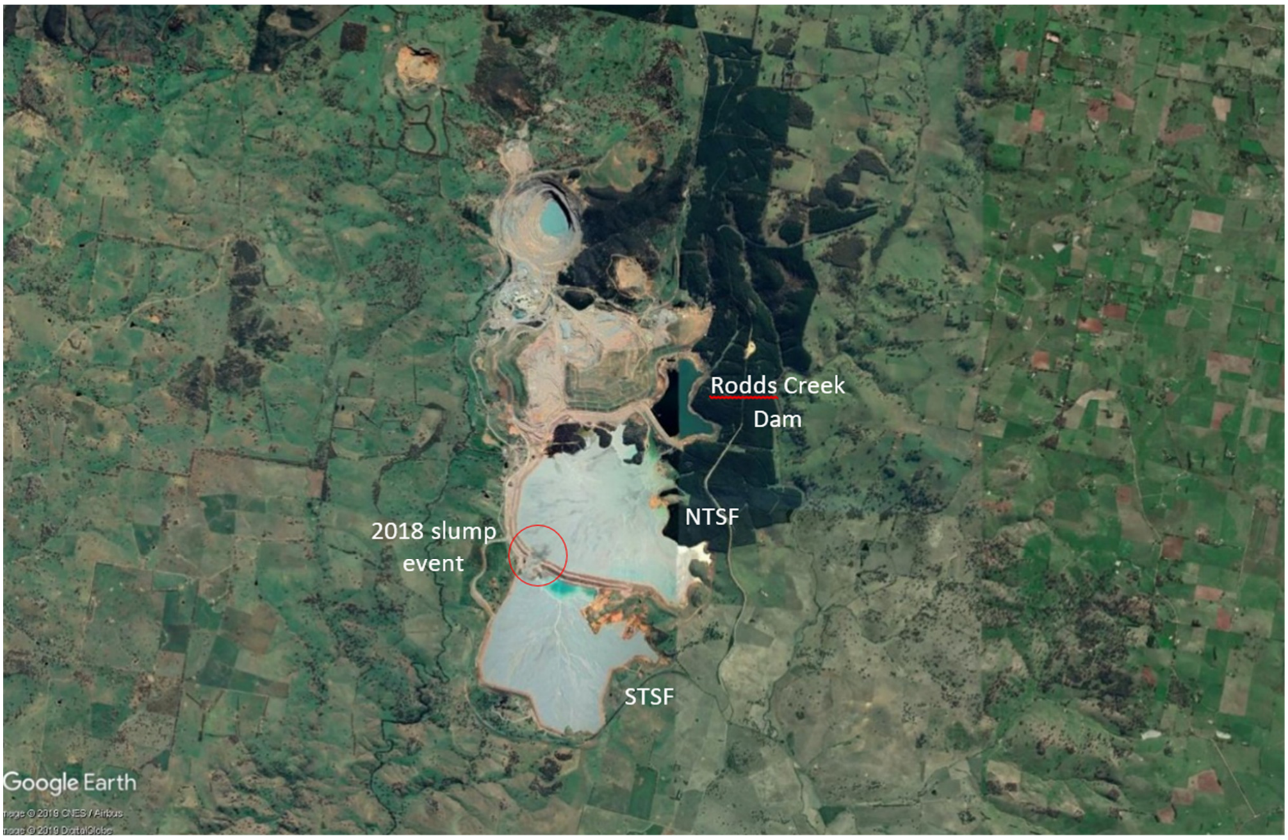

Figure 1: Cadia Mine General Layout (May 2018)

1.1.2 The NTSF Slump Event

There are two operational tailings storage facilities (TSF) at CVO; the Northern TSF (NTSF) and the Southern TSF (STSF) (Figure 1). Both TSF embankments were constructed across the former Rodds Creek. Construction of Stage 1 of the NTSF was completed in 1998, while construction of Stage 1 of the STSF was completed in November 2001. By mid-2007, tailings and decant water impounded by the STSF had commenced to encroach on the downstream toe of the NTSF (Hatch, 2018).

The NTSF is a Prescribed Dam under the requirements of the NSW Dams Safety Act 1978, with the NSW Dam Safety Committee (DSC) being the administering authority. At the time of the failure (March 2018), the NTSF was assigned a Consequence Category of Significant with an environmental approval for a final crest level of 779 mAHD. In the late afternoon of Friday 9th

March 2018, following the identification of cracks on the dam crest earlier in the day, a slump occurred on the western side of the southern embankment of the NTSF (Figure 2). The NTSF has been in operation for approximately 20 years and has been raised on average every two years (Hatch, 2018).

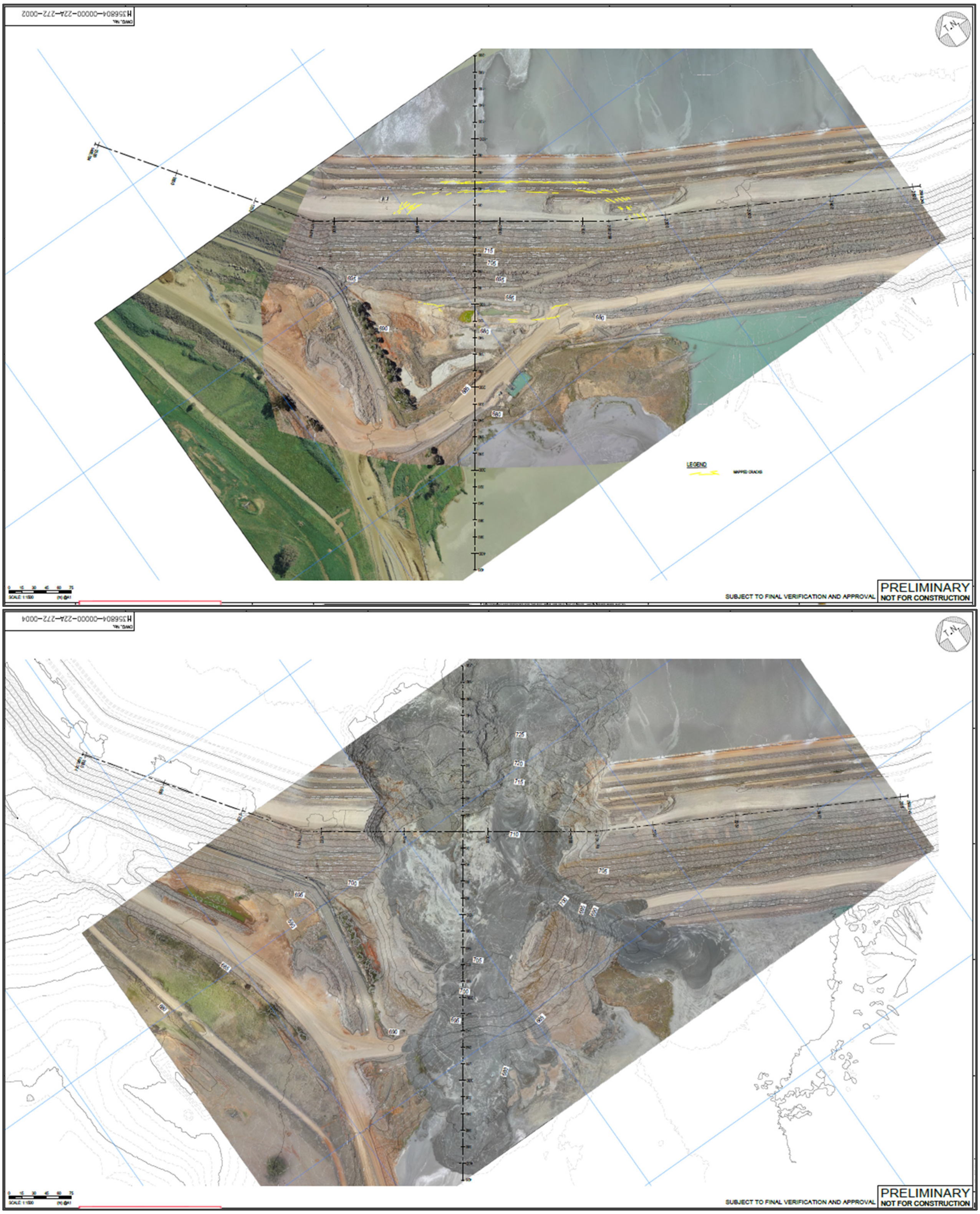

Figure 2: NTSF Area of Slump, Pre-slump (above), and Post-slump (below) (Hatch, 2018)

1.1.3 Intent of this Report

This report provides a technical assessment of pressure and seepage conditions in the period leading up to the slump event. This work is to provide key input to deformation and stability analysis being undertaken independently.

2 CONCEPTUAL HYDROGEOLOGY OF THE NTSF AREA

2.1 Regional Setting

2.1.1 Geological Framework

The project area lies within the eastern Lachlan Fold Belt of NSW. The Lachlan Fold Belt (the Belt) is divided into northerly trending metamorphic, volcanic, and sedimentary belts intruded by numerous igneous rocks. The rocks of the Belt are primarily of Ordovician, Silurian and Devonian age (AGE, 2009). A simplified summary of the Ordovician geology of the study area is provided in Figure 3, after (Wilson, 2003). The major Ordovician sequences of relevance to this assessment and which form part of the Belt are the mid Ordovician Weemalla Formation, and the late Ordovician Forest Reefs Volcanics.

Overlying the Ordovician across a large proportion of the NTSF and STSF footprint are rocks of the Silurian Ashburnia Group. Tertiary basalt and Quaternary alluvium conformably overlie Silurian and Ordovician units where they outcrop.

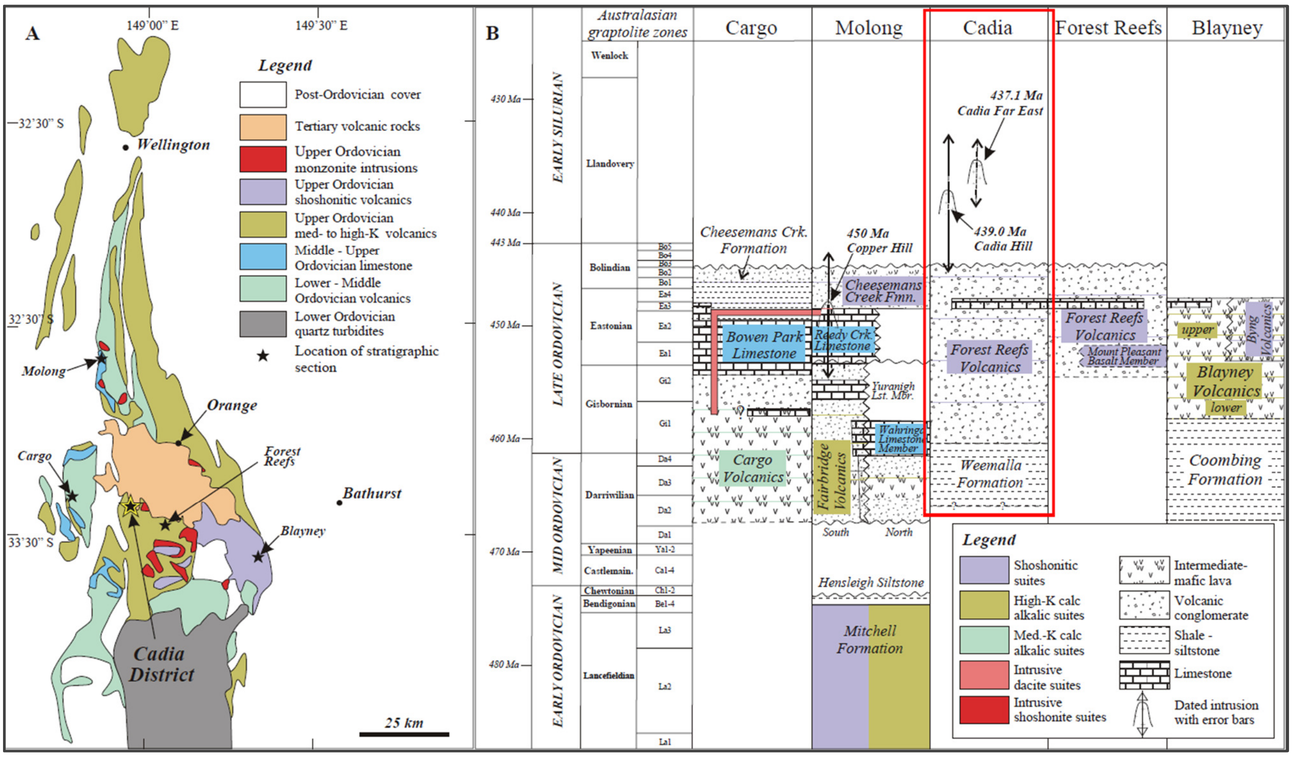

Figure 3: Simplified Ordovician Geology of the Molong Volcanic Belt after (Wilson, 2003), (Figure 2.4) (modified from Glen et al, 1998), Cadia area marked

The dominant regional structural features are a series of north trending reverse faults and related splays. Faults can form barriers to groundwater flow or can act as more transmissive conduits for water (AGE, 2009). The regional geology of the area is shown in Figure 4.

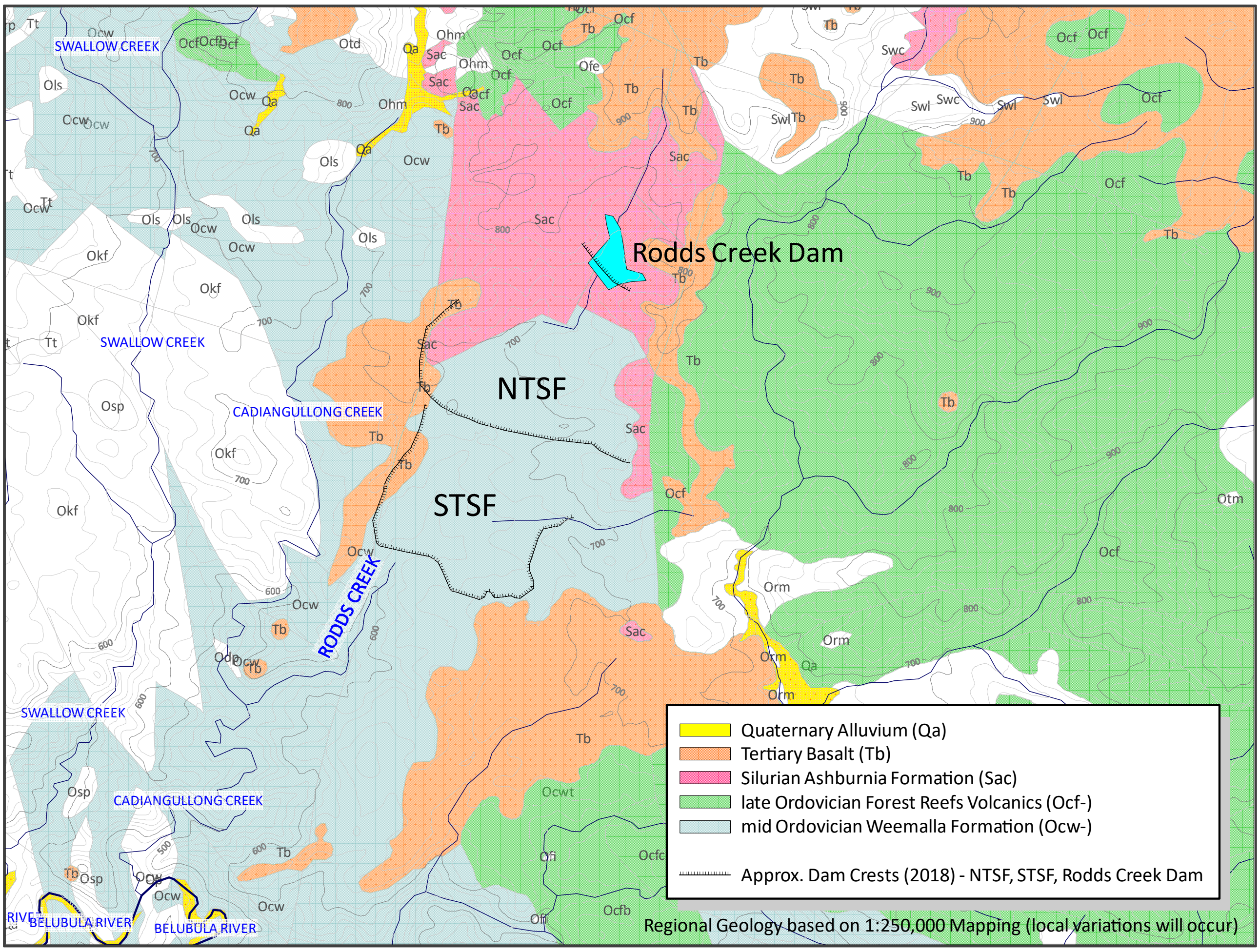

Figure 4: Regional Geology of the NTSF / STSF Area

2.2 Hydrology & Meteorology

Rainfall and creek flow monitoring data from five locations have been used to assess hydrology and rainfall conditions in the period before the slump. The location of these stations is provided in Figure 5, and the data are discussed in the following sections. The stations are:

Rainfall (daily, and long term CRD)

- 063133 Angullong, ~7.5 km southwest of the STSF
- 063254 Orange Agricultural Institute, ~25 km north-northeast of the NTSF

Creek Flow (gauge height and flow) for three stations, all within a few km of the NTSF, being:

- 412702 Cadiangullong Creek, upstream and west of the NTSF.
- 412161 Cadiangullong Creek, downstream and southwest of the STSF.
- 412147 South flowing creek northeast of the NTSF and upstream of Errowanbang.

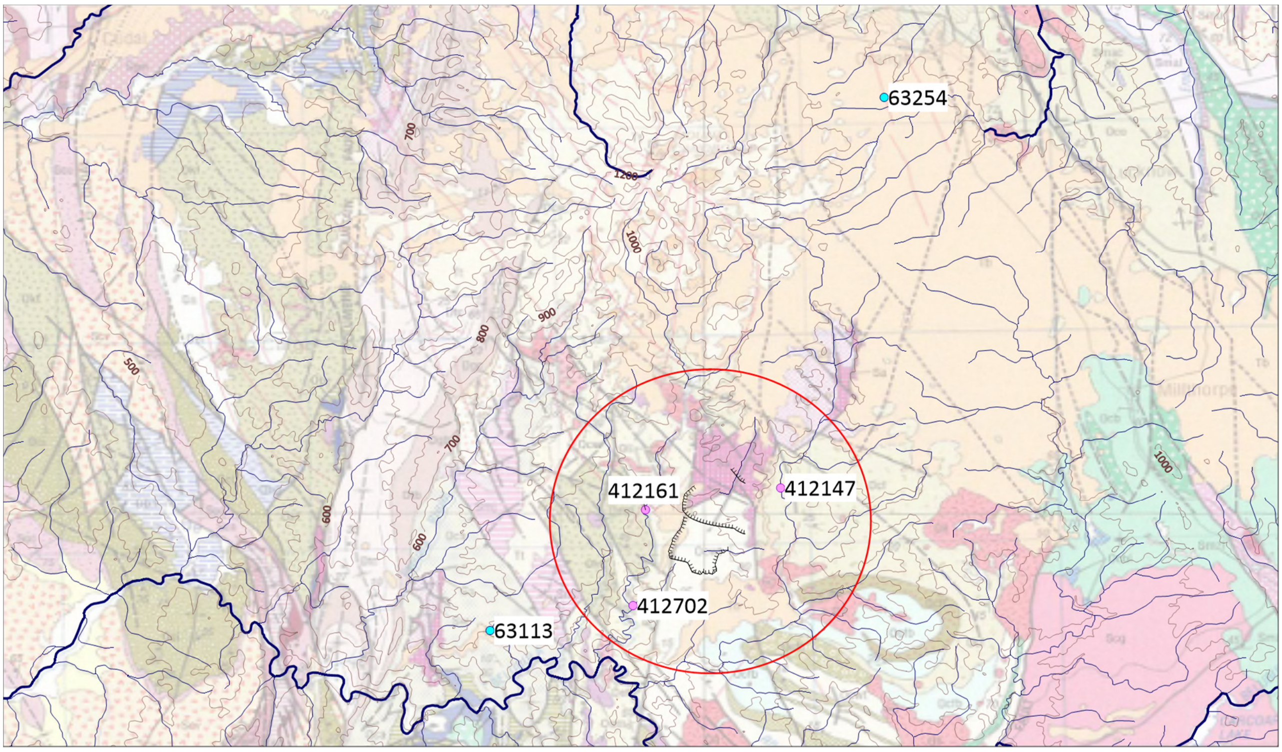

Figure 5: Location of Rainfall and Creek Flow Monitoring Stations

2.2.1 Meteorology

CRD (Cumulative Rainfall Departure) trend analyses has been applied in most of the recent hydrogeological reports for the mine. This data has been updated to after the slump for station 063254 (Orange Agricultural Station), which is applied in the recent works of AGE. This update is presented in Figure 6, and shows that rainfall has been below average for the 15 months preceding the slump event. A brief period of above average conditions producing an excess of about 500mm occurred between May and November 2016. Conditions were below average before this period, as far back as 2011.

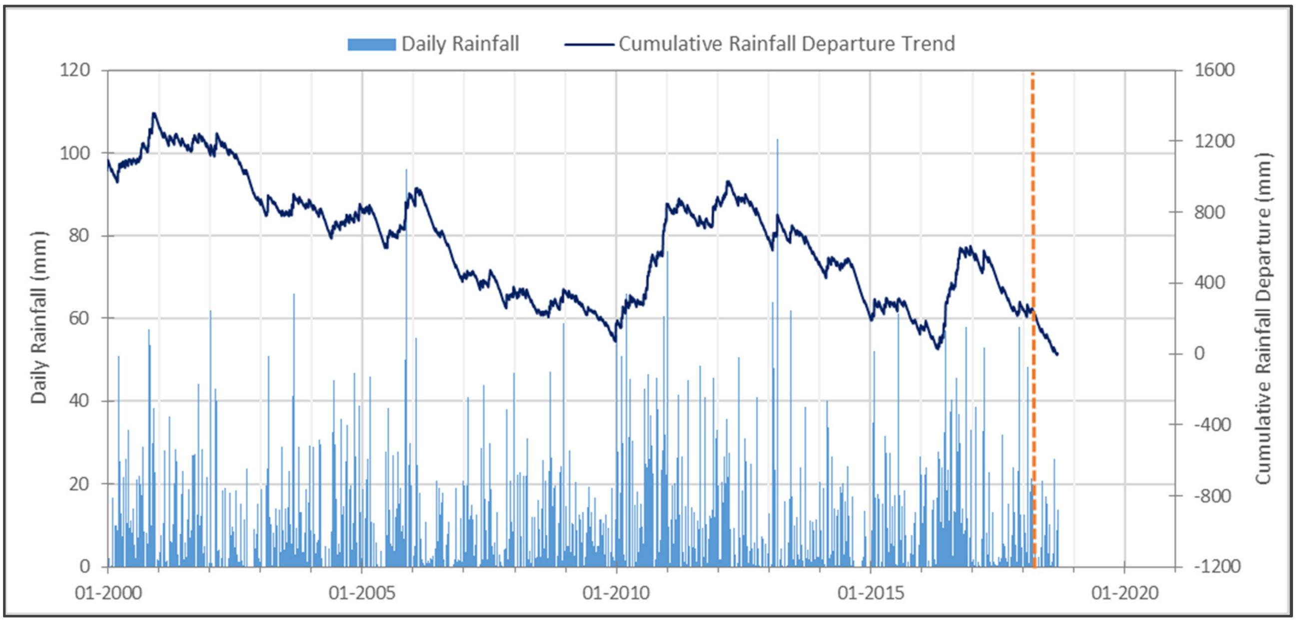

Figure 6: Long Term Rainfall (Daily Totals) and Daily CRD Trend for the Orange Agricultural Institute (063254), for the Period 2000 to 2020

Figure 7 shows daily rainfall totals for Stations 063133 and 063254 for the period leading up to the slump, marked as an orange bar for readability. Both stations observe good rainfall events in late January and late February as well as mid-May 2018. Stations 063254 observed ~20 mm rainfall ~3 days prior to the slump, although this event appears more local in nature with no rainfall recorded at Station 063133.

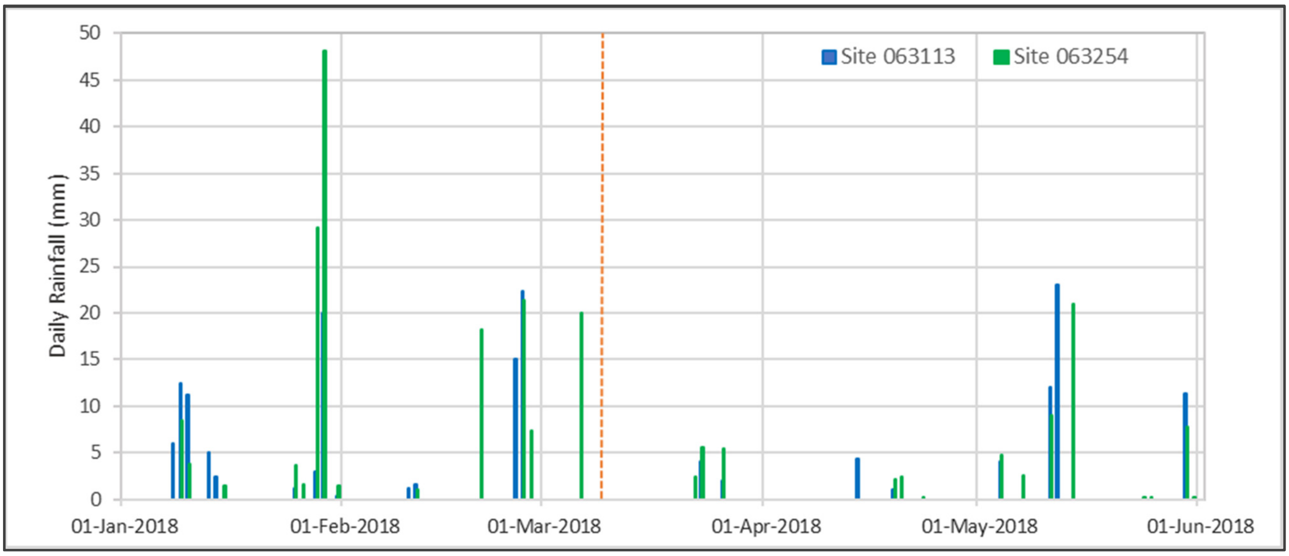

Figure 7: Daily Rainfall Totals Stations 063254 (Orange Agricultural Institute) and 063133 Angullong for the Period 2010 to 2015

2.2.2 Drainage

The NTSF and STSF (and the Rodds Creek Dam) each lie in the original Rodds Creek drainage (Figure 4). There are two stream gauging locations to the west of the NTSF/STSF complex located on Cadiangullong Creek, being stations 412702 and 412161. In the east, there is one location on the southerly flowing Flyers Creek. All three stations (Figure 8) show similar response to rainfall for the 2018 period of record surrounding the slump event (Figure 7).

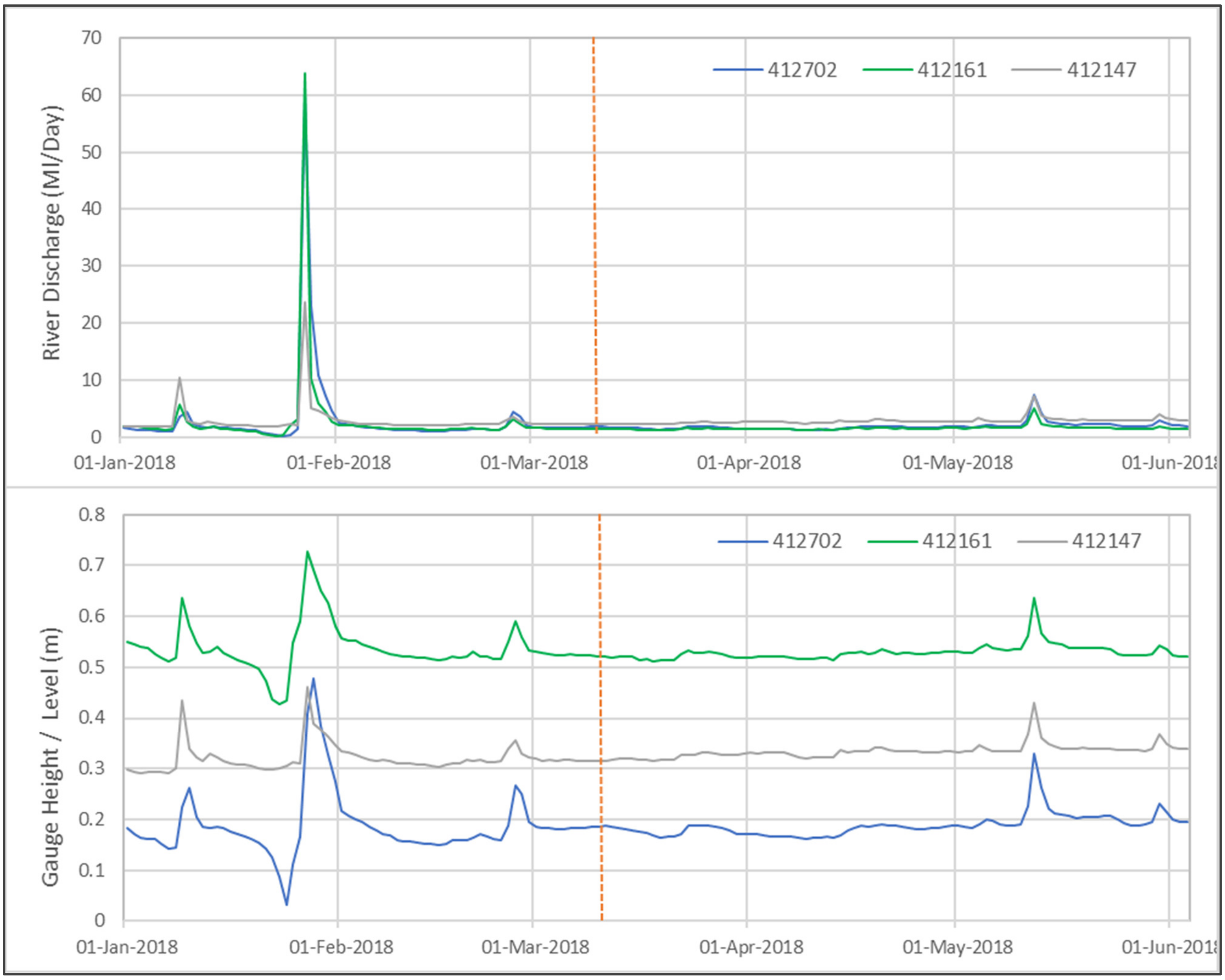

Figure 8: Stream Gauge Height and Discharge, Period of Slump Event

2.3 Geology & Structure

2.3.1 Main Geological Units

A simplified geological map showing only units described in this report is provided in Figure 4. Each of the units shown are discussed in the following section.

Quaternary Alluvium

Quaternary alluvium is common throughout the region, although only significant sequences are regionally mapped. Alluvium generally comprises clays, sands and gravels deposited by modern meandering fluvial systems which are generally well incised with poorly developed backplains (Pogson D.J. & Watkins J.J., 1998). Alluvium may be present in the form of buried palaeo-channels beneath valley fill Tertiary basalt. Local logs indicate these may be several metres thick in some locations. Hydrogeological conditions of alluvium would be expected to be highly variable depending on the nature of sediment, depositional conditions and post-deposition impacts such as weathering, reworking, and deposition under basalt.

Recharge of alluvium will be a combination of rainfall infiltration, creek (and flood / overbank) flow and spring / seep contributions from underlying basement geology or flanking Tertiary basalt. Discharge from alluvium may occur via losses to reaches of gaining streams, losses to underlying geology and in areas where the aquifer is sufficiently developed, abstraction from bores.

Tertiary Basalt

Prominent outcrop of Tertiary basalt is expressed as lava plains resulting from the outpouring of several basalt flows from Mount Canobolas to the southeast, south and west of Orange (Pogson D.J. & Watkins J.J., 1998).

Tertiary basalt crops out along elevated ridgelines adjacent to both the NTSF and STSF. The basalts are typically olivine basalt and are part of the now dissected Conobolas Volcanic Complex. The basalts are up to 80m thick at Cadia East and comprise at least six separate flows (Wilson, 2003). Potassium-Argon dating of the Canobolas Basalt (Gibson,2007) provides a Middle Miocene age of 12.7 to 11.2 Ma. The basalts were extruded over a paleo terrain and initial flows would have been along paleo drainage channels which now occupy the thickest accumulations of basalt (Hatch, 2019).

In the south west corner of the NTSF, a remnant sequence of valley fill basalt exists and underlies a portion of the western embankment. The portion underlying the western embankment was reviewed and re-interpreted, with an updated isopach assessment and a sectional assessment of the unit provided in Figure 9. All drill control available were used (partial and fully penetrating sites), underlying palaeo-alluvium of up to 4m thickness was identified. Red contours represent elevation of the base of the basalt, while blue contours represent unit thickness. The base of the Tertiary basalt varies from a high of 710m in the north, to 655m in the south.

Groundwater recharge of the Tertiary basalt is most likely through rainfall infiltration and may also occur where drainages flow over the unit and surface water is able to infiltrate to the basalt. Discharge occurs though bore abstraction, discharge into creeks, seepage to underlying rock formations (AGE, 2009) and through contact spring losses.

The basalts and covered palaeo-alluvium which underlie them are recognised aquifers of significance. (AGE, 2013) notes that Tertiary basalt forms a productive aquifer with variable yields and consistently good quality water suitable for potable use. Local permeability and storage characteristics can be highly variable depending on the nature, thickness and continuity of the basalt and the extent and inter-connectivity of primary and secondary permeability features. The basalts have the ability to store and transmit water and will also provide active drainage depending on system geometry and connectivity. Springs are often located along the margins of Tertiary basalts.

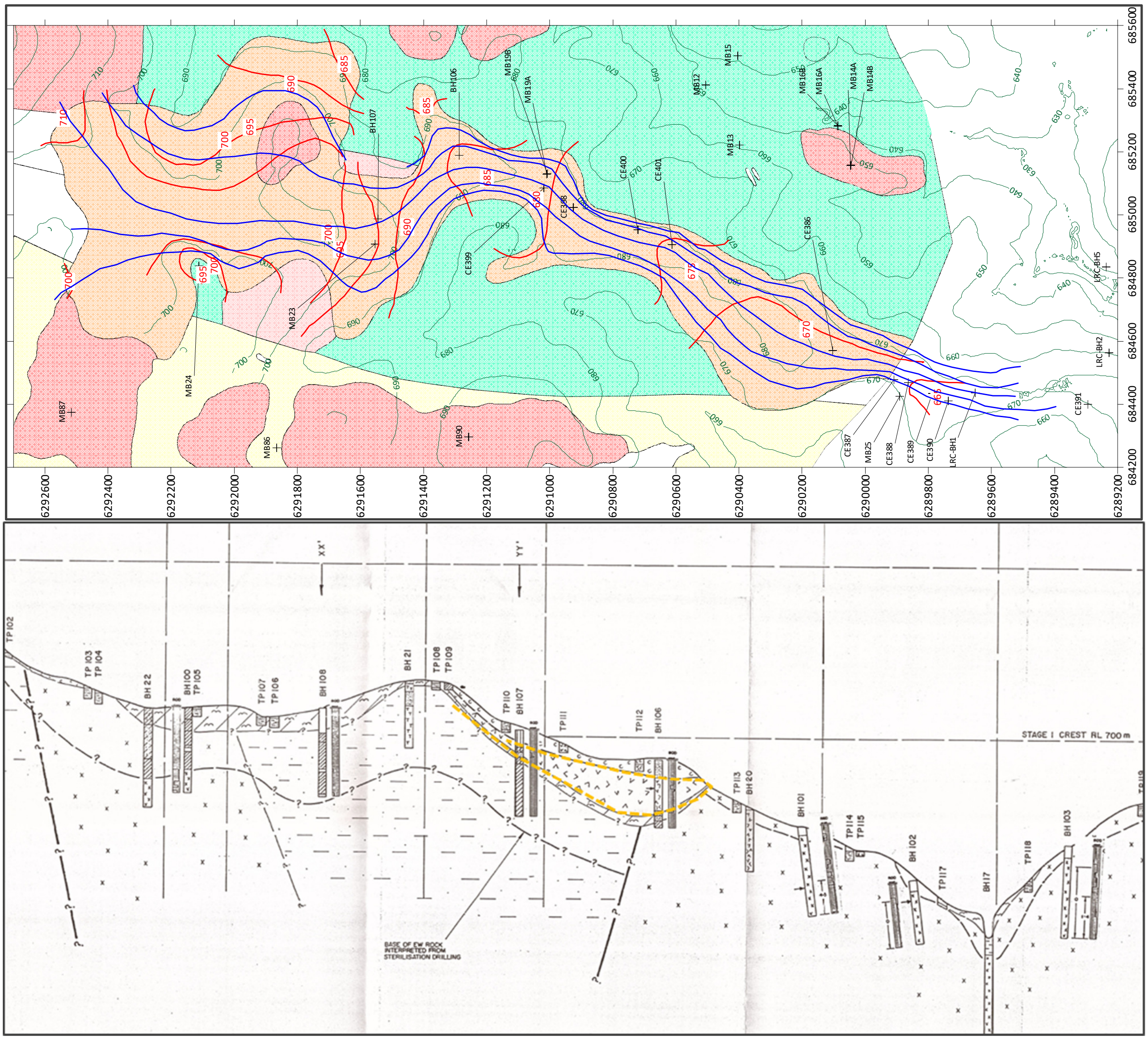

Figure 9: Local Interpretation of the Tb Flanking the Southwest of the NTSF: Upper Image represents Isopach of the Tb (rotated), Lower image is an Earlier Sectional Interpretation of the unit for a section located along the approximate centreline near the western embankment

(AGE, 2013) apply a K_h and K_v value of $1.6x10^{-6}$ m/sec, with a specific yield (Sy) of 0.2% and a specific storage (Ss) of $1x10^{-6}$. Of note, the vertical permeability is around three orders of magnitude higher than the vertical permeability of the underlying Silurian sediments and Ordovician volcaniclastics (under fresh conditions).

Early Silurian Ashburnia Formation

The Ashburnia Group comprises Silurian limestones, mudstones, siltstones, sandstones and shales. The unit represents fluctuating transgressive / regressive depositional conditions in a variable supratidal to sublittoral depositional environment. Rapid deepening provided relatively quiet conditions for the accumulation of the turbidite and muds of the Cadia Coach Shale (Pogson D.J. & Watkins J.J., 1998).

(AGE, 2013) divide the Silurian sediment sequence into three sub units – an upper sandstone comprising interbedded siltstone and sandstones, and an overlying massive sandstone, a lower siltstone, and a basal unit which varies locally. The basal unit may be boulder conglomerate, limestone or oxidised siltstone. Groundwater depths vary between about 25m to 64m (depth below ground), and aquifer water quality is typically fresh, and calcium-bicarbonate dominated (AGE, 2009).

Recharge is expected to be dominated by two processes: rainfall infiltration to exposed areas of the sequence, and vertical leakage from the Tertiary basalt where this unit overlies the Silurian sediments. Groundwater discharge is likely where creek incision causes seeps and spring discharge.

(AGE, 2013) provides median hydraulic conductivity data for Silurian sediments, which are K_h $6.1x10^{-8}$ m/sec, and K_v $7.2x10^{-9}$ m/sec. Sy is estimated at 0.5% and Ss is estimated at $1x10^{-6}$ (unitless). Weathered Silurian sediments are estimated to have hydrogeological parameters two orders of magnitude higher than those of fresh rock.

Late Ordovician (to Early Silurian) Forest Reefs Volcanics

The Forest Reefs Volcanics comprise stratified clastic volcanic derived conglomerates and breccias, sandstones and siltstones. Rocks are high K calc-alkaline and vary in composition from basaltic to basaltic andesite (Harris, 2014). The volcanic and volcaniclastic components of this unit are formed by effusive and explosive processes. (Harris 2014). Volcanic eruptions appear to have occurred from a low relief, submarine volcanic complex with multiple vents, producing thickly stacked lava sequences. Explosive volcanism occurred during the later stages resulted in ash fall deposits in a shallow water environment (Hatch, 2019)). Rock types range from basaltic lava and breccia, matrix supported volcanic conglomerate, volcaniclastic sand and ash and other fractionated volcanic deposits (Pogson D.J. & Watkins J.J., 1998).

(AGE, 2009) notes that Ordovician volcaniclastic basement rocks appear to have a widely spaced and poorly interconnected fracture network beyond the major fault zones and form an aquitard with very low groundwater yields and slightly brackish water quality. (AGE, 2013) provides median hydraulic conductivity data for Ordovician volcaniclastics, which are K_h $5.4x10^{-8}$ m/sec, and K_v $2.8x10^{-9}$ m/sec. Sy is estimated at 0.1% and Ss is estimated at $1x10^{-5}$. Hydrogeological properties for weathered Ordovician are also presented in (AGE, 2013), estimated hydraulic conductivity around 2 orders of magnitude higher than fresh rock. Sy is estimated at 1%, and Ss remains unchanged at $1x10^{-5}$.

Ordovician Weemalla Formation

The Weemalla Formation comprises Ordovician aged laminated siltstone and lesser siliceous siltstone, mudstone and feldspar-rich sandstone that include pillow basalts. It has been suggested that the deposition of this unit occurred in a proximal to distal wedge of shallow marine volcanic debris developed on the slopes of a marine volcanic edifice (Pogson D.J. & Watkins J.J., 1998). The fine grained and well sorted nature of the Weemalla Formation and presence of abundant volcanic detritus is consistent with deposition in a deep low relief, marine sedimentary basin on the flank of an eroding volcanic arc (Hatch, 2019). In the study area the top of the Weemalla Formation is defined as the contact with the basal volcanic conglomerate of the overlying Forest Reefs Volcanics (Pogson D.J. & Watkins J.J., 1998). The upper contact of this unit has been described as gradational and intercalated. Although the regional contact between the Weemalla Formation and overlying Forest Reef Volcanics is gradational, the contact in the vicinity of the NTSF is faulted, with the Weemalla lying to the west of the NTSF (Hatch, 2019).

Recharge and discharge conditions for each of the Ordovician sequences is the same as that expected for the Silurian. Recharge is expected to be dominated by rainfall infiltration to exposed areas of the sequence, and vertical leakage from the Tertiary basalt. Discharge is likely where creek incision causes seeps and spring discharge.

Most previous hydrogeological works differentiate between Silurian and Ordovician units, but do not differentiate between individual units. Hydrogeological conditions for the Weemalla Formation are therefore assumed to be similar to the Forest Reefs Volcanics.

2.3.2 Prominent Local Structure

Wyangala-Werribee Fault System

The Werribee Fault is a regionally mapped north to north-northeast trending, westerly dipping (60°-70°) thrust with a strike-slip component. In the north of its mapped extent and near to the Cadia Mine, it truncates several NNW trending faults indicating it may be a late stage feature. In the area of the mine the fault lies under cover of Tertiary basalt and passes close to the Cadia Mine juxtaposing Ordovician volcanics on the west against Silurian sediments on the east (Pogson D.J. & Watkins J.J., 1998). A regional scale section provided with 1:250,000 mapping (NGMA, 1998) passes across the Werribee Fault approximately 15 km south of the NTSF and shows the general nature of its influence on surrounding rock described above. A portion of this section is reproduced in Figure 10.

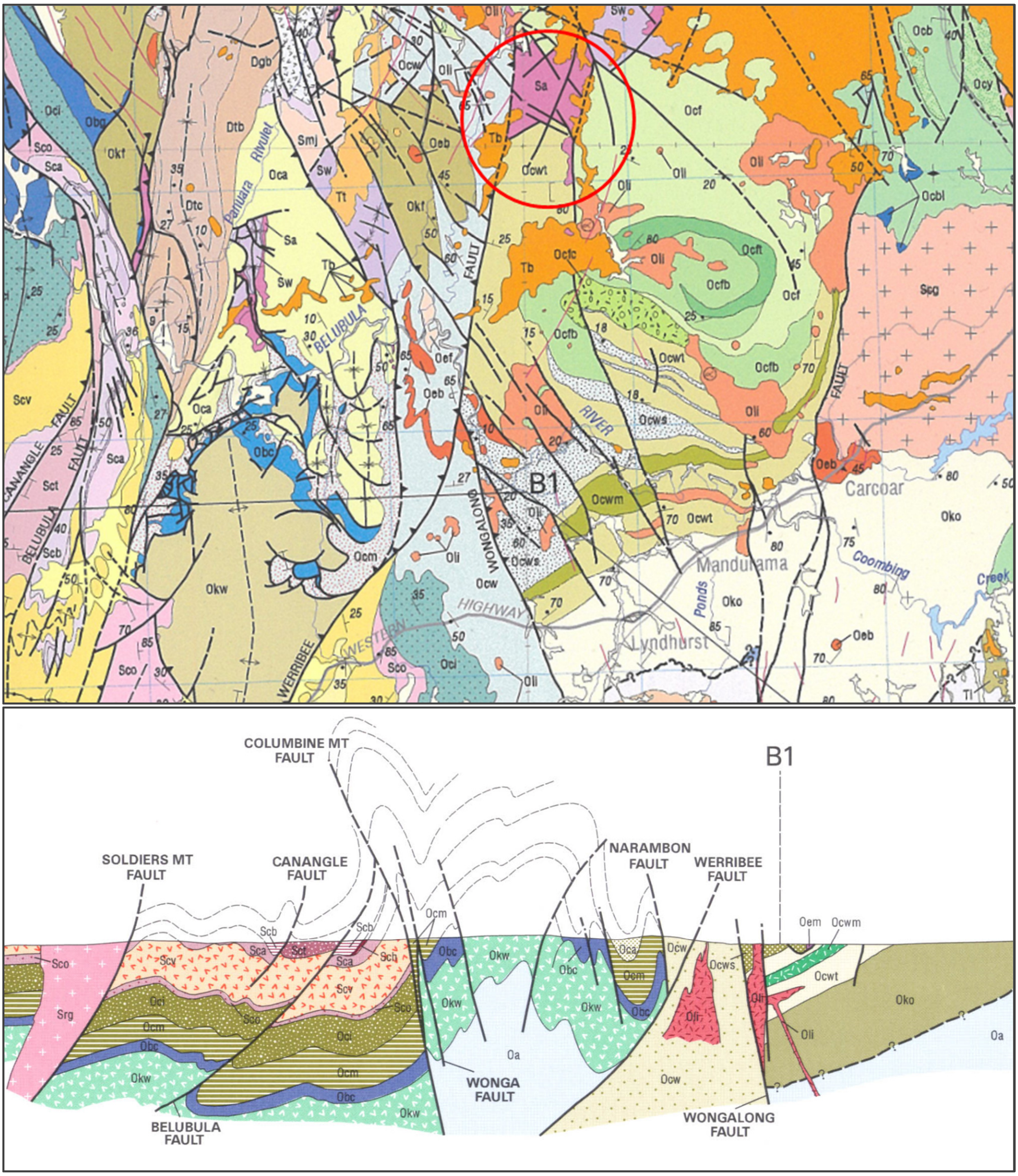

Figure 10: **1:250,000 Regional Geology, approximate NTSF Area (red circle) and Regional Cross Section of the Werribee Fault (NGMA, 1998) to the South of the NTSF**

Newcrest have completed a more focussed evaluation of the structural architecture of the Wyangala-Werribee Fault System (Newcrest Mining Ltd., 2016?). This interpretation has been completed for the whole of the mine area including the tailings facilities to the south of the mine, and defines the structural feature as:

- About 30 km long (strike length)
- Well defined in geophysics and surface mapping;
- Represented as two-three parallel thrust faults
- Damage zone 200-400m wide
- Moderately dipping to the west
- Significant (vertical) offset, up to 300 m

Definition of the system is based on a number of data sources and fault mapping exercises. The colour coding of this structure shown in Figure 11 reflects these assessments, with the red being 1997 Geological Survey mapping, and the yellow and blue being project mapping completed in the 2000s and 2007 respectively. Tertiary basalt flows cover most of the fault architecture associated with the Wyangala-Werribee Fault System (Newcrest Mining Ltd., 2016?).

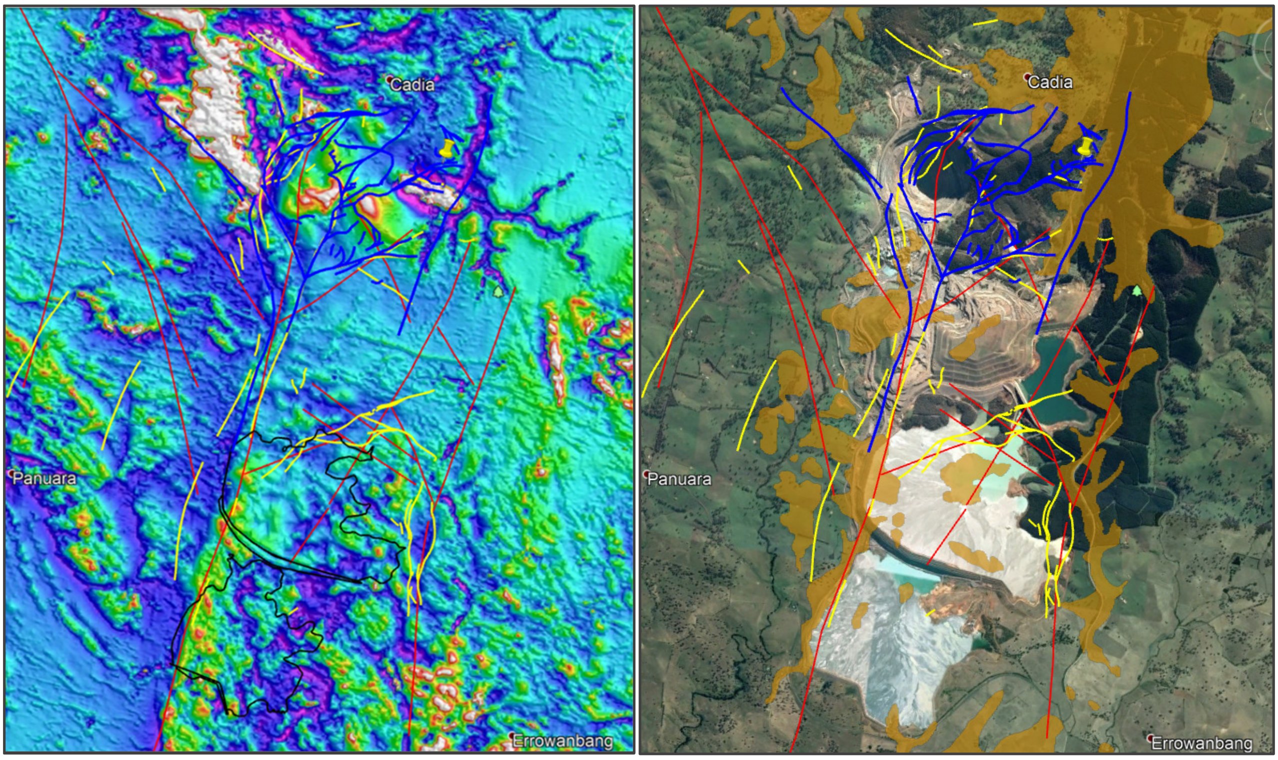

Figure 11: Geophysical Constraints (left) and Relevance of Basalt Cover (right) after (Newcrest Mining Ltd., 2016?)

In the immediate area of the NTSF, updated interpretation of the location of this fault system has been undertaken, with current interpretation of Hatch (Sep-2018) provided in Figure 12. This indicates a westerly displacement of the surface expression of the fault of about 150 m, immediately west and south west of the NTSF. Geologically, this interpretation also shows the late Ordovician Forest Reef Volcanics to the east, and middle Ordovician Weemalla Formation to the west, which is overlain by Quaternary alluvium and Tertiary basalt.

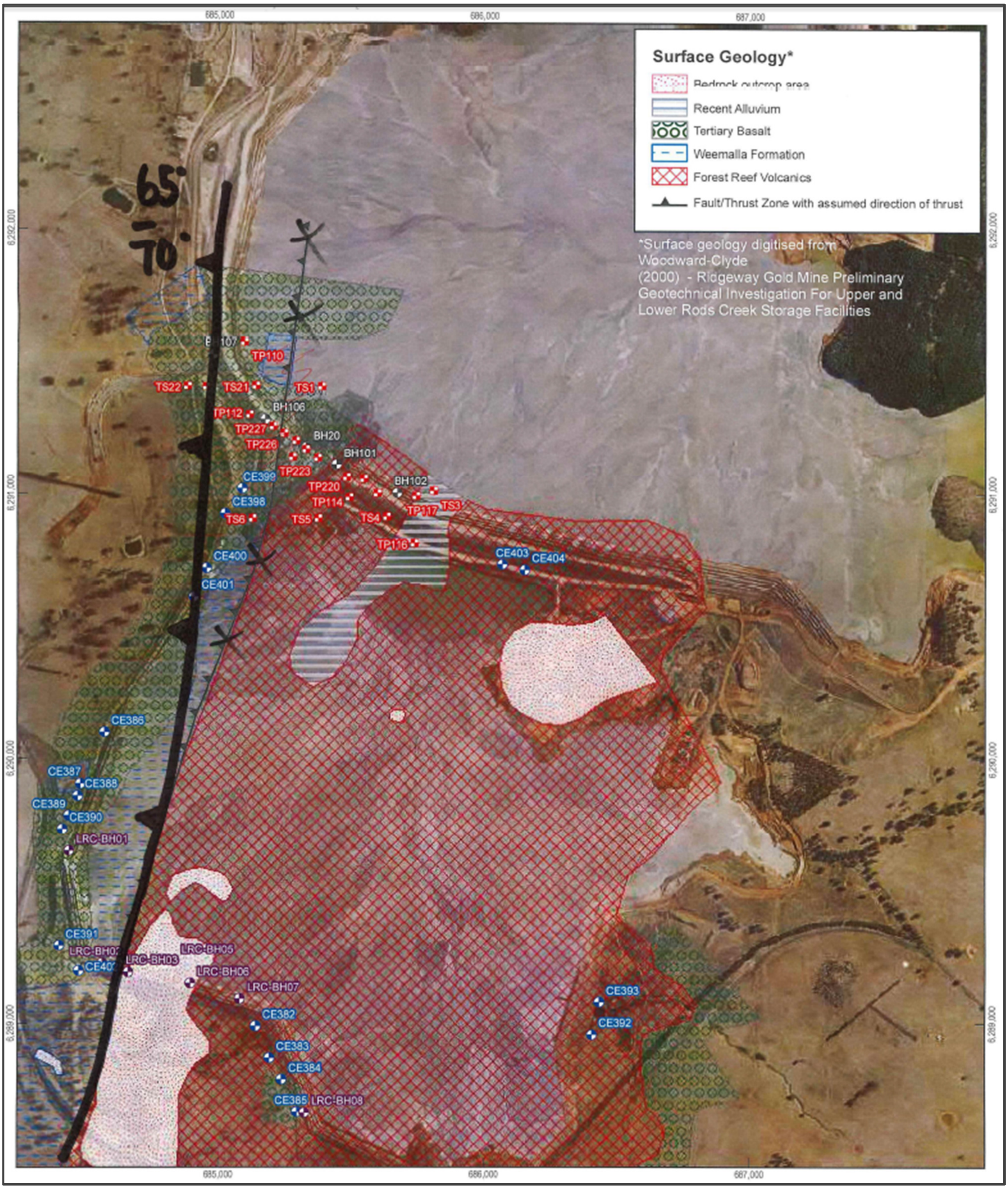

Figure 12: **Hatch (2018) Revision to the Local Alignment of the Werribee Fault near the NTSF, using GHD Mapping (reference) as a Base Map**

2.4 Hydrogeology of the NTSF

Description of the construction of the NTSF is provided in detail in (Hatch, 2019). Elements of construction relevant to seepage modelling are provided in the following section. This information is taken verbatim from Appendix B (NTSF TimeLine) of (Hatch 2019).

2.4.1 NTSF Construction Sequencing

Initial construction of the NTF commenced in August 1997 to a height of 50 m. Since then, the TSF has been raised eleven times, with the most recent raising being Stage 10 which commenced in 2017. A summary of the design and construction details of the NTSF is provided in Table 1.

Table 1: Summary of Design & Construction (after Hatch 2019, Appendix B)

Stage	Crest Level (mAHD)	Max Height (m)	Construction Type	Design By [1]	Construction Completed
1	700.0	50.0	Conventional	Knight Piesold	May 1998
2A	707.0	57.0	Downstream	Woodward Clyde	Aug 2000
2B/1	710.5	60.5	Downstream	URS	May 2002
2B/2	714.0	64.0	Downstream		Jun 2003
3	718.5	68.5	Centreline	URS	Nov 2005
4	723.0	73.0	Upstream	URS	Oct 2008
5	729.0	79.0	Upstream	URS	Aug 2011
6	732.0	82.0	Upstream	URS	Dec 2012
7	735.0	85.0	Upstream	URS	Feb 2014
8	738.0	88.0	Upstream	URS/AECOM	Oct 2015
9	741.0	91.0	Upstream	AECOM	Dec 2016
10	744.0	94.0	Upstream	ATC Williams	Mar 2018 [2]

(1) Woodward Clyde was acquired by URS who were subsequently acquired by AECOM.
(2) Stage 10 was incomplete at the time of the NTSF Failure

2.4.2 NTSF Construction Elements

Starter Embankment

The Stage 1 starter embankment is an earth and rockfill dam, with a 1,680 m long embankment and a 16 m wide crest at RL 700. A 5 m wide clay core is bounded by rockfill shoulders, with a 15 m wide transition / filter zone between the clay core and the downstream rockfill shoulder of the embankment.

Rodds Creek Diversion

Rodds creek was diverted through the dam foundation via a 1,350 mm concrete encased (through the clay core) steel conduit. A sediment dam was integrated into the upstream face to control runoff during construction and emergent groundwater from springs in the creek channel. The sediment dam includes a 10 m wide zone of drainage gravel between RL 661 and RL 665.

Clay Blanket

A 1 m thick clay blanket (permeability 1.0×10^{-9} m/sec) was constructed upstream of the dam in Rodds Creek and a 1 m thick clay layer was constructed between the sediment dam and the clay core at RL 658.

Any areas of exposed fractured rock or permeable soil on the storage floor were covered with low permeability clayey soil to provide an overall average base permeability equivalent to 1 m thickness of material with a permeability of 1×10^{-9} m/sec or better (ATC Williams, 2017).

Underdrain

During Stage 3 construction, an underdrain system consisting of a slotted collection pipe encapsulated within a filter blanket was provided over the full length of the upstream toe of the Stage 3 embankment. Outlet pipes were provided to the downstream rockfill batter at 200 m intervals, which were concrete encased through the clay core with a filter sand plug immediately downstream of the concrete encasement.

For drainage under the clay liner, ABS pipe was laid on the base of Rodds Creek channel and rock drainage material placed on top. All water collected by this system was returned back into the NTSF via a drainage collection pond, nor covered by tailings within the STSF (ATC Williams, 2017).

Tailings Deposition

Tailings deposition is sub aerial using multiple spigots. Deposition planning is achieved by splitting the dam embankment into zones, each containing five to seven discharge spigots. Modelled tailings rate of rise is ~1.9m/year prior to 2010 and ~2.4m/year after 2010. The NTSF has an average beach slope of 0.3%.

Buttressing

In mid-2007, a 35 m wide berm of igneous mine waste was placed at the toe of the NTSF. Over the following years, the berm was progressively raised and lengthened to keep it above the STSF decant pond level. As a consequence of cone penetration tests completed in 2017, ATCW recommended the construction of two buttresses (the Stage 1 buttress and the Stage 2 buttress). The Stage 1 buttress extends from the Stage 3 crest to the Stage 7 crest, the Stage 2 buttress extends from natural ground at the toe of the NTSF to the Stage 3 crest.

2.4.3 Drainage & Seepage

The Stage 3 underdrains have remained largely dry, except for the western drain. Although seepage from this drain was noted for some time, it was not until a pipe was attached that the measurements of flow rate were possible. Drain flow for the period 2015 to early 2018 range between 30 L/min and 50 L/min (Figure 13). Extension of a trend line through this data indicates flow may have commenced around mid-2006. Prior to the slump event, a 10 L/min increase in flow rate was observed for each 5 m rise in the decant pond level.

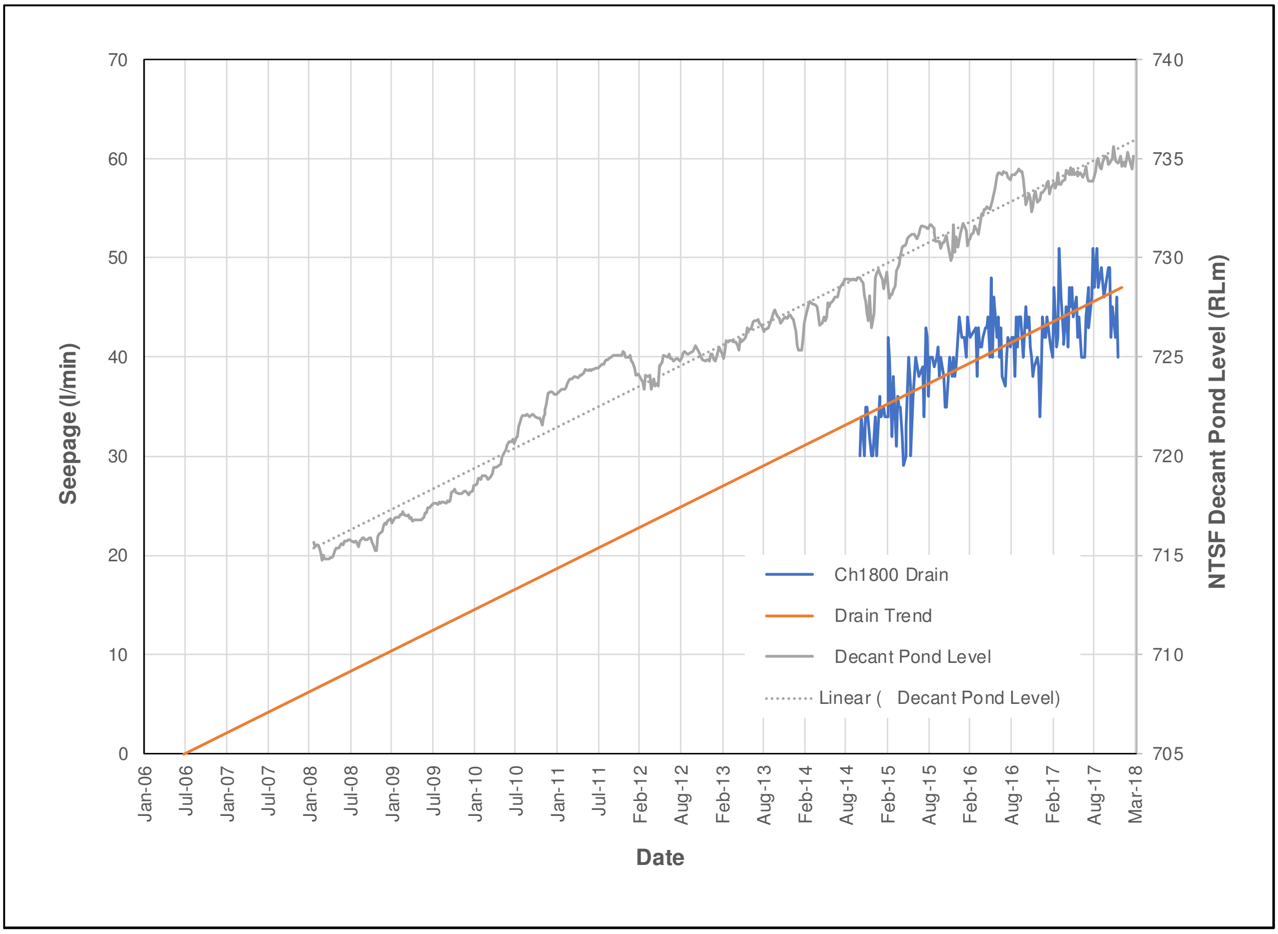

Figure 13: Ch.1800 Drain Flow and NTSF decant Pond level

Seepage observed as semi-permanent wet spots have been noted on a number of berms on both the Southern and Western Embankments. As most of the wet spots appear to dry out during dry weather, Hatch concluded that they most likely result from rainfall runoff and infiltration into the rockfill collecting at low points. This is consistent with the concept of shallow interflow discussed in the Ridgeway EIS (Kalf, 2000).

2.4.4 NTSF (& STSF) Decant Ponds

Stage 4 to Stage 10 elevation data for the NTSF and STSF dam crest and decant pond elevation, and the water elevation of the Rodds Creek Dam, is provided in Figure 14.

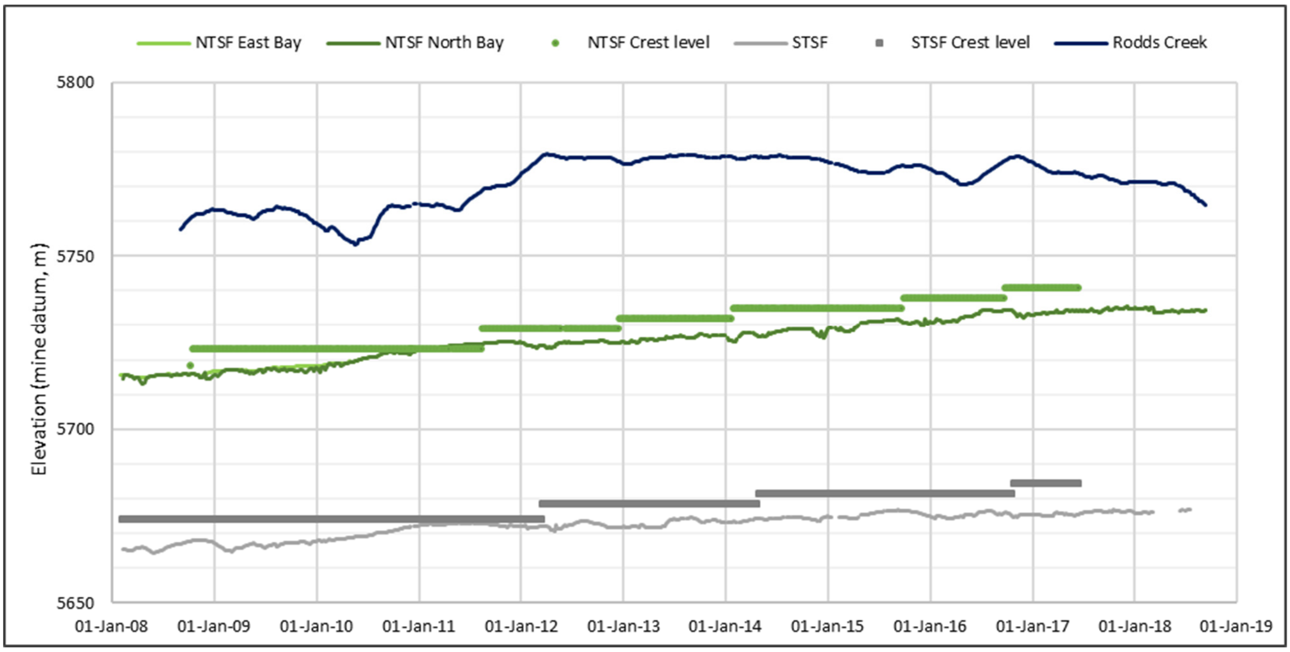

Figure 14: NTSF & STSF Dam Crest and Pond Elevations, Rodd Creek Dam Water Elevation

Spatial representation of pond location has been assessed by KCB using available air photography, from site held data and Google Earth imagery. A summary of this information is presented in Figure 15, observations include:

- For the three recent images, the pond sizes in each of the NTSF and the STSF are not large compared with the cluster image of longer-term pond records;
- The NTSF pond has generally maintained a lateral distance of 1,000 m or greater from the area of the slump, with exception of a period in late 2010 when both TSFs experienced large pond extents. Under these conditions the pond was still several hundred metres from the slump area.
- In 2010, the area experienced a year of above average rainfall which produced a CRD excess of about 800 mm. The period is also reflected in crest versus pond elevation data presented in Figure 14, which shows a brief period of merged elevations.
- Post slumping, pond sizes in each facility are comparatively very small.

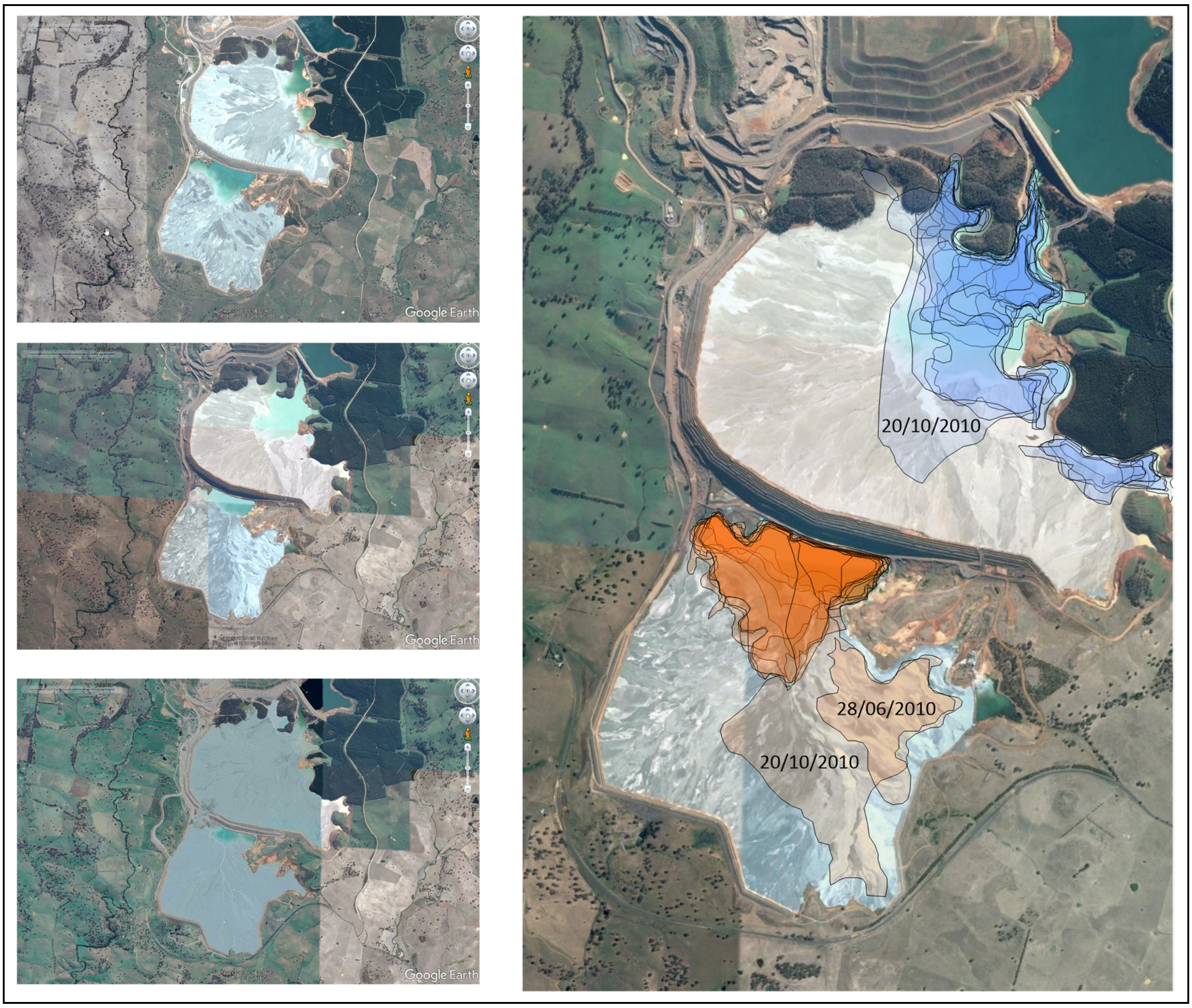

Figure 15: NTSF and STSF Pond Location (Upper Left Nov-2015, Centre Left Dec-2016, Lower Left May-2018, Right Cluster Map of All Data Available)

2.4.5 Piezometric Monitoring Data

There is a large inventory of monitoring established at the mine. With focus on the seepage performance of the NTSF for the period leading up to the slump event, a reduced subset of data is presented. Figure 16 provides a location map of monitoring facilities (bores and VWPs) used in this assessment. Table 2 provides a tabulated summary of these facilities.

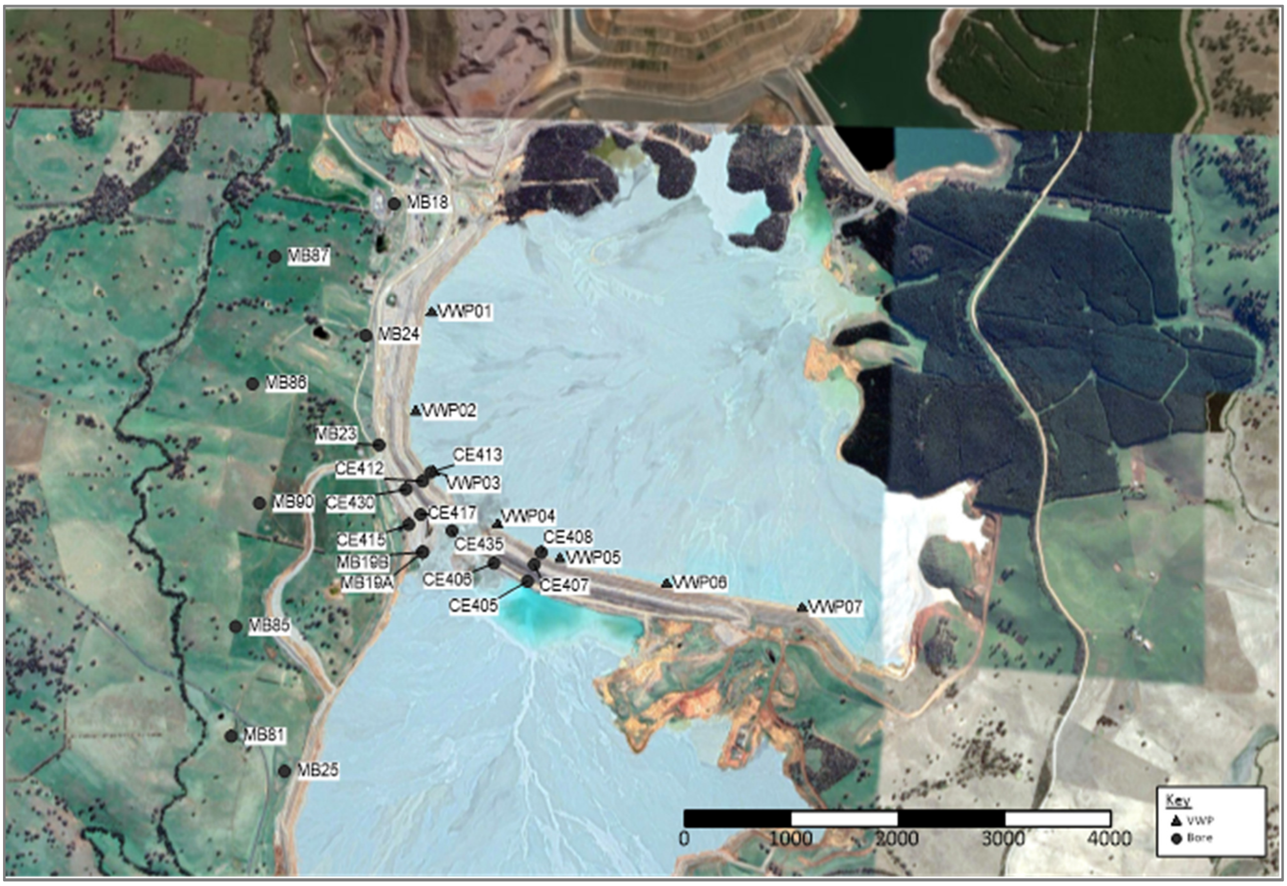

Figure 16: **Location of Key Monitoring Locations (Bores and VWPs) (figure needs improvement / clarity)**

Table 2: **Bore & VWP Completion Details for Sites Used in Hydrograph Interpretations**

Bore	Easting	Northing	RL (mAHD)	Total Depth (m)	Unit	Type
CE405	685,666	6,290,860	687.83	30.5	Fresh Volcanics	VWP
CE406	685,495	6,290,952	688.04	31.8	Fresh Volcanics	VWP
CE407	685,700	6,290,945	731.80	61.6	Core	VWP
CE408	685,737	6,291,006	743.80	57.0	Tailings	VWP
CE412	685,129	6,291,369	732.14	67.5	Basalt	VWP
CE413	685,171	6,291,414	743.85	58.4	Basalt	VWP
CE415	685,059	6,291,149	686.16	31.3	Fresh Volcanics	VWP
CE417	685,120	6,291,200	701.00	39.0	Basalt	VWP
CE430	685,045	6,291,328	706.32	44.5	Basalt	VWP
CE435	685,280	6,291,117	708.33	45.0	Fresh Volcanics	VWP
MB18	684,985	6,292,785	722.00	40.0	Silurian Sediments	Bore
MB19A	685,131	6,291,009	688.12	39.7	Ordovician Volcanics	Bore
MB19B	685,130	6,291,007	688.14	7.6	Soil/Clay	Bore
MB23	684,908	6,291,554	703.49	41.3	Ordovician Volcanics	Bore
MB24	684,839	6,292,112	696.44	30.9	Ordovician Volcanics	Bore

Bore	Easting	Northing	RL (mAHD)	Total Depth (m)	Unit	Type
MB25	684,425	6,289,890	668.90	30.5	Ordovician Volcanics	Bore
MB81	684,153	6,290,069	657.48	19.0	Silurian Siltstone	Bore
MB85	684,175	6,290,626	676.50	26.0	Silurian Sediments	Bore
MB86	684,261	6,291,865	685.65	22.0	Ordovician Volcanics	Bore
MB87	684,375	6,292,516	693.56	21.5	Ordovician Volcanics	Bore
MB90	684,297	6,291,257	644.00	60.0	Tertiary Basalt	Bore
N1-2	685,908	6,288,934	731.71	24.9	Tailings	VWP
N2-2	685,557	6,289,718	731.67	35.0	Tailings	VWP
N3-2	685,943	6,290,405	730.67	36.0	Tailings	VWP
VWP01(NO1)	685,177	6,292,229	740.68	10.0	Tailings	VWP
VWP02(NO2)	685,097	6,291,723	741.16	10.0	Tailings	VWP
VWP03(NO3)	685,188	6,291,417	740.86	10.0	Tailings	VWP
VWP04(NO4)	685,514	6,291,149	740.39	16.0	Tailings	VWP
VWP05(NO5)	685,833	6,290,973	740.08	16.0	Tailings	VWP
VWP06(NO6)	686,377	6,290,845	739.02	16.0	Tailings	VWP
VWP07(NO7)	687,069	6,290,719	738.96	16.0	Tailings	VWP
NTSF20001	685,472	6,291,067	705.50	10.0	Tailings	VWP
NTSF20002	685,472	6,291,067	719.77		Decommissioned	VWP
NTSF20003	685,472	6,291,067	720.69		Decommissioned	VWP
NTSF20004	685,472	6,291,067	726.64		Decommissioned	VWP
NTSF20017	685,472	6,291,067	721.10		Decommissioned	VWP

There are five hydrographs presented for bores completed in natural strata and proximal to the NTSF. These are MB18, MB19A/MB19B, MB23 and MB24 (Figure 17). The bores are located immediately west and south west of the NTSF, close to the abutment of the STSF into the southern NTSF embankment. All the bores are within 500 m of the toe of the western or southern embankment of the south west corner of the NTSF.

Long term trends for four of these bores are shown and indicate a consistent head increase of 0.35 m to 0.55 m per year. No unique spikes in the record due to sudden recharge events such as rainfall or creek flow are evident. The equivalent lineal trend on the NTSF and the STSF decant ponds are 2.0 m/year and 1.0 m/year respectively. These data indicate translation of the developing pressure response from raising of the NTSF into local groundwater conditions within the Silurian and Ordovician strata.

The absence of local peaks in the data (exception being MB19B which is the shallowest completion at 7.6 m) and the large difference in vertical elevations between the bores and the decant pond elevation in the NTSF (30 m-50 m), indicates that this trend is a muted pressure response to the TSF’s presence rather than an indicator of direct and efficient hydraulic continuity. This is a relevant observation in considering the interaction between the NTSF and natural ground from a modelling context. If the efficiency of the interaction between these systems is represented too strongly, then the prediction of heads in natural ground will be dominated by the NTSF, and likely over-estimated to the order of 10’s of metres.

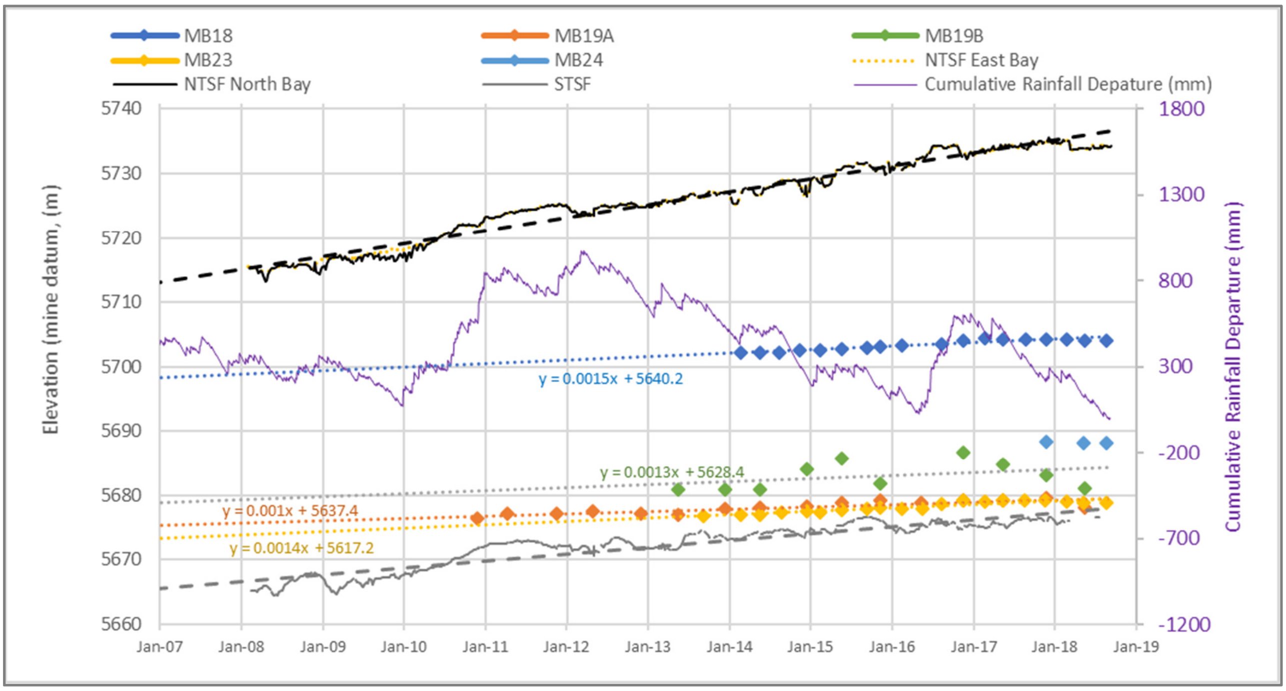

Figure 17: NTSF Proximal Foundation Head Monitoring, 2007 to 2018

Figure 18 shows a similar composite hydrograph, however, these are for sites slightly further away from the NTSF / STSF complex, to the west and south of the facilities. These bores are between 800 m and 1,700 m from the NTSF. In the lower section of the figure, the graphs have been reproduced to show detail for the cluster of bores between RL (5)640 and (5)660.

The long-term rising trends apparent in the proximal sites is not present in data from these more distal bores. Their response is considered more typical of that expected from groundwater unaffected by influences other than rainfall, with two sites (MB81 and MB25, and possibly MB85) of longer record showing a strong recharge and decline response to a period of prolonged above-average rainfall. Consistent with the current CRD trend, all distal bore hydrographs are now showing a steady rate of decline, which is in contrast to pond conditions in the NTSF and the STSF over the same period.

These data are indicating no translation of the NTSF / STSF pressure effects at distance, placing the likely lateral extent of NTSF pressure impact to be in the range of 500 m to 800 m from the TSF complex.

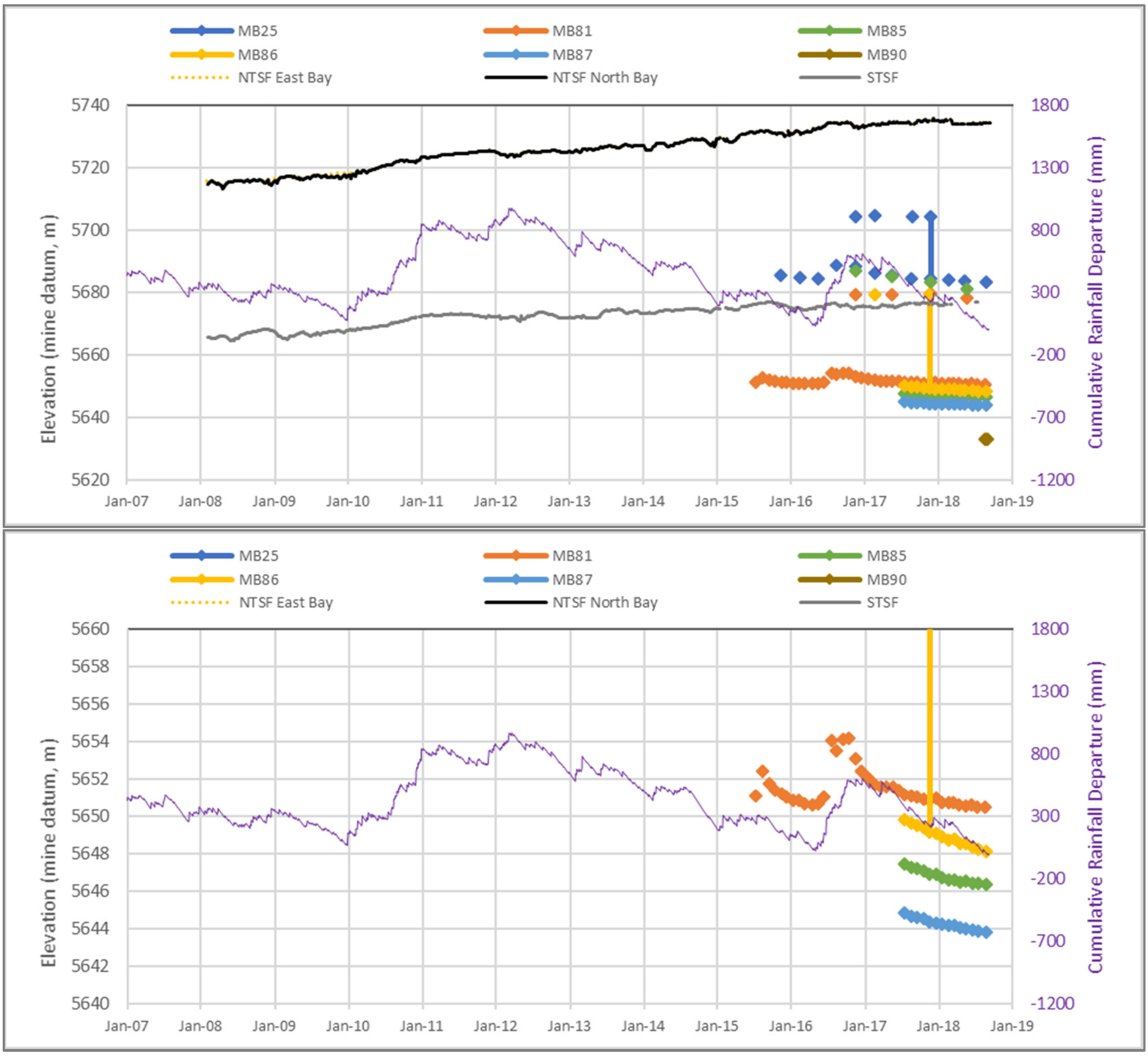

Figure 18: NTSF Distal Foundation Monitoring, 2007 to 2018

Figure 19 provides time series monitoring of piezometric conditions in the tailings and in the Tertiary basalt (from VWPs installed during the 2018 campaign). A section showing the relative location of these CE sites is also provided after Hatch (2019). Of the VWP's, location VWP-N03 is closest to these basalt VWP monitoring locations.

An observation from these data is the vertical head differential between the tailings and the basalt, particularly sites CE412 and CE430. These data indicate that seepage and head translation from the tailings to the underlying basalt is either (i) not significant compared to the basalt's ability to accommodate these flows, or (ii) absorbed by the basalts' ability to rapidly discharge this additional water. Because the conditions in the tailings do not indicate presence of drainage effects over the basalt, the former condition is considered more technically likely.

The gradient between the downstream basalt VWPs is also important for two reasons (i) it is relatively 'gentle' at ~1:30 (considering its proximity to the embankment), indicating seepage contribution from the tailings which would be controlling features to the saturated section of the sequence are not significant, and (ii) the heads are below the interpreted top of the Tertiary basalt, indicating seepage from tailings into the basalt is not significant enough to pressurise the basalt, which in turn reduces its potential to create spring discharge back into the tailings (at this location)[1].

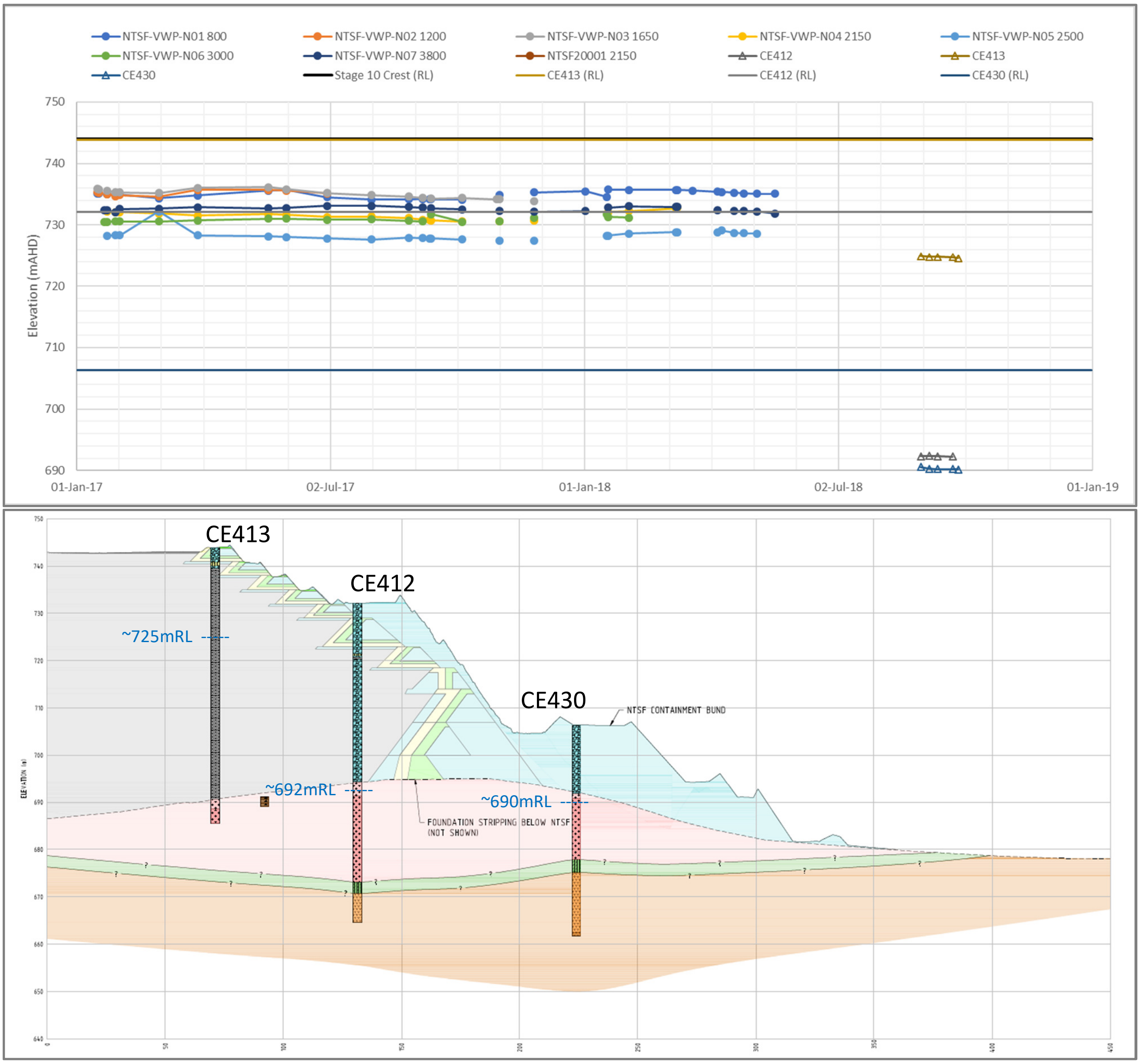

Figure 19: NTSF Internal Monitoring, Time Series Jan-2017 to May-2018, and 2018 Installed Tertiary Basalt VWPs, lower image location of CE series holes (Hatch, 2019)

[1] It is noted these observations are based on comparison of Tertiary basalt conditions measured after the slump event.

Equilibrium pore pressures (Figure 20) from pore pressure dissipation tests completed as part of the 2013 and 2017 CPTu investigations indicate a pressure gradient below hydrostatic at a number of test locations (Hatch, 2019). The pressure gradient is closest to hydrostatic along the western embankment (N1-2) and well below hydrostatic at sites N05 and N302, which are located on the southern embankment. At these sites the inferred water level is ~8m below the tailings surface, and 3-4m below the tailings surface elsewhere (Hatch, 2019).

The deeper groundwater surface in the vicinity of Ch2500 can also be seen in a longitudinal profile of the piezometric surface for a number of dates (Figure 21). This, and the pressure gradient less than hydrostatic, can most likely be attributed to downward drainage toward the Stage 1 underdrain system between Ch2300 and Ch2600 to assist in consolidation of the tailings (Hatch, 2019).

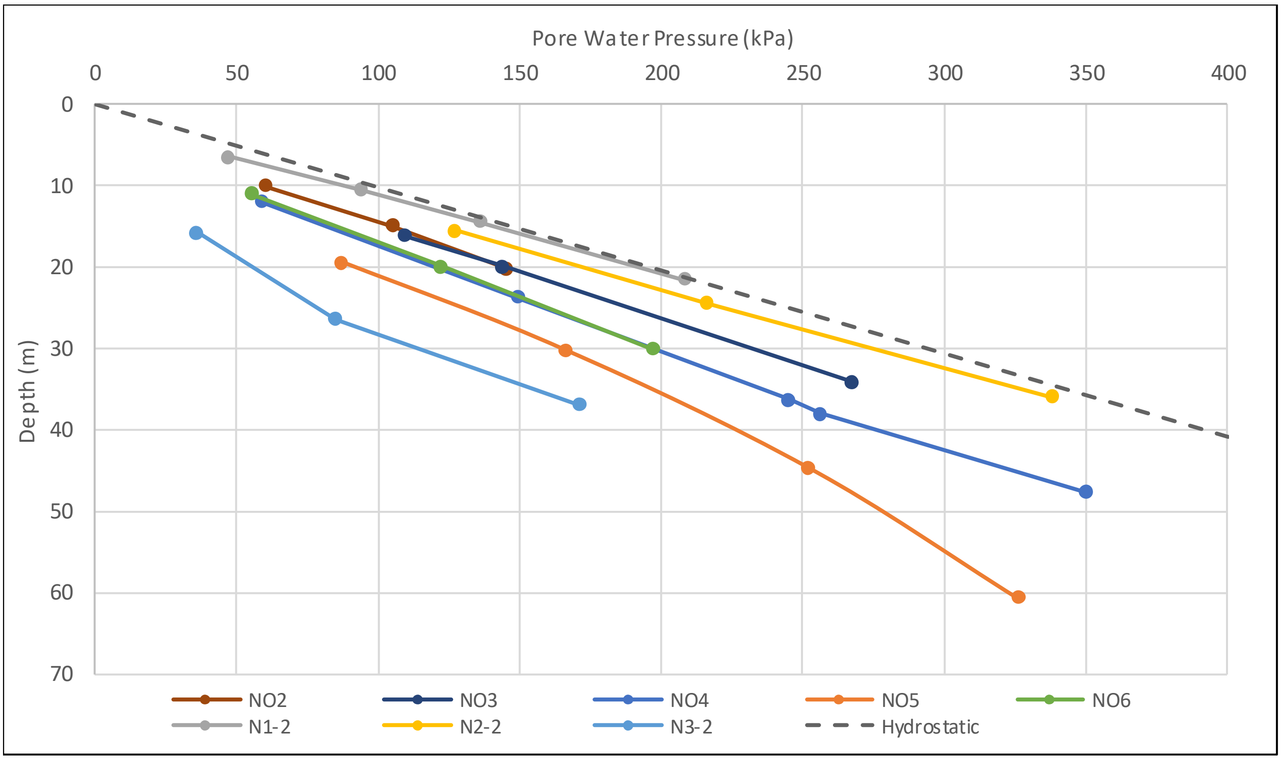

Figure 20: CPTu Pore Water Pressure Gradients (Hatch, 2019)

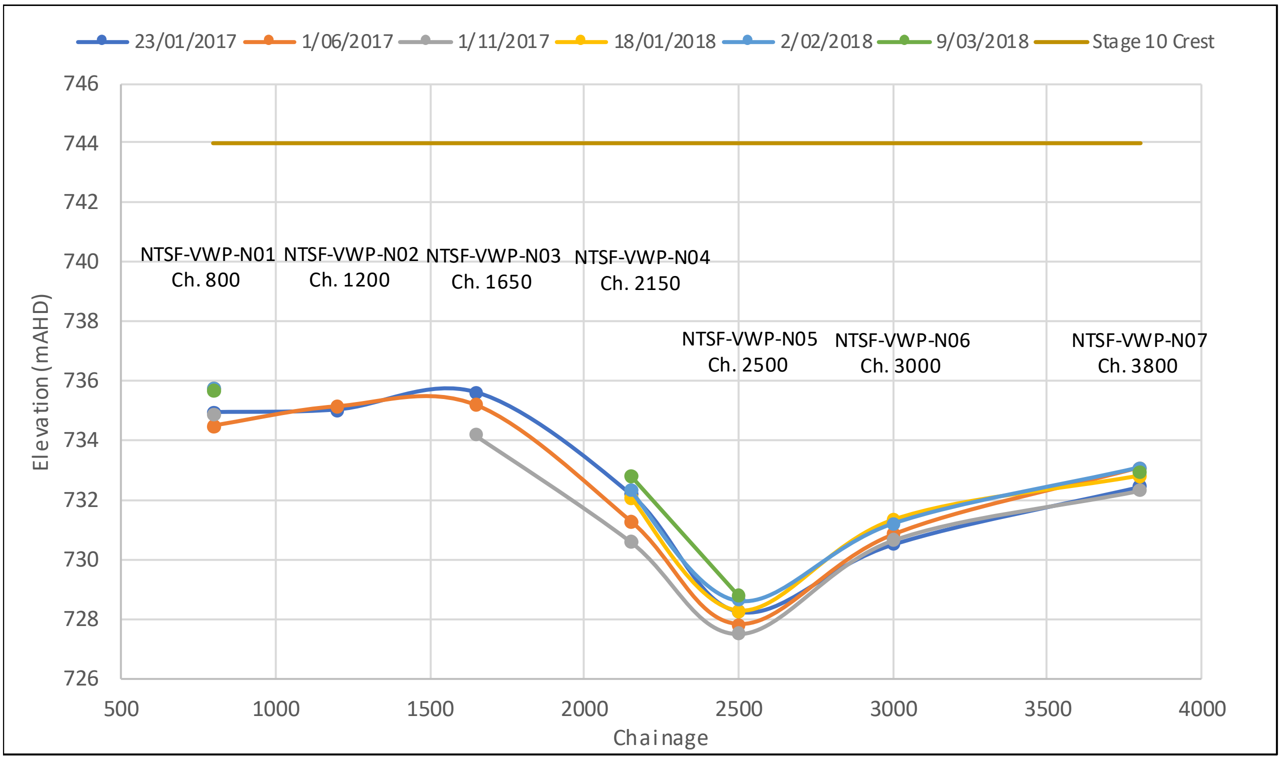

Figure 21: Longitudinal Profile of Piezometric Surface with Time (Hatch, 2019)

2.4.6 Springs

Numerous studies, including those related to the design, construction and performance assessment of the NTSF have acknowledged the presence and relevance of springs at the site. Examples of such references are provided in Table 3.

Table 3: Example Spring Referencing from Previous Technical Documentation

Reference	Comment
Woodward-Clyde (1995). *Cadia Project Tailings Disposal Study – Geotechnical; Investigation Report*	▪ Pg.5 “Baseflow appears to be recharged through leakage from basalts that outcrop within the upper reaches of the catchment, or through “Spring” flow fed from fault/fractured zones. ▪ Pg. 14 “Some groundwater springs have been observed from the boundary between the Tertiary basalt and the Silurian sediments”
Knight Piesold and PSM (1997). *NTSF1 Construction Report*	▪ Natural Springs (pg.9) ▪ Spring during construction (pg.10) ▪ Has recording of pore pressure during NTSF constructions (get copy of App C ref from Hatch*)
Newcrest Mining Limited (2000). *Geology of Southern Tailings Storage Facility Site, Rodd’s Ck-Spring Dell-Wire Gully; Cadia Hill Gold Mine Region*	▪ Map ▪ “Dell Spring” which is STSF

Reference	Comment
Kalf (2000). *Ridgeway Project Groundwater Management. In: Ridgeway Project – Environmental Impact Statement, Appendix B*	▪ "Seepages emerging from the basalt at Ridgeway tend to occur at the head of drainage gullies." ▪ "Groundwater within the volcaniclastic rocks also emerges at the ground surface along gullies and this is thought to be controlled by local fracture systems associated with the drainage system." ▪ "In mid to second half of 1998 the area experienced very high rainfall which also recharged the groundwater system substantially (see Attachment B-B). These conditions have indicated the presence not only of baseflow but a substantial interflow component in the stream hydrographs (Gilbert and Associates, 2000)." ▪ "…there is also a significant interflow component where recharge water drains relatively quickly into the stream gullies after heavy rainfall."
Woodward-Clyde (2000). *Cadia Hill Gold Mine Tailings Storage Facility Surveillance Report*	▪ Pg. 19 & Pg.20 ▪ Natural Spring at CH1650 found during inspection ▪ Seepage cannot be separated from runoff (pg.11)
URS (2002). *Southern Tailings Storage Facility Construction Report (Memorandum)*	▪ Soft wet zones encountered during TSF foot print preparation (pg.15) ▪ Spring exposed in foundation of cut-off (pg.18)
Kalf & Associates (2004). *Ridgeway Deeps: Groundwater Model Simulation Update and Hydraulic Impact of Mining To -500 m RL (Draft)*	▪ Sec 2.2. Spring waters are predominately sodium bicarbonate type.
AGE (2009). *Cadia East Project Groundwater Assessment. In: Environmental Assessment Cadia East Project, Appendix G*	▪ Many mentions of "Spring". All not in zone of interest. Small seepage zone east of Rodd's creek (pg.30) ▪ Baseflow in Flyers Creek is partially maintained by an area of (Silurian) springs approximately 1,200 m downstream of Long Swamp Road. An individual spring in this area had a visually estimated flow of about 20 L/s in autumn 2007 (Gilbert & Associates, 2009). Monitoring bores MB47A/MB47B are located approximately 300 m to the north-west of the spring zone and were located to provide data on the strata which feed the springs and to act as long-term monitoring points. ▪ Spring census work completed by (AGE, 2009) focussed on the area to the north and north east of the mine, where the broader sequence of Tb is mapped. This work presents census results for 53 springs mapped, however these have little relevance to the NTSF area other than to assist in understanding the types of spring that may occur.
GHD (2015). *Southern Tailings Storage Facility Seepage Investigation Review Data*	▪ "Increasing groundwater levels near the STSF may be associated with seepage from the tailings dam and/or the influence of the STSF structure on localised flow within the fractured groundwater system" ▪ Study focussed on understanding seepage from the STSF – limited relevance to this investigation.
AGEC (2016). *Cadia Mine. Update to Groundwater Model. Ref.G1383C.*	▪ Represents interaction (numerical) between the groundwater system and a number of springs – the approach assumed springs are associated with drainage alignment and local discharge conditions.
ATC Williams (2017). *Cadia Valley Operations, Northern Surveillance Report 2017*	▪ Contains record of seepage, monitoring sites appears to be on embankment benches, post construction
GHD (2018). *Cadia Valley Operations – Tailings Storage Facilities. Seepage Management Options Study. Options Report.*	▪ Section 2.5, "In some places the basalt and volcanoclastic groundwater appears as springs along or near the drainage lines where the topography falls (Kalf and Associates, 2000; Newcrest, 2016)"

Cadia Spring Occurrence and Type

There are four general types of springs occurring across the Cadia area based on the notations provided in Table 3:

- Contact springs, located at the margins of the higher permeability Tertiary basalt, with seepage from the basalt discharging at the contact with the lower permeability rock beneath. As natural recharge raises the saturated profile in the basalt, discharge rates at the margins will increase;
- Baseflow springs for aquifers and aquitards which are incised from drainage development and where topographic lows intersect natural groundwater. These are also sensitive to the saturated profile in the aquifer / aquitard: in the case of Silurian and Ordovician strata, their generally low permeability limits the variability in spring flow rate. Spring discharge may not always be evident if discharge occurs into alluvial bedloads;
- Structurally derived springs, where regional or sub regional structure acts as either a:
  - conduit to flow, permitting higher heads to be laterally translated to lower elevation areas, or;
  - barrier to flow, with spring discharge occurring where the fault acts as a ‘dam’ to groundwater, locally raising heads which may discharge at surface.
- Shallow interflow springs, which represent short distance and duration springs caused from local rainfall recharge discharging in creek alignments or breaks in slope. This form of spring is effectively rejected recharge, short lived and closely related to rainfall conditions.

Based on the above the springs at Cadia are not believed to have deep seated sources. Variability in spring head and consequent flow are likely driven by local recharge events, with flow rate a result of the spring head and the permeability of the spring source aquifer. Although there are some substantial spring flows noted, these appear mostly related to the main outcrop of Tertiary basalt to the north of the mine, and are limited relevance to the NTSF performance.

NTSF Area Springs

All four of the spring mechanisms described above have the potential to occur in the NTSF area. The eastern flank of the Tertiary basalt beneath the western embankment may provide contact spring flow. The Werribee Fault strikes beneath the NTSF and is regional is scale – this feature may provide either of conduit or barrier to flow conditions. Baseflow and interflow springs are also possible and based on visual descriptions provided of observed springs are probably the main mechanism in place beneath the facility.

Some NTSF area observations include:

- Woodward-Clyde (1995): *“It is understood that creekflow is perennial. This baseflow appears to be recharged through leakage from basalts that outcrop with the upper reaches of the catchment, or through ‘spring’ flow fed from fault / fracture zones.” And “The Tertiary basalt and trachyte flows are a known groundwater resource which are used for domestic and stock water supplies. Some groundwater springs are found at the contact between the Tertiary flows and underlying formations. Groundwater flows have been* *observed from the boundary between the Tertiary basalt and the Silurian Sediments / Angullong Formation in the catchment area of Rodds Creek."*

- Knight Piesold and PSM (1997): Noted *"During construction of the Stage 1 embankment several small springs were encountered in the base of Rodds Creek both upstream and downstream of the Zone A core. Springwater trapped upstream of the core will be collected by the upstream drainage system and discharged to the drainage collection pond."* And *"…a small homogenous earthfill embankment was constructed in Rodds Creek to provide a seepage collection pond to trap any spring water seeping into the channel through the rockfill placed within the footprint."*
- Woodward-Clyde (2000): Photograph of a natural spring at Chh1650, noted to be very wet due to recent rain.

The observations at the NTSF and other references indicate that the springs observed are not large in yield, are not likely to have a substantial driving head, and their variability in flow appears related to local rainfall conditions rather than regional hydraulic stresses. The construction of the NTSF recognised the presence of these springs and included internal components to address water produced by the springs during and after construction (Section 2.4.2). The piezometric records shown throughout Section 2.4.5 indicates that the NTSF drain was operational and that potential increasing tailings saturation as a consequence (say) of unmitigated spring contributions does not appear to be apparent.

As the NTSF was progressively raised, the increased head over the springs would be expected to further reduce their ability to flow and contribute water to the base of the tailings. The occurrence of interflow or baseflow springs would be diminished due to this suppressing head, and also due to the loss or reduction of natural recharge which might be expected to be the source of their flow in the first instance.

2.5 Hydrogeological Processes Discussion

The following summarises the preceding content to provide a general description of the hydrogeology at the NTSF:

- There are four broad groundwater systems, being:
  - Low permeability Ordovician Volcanics of the Weemalla Formation and the Forest Reefs Volcanics.
  - Low permeability Silurian sediments of the Ashburnia Group, which comprise limestones, mudstones, siltstones, sandstones and shales[2].
  - Moderate to high permeability Tertiary basalt, which may include a buried palaeo channel sequence where vent flows infilled pre-Tertiary drainages. The main outcrop of this unit is north of the mine, however there is an elongate sequence of basalt which lies beneath and west of the western embankment of the NTSF

[2] Previous assessments have often considered the Ordovician and Silurian sequence as a singly hydrostratigraphic unit because of the similarity of conditions in each sequence, and their strong hydrogeological contrast to the Tertiary basalt and Quaternary alluvium (where developed).

    - Quaternary alluvium, which in the immediate study area is poorly developed. This is also of limited relevance to the performance of the NTSF due to foundation preparation activity as part of construction.

- Structurally, the Werribee Fault underlies the NTSF and is a regionally mapped north to north-northeast trending, westerly dipping thrust with a strike-slip component. Near to the Cadia Mine, it truncates several NNW trending faults indicating it may be a late stage feature. The structure has a damage zone 200-400m wide, and a vertical offset of about 300m. Local faulting and fracturing is likely and may cause localised areas of higher permeability in the Ordovician / Silurian basement rocks.
- Groundwater recharge of the Tertiary basalt is most likely through rainfall recharge. Recharge of alluvium will be a combination of rainfall, creek flow and spring / seep from underlying basement or flanking Tertiary basalt. Recharge into the Silurian / Ordovician will be via rainfall recharge and will also occur where saturated Tertiary basalt overlies these systems. Rates of recharge into the Silurian / Ordovician are expected to be low to negligible, and variable for the Tertiary basalt and Quaternary alluvium depending on their condition at surface. Groundwater discharge may occur from all units via springs and seeps. Additionally, bore abstraction may occur for permeable sequences such as the Tertiary basalt and alluvium of spatial and hydrogeological significance.
- The NTSF design recognised, and construction had accounted for, the presence of springs and the potential impacts of a high permeability aquifer beneath the western embankment. NTSF performance monitoring has indicated the underdrain installed during Stage 3 construction has performed as intended. Phreatic conditions within the tailings indicate downward drainage effects toward to the drain, and unsaturated tailings conditions of up to 8m below the tailings elevation at the upstream of the embankment. Foundation seepage loss appears to be low and does not appear to have pressurised the contrastingly permeable underlying basalt. Based on this observation, it is assumed that the Werribee Fault has also not been pressurised.

3 SEEPAGE MODELLING

3.1 Two-Dimensional Seepage Modelling

Two-dimensional (2D) seepage modelling was undertaken using Seep/W to test hydraulic concepts and to inform the construction requirement of boundary conditions and hydraulic stresses for the three-dimensional (3D) modelling.

3.1.1 2D Model Details

Two models were constructed:

- Section CH1950 across the NTSF dam with a section length of ~850 m (which is the same dimensions and alignment of the early Slope/W model), or the short section, and,
- An extended version of this section of Ch1950, extending the model in both directions (4,738m) to reach the northern decant pond and the upper level Rodd Creek Dam upstream of the NTSF – the long section.

Assigned model parameters are consistent with parameters used in the initial Slope/W simulations (reference) with judgement-based values assigned where additional input was required. A summary of the material parameters used in the 2D modelling is provided in Table 4.

Table 4: 2D Seep/W Sectional Models for Testing of Hydraulic Stressors

Geology / Strata	K_h(Sat) m/s	K_v/K_h	Porosity	Ss 1/m
NTSF with depth 0 to 3m	1.00E-05	0.1	0.35	9.80E-05
NTSF with depth 3 to 6m	5.00E-06	0.1	0.35	9.80E-05
NTSF with depth 6 to 10m	1.00E-06	0.1	0.35	9.80E-05
NTSF with depth >10m	1.00E-07	0.1	0.35	9.80E-05
Dam Core	1.00E-09	1	0.35	9.80E-05
DS Berm	2.00E-05	1	0.3	9.80E-05
DS Rockfill	2.00E-05	1	0.3	9.80E-05
2B Rockfill	2.00E-04	1	0.3	9.80E-05
2A Transition	1.00E-06	1	0.3	9.80E-05
Foundation	1.00E-07	1	0.35	9.80E-05
Weathered Rock	5.00E-08	0.1	0.2	9.80E-05
Bedrock	1.00E-08	0.1	0.1	9.80E-05
Tertiary basalt	1.00E-04	0.1	0.2	9.80E-05
Palaeo Pathway – Tb buried	1.00E-02	0.1	0.2	9.80E-05

3.1.2 2D Model Results

Model output are shown in Figure 22 and Figure 23.

For the short section model (Figure 22) phreatic conditions are largely controlled across the dam with drainage elements effectively maintaining partially drained conditions in the tailings upstream of the dam, consistent with general piezometric observations.

Foundation conditions in this model do not permit differentiation in material parameters, so the highly contrasting conditions of the Tertiary basalt are not able to be separately modelled, neither are pond conditions in the NTSF and their relative influence on phreatic conditions across the tailings.

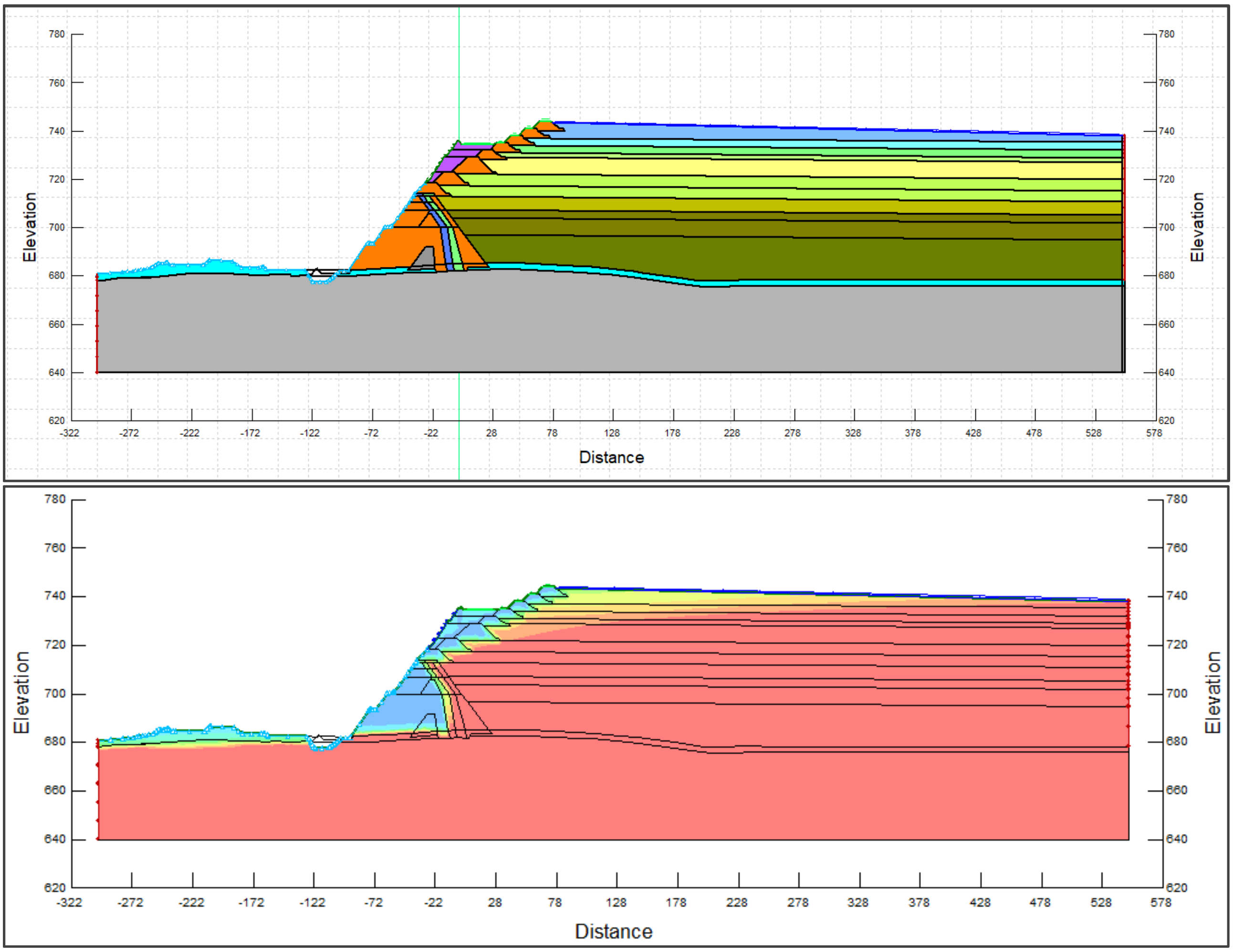

Figure 22: Short Section Model Domain (upper) and Modelled Phreatic Conditions (lower), Steady State

The long section model was developed to reduce the identified limitation in the short section model, and is shown in Figure 23. The modifications to this domain are extension upstream of the NTSF to permit inclusion of the NTSF pond and the potential effect of the Rodds Creek Dam, and increased layer partitioning of the foundation conditions to permit definition of the Tertiary basalt and a palaeo-alluvium sequence (between the base of the basalt and the underlying Silurian or Ordovician basement).

Three steady state scenarios are shown: the base case conditions (Silurian / Ordovician foundation materials), a Tertiary basalt (and palaeo-alluvium) sequence beneath and downstream of the dam, and another version of this with the Tertiary basalt and palaeo-alluvium extending approximately 1/3rd upstream of the dam.

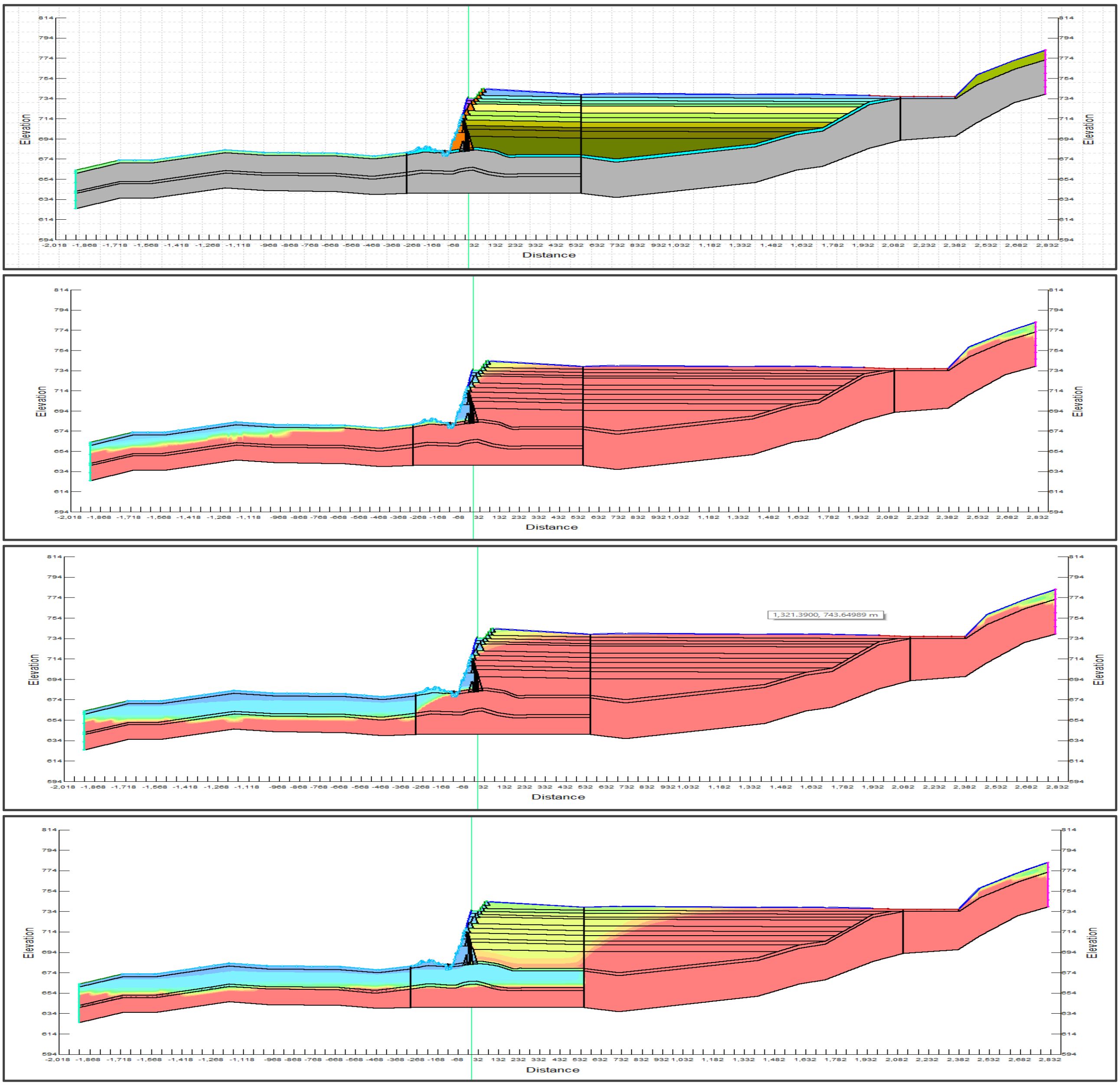

Figure 23: Long Section Model Domain (upper) and Modelled Phreatic Conditions a) Base Simulation Conditions, b) Tertiary basalt and palaeo-alluvium to Dam Toe, and c) Tertiary basalt and palaeo-alluvium to ~30% of Dam U/S of Crest

Discussion of the results of these three simulations is provided:

1. **Base Case Silurian / Ordovician foundation model case.**

   Similar results to the short section are observed, although this model gives a better appreciation of the relevance of the decant pond as a constant head source. With low permeability foundation materials, the model predicts largely saturated conditions at the downstream toe of the dam, although the drainage elements within the dam appear to remain effective.

Resultant variability of the degree of saturation of the tailings is a combination of the applied boundary conditions at either end of the model – the decant pond elevation in the upstream area of the section, and drainage elements in the dam itself. Differing recharge rates across the tailings provided some variability in this saturation but was not the primary factor influencing saturation upstream of the dam.

2. **Tertiary basalt and palaeo-alluvium downstream of the NTSF model case.**

   This scenario showed that strong downstream drainage via the higher permeability basalt occurs. This prediction is consistent with observations shown in Figure 19, indicating that the underlying basalt allows the seepage to be distributed. These model results also suggest the rate of seepage into the Tertiary basalt for the section shown does not pressurise the system and that the geometry and material parameters of the basalt are sufficient to carry seepage water away.

3. **Tertiary basalt and palaeo-alluvium downstream and upstream of the NTSF model case.**

   This section was simulated to consider the drainage effect of the basalt (without seepage mitigation prevention) in contrast to the generally lower permeability material of the Silurian and Ordovician foundation and the tailings.

   This is intended to reflect conditions where the basalt underlies the dam and tailings with the potential to act as a high capacity drain. No clay cover of the basalt is modelled in this case.

   As expected under this scenario, the basalt is the dominant drainage material, pushing the upstream extent of saturation further upstream, and increasing the gradient in the tailings between the extent of basalt simulated and the decant pond. (This may also be a response to the steady state condition modelled.) This is not consistent with data observed (Section 2.4.5), which shows no such dominant drainage effects attributed to the basalt where it underlies tailings.

3.1.3 2D Model Discussion and Relevance to the 3D Domain

The following points are noted:

- The 2D system is sensitive to foundation permeability, decant pond conditions and dam drainage construction elements, and to a lesser extent rainfall infiltration on the NTSF beach. Spigot water contributions were not modelled in the 2D scenario.
- Lower foundation permeability limits the vertical losses from the NTSF, with removal of water and the shape of the phreatic condition within the tailings most influenced by the efficiency of the dam drainage construction elements and the location and elevation of the decant pond.
- The effect of the Tertiary basalt as a drain without preventative seepage measures is powerful, and does not appear present in observational data. Piezometric records indicate

dam construction methods to address the potential high drainage this unit may create as being effective. This concept should be carried to the 3D model domain.

- Hydraulic gradients within the basalt appear to dissipate relatively quickly downstream of the dam, consistent with observed (post slump event) data.
- Decant Pond – the elevation and location of the decant pond has a strong influence on the degree of saturation and the position of the fully and partially saturated tailings.;
- Staged TSF – field results suggest that the tailings do not exhibit strong reduction in permeability due to settlement / consolidation but do show a downward drainage effect. The effect of this drainage on conditions in the tailings needs to be replicated in the 3D model construction and calibration process.

3.2 Three-Dimensional Numerical Modelling

3.2.1 3D Modelling Preamble

Three-dimensional (3D) modelling was required to:

1. Predict NTSF seepage and phreatic conditions for the period leading up to the slump event in March 2018;
2. Account for the primary sources of potential hydraulic stress internal and external to the NTSF; being both construction elements of the facility and natural strata. In this regard the model is to reflect the conceptual system described in Section 2 of this report;
3. Represent pre-slump-event conditions with a suitable level of confidence in model calibration and predictive performance.
4. Provide predicted conditions to others for independent stability or deformation analysis.

A 3D domain is preferred over the 2D domain because of its ability to reflect the geometric uniqueness of the NTSF construction elements and the underlying geology, and it permits are more spatially calibrated condition to be achieved which can then be used for either 2D or 3D analysis by others.

The model does not assess potential failure of NTSF design elements, and is intended to reflect the as-built condition as close as possible, so that predictions of hydraulic conditions based on operational performance of design and construction, as is understood to be the case, can be carried forward to deformation and stability analysis by others.

3.2.2 Model Construction

Model Selection, Limits & Spatial Extent

The three-dimensional, finite-element model platform FEFLOW was selected to meet the objectives and requirements of this investigation.

The 3D NTSF model domain is shown in Figure 24, with key line-data which is used to develop nodal distribution (dam infrastructure and drainage) also shown. The domain includes the full domain of the NTSF and extends far enough west to capture the Tertiary basalt which underlies the western embankment. To the south, the model domain extends far enough to capture the STSF ponding which is a critical boundary condition. The model domain covers a planar area of 1.39x10^7 m^2 (~14 km^2), with model dimensions of 4.7 km x 4.0 km x 150m.

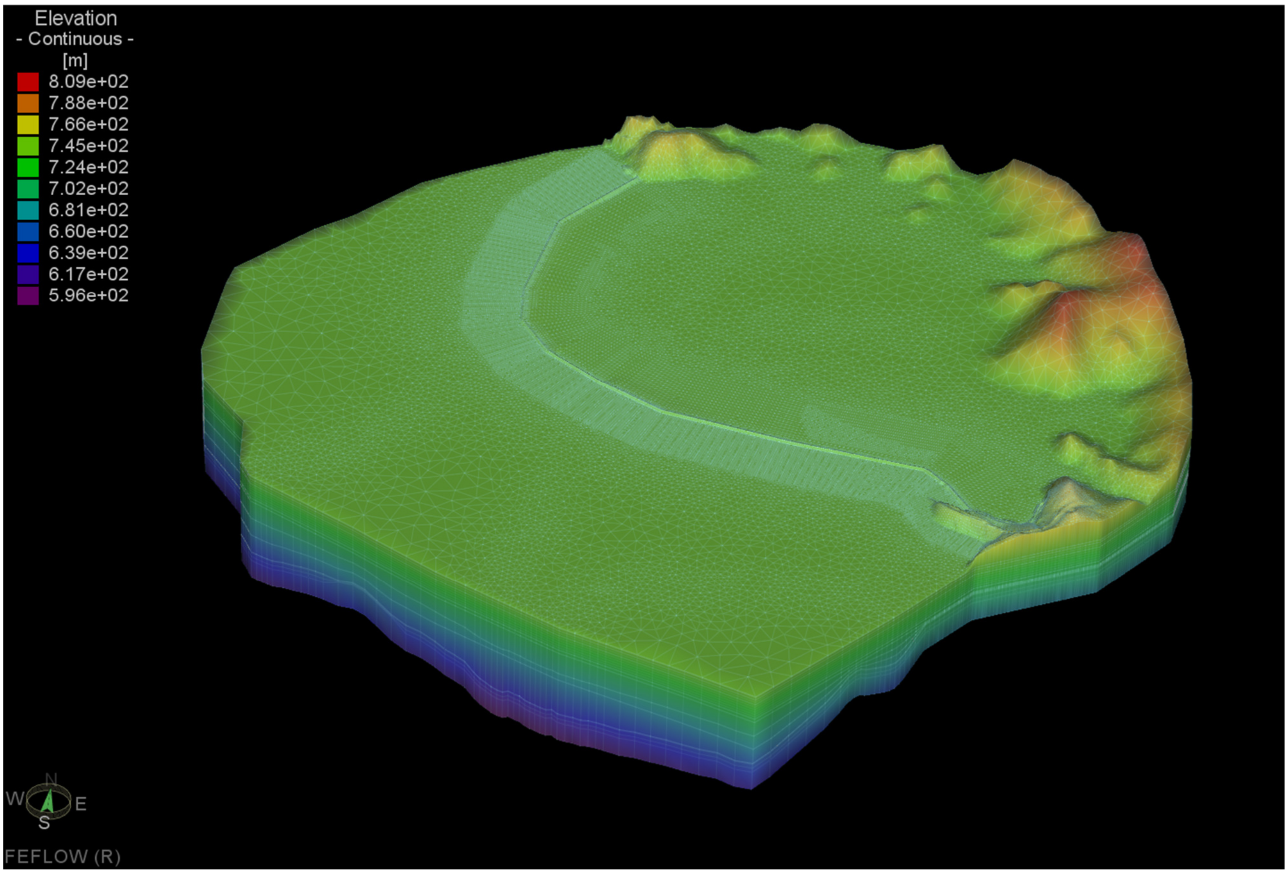

Figure 24: Cadia NTSF 3D Model Extent, Oblique View

Geological Basis

The model domain has been vertically extended to a nominal depth of ~5 x the maximum depth of the placed tailings. This is to provide sufficient depth definition to permit development of deeper groundwater flow regimes if required. Regional hydrogeology and dam construction have been represented consistent with the conceptual description provided in Section 2, and comprises:

- Dam Construction Elements:
  - Tailings, NTSF and STSF, with depth variability included in construction;
  - Dam Core;
  - Class 2B Fill;
  - Upstream clay liner;
  - Underdrain / gravel fill; and
  - Dam lifts (combined fill and lining).

- Geology:
  - Silurian / Ordovician, fresh and weathered;
  - Tertiary basalt, fresh and weathered;
  - Palaeo-alluvium where interpreted to exist;
  - Werribee Fault alignment; and
  - Top soil.

Calibrated material parameters are discussed in Section 3.2.3.

Domain / Nodes / Layers

The model was discretised using six-noded three-dimensional prism elements. A process of mesh refinement based on hierarchical areas of model interest was used to arrive at the final mesh configuration, which is shown in Figure 25.

There are ~73,000 elements per layer, across 19 layers for ~1.4M elements in total. Model layers 1-15 for the area of the NTSF are assigned for TSF construction and are aligned with the Stage development of the facility (e.g. model layer 5, is dam stage 5). Layer 15 is an allowance for engineering foundation transition conditions, and layers 16 to 19 represent natural strata. A summary of the model layering and NTSF staging is provided in Table 5.

Table 5: NTSF Construction Stage and Model Layer Development

Stage	Elevation	Layers
Natural geology	Variable	16-19
Engineering Layer/Top Soil	1m thickness	15
NTSF Stage 1	700	14
NTSF Stage 2A	707	13
NTSF Stage 2B/1	710.5	12
NTSF Stage 2B/2	714	11
NTSF Stage 3	718.5	10
NTSF Stage 4	723	9 and 8
NTSF Stage 5	729	6 and 7
NTSF Stage 6	732	5
NTSF Stage 7	735	4
NTSF Stage 8	738	3
NTSF Stage 9	741	2
NTSF Stage 10	744	1

This geometric arrangement resulted in reasonable model run times (generally ~2 hours for a quasi-steady state, and 1 hour for the 67-day transient with daily time steps), and relatively stable model simulations.

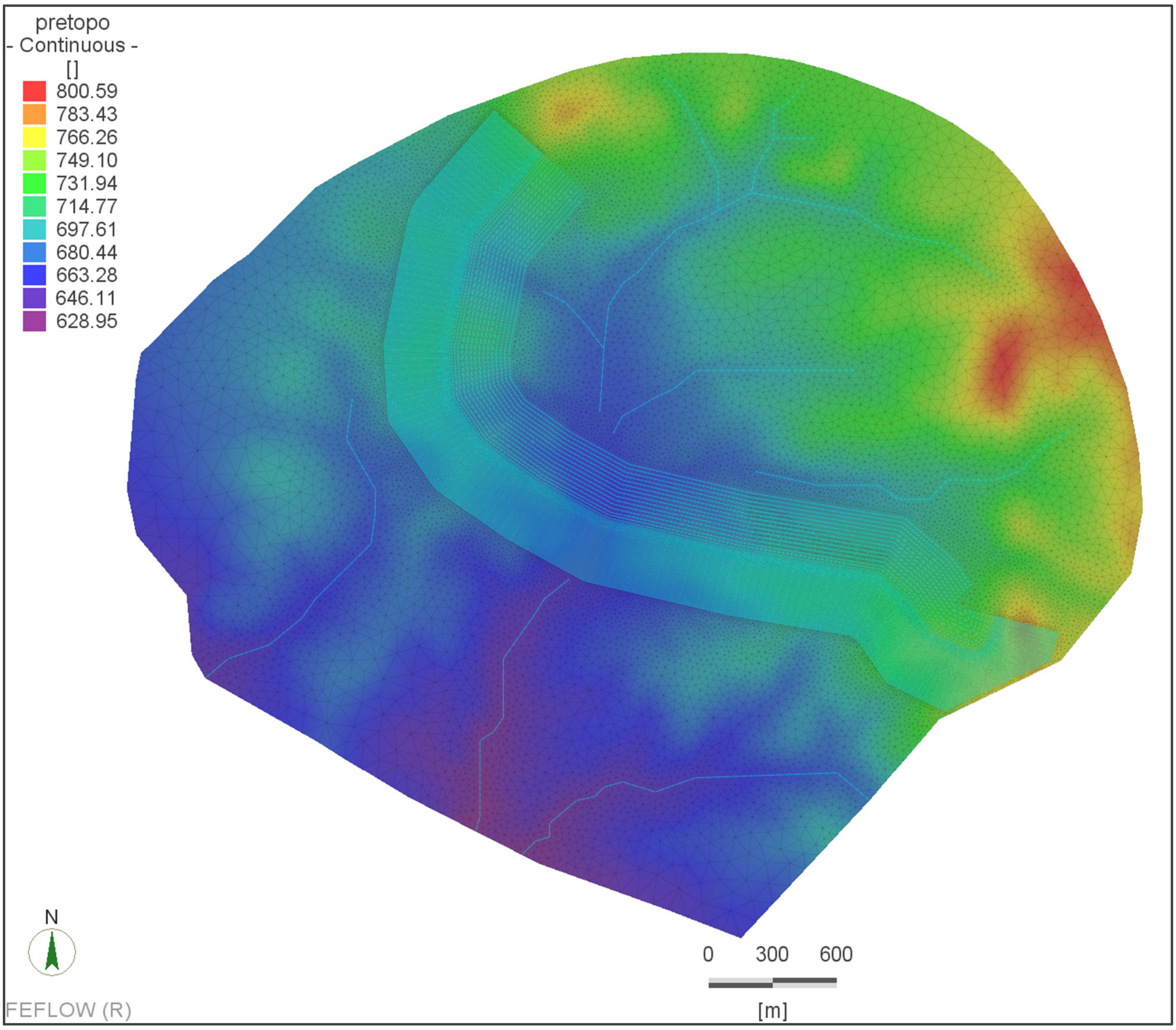

Figure 25: Cadia NTSF 3D Model Node Distribution

Model Boundary Conditions

Model boundary conditions comprise:

- Rainfall recharge, as a variable rate based on percentage of mean annual rainfall and dependant on the hydraulic properties of the upper most unit in the model;
- Decant pond area and elevation as a varying fixed head, for the NTSF and STSF, based on mapped extents and stage development of the tailings dam(s) and consequent ponded water levels (Figure 14);
  - Spigot water distribution across the NTSF beach was zoned based on distance from the dam crest and location to the pond. Rates were manually calibrated to assist in constructing a plausible water balance for the tailings, and were:
    - 400-600 mm/annum for the area up to 100m from the dam crest;
    - 100-200 mm/annum for beach areas 100 m to 400 m from the dam crest,
    - 30mm/annum for the balance, which is approximately equivalent to 4% of MAR.

- No flow boundary conditions were established at the model base and on the lateral limits of the model domain.

Constrained seepage face conditions were established across the face of the dam. The constraints on the seepage face dictate that once phreatic conditions intersect the top of the upper active layer in the model at the time of the simulation, water is removed from the system and reports to the water balance as an outflow. This representation of seepage faces is established to reflect the process of emerging seepage due to rising phreatic conditions “daylighting” at surface.

Drain discharge was measured from model output, no fixed heads were applied in forcing the model to exit excess water. The STSF southern outflow was modelled as a seepage face (665.0 to 671.0 mRL).

Model Timing & Stress Periods

Timing and evaluation of model calibration is discussed in Section 3.2.3

A steady state model of the Stage 9 NTSF condition was run and calibrated. This calibrated steady state model was then used to create starting conditions for the transient simulation of Stage 10 of the NTSF.

The Stage 10 model was constructed to run from 1-Jan-2018 to the 9-Mar-2018, for a 67-day period. Recharge on both the NTSF and the dam raise material was established as a daily time sequence based on actual conditions as recorded by site. Pond elevations reflected actual data, and model results were extracted for the final time step, which is coincident the slump event.

Results of this process are discussed in Section 3.2.4.

3.2.3 Model Calibration

Calibration Approach

The conceptualisation of the system, review of observation data and outcomes from the 2D sectional analysis indicate the NTSF has moderate to limited connectivity with foundation materials, and that the phreatic condition within the tailings are more dominated by dam construction elements and decant pond location. The calibration strategy was developed to reflect these system attributes with focus brought to NTSF observational data. Data outside the facility were still used, but were not considered the primary drivers to achieve a satisfactory level of model calibration.

Steady state model calibration was undertaken on the Stage 9 NTSF condition, with focus on three primary sets of observation data:

- CPTu Pore Water Pressure Gradients (Figure 20) measured in the NTSF, showing downward vertical gradient profiles within the tailings;
- 2017/18 piezometric data for tailings locations around the upstream area of the dam crest (Figure 21), which show the prominence of drain effects on the tailings profile;
- Measured drain flow between 2015 and 2018 (Figure 13), which for Stage 9 were generally between 40 L/min to 50 L/min.

Post-slump groundwater levels in the Tertiary basalt were also considered, however, it is noted these were measured after the event.

Initial calibration was manually completed modifying boundary condition and parameter ranges. Automated and manual calibration was then completed firstly on the foundation geology properties, and then on the permeability of the tailings inside the NTSF.

Calibration Results

A summary of model material parameters post calibration is provided in Table 6. Permeability modified during the calibration process is summarised in the following:

- Tertiary basalt Kh / 100 from the pre-calibration value
- Weathered rock Kh x 2.5 from the pre-calibration value
- NTSF Tailings Kh Variable, range 'tightened' and depth varying

As expected, the modification of tailings permeability had the greatest impact on model performance. A depth-variant hydraulic conductivity is included and is summarised in Figure 26. Tertiary basalt permeability was reduced; however, the basalt remains the unit with the highest permeability in both tailings and bedrock. High permeability underdrain materials and low permeability clay blanket conditions are the main controlling factors on the rate of water transfer vertically into foundation materials, and through the dam.

Table 6: Model Calibrated Hydraulic Parameters

Material	Kh (Sat) m/sec	Kv/Kh	Porosity	Ss 1/m
Bedrock	1.00E-08	0.1	0.1	1.00E-04
Faults	5.00E-09	1	0.1	1.00E-04
Lifts (Combined Fill and Liners)	1.00E-06	1	0.3	1.00E-04
2B Fill (Core side Fill)	2.00E-04	1	0.3	1.00E-04
Dam core	1.00E-09	1	0.35	1.00E-04
Basalt	1.50E-06	1	0.2	1.00E-04
Palaeo Pathway	1.50E-06	1	0.2	1.00E-04
Top Soil	2.00E-08	1	0.35	1.00E-04
Upstream Clay liner	1.00E-09	1	0.1	1.00E-04
Slotted piping/Gravel fill	1.20E-02	1	0.1	1.00E-04
Weathered Rock	2.00E-08	0.1	0.1	1.00E-04
NTSF	1.00E-7 to 2.65E-6	0.1	0.35	1.00E-04
STSF	5.00E-07	0.1	0.35	1.00E-04

Permeability modified during the calibration process is summarised in the following:

- Tertiary basalt Kh / 100 from the pre-calibration value
- Weathered rock Kh x 2.5 from the pre-calibration value

- NTSF Tailings Kh Variable, range 'tightened' and depth varying

The modification of tailings permeability had the greatest impact on model performance. A modified depth-variant hydraulic conductivity has been included in the model and is summarised in Figure 26. Reduction of two orders of magnitude of the basalt is also a noted significant modification. Initial estimates are considered more representative of the unit where it is more regionally mapped and recognised as an aquifer to the north. The modifications to ground conditions discussed in Section 2.4.2 may also contribute to a lowered value for this unit.

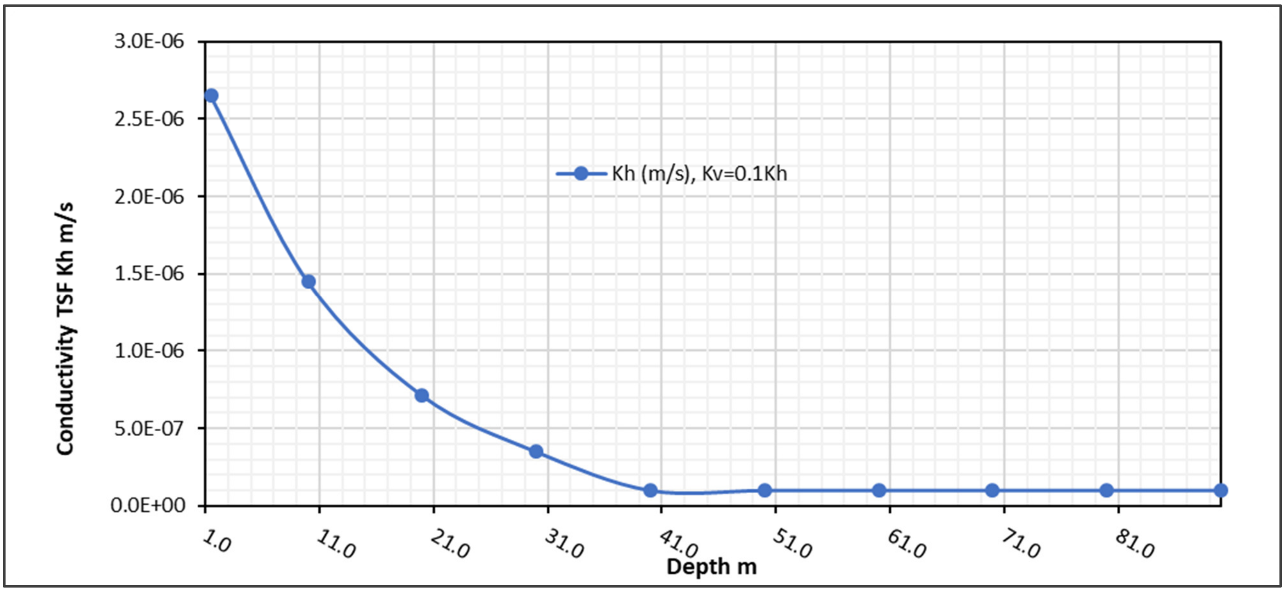

Figure 26: Inferred Tailings Permeability Modified Depth Variant Range

A summary of observed versus modelled head values for the calibrated Stage 9 model is provided in Table 7. Values used which post-date the event are shaded orange.

Table 7: Summary Observed versus Modelled Head Values, Calibrated Model

Name	Depth	Tip El. (m)	Observed Head m	Computed Head m	Observed Pressure kPa	Computed Pressure kPa	Head Residual (m)	Observation Date
VWP-N01	10.00	730.70	734.50	736.10	37.28	52.97	-1.60	2017-06-30
VWP-N02	10.00	731.20	735.10	735.02	38.26	37.44	0.08	2017-06-30
VWP-N02a	10.06	731.14	737.26	735.01	60.04	37.93	2.25	2017-xx-xx
VWP-N02b	15.00	726.20	736.90	734.17	104.97	78.18	2.73	2017-xx-xx
VWP-N02c	20.26	720.94	735.72	733.32	144.99	121.42	2.40	2017-xx-xx
VWP-N03	10.00	730.90	735.20	733.95	42.18	29.97	1.25	2017-06-30
VWP-N03a	16.11	724.79	735.90	732.75	108.99	78.12	3.15	2017-xx-xx
VWP-N03b	20.00	720.90	735.58	732.03	144.01	109.21	3.55	2017-xx-xx
VWP-N03c	34.09	706.81	734.03	726.85	267.03	196.63	7.18	2017-xx-xx
VWP-N04	16.00	724.40	731.30	733.01	67.69	84.47	-1.71	2017-06-30
VWP-N04a	12.01	728.39	734.40	733.76	58.96	52.67	0.64	2017-xx-xx
VWP-N04b	23.80	716.60	731.79	731.64	149.01	147.59	0.15	2017-xx-xx
VWP-N04c	36.35	704.05	729.02	726.18	244.96	217.14	2.84	2017-xx-xx
VWP-N04d	38.05	702.35	728.45	725.39	256.04	226.05	3.06	2017-xx-xx

Name	Depth	Tip El. (m)	Observed Head m	Computed Head m	Observed Pressure kPa	Computed Pressure kPa	Head Residual (m)	Observation Date
VWP-N04e	47.67	692.73	728.41	722.19	350.02	289.00	6.22	2017-xx-xx
VWP-N05	16.00	724.10	727.80	730.27	36.30	60.48	-2.47	2017-06-30
VWP-N05a	19.47	720.63	729.50	729.67	87.01	88.68	-0.17	2017-xx-xx
VWP-N05b	30.22	709.88	726.80	725.86	165.99	156.77	0.94	2017-xx-xx
VWP-N05c	44.66	695.44	721.13	718.45	252.02	225.75	2.68	2017-xx-xx
VWP-N05d	60.67	679.43	712.66	713.13	325.99	330.64	-0.47	2017-xx-xx
VWP-N06	16.00	723.00	730.80	731.67	76.52	85.05	-0.87	2017-xx-xx
VWP-N06a	11.07	727.93	733.54	732.39	55.03	43.73	1.15	2017-xx-xx
VWP-N06b	20.00	719.00	731.44	731.13	122.04	118.97	0.31	2017-xx-xx
VWP-N06c	30.07	708.93	729.01	728.60	196.98	193.00	0.41	2017-xx-xx
VWP-N07	16.00	723.00	733.10	732.26	99.08	90.83	0.84	2017-06-30
CE405	*30.25*	*657.58*	*682.68*	*677.26*	*246.23*	*193.09*	*5.42*	*2018-09-06*
CE406	*30.15*	*657.89*	*677.83*	*679.90*	*195.61*	*215.89*	*-2.07*	*2018-09-06*
CE407	*51.00*	*680.80*	*697.71*	*703.83*	*165.89*	*225.96*	*-6.12*	*2018-09-06*
CE408	*56.95*	*686.85*	*710.78*	*713.58*	*234.75*	*262.21*	*-2.80*	*2018-09-06*
CE412	*56.50*	*686.65*	*692.36*	*702.83*	*56.02*	*158.68*	*-10.47*	*2018-09-06*
CE413	*57.35*	*697.00*	*724.87*	*719.97*	*273.40*	*225.30*	*4.90*	*2018-09-06*
CE415	*25.00*	*661.16*	*684.77*	*687.22*	*231.61*	*255.67*	*-2.45*	*2018-09-06*
CE417	*12.40*	*688.60*	*691.21*	*694.03*	*25.60*	*53.29*	*-2.82*	*2018-09-06*
CE430	*26.15*	*680.17*	*690.57*	*698.44*	*102.02*	*179.22*	*-7.87*	*2018-09-06*

Contoured calibrated head conditions for Stage 9 are provided in Figure 27 for the NTSF tailings. A series of cross sections as shown on this figure, are provided for the calibrated model in Figure 28.

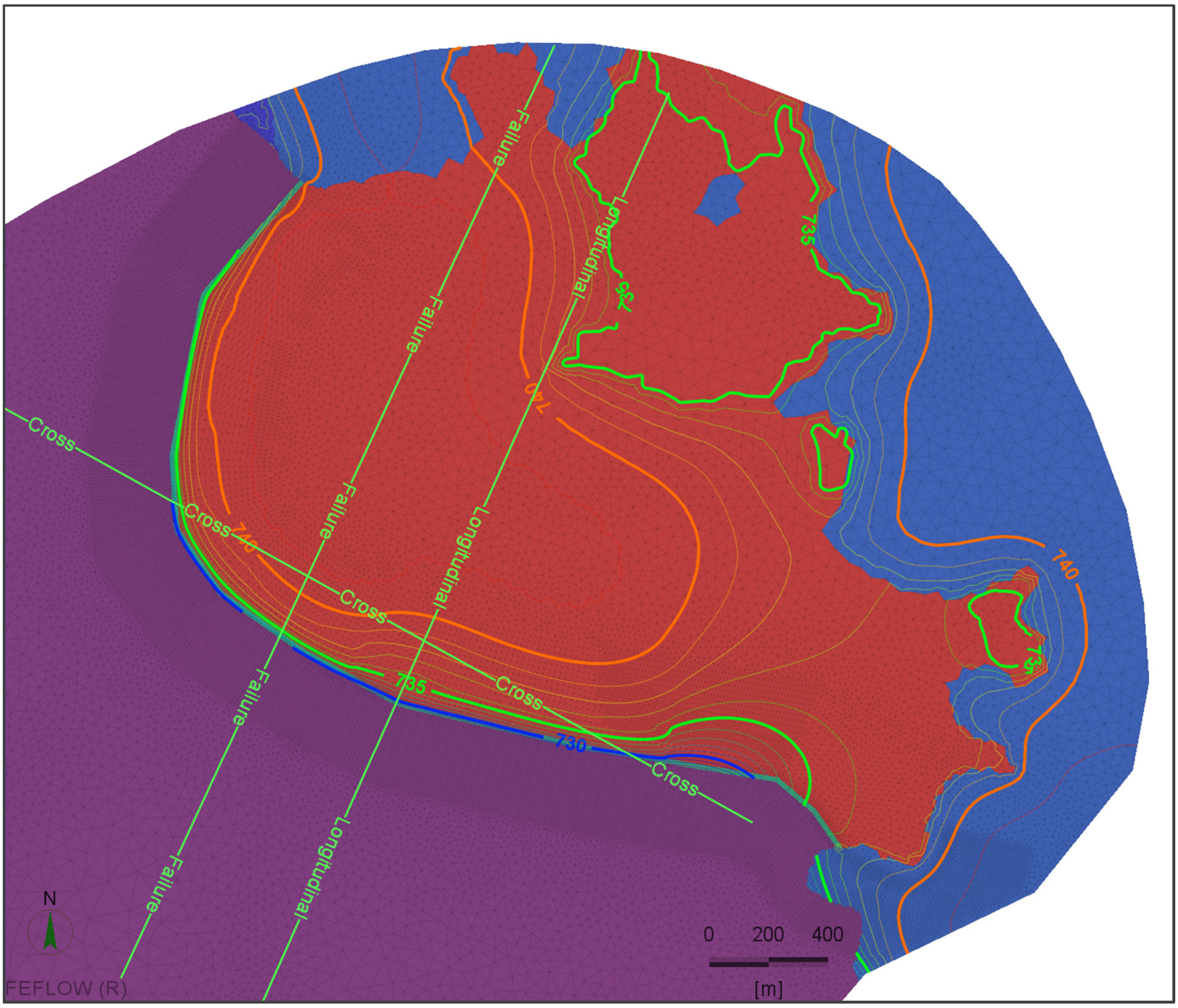

Figure 27: Calibrated Model Head Conditions, Tailings Conditions

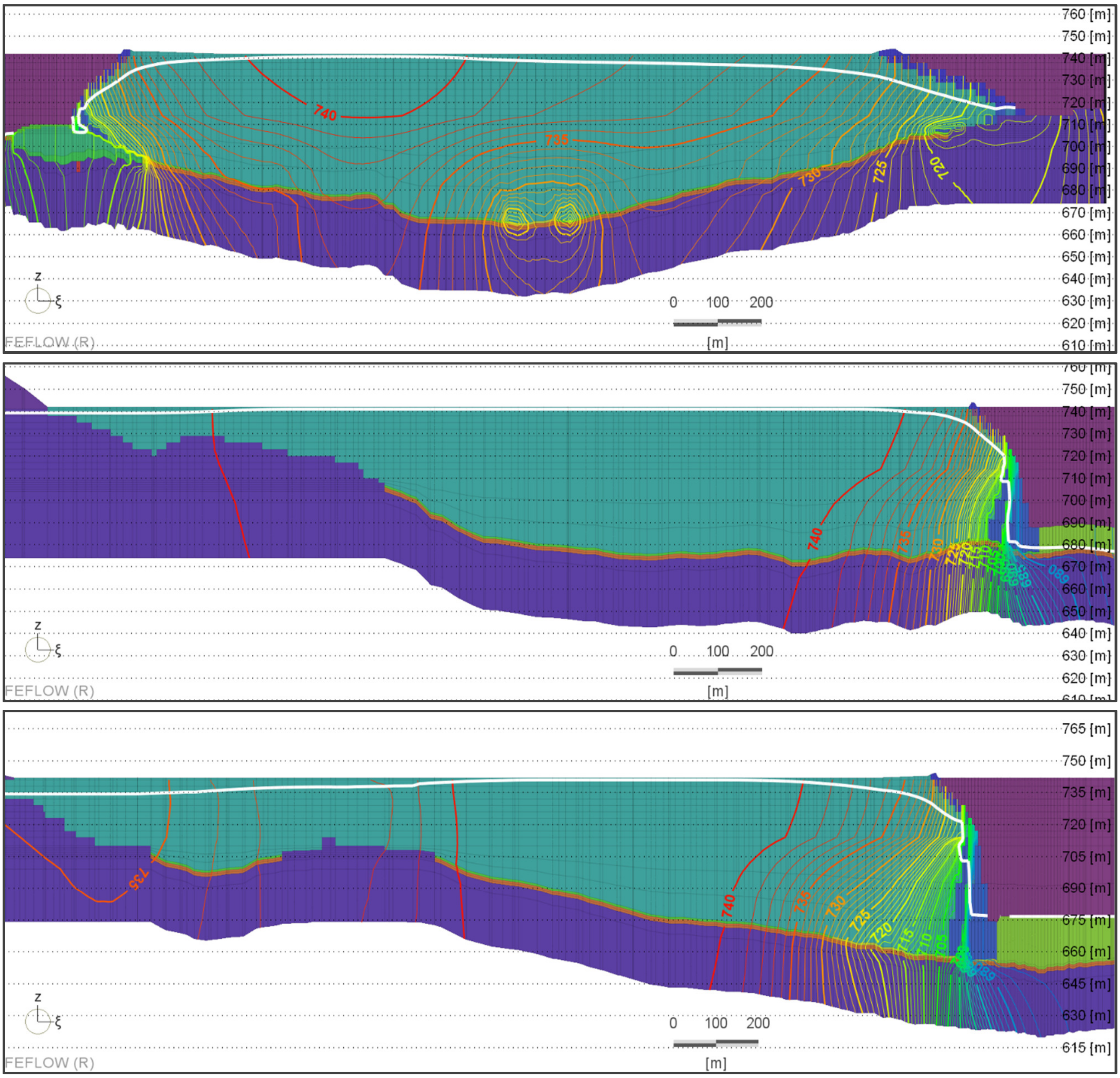

Figure 28: **Calibrated Model Head Conditions, Model Sections: Cross (upper), Failure (middle), Longitudinal (lower)**

Calibration Performance

Additional discussion of calibration performance is provided in the following sections and comprises review of the three components of the predictive model required to replicate the conceptual understanding of the performance of the NTSF, being: statistical measure of measured versus observed heads, replication of pore pressure response and downward gradient trends, prediction of drain flow discharge from the NTSF.

Measured versus Observed Conditions

Measured versus observed conditions for the Stage 9 model, for TSF VWPs are shown in Figure 29. Note this suite of data includes the 2018 installed CE sites at the base of the NTSF embankment.

Although these were installed post-slump-event, they are important in understanding the performance of the model to replicate key hydraulic stresses.

Calibration statistics are within industry accepted metrics. The correlation co-efficient between measured and modelled data is 0.95, the RMS error is ~3.69 m, and the mean error is -0.3m (indicating the model is computing heads slightly below measured). The scaled RMS is 6.2%, and the measured data has a 60 m vertical range between about 676 mRL and 736 mRL.

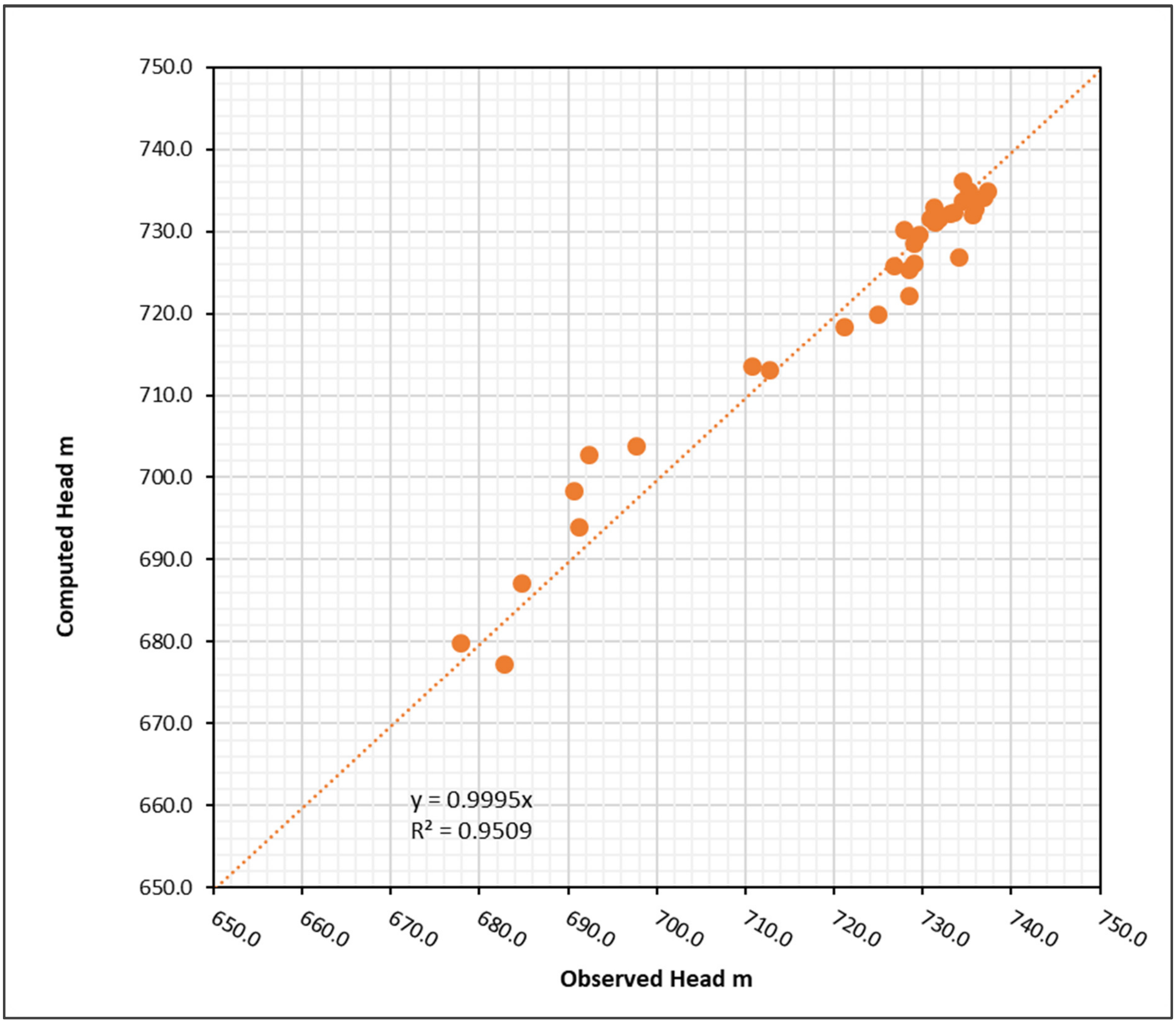

Figure 29: Measured versus Modelled Head Conditions, NTSF Tailings and Foundation Tb

Tailings Gradient Replication

CPtu derived pore water pressure data shown in Figure 20 are also used to assess whether the model is replicating the downward gradients observed in the field collected data. These results are shown in Figure 30. Visual comparison of these graphs indicates the model is replicating this process in all locations, at a similar scale to that observed.

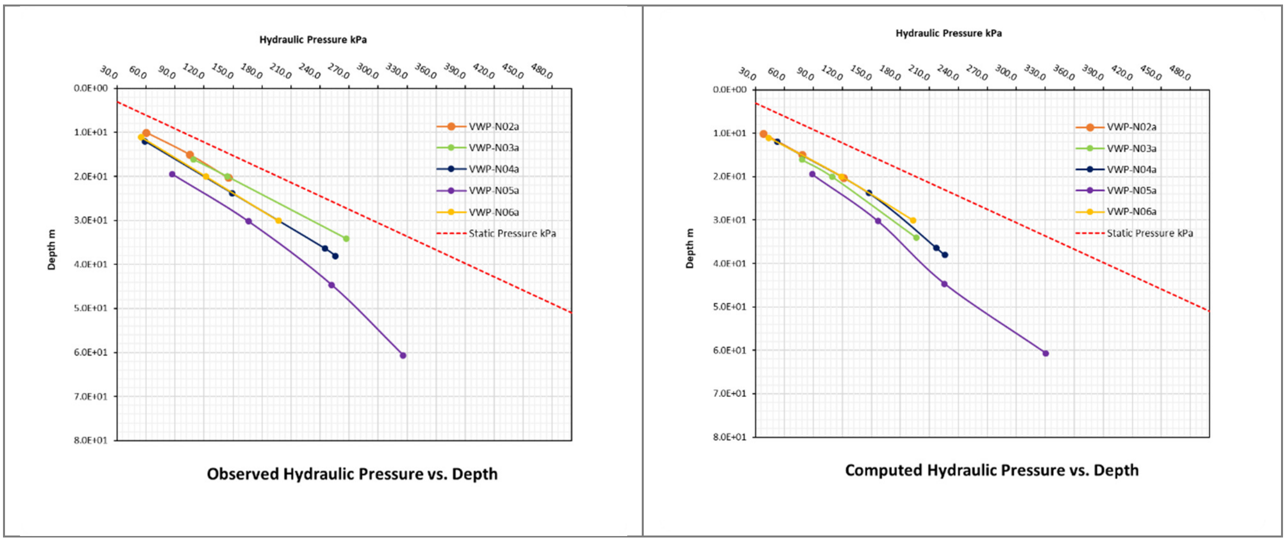

Figure 30: Comparison between Observed (left) and Computed (right) Tailings Gradients

NTSF Drain Flow Estimation

Model simulated total drain flow under steady state conditions for the calibrated model is estimated at 68.0 L/min. This is higher than 2018 measured data of 40 L/min to 50 L/min as the drain measurement does not collect all the seepage, whereas the modelled estimate captures seepage as a total loss form the model. The measured value therefore is considered to underestimates total. A summary of transient drain predictions from this feature is shown in Figure 31.

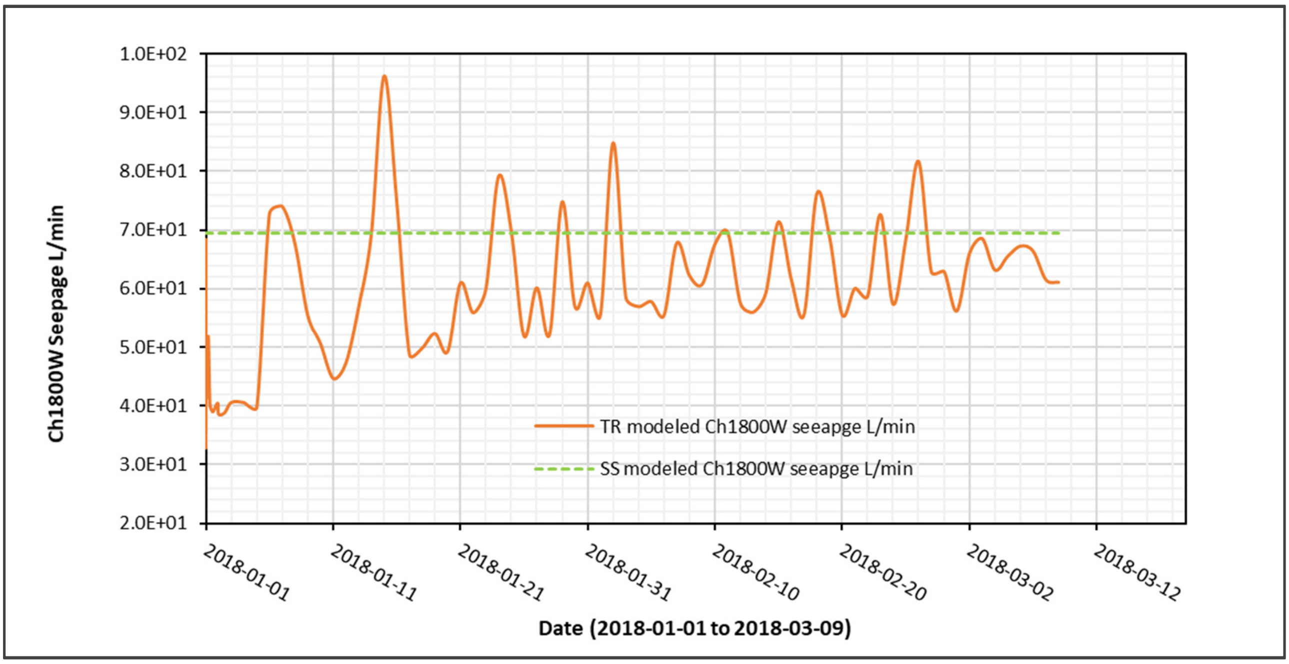

Figure 31: Transient Model Drain Flow Predictions, Ch1800W Drain

3.2.4 Model Results

3D Model Output

The results of the transient simulation are provided in a series of figures and cross sections between Figure 32 and Figure 37.

Generally, conditions are similar to those of the calibration model. Drainage via the Ch1800W drain remains a prominent visual component to phreatic conditions, particularly in the upper tailings sequence. The decant pond imposes a skew in these contours, and in lower levels of the model and foundation conditions the drainage effect of the Tertiary basalt becomes more prominent, as would be expected. The area of the slump event is located mid-way between the drainage effect to the east of the slump area, and the sub-crop of the Tertiary basalt.

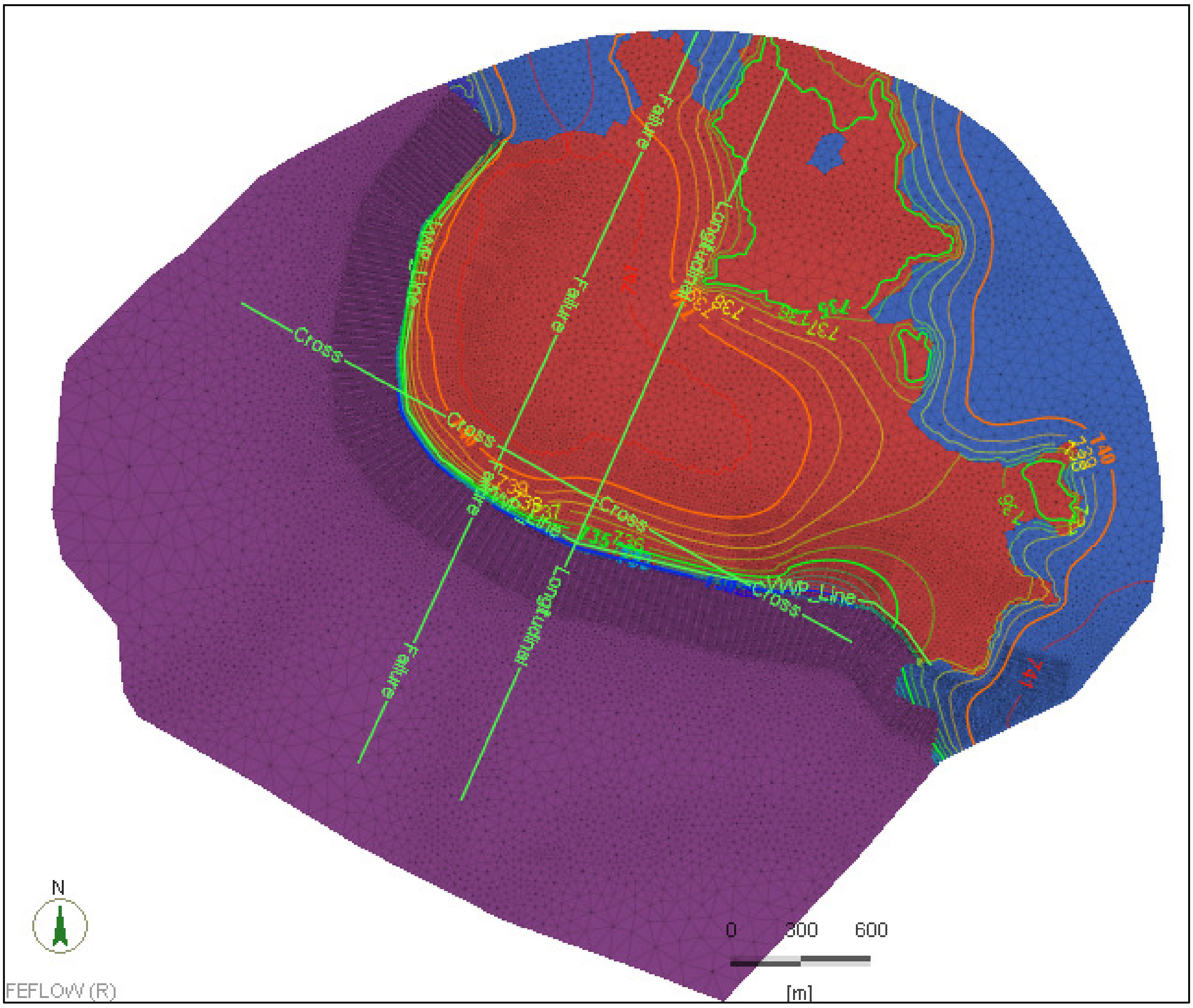

Figure 32: Transient 3D NTSF Model, Upper Layer Conditions, Time of Slump Event

A detailed image of the slump event failure section is provided in Figure 33. Modelling results suggest that the internal dam construction components appear to continue to perform as intended, with the phreatic surface predicted to be about 6-7 m below the Stage 10 dam crest, and the phreatic condition above the Stage 3 crest elevation of about 718.5 m maintained behind (upstream) of the NTSF lifts.

Transient modelled drain discharge (Figure 31) fluctuates but remains within a relatively constant range for the six weeks or so preceding the failure date, and mostly below the steady state calibrated amount for this feature.

The climatic and dam raise conditions modelled do not appear to have created a disproportionate increase in either the phreatic condition of the tailings or drain flow estimation at the time of the slump event.

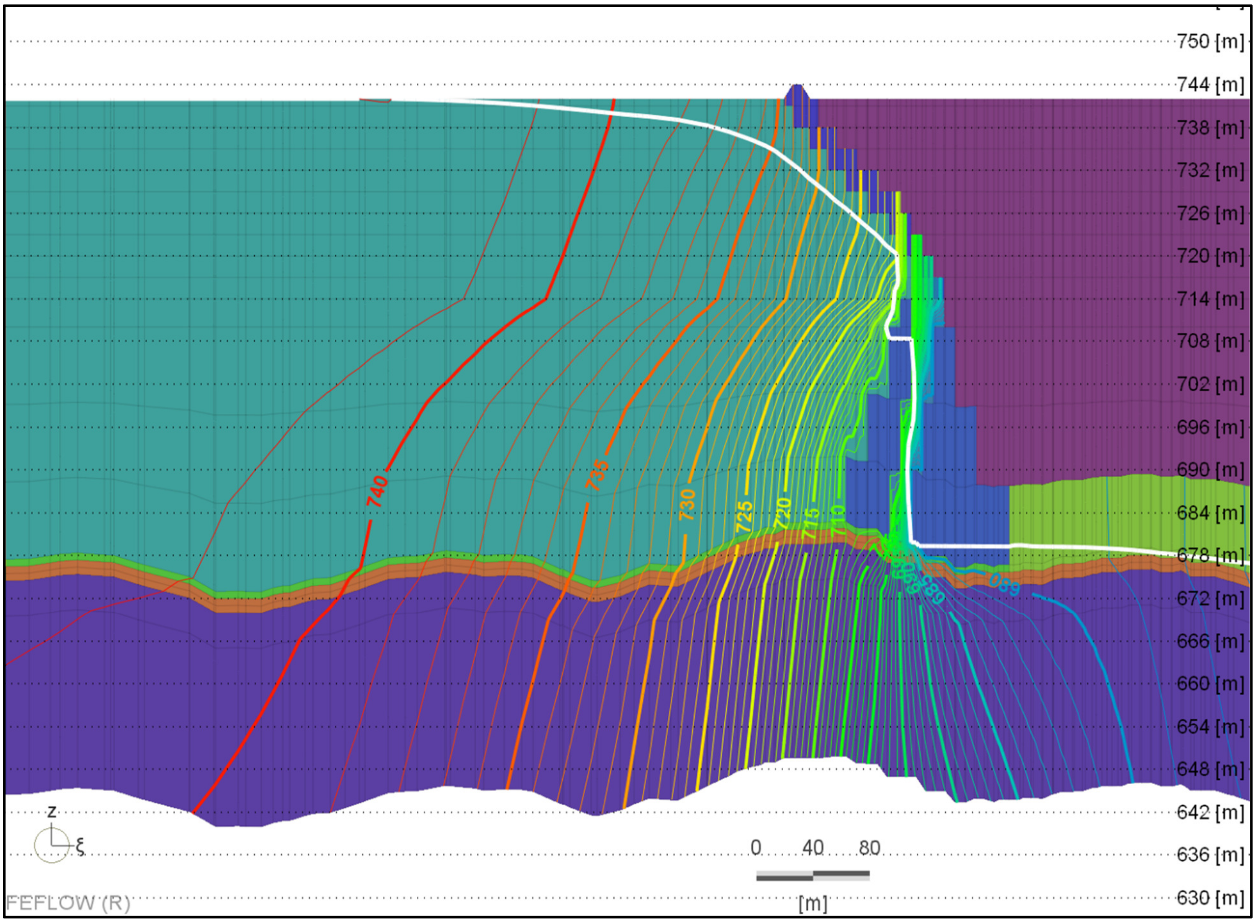

Figure 33: Detailed Piezometric Detail, Failure Section, Time of Slump Event

An important observation in Figure 32 is that visually the area of the slump coincides with the area of the NTSF which appears to experience the highest degree of saturation nearest to the dam (with exception of the western embankment). The detailed cross section (Figure 33) and the predicted drain discharge do not indicate that the phreatic condition has conceptually changed and has either encroached on the dam lifts or resulted in emergent seepage on the face. This is also consistent with the available monitoring data (Section 2.4.5) which confirms the same.

This area of the dam is simulated to have a higher degree of saturation than further to the east where drain effects are more prominent, but the dam construction elements built into the model appear to be continuing to manage the system. Further to the west, and around the western embankment, greater degrees of near dam saturation are noted, so this does not appear to be a unique or singular observation, however it is visually prominent when compared with conditions toward the east.

The next four figures provide model predicted output for NTSF conditions in the lower sections of the system at the interface of the tailings system and the transition back into natural ground. The effect of the Tertiary basalt starts to be noted in layer 15 and is more visually prominent in lower layers; however due to the foundation preparation preventing this unit from creating a drainage effect in the tailings, as evident in NTSF performance data, this observation is relevant only below or downstream of the NTSF. The modelled phreatic conditions in the tailings, above the sub-crop of the Tertiary basalt, reflect the observation data and system performance discussed in Section 2.4.5

The Ch1800W drain which is a prominent feature throughout the tailings also increases in definition in lower elevations of the tailings as permeable strata associated with the pre-construction drainage assist in removing water from deeper areas of the system.

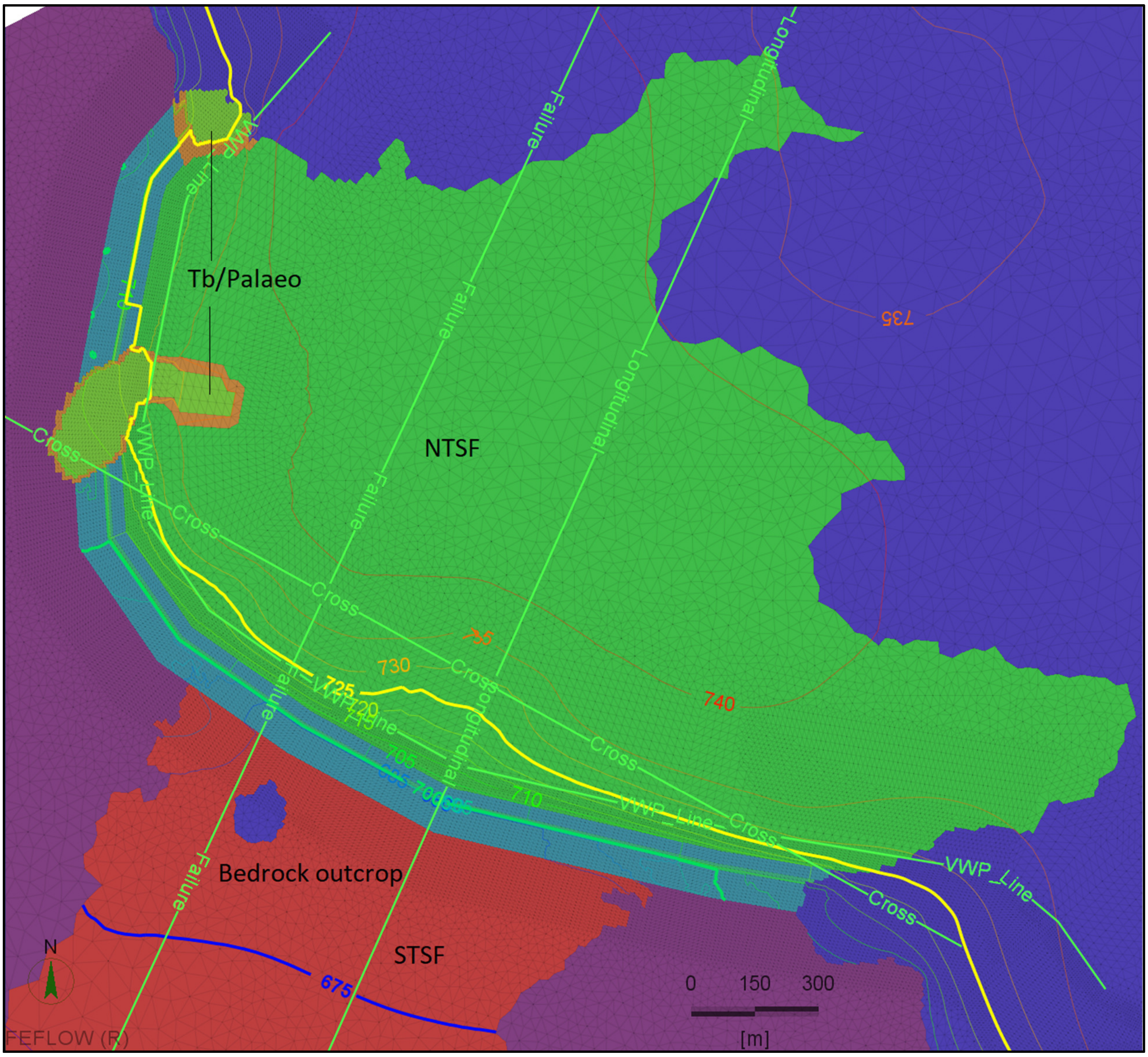

Figure 34: Transient Conditions & Geology, Layer 14, Base of NTSF, Time of Slump Event

Figure 35: Transient Conditions & Geology, Layer 15, Time of Slump Event

The imagery in Figure 34, Figure 35, Figure 36 and Figure 37 show predicted pressure conditions with increasing depth and transitioning geology, across model layers 14, 15, 16 and 17. The 725 m contour (yellow) and the 700 m contour (green) are useful visual guides in reviewing these figures to assess conditions with depth.

Below the tailings, underlying hydrogeological contrasts (for example, between the Tertiary basalt (high) and the Forrest Reef Volcanics, become dominant features on the shape of pressure conditions and the movement of groundwater. Tertiary basalt becomes more influential as a drain, as does the existing and covered Rodds Creek channel. Pressure contours indicate very little change in vertical gradients in the area of the slump.

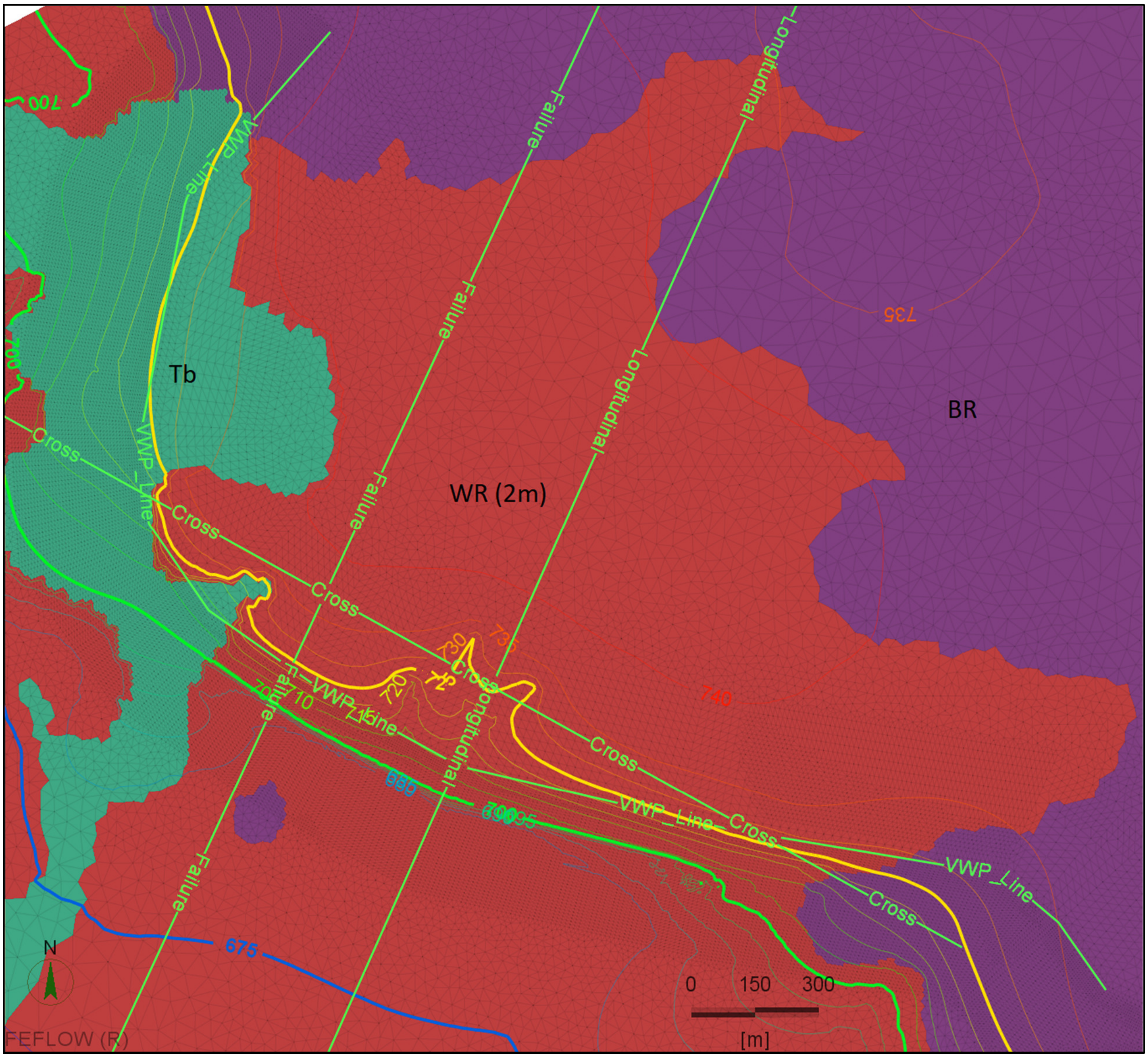

Figure 36: Transient Conditions & Geology, Layer 16, Time of Slump Event

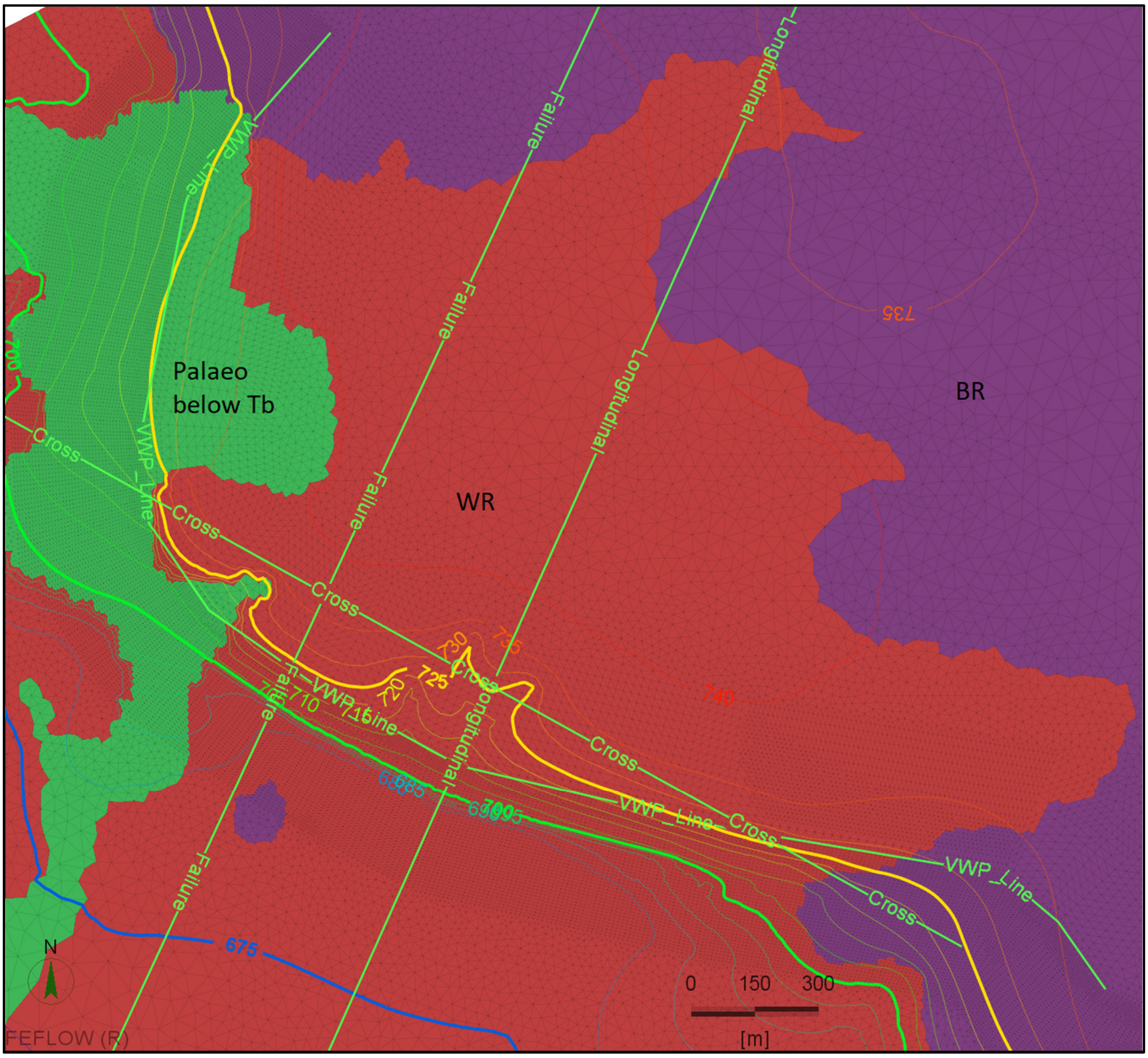

Figure 37: Transient Conditions & Geology, Layer 17, Time of Slump Event

3.3 3D Modelling Summary

A 3D model has been constructed to replicate performance of the NTSF in the period leading up to the slump event that occurred in March 2018. The model was constructed based on the conceptual understanding of the site described in Section 2 and informed through 2D modelling to assess prominent hydraulic concepts of greatest relevance to prediction of conditions inside the NTSF.

The model was calibrated to three primary performance criteria: piezometric conditions of the tailings, vertical gradients within the tailings derived from CPtu testing, and estimation of drain flow emerging from the Stage 3 underdrain. The model calibration was able to replicate each of these criteria through a manual and automated calibration process, and the model was then set up to simulate the Stage 10 construction from 1-January-2018 to the time of the slump event, under transient conditions.

During the period of transient simulation, no significant rainfall or creek flow was noted, pressure conditions within the tailings did not exhibit any abnormal trends compared with prior or recent data, and the decant pond elevation was not substantially increased. Model simulated conditions for the time of failure do not indicate any occurrence of new or abnormal seepage emergence on the dam face, and the effect of the Stage 3 underdrain maintained phreatic conditions upstream of the dam lifts. Review of deeper predicted pressure conditions does not indicate generation of higher pressures at the area of the slump.

The data from this simulation were compiled and forwarded for use in other elements of the study. The simulation did not consider failure of any element of the dam construction and modelled the conditions as close to actual as possible. No sensitivity or uncertainty analysis has been completed.

4 REGULATORY QUESTION RESPONSE

Two points in relation to the seepage and hydraulic performance of the NTSF have been raised by the regulator. These, and comments addressing each, are provided in the following, noting some section reproduction is provided in the following to permit the response to be located in one location:

4.1 Question 1

> ***"an assessment as to the contribution that seepage has had on the integrity of the NTSF wall at the site of the wall slump event"***

4.1.1 Groundwater Modelling Analysis

Groundwater modelling was undertaken to construct a best estimate of phreatic conditions in the NTSF at the time of failure. A 3D model was constructed and calibrated to NTSF performance observations, and then run under transient conditions using true meteorological records to estimate phreatic conditions and seepage at the location of the slump, at the time of the event.

This work is documented in detail in this report, with the modelling results discussed in Section 3.2.4. A summary, specifically related to seepage at the NTSF wall at the site of the slump event, is provided:

- The climatic and dam raise conditions modelled do not appear to have created a disproportionate increase in either the phreatic condition of the tailings or drain flow estimation at the time of the slump event.
- Visually, although the area of the slump coincides with the area of the NTSF which appears to experience the highest degree of saturation, dam construction elements intended to manage water and built into the model appear to be continuing to manage the system. In this regard, the model results do not indicate that saturated conditions have either encroached on the dam lifts or resulted in new emergent seepage on the dam face.
- Model simulated conditions for the time of failure do not indicate any occurrence of new or abnormal seepage emergence on the dam face, and the effect of the Stage 3 underdrain maintained phreatic conditions upstream of the dam lifts.

4.1.2 Monitoring Data Analysis

Piezometric records form a substantial component of base information to this investigation, through informing the assessment of the conceptual system, and calibrating the 3D groundwater modelling. A detailed review of piezometric data is provided in Section 2.4.5, with data recorded for the period leading up to the slump event inside the NTSF reproduced for about 15 months preceding the slump event shown in Figure 38. Decant pond elevation for the same period is also shown:

- VWP-001 & VWP-002 are located along the western embankment. Levels in VWP-002 do not include the immediately preceding period of the slump. VWP-001 shows a rise in levels coincident with decant pond elevation increase.

- VWP-003 is located west of the slump event and over Tertiary basalt. The record stops in November 2017 on a downward trend. This site may have experienced a rise in levels after this time as observed in other locations.
- VWP-004 is located close to and east of the slump. Pressure ranges between 730.5 mRL and 732.8 mRL, with the high value about 11 m below the Stage 10 crest. This site indicates a change of 2m rise from October to March 2018, which may be responding to two stresses resulting from the same trigger (decant pond elevation):
  - Decant pond increases over this period to a high of about 735 mRL, and,
  - Secondary response to increase in levels across the TSF which is noted along the western embankment and upstream of this site in VWP-N005, with a high of about 735.8 mRL. The rate of rise between this VWP and VWP-003 is very similar. A rise is also noted in VWP-005 although this site remains strongly affected by the drain discharge.
- VWP-005, VWP-006 and VWP-007 are located further to the east, with VWP-005 closest to the main area of drain impacts.

All sites with 2018 data observed a similar rising trend in the 6 months of late 2017 / early 2018, probably attributed to the progressive rising of the NTSF decant pond and the resulting re-saturation of the general tailings profile throughout the system. VWP levels generally show 1-2 m of vertical variance, and all remain 8-14 m below the Stage 10 crest elevation. For those VWPs with early time data, the elevation of conditions at the time of the slump event are similar to their conditions at the earlier 'high' in early 2017, when the crest elevation and the decant pond operating level were both lower.

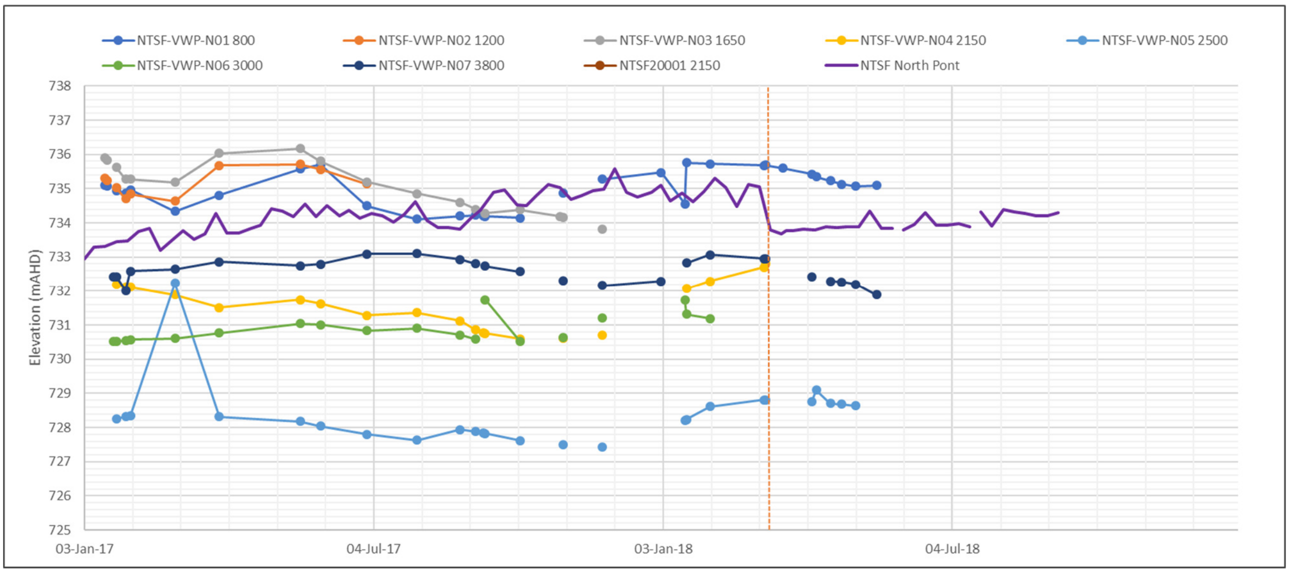

Figure 38: VWP Data NTSF, 2018 and 2018, and NTSF Decant Pond Elevation

In the months preceding the slump, no substantial rainfall was noted (Figure 7), and creek flows measured at the mine did not exhibit any significant events (Figure 8). Changes to conditions discussed above in the VWPs are consistent with pond elevation increases and re-saturation of the tailings profile across the whole NTSF. This hydraulic response mechanism also reinforces the relevance of the decant pond elevation as a key boundary condition in the modelling reported earlier.

4.1.3 Question Response Summary

Summary points from this discussion are:

1. Modelling, informed by monitoring data and detailed conceptualisation of the tailings and foundation conditions, does not predict additional emergent seepage on the dam face at the time of the slump. This modelling also does not predict development of phreatic conditions or drain flows which have not been previously observed at the site;
2. Piezometric observation data shows the tailings system responding to decant pond level. Pressure elevations in VWPs at the time of the slump are similar to elevations observed in early January 2017, when the dam crest was 3 m lower, and the decant pond 2m lower, than conditions at the time of the slump.

4.2 Question 2

"an assessment of historical piezometer data for the NTSF and the contribution that groundwater levels has had on the integrity of the NTSF wall at the site of the wall slump event"

Understanding the potential impact of groundwater levels on the stability of the dam, at the location of the slump event, is very difficult because of the hydrogeological influence of the STSF on conditions at and near the site.

This question is addressed in three parts: observation of conditions inside the NTSF as they relate to the NSTF and STSF decant ponds, observation of groundwater level responses in proximal and distal monitoring bores as reported elsewhere in this report, and consideration of hydrogeological conditions as they relate to the construction of the NTSF at the slump location.

4.2.1 Groundwater Modelling Analysis

The groundwater model was constructed in a manner to permit review of predicted conditions at the time of the slump event in deeper, natural geology. These results are shown and discussed earlier in this report in Section 3.2.4. Table 8 provides a numerical summary of results with deepening strata at three locations near the slump. These data indicate that head differentials across layers are generally small, further locational observation discussion on these is provided:

- Upstream, downward gradients are maintained across both layer transitions
- At the dam, an upward gradient with a head differential of about 1.3 m is noted from layer 16 into layer 15 (weathered rock to the base of tailings / clay liner). Fresh rock to weathered rock contact indicates a downward gradient with a head differential of 0.15 m.
- At the downstream area, the gradient between layer 15 and 16 is almost negligible, very weakly downward gradient of <0.01 m, and an upward gradient from fresh rock into weathered rock of ~0.07 m head differential is predicted.

- The scale of these model predicted head differentials are well within the range of measured pressure changes within the NTSF tailings, and naturally fluctuating groundwater conditions for proximal and distal monitoring locations.

Table 8: Summary Pressure Conditions with Depth, 9-March-2018, NTSF Slump Location

Location	Model Layer	Computed Head (m)	Vertical Gradient (down +ve, up -ve)	Node Locations
Upstream	15	715.2535	L15 > 16, +0.2966 m L16 > 17, +0.1621 m	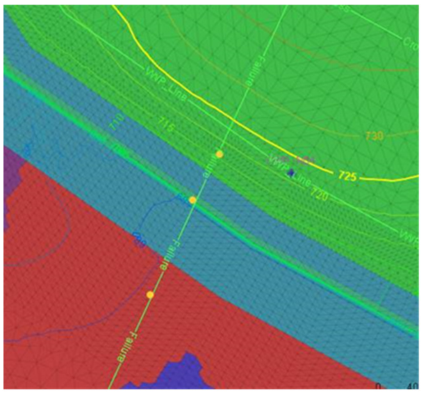
	16	714.9569		
	17	714.7948		
Dam	15	693.3675	L15 > 16, -1.2872 m L16 > 17, +0.1525 m	
	16	694.6547		
	17	694.5022		
Downstream	15	679.2957	L15 > 16, +0.0039 m L16 > 17, -0.0695 m	
	16	679.2918		
	17	679.3613		

4.2.2 Monitoring Data Analysis

Figure 39 shows post-slump-event performance of the dam construction components as they relate to foundation geology conditions in the Tertiary basalt. Dam construction components and the relative head of VWP data at these locations indicate the dam continued to manage the seepage, and that water into the basalt was not causing problematic or high-pressure conditions in that sequence. This is consistent with the concept that the basalt will act as a natural drain to water which enters it from the NTSF, as long as the recharge from the NTSF does not overcome the ability of the basalt to naturally drain.

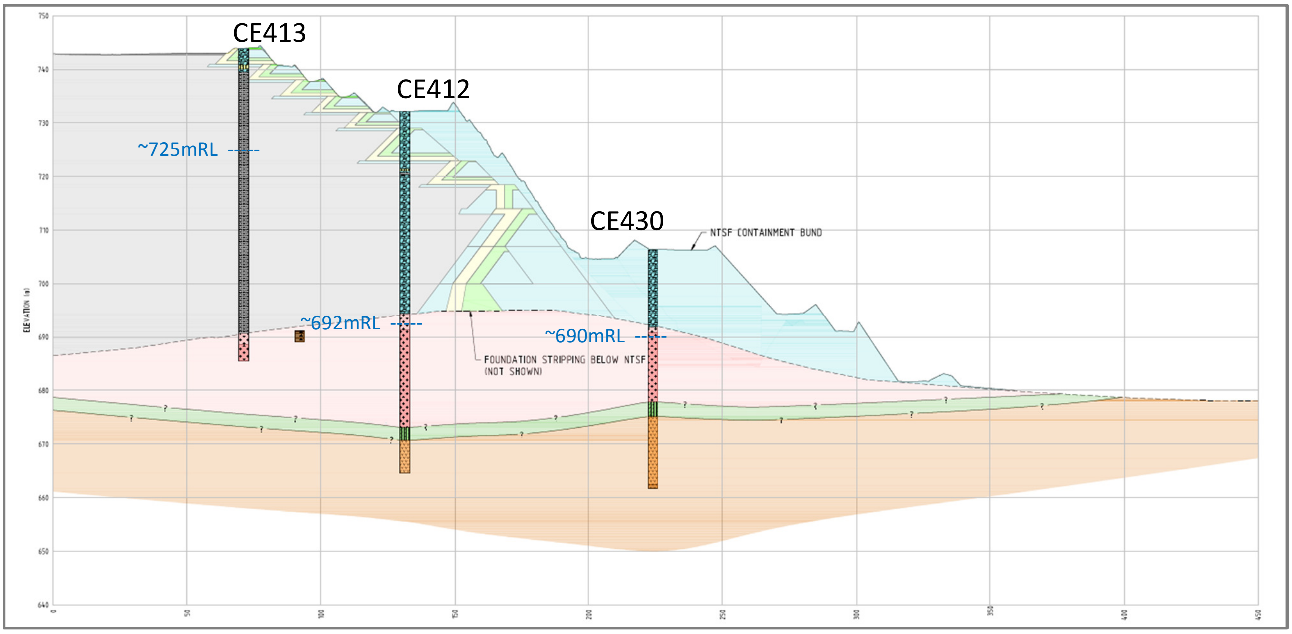

Figure 39: 2018 Installed Tertiary Basalt VWPs, CE series holes (Hatch, 2019)

Decant pond conditions in the STSF have observed a much slower rate of rise than those of the NTSF. In the 2 years preceding the slump, the STSF decant pond has observed 2.2 m of rise, while the NTSF has observed 4.4 m. During 2018 in the period leading up to the slump event, the STSF decant pond varied across a range of 0.58 m: the maximum elevation of STSF decant pond levels for this period is 676.6 m, which is below the starter dam for the NTSF (Figure 40), and approximately 14 m lower than the piezometric conditions observed in CE430. These levels are also lower than three Forrest Reefs Volcanics VWPs installed after the slump, at CE405, CE406 and CE415, which have a range of pressure elevations between 678 m and 685 m, which are 1-10 m below their installed collar elevations. These values although similar, are not consistently close to pond elevation in the STSF, and they do not indicate direct and efficient connectivity into the underlying volcanics.

There are five hydrographs presented for bores completed in natural strata and proximal to the NTSF. These are MB18, MB19A/MB19B, MB23 and MB24 and their hydrograph data are reproduced in Figure 40. These bores are immediately west and south west of the NTSF, close to the abutment of the STSF into the southern NTSF embankment. All the bores are within 500 m of the toe of the western or southern embankment of the south west corner of the NTSF.

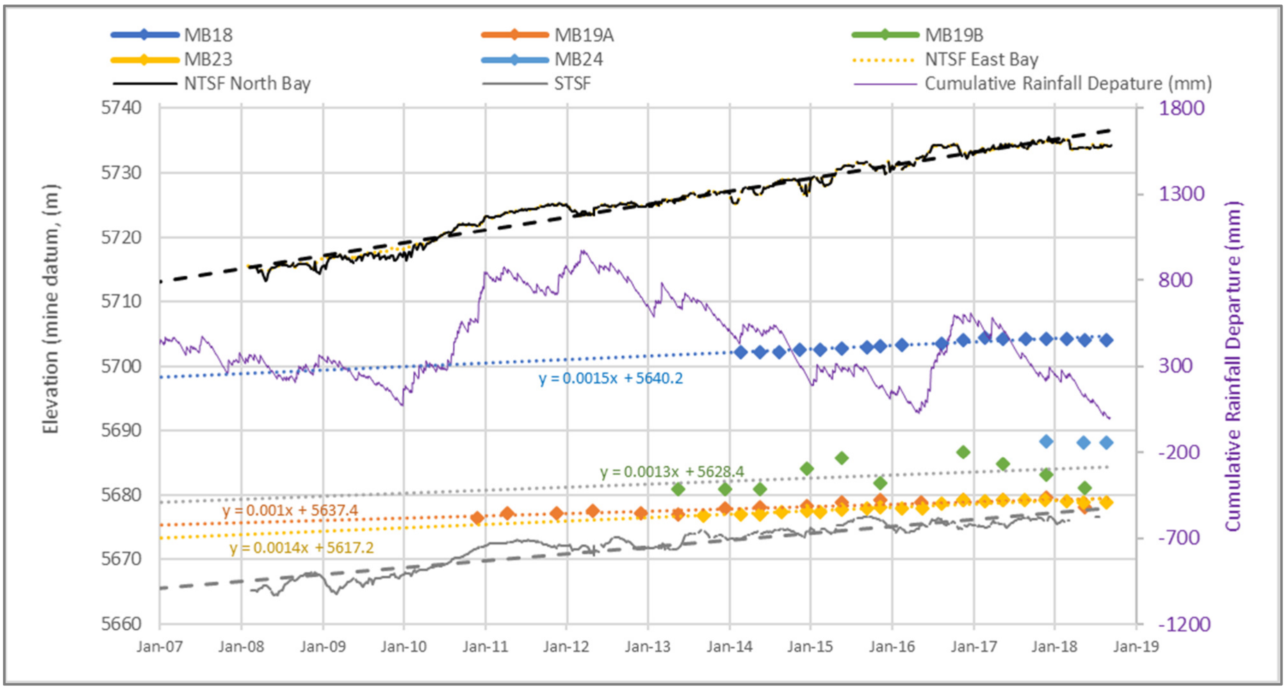

Figure 40: NTSF Proximal Foundation Head Monitoring, 2007 to 2018

Long term trends for four of these bores are shown and indicate a consistent head increase of 0.35 m to 0.55 m per year. This trend appears to be present for several years for a number of the bores and may be attributed to either or both of the NTSF and STSF operations. No unique spikes in the record due to sudden recharge events such as rainfall or creek flow are evident, although this may be a function of the gap between records. These data indicate translation of the developing pressure response from raising of the NTSF (and the STSF) into local groundwater conditions within the Silurian and Ordovician strata.

The absence of local peaks in the data (exception being MB19B which is the shallowest completion at 7.6 m) and the large difference in vertical elevations between the bores and the decant pond elevation in the NTSF (30 m-50 m), indicates that this trend is a muted pressure response to the TSF's presence rather than an indicator of direct and efficient hydraulic continuity. There do not appear to be any late time increases in the trends in these data either – sites MB18, MB19A and MB23 may be observing a flattening of their response in 2018.

A similar exercise was conducted for a series of distal bores and is discussed earlier in this report. All of these distal bores however experienced trends consistent with regional conditions and did not show the same pressure response as the proximal bores to the tailings dams. These data are indicating no translation of the NTSF / STSF pressure effects, placing the likely lateral extent of NTSF pressure impact to be in the range of 500 m to 800 m from the TSF complex.

To bring this into context and to consider the potential for TSF operations to impact conditions in natural groundwater, a summary of depth to water records is provided for both the proximal and distal data (Table 9). Over the past three years, all the distal bores experienced an increase in the depth of water from collar, consistent with the regional trend of below average rainfall conditions. Pressure translation from the TSFs has not only not occurred, but groundwater levels have fallen.

For the proximal sites, three of the five locations have experienced a rise in groundwater levels of between 0.4 m and 1.3 m between 2015 and 2018, lower than the rate of rise of either of the TSFs. None of these bores are approaching artesian conditions, two are observing a decline in groundwater level.

Table 9: Averaged Depth to Water Records, 2015 and 2018

Bore		Ground Elevation	2015 Depth To Water Average (mbCol)	2018 Depth To Water Average (mbCol)	Change (+ve = rise -ve = fall)	Notes
MB18	Proximal	722	19.6	18.3	1.3	
MB19A		688.12	9.4	10.3	-0.9	
MB19B		688.14	4.6	7.3	-2.7	
MB23		703.49	26	24.9	1.1	
MB24		696.44	9.7	9.3	0.4	
MB25	Distal	668.9	14.2	15.8	-1.6	
MB81		657.48	6.5	7.4	-0.9	
MB85		676.50	15.8	16.7	-0.9	First reading 15/7/17
MB86		685.650	13.4	14.7	-1.3	First reading 15/7/17
MB87		693.56	18.4	19.2	-0.8	First reading 15/7/17
MB90		644	30.4	30.4	0	First reading 17/8/18

4.2.3 Question Response Summary

Summary points from this discussion are:

1. Modelling, informed by monitoring data and detailed conceptualisation of the tailings and foundation conditions, does not predict generation of substantial vertical pressure gradients across the area of the slump at the time of the event.

2. Focussed review of conditions from the model at the area of the slump indicate head conditions with depth do not vary substantially, a mix of upward and downward gradients are predicted, with their scale within the range of regional groundwater monitoring and NTSF tailings head variability.

3. Monitoring indicates that natural groundwater conditions in low permeability strata are experiencing a muted response to TSF operations at the NTSF and the STSF, observed as a consistent increase in their levels over a long period of time. None of these sites appear in direct and efficient hydraulic connection with either of the NTSF or STSF decant ponds, and none are artesian in hydrogeological nature.

4. Monitoring data (post slump event) indicates that natural groundwater conditions in the Tertiary basalt near the slump event are currently not under confining pressure, and that the basalt appears to be operating as an effective drain to seepage which does bypass the dam components designed for seepage and pressure control.

5 CLOSURE

This report is an instrument of service of Klohn Crippen Berger Ltd. The report has been prepared for the exclusive use of Ashurst Australia (Client) for the specific application to the Newcrest - ITRB Report on NTSF Embankment Failure Hydrogeology Assessment. The report's contents may not be relied upon by any other party without the express written permission of Klohn Crippen Berger. In this report, Klohn Crippen Berger has endeavoured to comply with generally-accepted professional practice common to the local area. Klohn Crippen Berger makes no warranty, express or implied.

Yours truly,

KLOHN CRIPPEN BERGER LTD.

Chris Dickinson, RPGeo (Hydrogeology)
Principal Hydrogeologist

CD:CD

REFERENCES

AGE. (2009). *Cadia East project Groundwater Assessment, prepared for Cadia Holdings Pty Limited.* Ref: G1383/D.

AGE. (2013). *Cadia East Mine Uodate of the Groundwater Model.*

Hatch. (2018). *Cadia Mine NTSF Apprndix B, NTSF History.*

Newcrest Mining Ltd. (2016?). *Cadia Architeecture (5-slide Power Point Presentation).*

NGMA. (1998). *Bathurst 1:250,000 Geology sheet SI55-8, 2nd Ed.*

Pogson D.J. & Watkins J.J. (1998). *Bathurst 1:250,000 Geological Survey Sheet SI/55-8: Explanatory Notes.* Geological Survey of New South Wales, Sydney, xiv + 430 pp.

Wilson, A. (2003). *The Geology, Genesis and Exploration Context of the Cadia Gold-Copper Porphyry Deposits.*

Advice to decision maker on gold mining project

IESC 2024-151: Cadia Continued Operations Project – Expansion

Requesting agency	The New South Wales Mining and Petroleum Gateway Panel
Date of request	16 August 2024
Date request accepted	22 August 2024
Advice stage	Gateway Application

The Independent Expert Scientific Committee on Unconventional Gas Development and Large Coal Mining Development (the IESC) provides independent, expert, scientific advice to the Australian and state government regulators on the potential impacts of unconventional gas and large coal mining proposals on water resources. Additionally, at the request of a relevant New South Wales, Queensland, South Australian or Victorian Minister and with the written agreement of the Australian Government Environment Minister, the IESC can provide advice on any other matter within the expertise of the IESC. The advice is designed to ensure that decisions by regulators on unconventional gas or large coal mining developments or any other matters within the expertise of the IESC are informed by the best available science.

The IESC was requested by the New South Wales Mining and Petroleum Gateway Panel to provide advice on the Cadia Holdings Pty Limited Cadia Continued Operations Project in New South Wales, and the request approved in writing by the Australian Government Environment Minister. This document provides the IESC's advice in response to the requesting agency's questions. These questions are directed at matters specific to the project to be considered during the requesting agency's assessment process. This advice draws upon the available assessment documentation, data and methodologies, together with the expert deliberations of the IESC, and is assessed against the IESC Information Guidelines (IESC 2024).

Summary

The Cadia Continued Operations Project (the 'project') is a proposed expansion of the existing Cadia Valley Operations (CVO), a polymetallic mining operation located in central New South Wales (Minesoils 2024, p. 6). The project is currently being reviewed by the New South Wales Mining and Petroleum Gateway Panel as it requires a Gateway Certificate due to the project's likely permanent impacts to Biophysical Strategic Agricultural Land (BSAL). The Mining and Petroleum Gateway Panel has requested the IESC's advice as required under the *State Environmental Planning Policy (Resources and Energy) 2021* (SEPP).

The project involves extension of operations to approximately 2050 via continuation of underground (cave) mining, tailings emplacement within existing and additional storages, development of an additional water storage, road realignments, and changed site infrastructure and facilities to enable the extended mining operations (Minesoils 2024, p. 6). This will result in disturbance of up to 1,253 hectares (ha) (Minesoils 2024, p. 10), of which 378 ha are verified BSAL (Minesoils 2024, p. 52). This disturbance occurs in the Gateway Application Area, which refers to the portion of the project area outside the existing CVO boundary.

The provided documentation lacks specific details as the Gateway Certificate assessment occurs prior to project referral and assessment under the New South Wales *Environmental Planning and Assessment Act 1979* (EP&A Act). The Gateway Assessment focuses on impacts to verified BSAL in areas which have not been previously assessed by the Gateway Panel. The IESC acknowledges that additional impact assessment and documentation will be required by the New South Wales EP&A Act, and the proponent indicates that such studies are underway (Minesoils 2024, pp. 10, 62). The IESC previously provided advice on upgrades to the tailings dam embankment for the CVO in August 2023 (IESC 2023).

<u>Key potential impacts</u> from this project are:

- disturbance of up to 1,253 ha outside the existing approved CVO project boundaries;
- emplacement of tailings in existing and proposed storages which could alter the water quality, rate and/or direction of leakage, impacting nearby groundwater-dependent ecosystems (GDEs) (including high-priority ones along waterways listed in the Water Sharing Plan), surface water systems and local groundwater;
- changes to instream habitat and downstream GDEs from construction of the South Water Storage on Cadiangullong Creek, including permanent inundation of a section of the creek, leading to impacts to ecologically important components of its flow and sediment regimes and water quality, and water logging of nearby GDEs;
- modification of surface flows due to different types of cave mining and associated localised fracturing and subsidence;
- increased drawdown from extension of cave mining, reducing groundwater availability to GDEs along Flyers Creek and Cadiangullong Creek; and
- cumulative impacts with the existing CVO project.

The IESC has identified areas in which additional work is required to address the key potential impacts, as detailed in this advice. These are summarised below.

- An improved understanding of surface water and groundwater resources, surface water-groundwater interactions and GDEs is required, which should include relevant baseline information on water quality, hydrological connectivity and flow regimes.
- Proposed project activities should be finalised and described in more detail so that potential impact pathways to water resources can be determined with greater certainty. Following this, an impact pathway diagram should be developed to refine and communicate understanding of how and where the project may impact water resources
- Site-specific investigations should be conducted to confirm the presence and groundwater-dependence of aquatic, terrestrial and/or subterranean GDEs in and near the project area. This information will guide assessment of likely impact pathways and potential impacts of the project on relevant GDEs.

- The likely extent and magnitude of groundwater level and water quality changes from underground mining, tailings deposition and water management infrastructure should be quantified to determine likely impacts to GDEs and surface waters.

- Further information is required regarding proposed avoidance and mitigation of potential impacts once water resources and project components have been adequately defined. This information should be complemented by detailed description of a monitoring program to assess the effectiveness of the avoidance and mitigation strategies and detect any residual impacts.

- An assessment of cumulative impacts is required that explicitly considers the existing CVO project and other relevant land and water uses in and near the project area.

The IESC strongly urges the proponent to draw on existing monitoring and information collected for the current operations to assist preparation of the Environmental Impact Statement.

Context

The Cadia Continued Operations Project (the 'project') is a proposed expansion of the existing Cadia Valley Operations (CVO), located approximately 20 km south-southwest of Orange in central New South Wales. CVO is a polymetallic mining operation which commenced in 1998, with current operations approved by the state (PA 06_2095), covering underground mining at the Cadia East and Ridgeway areas and Cadia Hill Open Pit (now used for tailings storage), and tailings deposition in the North Tailings Storage Facility (NTSF) and South Tailings Storage Facility (STSF) (AGE 2021, p. 8).

The proponent seeks to extend the mine life from 2031 to 25 years after approval is granted (nominally 2050). This will involve extension of underground (cave) mining, extension of the STSF (referred to as the STSFx) and continued use of existing tailings storages, development of the South Water Storage on Cadiangullong Creek, realignment of an unspecified section of Cadiangullong Creek, construction of surface water infrastructure such as drains and reclaim ponds, road realignments, and changes to site infrastructure and facilities (Minesoils 2024, p. 6).

The Gateway Application Area (GAA) refers to land where new mining leases are required for the activities proposed. The GAA totals 2,265 hectares (ha) (Minesoils 2024, p. 41), within which 1,253 ha will be directly disturbed (Minesoils 2024, p. 10). The project is anticipated to directly impact up to 378 ha of Biophysical Strategic Agricultural Land (BSAL) (Minesoils 2024, p. 52). The GAA is within the Lachlan River Catchment, in the Murray-Darling Basin. Cadiangullong Creek is the major watercourse in the GAA, fed by Rodds Creek, flowing generally southward into the Belubula River which then flows west to the Lachlan River (Minesoils 2024, p. 18). Flyers Creek, east of the GAA, has springs and perennial reaches supported by groundwater (Minesoils 2024, p. 57). Within and surrounding the GAA, high-potential terrestrial groundwater-dependent ecosystems (GDEs) and moderate- to high-potential aquatic GDEs are associated with Cadiangullong Creek, Flyers Creek and the Belubula River, and low-potential terrestrial GDEs occur in the Cadia East subsidence zone (Minesoils 2024, Figure 5, p. 17). Some of these GDEs along the Belubula River and Cadiangullong and Flyers creeks are likely to be high-priority ones listed in the Water Sharing Plan.

The GAA is located in the Lachlan Fold Belt of NSW, where the Orange Basalt Aquifer Source associated with Tertiary basalts is considered a highly productive aquifer under the *NSW Aquifer Interference Policy* (AIP). The Lachlan Fold Belt Groundwater Source is considered a less-productive fractured groundwater source in the area. The proponent notes potential discrepancies between regional mapping and site investigations of the extent of the Orange Basalt aquifer (Minesoils 2024, p. 15).

At the Gateway Certificate stage, the proponent must verify whether the proposed site is on BSAL and, where present, assess the likely significance of impacts on BSAL and associated groundwater resources (Minesoils 2024, p. 9). As such, the current documentation is limited in scope, and lacks specific details that would be required of the Environmental Impact Statement (EIS) once a Gateway Certificate is acquired.

Response to questions

The IESC's advice in response to the requesting agency's specific questions is provided below.

Question 1: Have all relevant water resources been adequately defined? If not, what further work is required?

1. The provided documentation presents limited or only high-level descriptions of relevant groundwater, surface water, GDEs and surface water-groundwater interactions within and surrounding the project area. Further work is needed to define the water resources, their distribution and interactions, and to determine if and how these resources and their interactions may be impacted by project activities.

    a. Groundwater resources have been described with limited detail, particularly the Orange Basalt Aquifer Source, a highly productive aquifer under the NSW AIP (Minesoils 2024, p. 15). Additionally, Quaternary alluvium is mapped along parts of Flyers Creek, Cadiangullong Creek and the Belubula River (Minesoils 2024, Figure 3, p. 13), but the potential presence of alluvial aquifers is not discussed. Further studies should aim to ascertain the extent of these and other relevant aquifers and characterise inter-aquifer connectivity and groundwater-surface water interactions. An assessment of how groundwater levels and water quality have changed due to approved mining operations would assist in understanding and predicting impacts from the project, especially to alluvial aquifers which may support springs, baseflow and/or riparian terrestrial GDEs.

    b. As groundwater flow likely occurs via fracture networks in fractured rock aquifers, the incidence, orientation, frequency and other characteristics of fractures, including mineral infilling, should be included within the groundwater investigations. This will assist in assessing how proposed mining activities will affect aquifers, such as increased fracturing from cave mining or seepage from tailings storages. Similarly, faults or structural features which could connect or compartmentalise groundwater flow, such as the Warrengengong Fault (Minesoils 2024, p. 57), or the Werribee/Cadiangullong Fault (identified in previous hydrogeological investigations – AGE 2021, p. 15), should be investigated and documented (see Murray and Power 2021).

    c. GDEs have not been adequately characterised. Under the Water Sharing Plan for the NSW Murray Darling Basin Fractured Rock Groundwater Sources (2020), high-priority GDEs could include groundwater-dependent vegetation along the Belubula River, Cadiangullong Creek and Flyers Creek, and groundwater-fed reaches and springs associated with Flyers Creek (Minesoils 2024, Figure 5, p. 17). Sources of groundwater supporting these GDEs should be identified, and may include the Cobblers Creek Limestone Formation (Minesoils 2024, p. 57) or any perched aquifers that could be present (AGE 2021, p. 19). Further work should aim to characterise GDEs and their groundwater-dependence using methods outlined in Doody *et al*. (2019) and, where present, quantify baseflow components in creeks. Groundwater levels and water quality near mapped GDEs should be measured for a period representative of natural climatic variability before the project commences to provide a baseline against which project impacts can be assessed and then monitored during and for a suitable period after operations.

    d. Hydrological and sediment regimes and baseline water quality of watercourses in the project area should be described, particularly for Cadiangullong Creek which will be directly impacted by diversions and construction of the South Water Storage. A baseline understanding of the hydrological regime with consideration of ecologically important flow components (e.g. timing, frequency and extent of overbank flows, duration and frequency of low flows) and NSW Water

Quality and River Flow Objectives is needed to assess potential impacts of the dam and to design appropriate managed releases downstream of the storage.

Question 2: Have all potential water resource impact pathways been adequately identified by the Applicant? If not, what further work is required?

2. Due to the limited documentation provided (consistent with the requirements of a gateway application) and the lack of information, the IESC is not confident that the proponent has adequately identified all potential water resource impact pathways.

3. The proponent presents a qualitative impact assessment (Minesoils 2024, pp. 57-59) which lacks adequate justification for conclusions drawn about residual impacts to water resources, evidenced in the following paragraphs. A more detailed and quantitative approach is needed in future impact assessments for the proposed project, and should include the identified impact pathways described below.

   a. Extension of underground mining operations and consequent increased extent and duration of groundwater drawdown could impact nearby GDEs and/or other groundwater users. Depending on the magnitude of drawdown, impacts could extend to terrestrial and aquatic GDEs along Cadiangullong and Flyers creeks (Minesoils 2024, Figure 5, p. 17). However, at this stage, the extent of impacts and specific impact pathways to particular GDEs cannot be determined.

   b. Potential leakage pathways from the STSFx could occur through fractures in the underlying bedrock, affecting groundwater flowpaths, increasing or decreasing groundwater levels, and impacting quality of groundwater that may be used by nearby GDEs. The proponent asserts that the hydrocyclone construction method for the STSFx will preclude infiltration to groundwater, and that consequent reductions in Flyers Creek baseflow will be negligible (Minesoils 2024, p. 58); however, no detail has been provided to support these conclusions.

   c. Water management infrastructure along Cadiangullong Creek (creek diversion and construction and operation of the South Water Storage) may alter downstream flows, introduce erosion and scour risks, impair water quality and impact in-stream and riparian habitats. Flows are stated to be maintained to ‘appropriate flow conditions’ (Minesoils 2024, p. 59), which would necessitate a comprehensive understanding and ongoing gauging of the hydrological behaviour of Cadiangullong Creek under a representative range of climate conditions that is not presented in the documents provided. Additionally, the existing Cadiangullong Dam located upstream of the diversion and South Water Storage should be considered when discussing cumulative impacts on flows, sediment regimes, water quality and aquatic and riparian habitats downstream.

   d. The South Water Storage will increase groundwater heads, recharge and seepage through the dam wall, increasing baseflows in Cadiangullong Creek downstream and potentially waterlogging terrestrial and riparian GDEs along the creek.

   e. Water management infrastructure to capture seepage and runoff from the STSFx wall, such as drains and reclaim ponds, could result in changes to surface flows (Minesoils 2024, p. 58), loss of catchment area and/or water quality impacts to Rodds Creek, Cadiangullong Creek and associated in-stream and riparian ecosystems. Further information on water infrastructure, locations and the scale of proposed changes is needed to assess these potential impacts and their pathways.

4. Impact pathways described in the documentation largely relate to project components sited in the GAA, outside the existing mining lease. As such, impacts from operations within the broader project are not investigated in detail. These impacts could include increased depressurisation and associated drawdown and subsidence from underground mining, changes to surface flows or interception of

surface flows from subsidence, and increased seepage from compaction and loading as tailings are deposited in existing storages. The extent of these impacts should be quantified once details of the project are finalised, such as volumes of tailings to be deposited in existing storages, or changes in water table as indicated by numerical groundwater modelling.

5. The IESC recommends that, once assessed, all impact pathways are presented as one or more impact pathway diagrams (see Commonwealth of Australia 2024) to illustrate their collective potential impacts and guide the monitoring of the effectiveness of management strategies to minimise or avoid these potential impacts.

Question 3: Is the Applicant’s proposed approach to assessing the potential impacts fit for purpose? If not, what further work is required?

6. The proponent states that the ‘EIS will address a range of interrelated water resource considerations’, and lists the guidelines that will be taken into consideration (Minesoils 2024, pp. 59-61). This high-level list is mostly fit for purpose and covers standard assessments needed to determine potential impacts to surface and groundwaters. However, further work is required and should include the following.

    a. Proposed assessments of surface and groundwater resources should include characterisation of surface and groundwater interactions to inform assessment of impacts resulting from the project to aquatic and terrestrial GDEs.

    b. The presence and groundwater-dependence of aquatic, terrestrial and subterranean GDEs should be assessed using established methods (e.g. Doody *et al*. 2019). Once GDEs have been ground-truthed and mapped, the proponent should evaluate potential impact pathways to each of these different GDEs from underground mining works and associated subsidence and drawdown, any alterations to surface flows and/or water quality from additional site infrastructure, and seepage from water and tailings storages.

    c. Additional details are required for the design and collection of data to inform an understanding of the baseline streamflow regime and water quality over a period sufficiently long to characterise inter- and intra-annual climate variability.

    d. Ecological surveys should be conducted of instream biota (e.g., invertebrates, fish, frogs, aquatic plants), stygofauna (especially in alluvial aquifers) and riparian vegetation and condition to obtain baseline data against which project impacts can be assessed. Specific details, guided by these surveys, should be used to describe how the effectiveness of mitigation measures will be monitored.

    e. Geotechnical studies should be conducted to confirm the areal extent of the caving impact zone to the surface, with additional localised fracturing and subsidence expected at Cadia East and Ridgeway underground mining areas. This information is needed because increases in the areal extent of the caving zone could result in additional loss of surface water and groundwater.

    f. The groundwater modelling approach includes assessing the potential for any impact on alluvial aquifers and surface water (Minesoils 2024, p. 59), but should also identify groundwater flow paths and the potential to impact private bores (Minesoils 2024, Figure 5, p. 17).

Question 4: Have appropriate strategies and measures to avoid, mitigate or reduce, to a practicable extent, the likelihood and significance of impacts to significant water-related resources been proposed? Are there additional strategies, mitigation or off-setting measures that should be considered to address any residual impacts of the project on water resources and related GDEs?

7. Limited information is provided in the Gateway documentation on strategies and measures to avoid, mitigate or reduce the likelihood and significance of potential impacts to significant water-related resources. Future impact assessments describing such strategies and measures should include:

    a. proposed measures to reduce or mitigate seepage from the STSFx, as well as ongoing monitoring and, if necessary, intervention to ensure leakage and downstream impacts are minimised;

    b. proposed measures to limit impacts to waterways and associated GDEs during construction of the STSFx, South Water Storage, and road and creek realignments. For example, options should be considered for the relocation of the proposed STSFx reclaim pond to avoid the need to realign Cadiangullong Creek;

    c. proposed measures to limit impacts to Cadiangullong Creek as a result of the stream diversion, such as replicating and maintaining appropriate stream and riparian habitats and associated ecological processes, and limiting excessive erosion and scour;

    d. options to offset impacts from clearing and/or reduced groundwater availability and water quality to listed ecological communities potentially present in the project area, such as White Box – Yellow Box – Blakely's Red Gum Grassy Woodland and Derived Native Vegetation (Minesoils 2024, pp. 22-23), that may also include GDEs;

    e. proposed monitoring programs with appropriate scope and sampling frequency, as well as suitable Trigger Action Response Plans (TARPs) for groundwater and receiving surface water levels and quality;

    f. information regarding timing and frequency of managed releases (and spills) from the South Water Storage, with consideration of water quality and river flow objectives;

    g. appropriate mitigation and management measures for GDEs, based on ground-truthed GDE distributions and assessment of potential impact pathways (see Paragraph 6c);

    h. proposed measures to remediate subsidence impacts in the northeastern area of the GAA should technical studies indicate the potential for this, as briefly indicated (Minesoils 2024, p. 62); and

    i. a clear description of the proposed mine closure plan, including appropriate measures for restoration of the TSF and the small segment of the stream diversion (if retained).

8. It is essential when preparing the coming EIS that the proponent draws on the existing information, including investigations and environmental monitoring, that has already been collected for and during the current operations.

Date of advice	10 October 2024
Source documentation provided to the IESC for the formulation of this advice	Minesoils Pty Ltd (Minesoils) 2024. *Gateway Report – Cadia Continued Operations Project*. Prepared for Cadia Holdings Pty Limited. July 2024. (Including Appendices 1-5). Available [online]: Independent Planning Commission - Cadia Continued Operations Project (nsw.gov.au) accessed 3 October 2024.
References cited within the IESC's advice	Australasian Groundwater and Environmental Consultants (AGE) 2021. *Cadia Groundwater Model Update 2021.* Prepared for Newcrest Mining. April 2021. Project No. G1383Y. Available [online]: G1383Y Report Cover Apr2021.cdr (caapp.com.au) accessed 17 September 2024.

Commonwealth of Australia 2024. *Information Guidelines Explanatory Note: Using impact pathway diagrams based on ecohydrological conceptualisation in environmental impact assessment.* Report prepared for the Independent Expert Scientific Committee on Unconventional Gas Development and Large Coal Mining Development through the Department of Climate Change, Energy, the Environment and Water, Commonwealth of Australia 2024. Available [online]: Information Guidelines Explanatory Note - Using impact pathway diagrams based on ecohydrological conceptualisation in environmental impact assessment | iesc accessed 25 September 2024.

Doody TM, Hancock PJ, Pritchard JL 2019. *Information Guidelines Explanatory Note: Assessing groundwater-dependent ecosystems.* Report prepared for the Independent Expert Scientific Committee on Coal Seam Gas and Large Coal Mining Development through the Department of the Environment and Energy, Commonwealth of Australia 2019. Available [online]: Information Guidelines Explanatory Note - Assessing groundwater-dependent ecosystems | iesc accessed 18 September 2024.

IESC 2023. *Advice to decision maker on gold mining project IESC 2023-143: Cadia Valley Operations Gateway Application – Expansion.* Available [online]: Advice to decision maker on gold mining project - IESC 2023-143: Cadia Valley Operations Gateway Application – Expansion accessed 2 October 2024.

IESC 2024. *Information Guidelines for proponents preparing coal seam gas and large coal mining development proposals.* Available [online]: Information guidelines for proponents preparing coal seam gas and large coal mining development proposals | iesc accessed 20 September 2024.

Murray TA and Power WL 2021. *Information Guidelines Explanatory Note: Characterisation and modelling of geological fault zones.* Report prepared for the Independent Expert Scientific Committee on Coal Seam Gas and Large Coal Mining Development through the Department of Agriculture, Water and the Environment, Commonwealth of Australia 2021. Available [online]: Information Guidelines Explanatory Note - Characterisation and modelling of geological fault zones | iesc accessed 2 October 2024.

Independent Expert Scientific Committee
on Coal Seam Gas and Large Coal Mining Development

Advice to decision maker on gold mining project

IESC 2023-143: Cadia Valley Operations Gateway Application – Expansion

Requesting agency	The New South Wales Mining and Petroleum Gateway Panel
Date of request	14 June 2023
Date request accepted	19 June 2023
Advice stage	Gateway Application

The Independent Expert Scientific Committee on Coal Seam Gas and Large Coal Mining Development (the IESC) provides independent, expert, scientific advice to the Australian and state government regulators on the potential impacts of coal seam gas and large coal mining proposals on water resources. Additionally, at the request of a relevant New South Wales, Queensland, South Australian or Victorian Minister and with the written agreement of the Australian Government Environment Minister, the IESC can provide advice on any other matter within the expertise of the IESC. The advice is designed to ensure that decisions by regulators on coal seam gas or large coal mining developments or any other matter within the expertise of the IESC are informed by the best available science.

The IESC was requested by the New South Wales Mining and Petroleum Gateway Panel through the New South Wales Minister for Planning and Public Spaces to provide advice on the Newcrest Mining Limited Cadia Valley Operations Gateway Application in New South Wales. The request has been approved in writing by the Australian Government Environment Minister. This document provides the IESC's advice in response to the requesting agency's questions. These questions are directed at matters specific to the project to be considered during the requesting agency's assessment process. This advice draws upon the available assessment documentation, data and methodologies, together with the expert deliberations of the IESC, and consideration of the IESC Information Guidelines (IESC, 2018).

Summary

Cadia Valley Operations Gateway Application Expansion Project (the project) is a proposed expansion of the existing Cadia Valley Operations (CVO) located in central New South Wales. The project is currently being reviewed by the New South Wales Mining and Petroleum Gateway Panel as it requires a Gateway Certificate due to permanent impacts to Biophysical and Strategic Agricultural Land (BSAL). The Mining and Petroleum Gateway Panel has requested IESC advice as required under the *State Environmental Planning Policy (Resources and Energy) 2021* (SEPP). The Gateway Application encompasses work

proposed to address damage that occurred to the Northern Tailings Storage Facility (NTSF) and Southern Tailings Storage Facility (STSF) in 2018. As presented for the Gateway Application, the project only includes enlarging the footprint of the STSF embankment, as recommended following technical and engineering reviews at CVO (Newcrest Mining Limited 2023, p. 6).

The project will temporarily impact 28.2 ha of land to enable construction of the modified embankment of the STSF and will permanently impact up to 2 ha (Minesoils 2023b, pp. 1-2), of which 0.8 ha is verified BSAL (Newcrest Mining Limited 2023, p. 6). Environmental impacts arising from the work on the embankment alone are likely to be limited, although the provided documentation lacks specific details because the Gateway Certificate assessment occurs prior to project referral and assessment under the New South Wales *Environmental Planning and Assessment Act 1979* (EP&A Act). It is unclear whether any clearing of native vegetation is required. The IESC notes that the White Box – Yellow Box – Blakely's Red Gum Grassy Woodland and Derived Native Grassland Ecological Community, listed as critically endangered under the *Environment Protection and Biodiversity Conservation Act 1999* (EPBC Act), may occur in the project area.

No changes are proposed to the mining method, processing rate, mine life, the footprints of the Cadia East and Ridgeway Mines, the maximum approved heights of the tailings storage facilities, or of waste rock management at CVO (Newcrest Mining Limited 2023, p. 5). The proponent is not proposing any additional take of groundwater, with minimal, if any change to water access licensing expected (Minesoils 2023b, p. 29). The documentation provided for the Gateway Application suggests that the project will be part of a larger and more complex modification application (Modification 15) when referred and assessed under the EP&A Act (Newcrest Mining Limited 2023, pp. 3-5). Little information was included in the documentation provided on the details of the changes proposed under Modification 15.

This advice applies only to the works to enlarge the STSF embankment footprint and not the full range of changes to potentially be proposed in Modification 15. The IESC understands that the potential impacts from this project and any other changes proposed under Modification 15 will require further investigation with additional impact assessment documentation to be prepared and submitted for assessment under the New South Wales EP&A Act.

Key potential impacts from this project are:

- embankment failure which could have severe and irreversible impacts for downstream surface waters, groundwaters and groundwater-dependent ecosystems (GDEs);
- changes to tailings storage facilities (TSFs) seepage which could alter the quality, rate and/or direction of leakage impacting on nearby GDEs, surface water systems and local groundwater; and
- increases in groundwater levels in the areas adjacent to the embankment works from compaction and loading that could result in waterlogging of nearby GDEs, increased discharge to surface water systems and potentially extend leakage flowpaths.

The IESC has identified areas in which additional work is required to address potential impacts, as detailed in this advice. These are summarised below.

- More information on the proposed embankment works is needed. Details of the design, construction and predicted performance of the modified embankment, including how the existing and new works will be keyed into the bedrock base and valley sides, operation of the TSFs, and tailings volumes to be stored, are essential to understanding the risks posed by the project. The project needs to be designed to minimise the risk of failure and subsequent impacts on downstream water resources.

- An improved understanding is required of the potential leakage pathways from the TSFs, the quantity and quality of leakage, and the potential receptors that could be impacted by the leakage. Although the proponent intends to design the embankment to limit leakage through it (Minesoils 2023b, p. 31), compaction and loading arising from the modified embankment may change the volume, rate and/or flowpaths of seepage currently occurring beneath the TSFs via Rodds Creek and the Cadiangullong Fault and its associated weathered and damage zone. These leakage pathways require more detailed evaluation (e.g., internal erosion pathways or those associated with faulting) to ensure that the embankment works are designed to minimise leakage.

- The likely extent and magnitude of groundwater level increases from the project and their potential impacts on nearby GDEs and surface waters have not been quantified. Historical increases in groundwater levels have been observed but only limited explanation is provided. The source of these increases needs to be comprehensively examined with consideration of tailings deposition (e.g., timing, volumes) to understand how the TSFs are affecting groundwater levels and risks to downstream water resources during and after construction and post-closure.

Context

The Cadia Valley Operations Gateway Application Expansion Project (the project) is located approximately 25 km southwest of Orange in central New South Wales (Newcrest Mining Limited 2023, p. 1). CVO is a gold and copper mine with current operations approved by the state (PA 06_2095 and subsequent modifications) and under the EPBC Act (EPBC 2006/3196 and subsequent variations). The existing approvals cover current operations at the Cadia East Underground, Cadia Hill Open Pit and Ridgeway Underground mine sites (Newcrest Mining Limited 2023, p. 1). Mining has occurred at the site since 1998 (AGE 2021, p. 8). Other land uses in the region include sheep and cattle farming, cropping and plantation forestry (Newcrest Mining Limited 2023, p. 9).

The project is in the Belubula River catchment, a tributary to the Lachlan River (Minesoils 2023a, p. 7), and part of the Murray Darling Basin. Cadiangullong Creek is the major watercourse at the site and is joined by Rodds Creek whose bed sediments occur beneath the NTSF and STSF. Sections of Flyers Creek to the east of CVO are perennial, receiving discharges from groundwater-fed springs (AGE 2021, p. 5). Groundwater discharge is also likely to enter Shallow, Cadiangullong and Rodds creeks (AGE 2021, p. 36). Low-flow discharges from CVO occur to Cadiangullong Creek (AGE 2021, p. 5).

The main groundwater sources at CVO include the Orange Basalt, a highly productive aquifer under the *Aquifer Interference Policy* (AIP), and the Lachlan Fold Belt Murray-Darling Basin Fractured Rock groundwater source (AGE 2023, Figure 2.2, p. 8). The extent of the Orange Basalt aquifer, and the fracture networks which are key for groundwater flow, are not well understood at CVO (AGE 2023, p. 6).

The IESC notes that there are indications of leakage from the TSFs into the shallow groundwater system due to currently approved activities, with potential for discharge to local surface waters and GDEs. The potential for these to be affected by the modification of the embankment needs to be clearly identified and quantified in future impact assessments undertaken in relation to the project, and the larger Modification 15.

Response to questions

The IESC’s advice in response to the requesting agency’s specific questions is provided below.

Question 1: Does the IESC consider that the surface water resources, groundwater resources and dependent ecosystems, and their interactions (including the nature of hydraulic connections within the underlying fractured rock aquifer system) have been adequately described and the impacts assessed?

1. The documentation provides only limited descriptions of the surface water resources, groundwater resources and groundwater-dependent ecosystems (GDEs). Some connectivity between the underlying fractured rock aquifer system and the surface water resources was identified, although the description was primarily qualitative. Impact assessment was not rigorous and does not explicitly consider potential stressors, their interactions and likely impact pathways from the proposed activities to the surface and groundwater water resources and dependent ecosystems.

    a. None of the GDEs or surface water systems were adequately characterised (see Doody *et al.* 2019), nor were potential project impacts considered in sufficient detail. High-priority GDEs were identified, including the vegetation along the Belubula River, Cadiangullong Creek and Flyers Creek. Potential impacts from the project would most likely occur in areas of GDEs along Cadiangullong Creek from compaction and loading raising groundwater levels. Some Cadiangullong Creek GDEs are within 200 m of the embankment works (AGE 2023, p. 16) and the proponent's impact assessment has asserted that groundwater level increases may occur at distances of up to 200 m (AGE 2023, p. 11). Future impact assessment should characterise the nearby GDEs and surface water resources to assess their likely responses to changes in groundwater levels. The potentially affected GDEs may include groundwater-dependent components of the EPBC Act-listed White Box – Yellow Box – Blakely's Red Gum Grassy Woodland and Derived Native Grassland Ecological Community.

    b. Potential leakage pathways from the TSFs occur through to the Rodds Creek bed sediments and through fractures in the bedrock underlying the TSFs. It is unclear from the project documentation whether the proposed changes to the STSF embankment will alter groundwater flowpaths, leakage rates and/or leakage volumes. Changes to leakage from the TSFs could alter the likelihood of groundwater discharge and/or the quality of the discharge to nearby GDEs and surface water systems, altering the extent and magnitude of potential impacts. The hydraulic connections within the underlying fractured rock aquifer system and their interactions with surface water resources and GDEs therefore require further analysis. This could include analysis of data from multi-level piezometers to characterise vertical hydraulic gradients, geophysics surveys to identify areas where enhanced leakage pathways could occur, and detailed analysis of relevant groundwater quality parameters (e.g., ion ratios, metals and other toxicants).

2. Impacts to groundwater were assessed qualitatively and the proponent concluded that there would be only limited changes to water levels and quality (Minesoils 2023b, p. 29). Insufficient information to support these conclusions was provided. A more detailed and quantitative assessment is needed in future impact assessments for the proposed project.

Question 2: Regarding groundwater

a. are the uncertainties relating to the extent and/or distribution and properties of the Orange Basalt highly productive groundwater resource adequately understood?

b. has the quantity and quality of seepage from the Southern TSF been adequately investigated, including in terms of the likely incremental and cumulative impacts on groundwater and/or surface water systems and dependent ecosystems, and existing users?

c. noting that the project is characterised as not exceeding the AIP Level 1 Minimal Impact criteria, have impacts been accurately assessed, including the uncertainties influencing the range impacts, such as climate change and hydrogeological uncertainties?

d. is the level of assessment of impacts on groundwater levels, flow and quality and dependent values adequate to assess the potential impacts on water resources?

3. Improvements are needed in understanding the extent and properties of the Orange Basalt highly productive groundwater resource. The potential leakage pathways from TSFs at CVO should be identified, including how the embankment works may alter leakage. Given that groundwater flow in this aquifer is strongly influenced by the location, extent and connectivity of the fracture network on a relatively local scale (AGE 2023, p. 3), inherent uncertainties will remain.

4. The proponent estimates the current quantity of seepage from the TSFs at approximately 0.6 ML/day and does not expect the project will materially change this value (AGE 2023, p. 11). This value is derived from modelling which was not provided to support this conclusion. Possible incremental or cumulative impacts to groundwater or surface water systems, GDEs or other water users are not reported.

    a. The water quality of seepage from the TSFs has not been thoroughly investigated, with only limited attempts based on absolute increases in sulfate concentrations (AGE 2023, p. 11). The proponent concluded that the proposed changes to the TSFs would not be expected to result in a "notable change in seepage water quality" (AGE 2023, p. 11). This conclusion has not been supported, nor is it clear whether chronic and/or sublethal effects on groundwater and/or surface water systems and dependent ecosystems are possible.

    b. Modifying the embankment of the STSF may increase compaction and loading in the vicinity of the works and this could alter the rate and/or direction of leakage. This in turn could change the quality of water being discharged at GDEs and to surface water systems. Further information is needed to demonstrate whether the current management system (pump-back/underdrainage) is sufficient and will continue to be, to manage the impacts of leakage.

5. Assessment of potential impacts against the *Aquifer Interference Policy* Level 1 Minimal Impact criteria has been qualitative with no consideration of climate change or hydrogeological uncertainties. Given that there will be no increased take (Minesoils 2023b, p. 29), it is likely that groundwater drawdown will not exceed these criteria. However, as outlined in paragraphs 1a and 1b, there is uncertainty as to whether compaction and loading could result in groundwater level rises at GDEs along Cadiangullong Creek and altered groundwater discharge to surface water systems. Additionally, it is unclear whether the project may alter leakage from the TSFs and potentially affect shallow groundwater quality. Further evidence and analysis of this are needed in future impact assessments to confirm that *Aquifer Interference Policy* Level 1 Minimal Impact criteria will be met.

6. The level of assessment of impacts to groundwater levels, flow and quality and dependent values provided in the Gateway Application is limited. The IESC acknowledges that this probably reflects the early stage in the impact assessment process at which the Gateway Assessment occurs. Although the potential impacts to water resources from modifying the STSF embankment are likely to be of limited magnitude and spatial extent, the information currently provided is not sufficient to confirm the proponent's conclusions. As outlined in this advice (Paragraphs 1a, 1b, 2-3, 4b, 5, 7a-7f), additional work will be needed in future impact assessment documentation to fully understand potential risks and impacts, and to confirm that these can be adequately managed.

Question 3: Regarding mitigation, monitoring, management and offsetting measures:

a. does the assessment propose reasonable strategies and measures to avoid, mitigate or reduce, to a practicable extent, the likelihood and significance of impacts to significant water-related resources?

b. are there additional strategies, mitigation or offsetting measures that should be considered to address any residual impacts of the project on water resources and related GDEs?

7. Limited information is provided in the Gateway Application on strategies and measures to avoid, mitigate or reduce the likelihood and significance of potential impacts to significant water-related resources. Given this limited information, it is premature for the IESC to suggest additional strategies, mitigation or offsetting measures that should be considered to address residual impacts of the project on water resources and related GDEs. The IESC suggests that the following be detailed further in future impact assessments.

    a. A geotechnical risk assessment. Further information is needed on the design, construction and monitoring of embankment integrity. Given prior performance of the TSFs, known leakage and the existence of faults and associated weathered zones, it is important that the geotechnical risks of the project are carefully detailed, and the embankment is designed to minimise the risks and ensure long-term integrity of the structure to prevent potential impacts on downstream water resources from catastrophic failure.

    b. The embankment design and construction. The proponent has stated that the core of the modified embankment will be designed to minimise leakage. Further details are need on this and other key design components to understand the leakage and failure risks, including details on the base and design of the embankment (including accounting for underlying thin and weak geological strata), consideration of the risks of failure of different design options, and how the embankment will be keyed into the bedrock base and valley sides.

    c. The monitoring network for identifying leakage from the TSFs. Given that leakage is expected to occur at shallow depths, most likely at the base of weathered materials (AGE 2021, p. 64), and through the weathered zone of underlying faults, multiple bores of suitable depth are required. Multi-level piezometers to monitor changes in vertical hydraulic gradient are also needed. The current network may already include suitable monitoring bores, although this should be confirmed. Additionally, an assessment of whether the compaction and loading may alter localised groundwater flowpaths is needed to determine whether additional monitoring bores are required to the south or east of the TSFs. Justification of the sampling frequency and parameter selection (e.g., specific analytes, including metals and other toxicants) is also needed to confirm the adequacy of the monitoring program.

    d. The proposed management of leakage from the TSFs. Currently, management appears to rely considerably on a pump-back/underdrainage system (AGE 2023, p. 11); however, minimal detail about this system was provided. To assess its adequacy, more details are needed, including its location, capacity, effectiveness and whether it has the capacity to handle increased leakage that may arise from the project. The risk of leakage and failure of the TSFs can be mitigated by controlling the water level within the TSFs during mine operation. Other mitigation options will need to be considered post-closure.

    e. Proposed measures to limit impacts to Cadiangullong Creek and associated GDEs from sediment during modification of the STSF embankment.

    f. Updates to existing monitoring and management plans. Future impact assessment documentation needs to clearly detail the updates proposed to current plans and outline suitable Trigger Action Response Plans (TARPs) that will ensure any leakage from the TSFs is identified and managed in a timely manner to minimise impacts to significant water-related resources. These plans should also describe responses and remedial actions in the event of an embankment failure, particularly if tailings or leachates subsequently enter water resources down-gradient.

Date of advice	1 August 2023
Source documentation provided to the IESC for the formulation of this advice	Newcrest Mining Limited 2023. *Cadia Valley Operations – Gateway Application Technical Overview*. Prepared for Newcrest Mining Ltd. 15 May 2023. (Including Appendices 1-3). Available [online]: Independent Planning Commission - Cadia Valley Operations Gateway Application (nsw.gov.au) accessed 26 July 2023.
References cited within the IESC's advice	Australasian Groundwater and Environmental Consultants (AGE) 2021. *Cadia Groundwater Model Update 2021.* Prepared for Newcrest Mining April 2021. Project No. G1383Y. Available [online]: G1383Y Report Cover Apr2021.cdr (caapp.com.au) accessed 26 July 2023. Australasian Groundwater and Environmental Consultants (AGE) 2023. *Cadia Groundwater Review to Support Gateway Application*. Prepared for Newcrest Ltd. March 2023. (Appendix 3 of Gateway Application). Doody TM, Hancock PJ and Pritchard JL 2019. *Information Guidelines Explanatory Note: Assessing groundwater-dependent ecosystems.* Report prepared for the Independent Expert Scientific Committee on Coal Seam Gas and Large Coal Mining Development through the Department of the Environment and Energy, Commonwealth of Australia 2019. Available [online]: Information Guidelines Explanatory Note - Assessing groundwater-dependent ecosystems | iesc accessed 26 July 2023. IESC 2018. *Information Guidelines for proponents preparing coal seam gas and large coal mining development proposals.* Available [online]: Information guidelines for proponents preparing coal seam gas and large coal mining development proposals | iesc accessed 26 July 2023. Minesoils 2023a. Cadia Valley Operations Modification 15 Agricultural Resources Assessment. Prepared for Newcrest Mining Ltd. March 2023. (Appendix 1 of Gateway Application). Minesoils 2023b. Cadia Valley Operations Modification 15 Agricultural Impact Assessment. Prepared for Newcrest Ltd. March 2023. (Appendix 2 of Gateway Application). Newcrest Mining Limited 2023. Cadia Valley Operations – Gateway Application Technical Overview. Prepared for Newcrest Mining Ltd. 2023. 15 May 2023.

Report

24 May 2024

To	Dirk Sanderson	**Contact No.**	PO 4501559263
From	Tegan Hopwood	**Project No.**	12640002
Project Name	Cadia surface water assessment		
Subject	Cadia surface water assessment - Belubula River		

Dear Dirk

1. Introduction

1.1 Background

Cadia Mine (Cadia) is a gold and copper mining and processing operation. Cadia is located approximately 25 km southwest of Orange, in the central tablelands of NSW. Cadia Holdings Pty Limited is the owner and operator of Cadia and is a wholly owned subsidiary of Newmont Corporation (Newmont), following the acquisition of Newcrest Mining Limited on 6 November 2023. Operations at Cadia occur under six Mining Leases (ML): ML1405, ML1449, ML1472, ML1481, ML1689 and ML1690.

Cadia comprises the Cadia Hill open cut (commenced in 1998 and completed in 2013), the Ridgeway underground mine (commenced in 2002) and the Cadia East underground mine (commenced in 2012). The site also maintains two waste rock emplacements (the rehabilitated North Waste Rock Dump (NWRD) and the active South Waste Rock Dump (SWRD)), as well as the Northern Tailings Storage Facility (NTSF), Southern Tailings Storage Facility (STSF) and Cadia Hill Pit TSF which commenced in 1998, 2002 and 2018, respectively. Newmont also operates the Cadia Dewatering Facility, located approximately 23.5 km to the east of Cadia, and east of the town of Blayney.

1.2 Scope of work

GHD Pty Ltd (GHD) were engaged by Cadia to undertake an assessment of surface water quality for two sites located on the Belubula River, upstream and downstream of Cadiangullong Creek, and provide a brief report of results to June 2023. The purpose of this report is to meet the internal and external reporting requirements for the 2022-2023 reporting period, which extends from 1 July 2022 to 30 June 2023.

Water quality data have been compared to the following guideline values:

– ANZECC (2000) livestock drinking water quality guidelines
– ANZECC (2000) irrigation guidelines, with long-term trigger values and values for sensitive crops applied as the most conservative values

Aquatic ecosystem monitoring of waterways within and surrounding Cadia has been undertaken for the reporting period as part of the Aquatic Ecosystem Monitoring Project.

1.3 Assumptions

All data received from Cadia Holdings Pty Ltd were assumed to be accurate, unless otherwise stated below. It is assumed that the collection methodology used for all sampling was appropriate to prevent contamination and that the holding times were adhered to.

1.4 Limitations

This report has been prepared by GHD for Cadia Holdings Pty Ltd and may only be used and relied on by Cadia Holdings Pty Ltd for the purpose agreed between GHD and Cadia Holdings Pty Ltd as set out in Section 1.2 of this report.

GHD otherwise disclaims responsibility to any person other than Cadia Holdings Pty Ltd arising in connection with this report. GHD also excludes implied warranties and conditions, to the extent legally permissible.

The services undertaken by GHD in connection with preparing this report were limited to those specifically detailed in the report and are subject to the scope limitations set out in the report.

The opinions, conclusions and any recommendations in this report are based on conditions encountered and information reviewed at the date of preparation of the report. GHD has no responsibility or obligation to update this report to account for events or changes occurring subsequent to the date that the report was prepared.

Where this report is relied on or used without obtaining this further advice from GHD, to the maximum extent permitted by law, GHD disclaims all liability and responsibility to any person in connection with, arising from or in respect of this report whether such liability arises in contract, tort (including negligence) or under statute.

The opinions, conclusions and any recommendations in this report are based on assumptions made by GHD described in this report. GHD disclaims liability arising from any of the assumptions being incorrect.

GHD has prepared this report on the basis of information provided by Cadia Holdings Pty Ltd and others who provided information to GHD (including Government authorities), which GHD has not independently verified or checked beyond the agreed scope of work. GHD does not accept liability in connection with such unverified information, including errors and omissions in the report which were caused by errors or omissions in that information.

The opinions, conclusions and any recommendations in this report are based on information obtained from, and testing undertaken at or in connection with, specific sample points. Site conditions at other parts of the site may be different from the site conditions found at the specific sample points.

2. Surface water assessment

2.1 Belubula River

The Belubula River is located to the south of Cadia, and flows in a westerly direction before joining the Lachlan River. The Belubula River receives water from Cadiangullong Creek, which flows in a southerly direction adjacent to Cadia.

The focus of this assessment is to identify potential impacts from Cadiangullong Creek on water quality in the Belubula River.

The following surface water sites are located on Belubula River:

– BRPS – located upstream of Cadiangullong Creek, downstream of Flyers Creek.
– CAWS71 – located downstream of Cadiangullong Creek and Flyers Creek.

2.2 Water quality

Summary statistics (minimum, median, and maximum values) for all analysed water quality parameters for data at upstream site BRPS and downstream site CAWS71 are presented in Table 2.1. Data analysed are for the period from January 2021 to June 2023, however it is noted that routine monitoring at CAWS71 did not commence until February 2022. No data are available for downstream site CAWS71 between February 2021 and February 2022, or in November and December 2022. These statistics have been compared to the ANZECC (2000) guideline for livestock drinking water, and the ANZECC (2000) guideline for irrigation. As outlined in Section 1.2, the lowest applicable guideline values for each analyte have been selected for comparison in this report, as the most conservative (lowest risk) values.

Total phosphorus (TP) was above the ANZECC (2000) irrigation guideline value at upstream site BRPS in the maximum value (and equal to the guideline in the median value), and above the guideline at downstream site CAWS71 in the median and maximum values. Therefore, approximately half of the TP concentrations reported for both sites were above the guideline value as shown in Appendix A. This guideline is for the prevention of bioclogging (clogging of irrigation infrastructure due to excessive algae or microbial growth) only. It is also the value for long-term (100 years) of irrigation, and is therefore considered to be of very low risk. All TP values at both BRPS and CAWS71 were below the short-term (20 years of irrigation) trigger value of 0.80 mg/L.

Similarly, dissolved iron was above the ANZECC (2000) long term irrigation guideline value at both upstream site BRPS and downstream site CAWS71 in the maximum values but below the short-term guideline value of 10 mg/L. All exceedances occurred in 2021 and 2022 and there have been no exceedances in 2023. The upstream dissolved iron concentrations were slightly higher than the downstream concentrations.

pH at downstream site CAWS71 exceeded the upper bound of the recommended pH range on one occasion (in 2022). The recommended pH range is to limit corrosion and fouling of pumping infrastructure for irrigation and stock watering systems. The pH graph in Appendix A suggests that this pH value is an outlier. No other pH exceedances were recorded.

All other water quality parameters were below both the ANZECC (2000) livestock and irrigation guideline values in all samples collected during the historical monitoring period at both the upstream and downstream Belubula River sites.

Further analysis of key water quality parameters, including comparison of results between the upstream (BRPS) and downstream (CAWS71) sites on the Belubula River are provided in sections 2.2.1 to 2.2.4 below. Time series figures for all analysed parameters have also been presented in Appendix A.

Table 2.1 Summary statistics for water quality results at BRPS and CAWS71, January 2021 to June 2023. All units are in mg/L unless otherwise stated.

Analyte	BRPS			CAWS71			ANZECC 2000	
Site	**Min**	**Median**	**Max**	**Min**	**Median**	**Max**	**Livestock**	**Irrigation [(a)]**
Physicochemical parameters								
Electrical Conductivity (EC) - Field (µS/cm)	221.9	457.0	724.3	244.1	540.0	770.1	NA	950 [(b)]
pH - Field (pH units)	7.22	8.13	8.50	7.17	8.09	10.80	NA	6-9
Redox Potential (mV)	51	275	340	24	262	335	NA	NA
Suspended Solids	<5	8	119	<5	6	52	NA	NA
Temperature (°C)	7.6	17.4	26.7	5.3	19.5	24.4	NA	NA
Total Dissolved Solids	178	279	469	155	302	495	2000 [(c)]	NA
Major ions								
Bicarbonate alkalinity	75	175	227	67	192	234	NA	NA
Calcium	17	39	67	19	41	69	1000	NA
Carbonate alkalinity	<1	<1	15	<1	<1	16	NA	NA
Chloride	16	33	63	12	39	63	NA	175 [(b)]
Hydroxide alkalinity	<1	<1	<1	<1	<1	<1	NA	NA
Magnesium	9	22	38	9	25	40	NA	NA
Potassium	2	3	6	2	3	6	NA	NA
Sodium	14	27	47	13	31	49	NA	115 [(b)]
Sulfate	14	40	114	16	50	137	1000	NA
Total alkalinity	75	178	235	67	193	236	NA	NA
Total hardness	80	183	324	84	201	337	NA	NA
Nutrients								
Nitrate as N	<0.01	0.13	0.53	<0.01	0.07	0.30	90.3 [(e)]	NA
Nitrite + Nitrate	<0.01	0.13	0.54	<0.01	0.07	0.30	NA	NA
Nitrite as N	<0.01	<0.01	0.02	<0.01	<0.01	0.02	9.1 [(f)]	NA
Total Kjeldahl Nitrogen	0.4	0.7	2.2	0.1	0.6	1.2	NA	NA
Total nitrogen	0.4	0.9	2.6	0.1	0.7	1.5	NA	5
Total phosphorus	0.02	0.05	0.24	0.02	0.06	0.26	NA	0.05 [(d)]
Dissolved metals								
Aluminium	<0.01	<0.01	0.34	<0.01	<0.01	0.40	5	5
Antimony	<0.001	<0.001	<0.001	<0.001	<0.001	<0.001	NA	NA
Arsenic	<0.001	0.004	0.013	<0.001	0.006	0.014	0.5	0.1
Cadmium	<0.0001	<0.0001	<0.0001	<0.0001	<0.0001	<0.0001	0.01	0.01
Chromium	<0.001	<0.001	<0.001	<0.001	<0.001	<0.001	1	0.1
Cobalt	<0.001	<0.001	0.003	<0.001	<0.001	0.003	1	0.05
Copper	<0.001	<0.001	0.003	<0.001	<0.001	0.010	0.4	0.2
Iron	<0.05	0.15	0.62	<0.05	0.06	0.58	NA	0.2
Lead	<0.001	<0.001	<0.001	<0.001	<0.001	<0.001	0.1	2
Manganese	0.016	0.029	0.141	0.014	0.025	0.046	NA	0.2

Analyte	BRPS			CAWS71			ANZECC 2000	
Site	Min	Median	Max	Min	Median	Max	Livestock	Irrigation [(a)]
Mercury	<0.0001	<0.0001	<0.0001	<0.0001	<0.0001	<0.0001	0.002	0.002
Molybdenum	<0.001	<0.001	<0.001	<0.001	<0.001	<0.001	0.15	0.01
Nickel	<0.001	<0.001	0.002	<0.001	<0.001	0.007	1	0.2
Selenium	<0.01	<0.01	<0.01	<0.01	<0.01	<0.01	0.02	0.02
Silver	<0.001	<0.001	<0.001	<0.001	<0.001	<0.001	NA	NA
Zinc	<0.005	<0.005	0.011	<0.005	<0.005	0.02	20	2

[(a)] Long-term (100 years) irrigation values used, as the most conservative value
[(b)] Value for sensitive crops used, as the most conservative value
[(c)] Most sensitive animal (poultry) value applied
[(d)] To minimise bioclogging of irrigation equipment only
[(e)] Nitrate guideline is 400 mg/L. Converted to nitrate as N.
[(f)] Nitrite guideline is 30 mg/L. Converted to nitrite as N.
Values in yellow are higher than the ANZECC (2000) irrigation guideline value

2.2.1 Physicochemical parameters

Field pH results recorded in the Belubula River were generally slightly alkaline, with most results during the January 2021 to June 2023 reporting period within the 7.5 to 9.0 range. Most pH results were very similar at sites upstream (BRPS) and downstream (CAWS71) of the Cadiangullong Creek confluence throughout the historical monitoring period. There was one elevated pH result observed at CAWS71 in June 2022, however, all subsequent results had returned to within the usual range.

Field electrical conductivity (EC) fluctuated at both sites across the historical monitoring period, with the highest EC results observed at both sites during early-2023 (Figure 2.1). One EC result (4025 µS/cm at BRPS in July 2022) was assumed to be incorrect as it did not match the laboratory result, and was consequently removed from the dataset.

A seasonal pattern in EC results was observed at both sites, with EC generally higher during the post-summer months (March and April in 2022, and February, March and April in 2023) and lower during the post-winter months (July to December). A weak relationship between EC and rainfall was observed during the 2022-2023 reporting period, with EC lowest between August and November 2022, when rainfall in the study area was well above average (refer Figure 2.1 in GHD 2023). Rainfall was also above average between February and April 2023 when EC results were at their highest, however, this is likely to have been influenced by lower rainfall in December 2022 to January 2023, coupled with increased evapoconcentration during the summer period. EC results were similar between the sites during most sampling events, although EC results in the January to June 2023 period were slightly higher at downstream site CAWS71 than upstream site BRPS. All results at both sites were well below the conservative guideline value for irrigation.

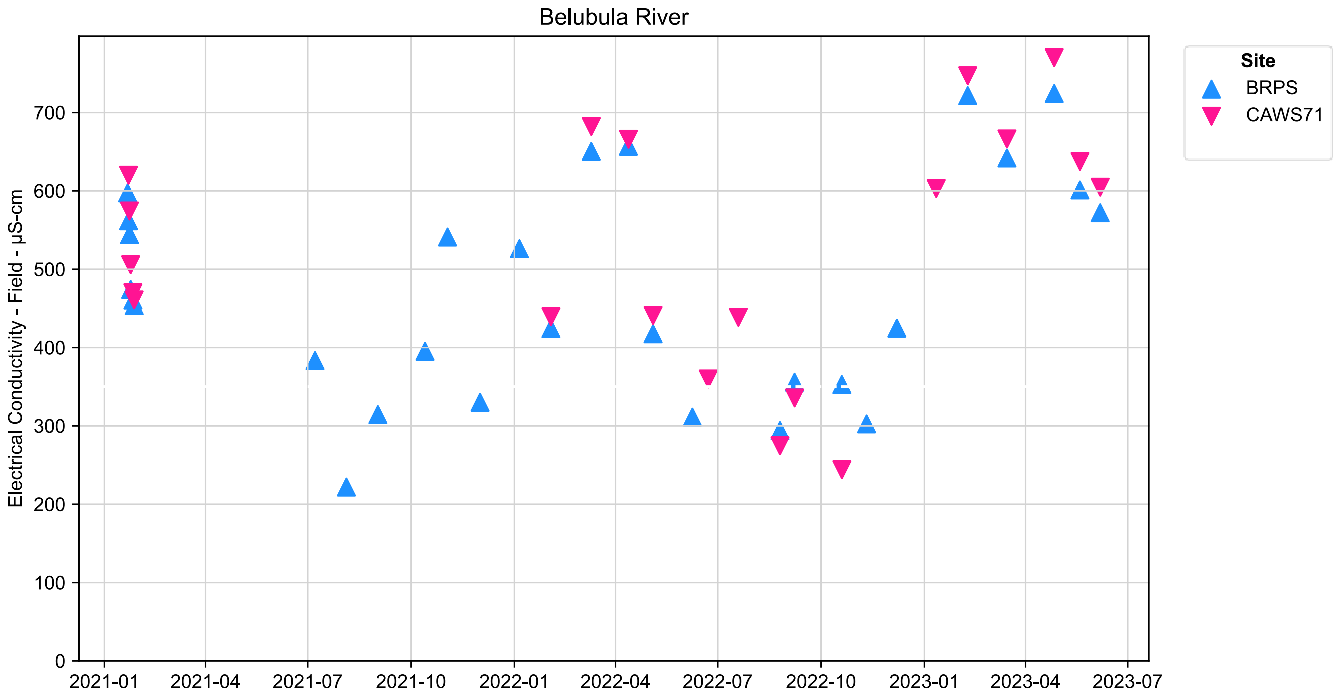

Figure 2.1 EC levels in the Belubula River

Total suspended solids (TSS) concentrations were generally low (<20 mg/L) at both sites, although infrequent elevated concentrations were observed between mid-2021 and mid-2022, most commonly at upstream site BRPS. Most TSS results were similar between the sites during events in which samples were collected from both sites. TSS results were frequently lowest from late-2022 to 2023.

2.2.2 Nutrients

Concentrations of nutrients have remained consistent at both BRPS and CAWS71 across the historical monitoring period, with all results during the 2022-2023 reporting period within the historical range of results. Concentrations of nitrate (and nitrate + nitrite) were lowest in January 2021, March 2022 and January to May 2023 at both sites, while concentrations were highest in August and September 2021 (BRPS only) and in mid-2022 (both sites).

Similar to nitrate concentrations, total nitrogen (TN) and total Kjeldahl nitrogen (TKN) concentrations were lower in early 2023 at both sites compared to most historical results. All nitrogen results were well below the relevant livestock and irrigation guideline values.

TP concentrations were also low in 2023 compared to some historical results, with the highest concentrations observed at both sites in 2021. As shown by the time series graph in Appendix A, TP concentrations at both sites have generally been decreasing over the past two years. As stated previously, approximately half of the TP concentrations reported for both sites over the monitoring period were above the long-term (100 years) irrigation guideline value for the prevention of bioclogging (clogging of irrigation infrastructure due to excessive algae or microbial growth). All TP values at both BRPS and CAWS71 were below the short-term (20 years of irrigation) trigger value of 0.80 mg/L.

TN, TKN and TP concentrations were similar between the two sites during all sampling events.

2.2.3 Major ion composition

Concentrations of most major ions (excluding potassium) followed a similar seasonal pattern, with the highest concentrations observed in February to April 2023, followed by March and April 2022. Concentrations of all of these major ions were slightly (less than 10 percent) higher at downstream site CAWS71 than upstream site BRPS. Potassium concentrations indicated no temporal pattern, with the highest concentrations observed at both sites in early 2021. Sulfate was higher at downstream site CAWS71 than upstream site BRPS in most samples of the historical monitoring period, particularly during the January to June 2023 period, although sulfate concentrations at both sites followed similar trends over the monitoring period and were well below the livestock guideline value.

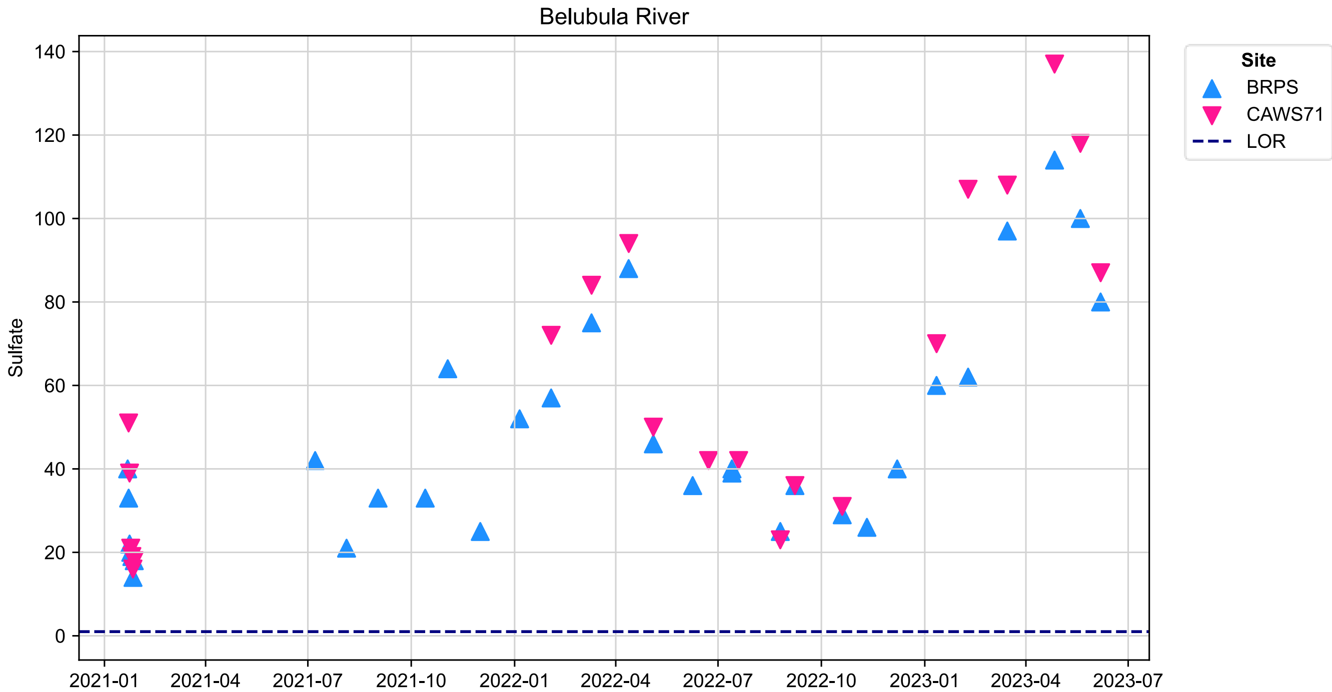

Figure 2.2 ***Sulfate concentrations in the Belubula River***

The piper plot in Figure 2.3 shows the ionic composition of Belubula River sites during the historical monitoring period, based on calculations of the median concentrations of each major ion for each time period (January 2021 to June 2022, and July 2022 to June 2023). The ionic composition of water at BRPS and CAWS71 was similar between sites and sampling period. Water at both sites demonstrated a mixed cation composition and a dominance of the bicarbonate anion.

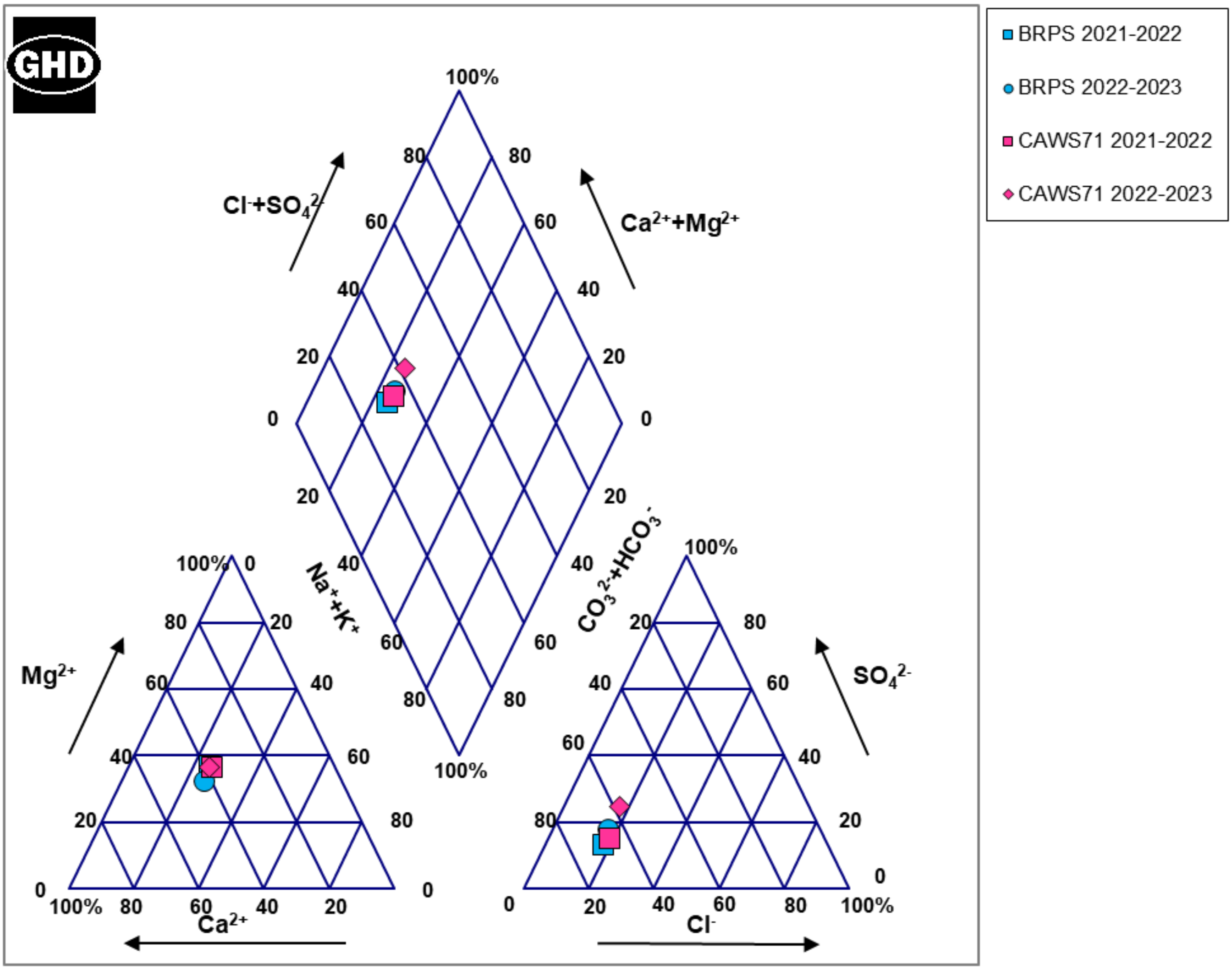

Figure 2.3 Piper chart showing differences in major ion composition at Belubula River sites

2.2.4 Dissolved metals

All dissolved antimony, cadmium, chromium, lead, mercury, molybdenum, selenium and silver concentrations were below the laboratory limit of reporting (LOR) at both sites across the historical monitoring period.

Dissolved aluminium concentrations were frequently elevated (compared to the LOR) at both upstream site BRPS and downstream site CAWS71 between July 2021 and November 2022 (Figure 2.4). There was no clear pattern in results between the sites during this time. A decreasing trend in aluminium concentrations was observed at both sites between August 2022 and December 2022, with all dissolved aluminium concentrations between December 2022 and June 2023 at both sites below the LOR. All results were well below the livestock and irrigation guideline values.

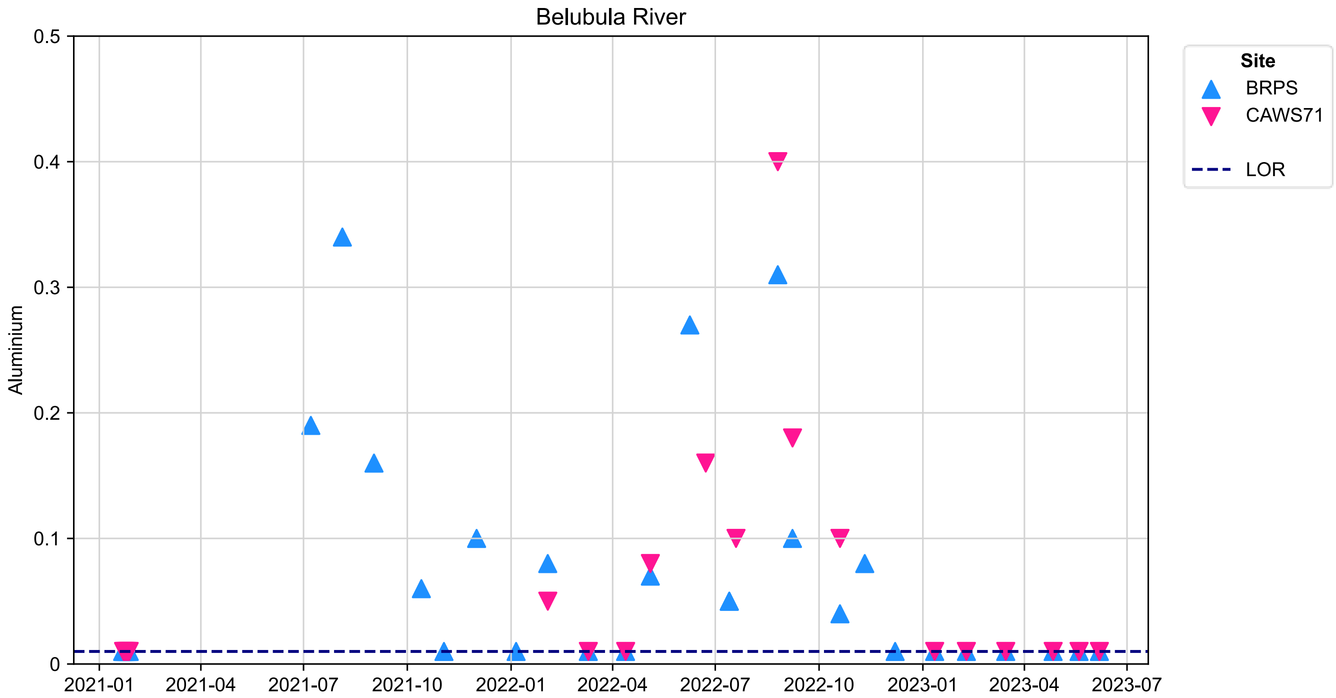

Figure 2.4 ***Dissolved aluminium concentrations in the Belubula River***

Dissolved arsenic concentrations (Figure 2.5) were similar between the sites (within 0.001 mg/L) during all sampling events of the historical monitoring period. Dissolved arsenic concentrations were highest at both sites in February and March 2023, but concentrations declined rapidly between March and June 2023, to be only slightly above the LOR and equal at both sites. All results were well below the livestock and irrigation guideline values.

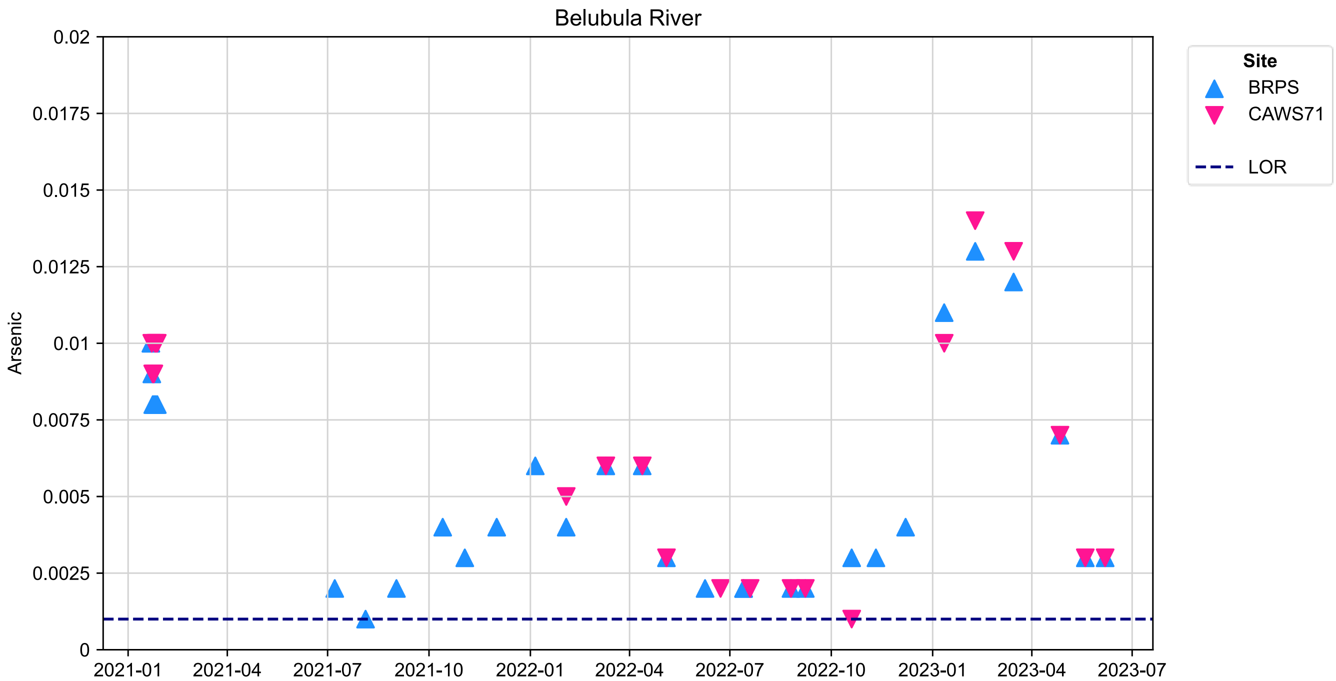

Figure 2.5 ***Dissolved arsenic concentrations in the Belubula River***

Dissolved cobalt concentrations at downstream site CAWS71 were equal to or lower than those at upstream site BRPS during all sampling events of the historical monitoring period. Dissolved cobalt concentrations were generally below the LOR at both sites, although there were some elevated concentrations observed (compared to LOR), particularly in early-2021 and early 2023. All results were well below the livestock and irrigation guideline values.

Dissolved copper concentrations were generally consistent between sites, with the majority of results below the LOR at both sites (Figure 2.6). The highest copper concentration observed during the historical monitoring period was recorded at CAWS71 in October 2022. However, this concentration was an isolated occurrence, and all subsequent copper concentrations had returned to within the typical range of results, with most below the LOR. All results were well below the livestock and irrigation guideline values.

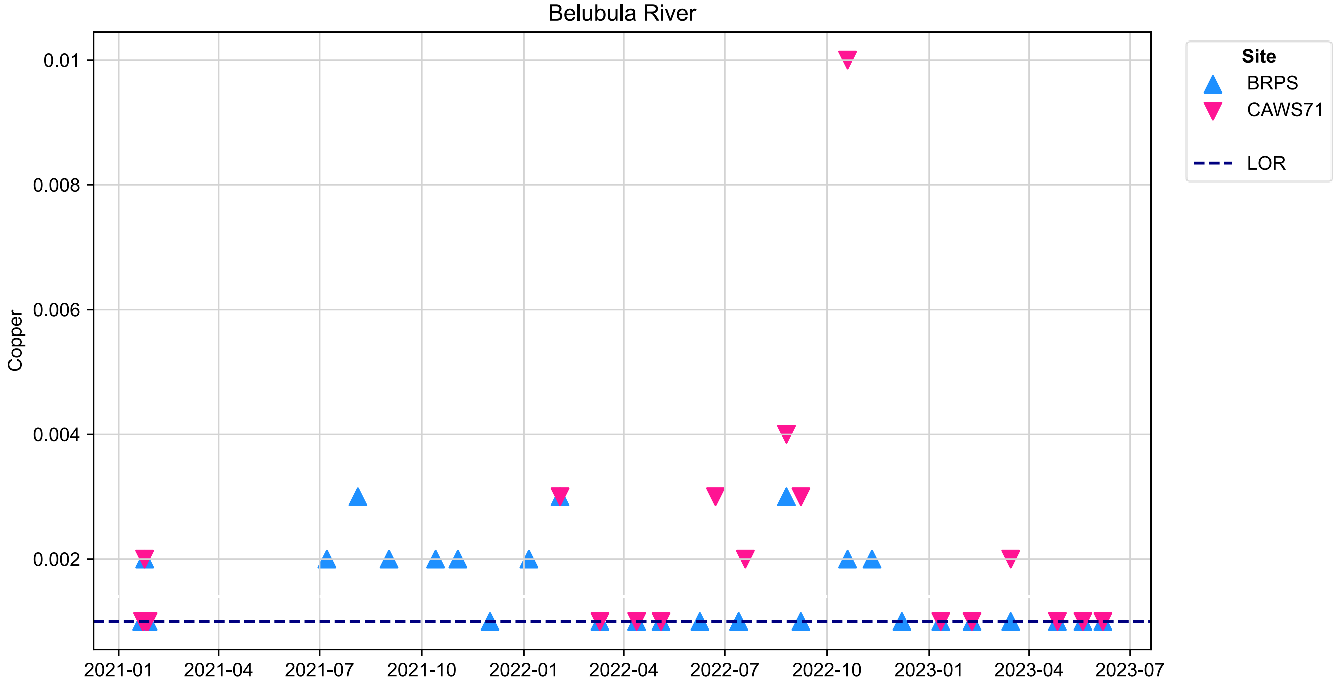

Figure 2.6 *Dissolved copper concentrations in the Belubula River*

Dissolved iron concentrations were generally elevated (compared to LOR) at both sites during much of the July 2021 to January 2023 period, while dissolved iron concentrations in the January to June 2023 monitoring period were consistently much lower. All exceedances of the long-term irrigation guideline value occurred in 2021 and 2022 and there have been no exceedances in 2023. Dissolved iron concentrations at upstream site BRPS were slightly higher than at the downstream site CAWS71 over the monitoring period and this is reflected in the slightly higher median value as shown in Table 2.1.

All dissolved manganese concentrations were very low, with all except one result (upstream site BRPS in February 2022) below 0.06 mg/L. All results were below the irrigation guideline value. Manganese concentrations were similar between the two sites during all other sampling events.

Concentrations of dissolved nickel were low (below the LOR) during most sampling events. The highest dissolved nickel concentration was observed at CAWS71 in August 2022; however, this concentration did not persist, with all subsequent nickel concentrations at CAWS71 returning to below the LOR. All results were well below the livestock and irrigation guideline values.

Concentrations of dissolved zinc were below the LOR during most sampling events. Like the nickel concentration, the dissolved zinc concentration at CAWS71 was also elevated above the usual range of results in August 2022. The zinc concentration observed at upstream site BRPS in August 2022 was also elevated, though the concentration was lower than that observed at CAWS71. Zinc concentrations were also elevated at upstream site BRPS only on several occasions in late-2021. These elevated zinc concentrations did not persist, with all subsequent zinc concentrations below the LOR. All results were well below the livestock and irrigation guideline values.

2.2.5 Summary

Results were generally consistent between the Belubula River sites upstream (BRPS) and downstream (CAWS71) of the Cadiangullong Creek confluence. Exceptions to this include slightly higher EC, and most major ions (mostly notably sulfate) at CAWS71, during most sampling events but particularly in the January to June 2023 period. In addition, TP concentrations were generally higher at upstream site BRPS.

There were minimal exceedances of the ANZECC (2000) irrigation and stock watering guidelines. The exceedances recorded were generally consistent between upstream and downstream sites and unlikely to be attributable to Cadiangullong Creek.

There were isolated incidences of elevated dissolved copper, nickel and zinc at CAWS71 that were not observed at BRPS, most of which occurred during the 2022-2023 reporting period. However, these detections were inconsistent and did not display clear trends, with subsequent concentrations following these peaks quickly returning to within the historical range.

Several dissolved metals have remained below the LOR in all samples of the historical monitoring period, including antimony, cadmium, chromium, lead, mercury, molybdenum, selenium and silver.

3. References

ANZECC and ARMCANZ (2000) *Australian and New Zealand Guidelines for Fresh and Marine Water Quality – Volume 1: The Guidelines*, Australia and New Zealand Environment and Conservation Council and Agriculture and Resource Management Council of Australia and New Zealand, Canberra.

ANZG (2018) *Australian and New Zealand Guidelines for Fresh and Marine Water Quality.* Australian and New Zealand Governments and Australian state and territory governments, Canberra ACT, Australia.

GHD (2023) *Cadia Annual Review 2022-2023: Surface Water Assessment (September* 2023).

Appendices

Appendix A

Surface water quality graphs

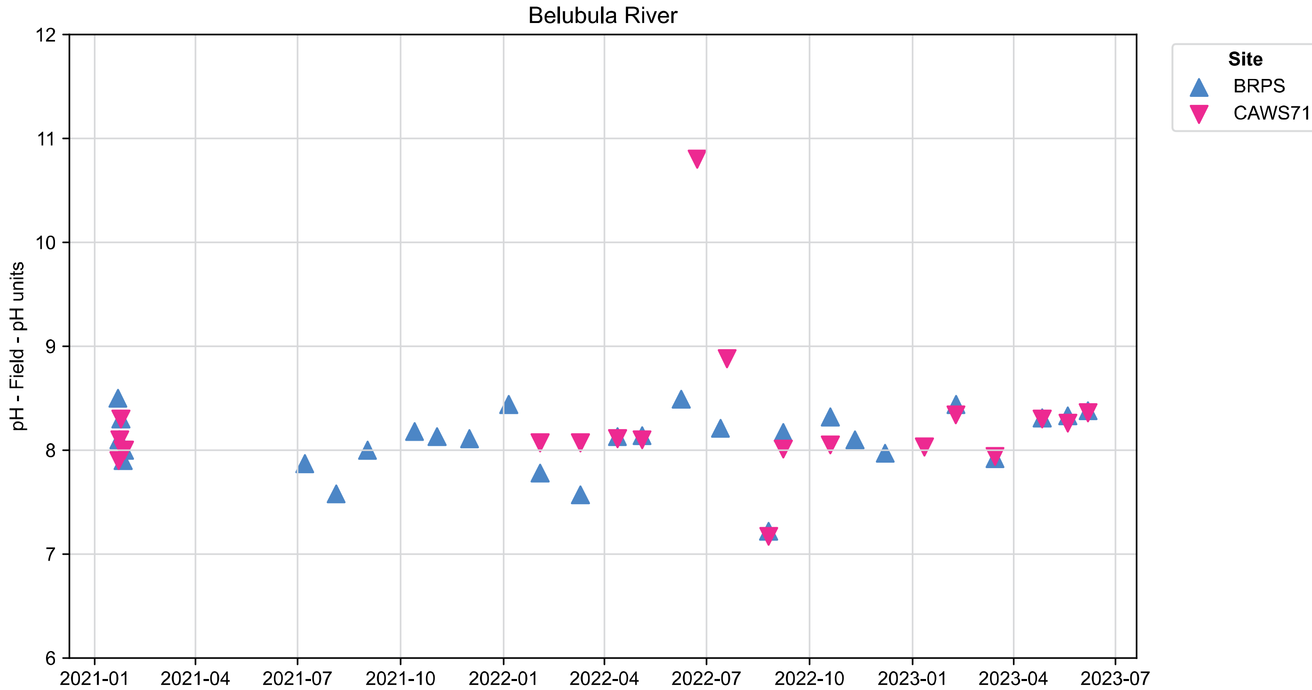

Belubula River
pH - Field - pH units
Site
BRPS
CAWS71

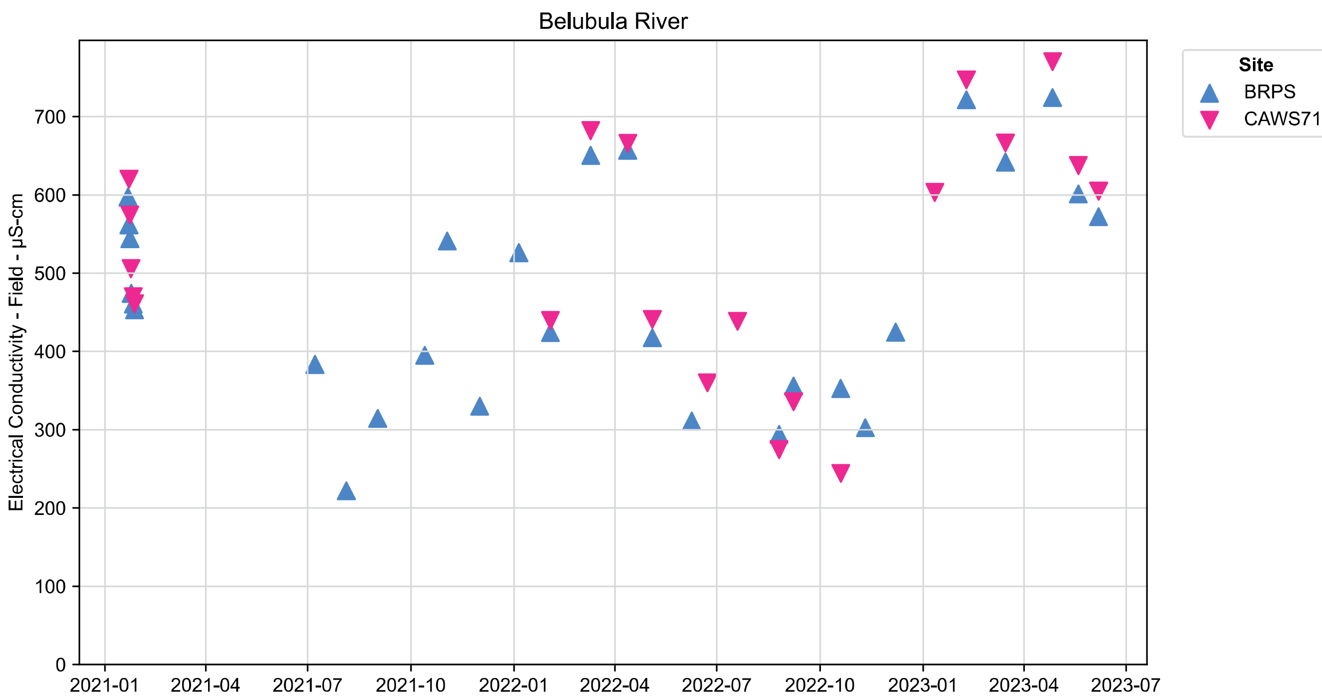

Belubula River
Electrical Conductivity - Field - µS-cm
Site
BRPS
CAWS71

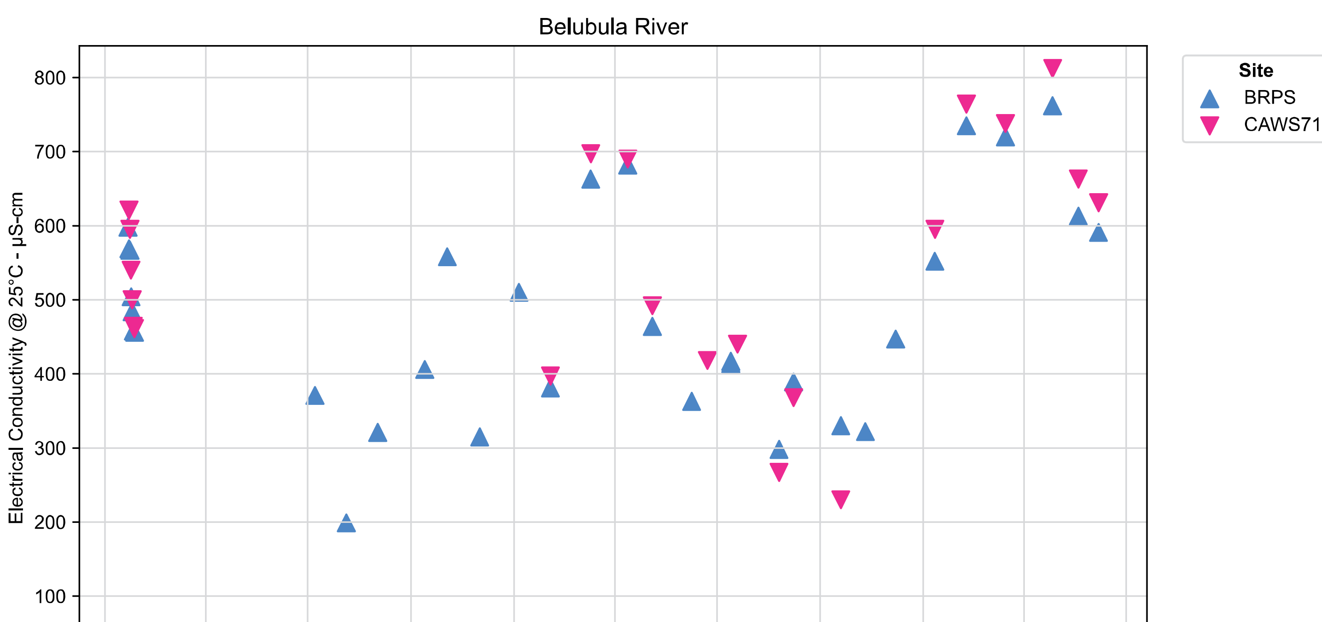

Belubula River
Electrical Conductivity @ 25°C - µS-cm
Site
BRPS
CAWS71

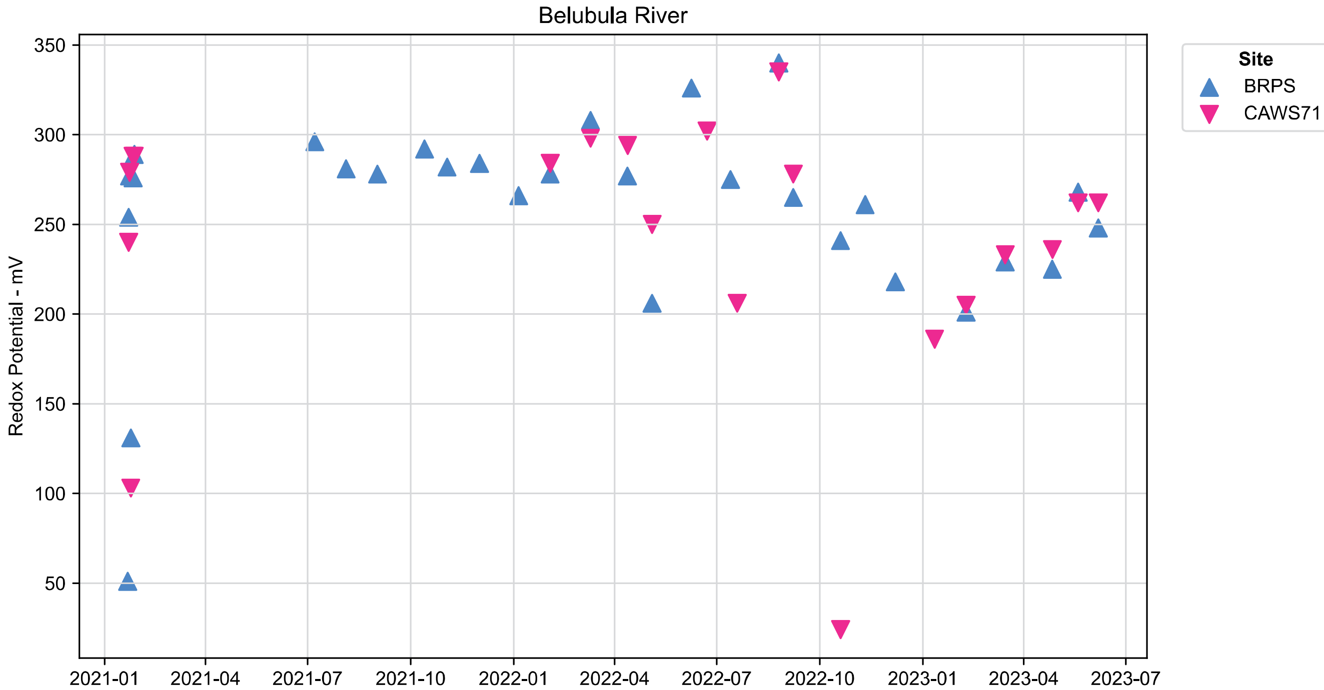
Belubula River
Redox Potential - mV
350
300
250
200
150
100
50
2021-01
2021-04
2021-07
2021-10
2022-01
2022-04
2022-07
2022-10
2023-01
2023-04
2023-07
Site
BRPS
CAWS71

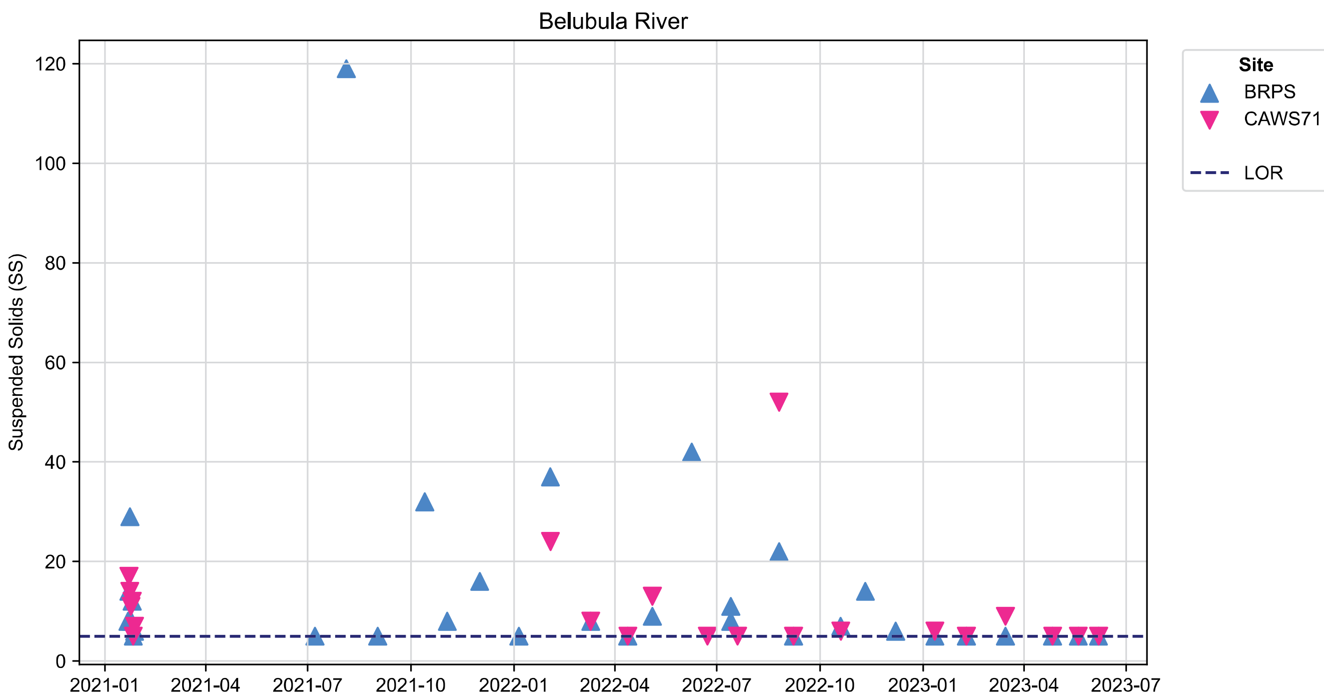
Belubula River
Suspended Solids (SS)
120
100
80
60
40
20
0
2021-01
2021-04
2021-07
2021-10
2022-01
2022-04
2022-07
2022-10
2023-01
2023-04
2023-07
Site
BRPS
CAWS71
LOR

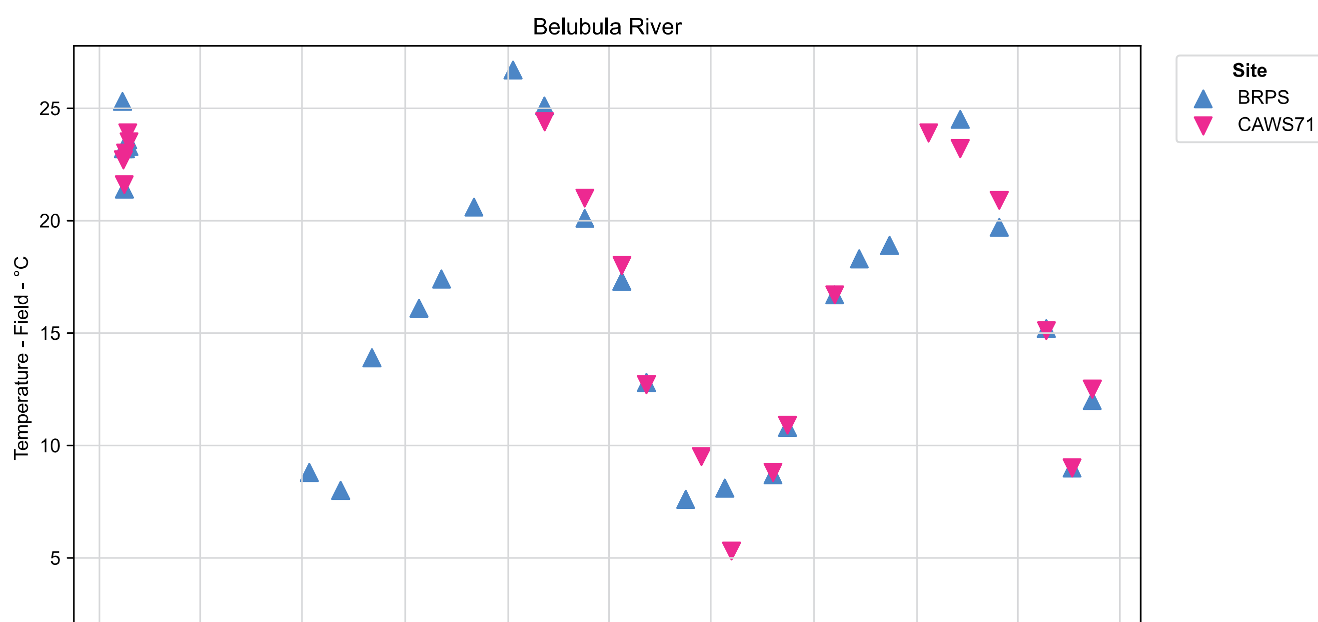
Belubula River
Temperature - Field - °C
25
20
15
10
5
Site
BRPS
CAWS71

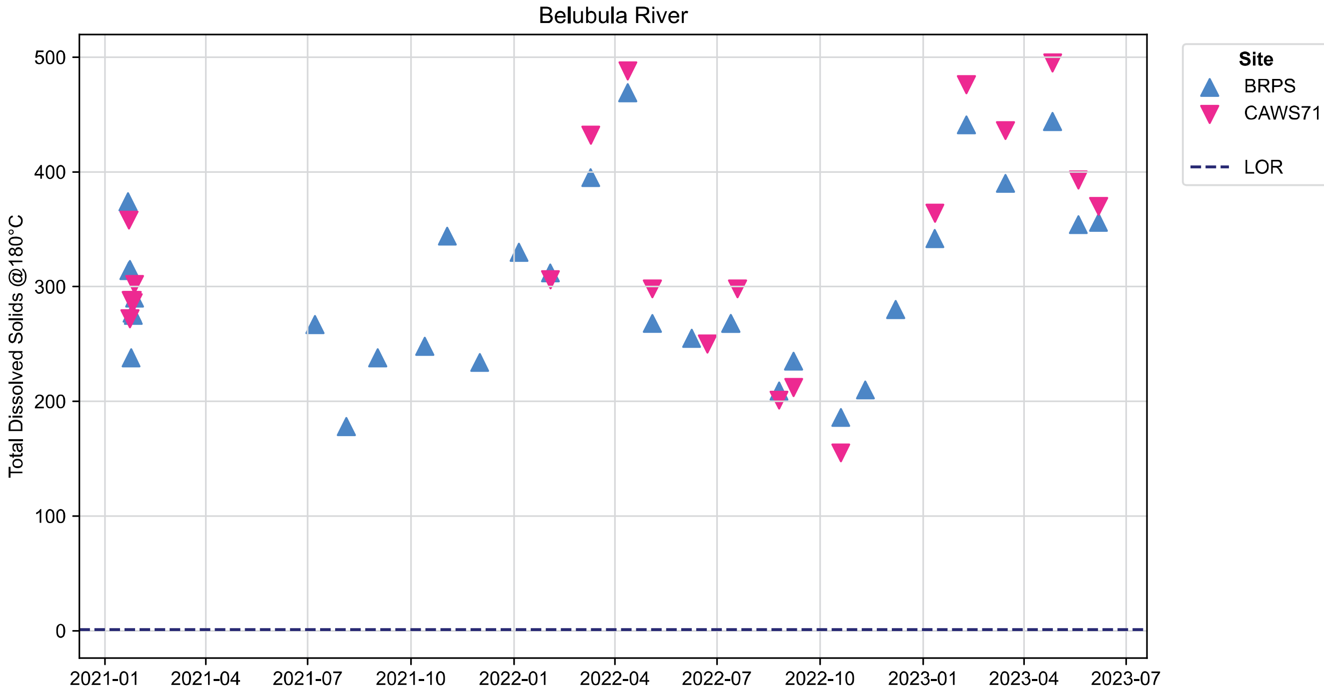
Belubula River
Total Dissolved Solids @180°C
Site
BRPS
CAWS71
LOR
0
100
200
300
400
500
2021-01
2021-04
2021-07
2021-10
2022-01
2022-04
2022-07
2022-10
2023-01
2023-04
2023-07

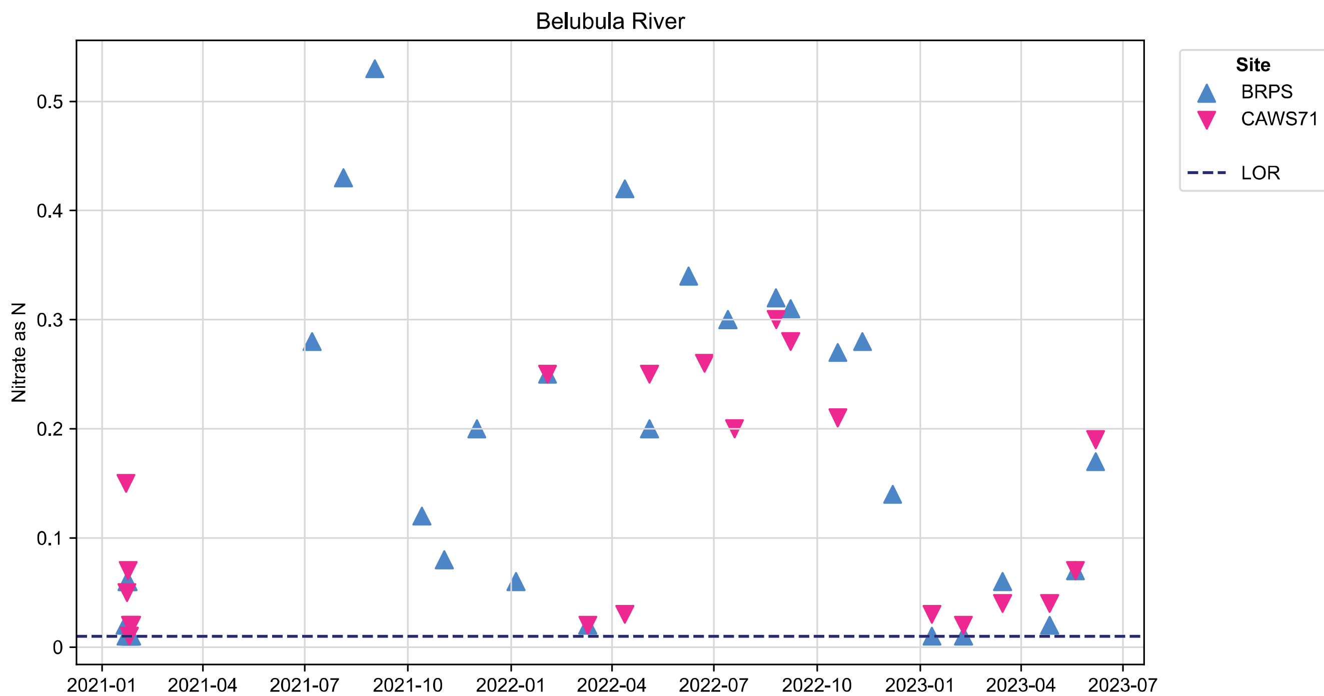
Belubula River
Nitrate as N
Site
BRPS
CAWS71
LOR
0
0.1
0.2
0.3
0.4
0.5
2021-01
2021-04
2021-07
2021-10
2022-01
2022-04
2022-07
2022-10
2023-01
2023-04
2023-07

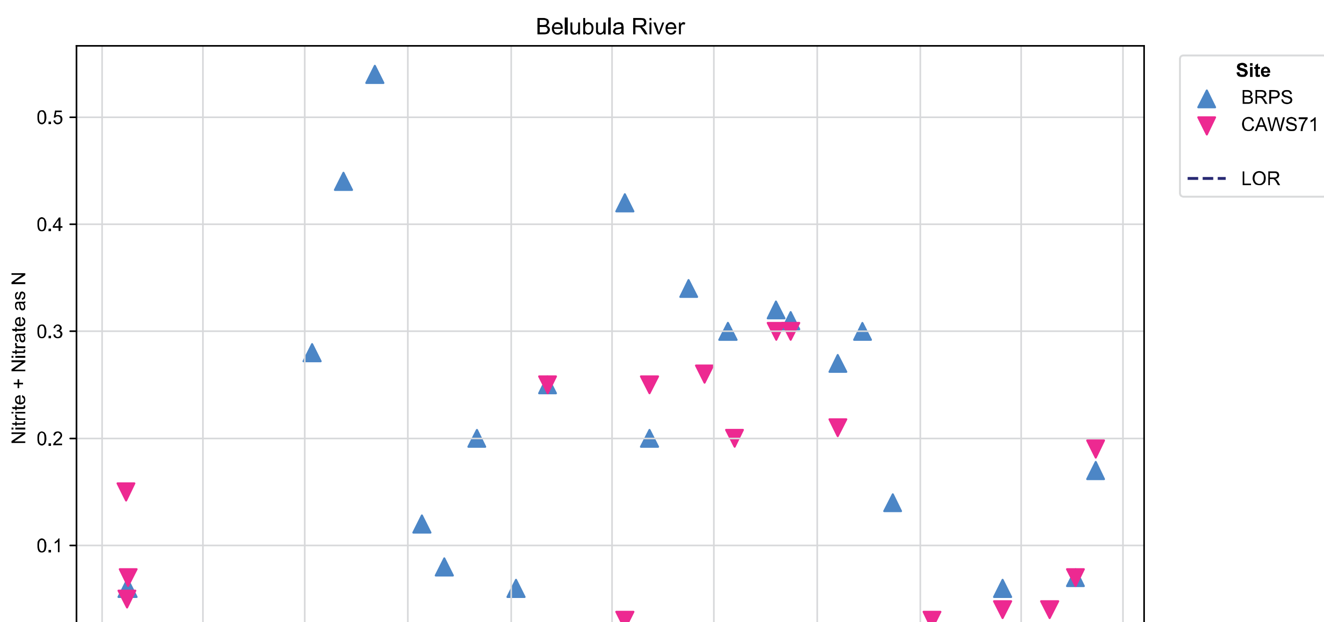
Belubula River
Nitrite + Nitrate as N
Site
BRPS
CAWS71
LOR
0.1
0.2
0.3
0.4
0.5

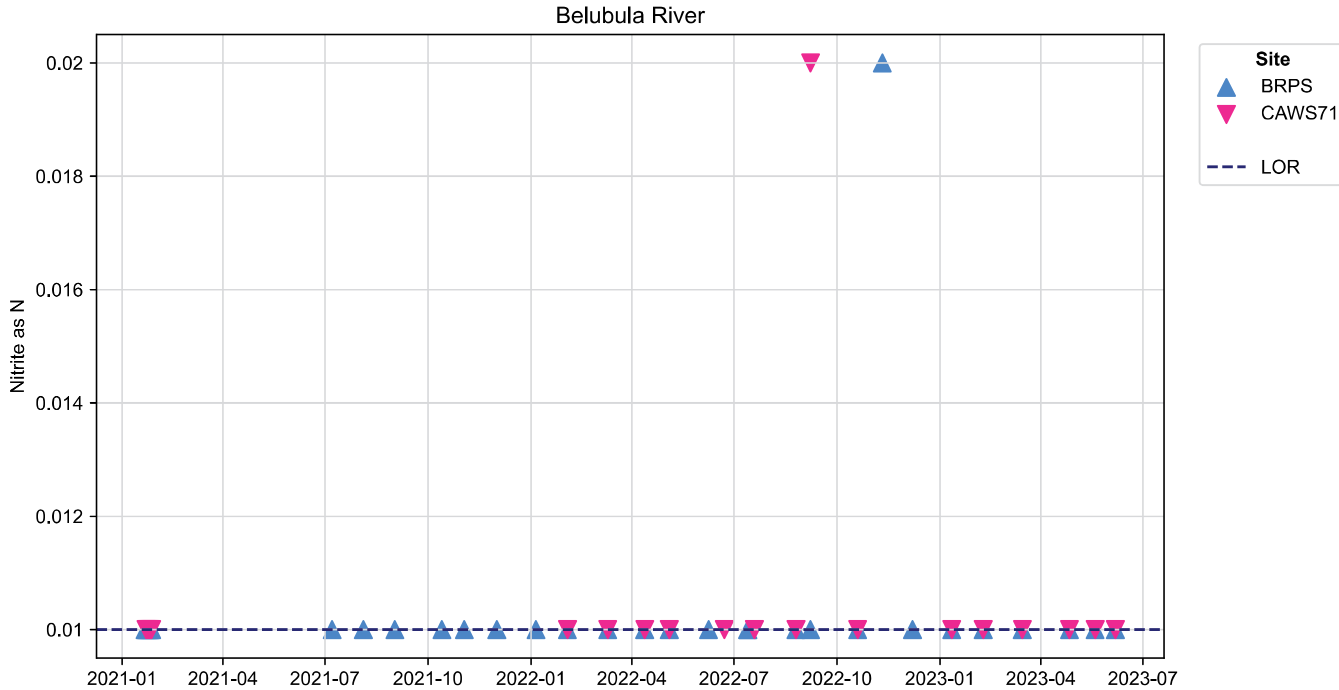
Belubula River
Nitrite as N
0.02
0.018
0.016
0.014
0.012
0.01
2021-01
2021-04
2021-07
2021-10
2022-01
2022-04
2022-07
2022-10
2023-01
2023-04
2023-07
Site
BRPS
CAWS71
LOR

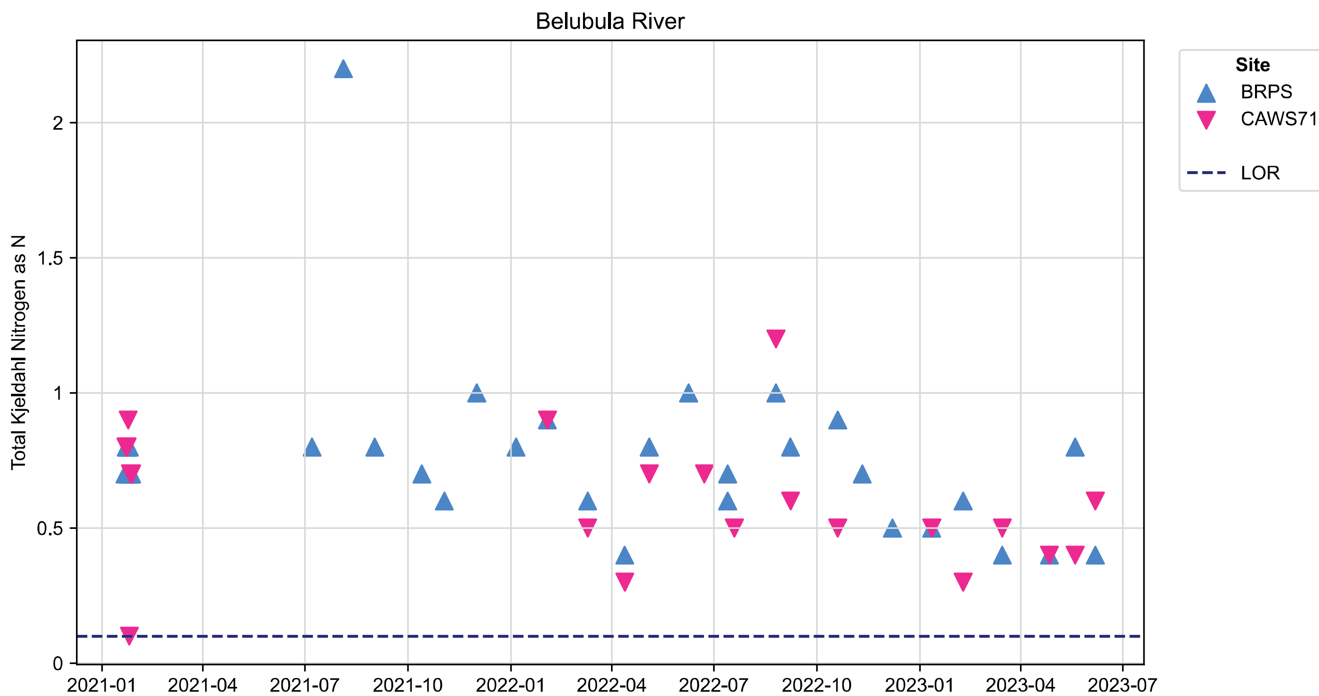
Belubula River
Total Kjeldahl Nitrogen as N
2
1.5
1
0.5
0
2021-01
2021-04
2021-07
2021-10
2022-01
2022-04
2022-07
2022-10
2023-01
2023-04
2023-07
Site
BRPS
CAWS71
LOR

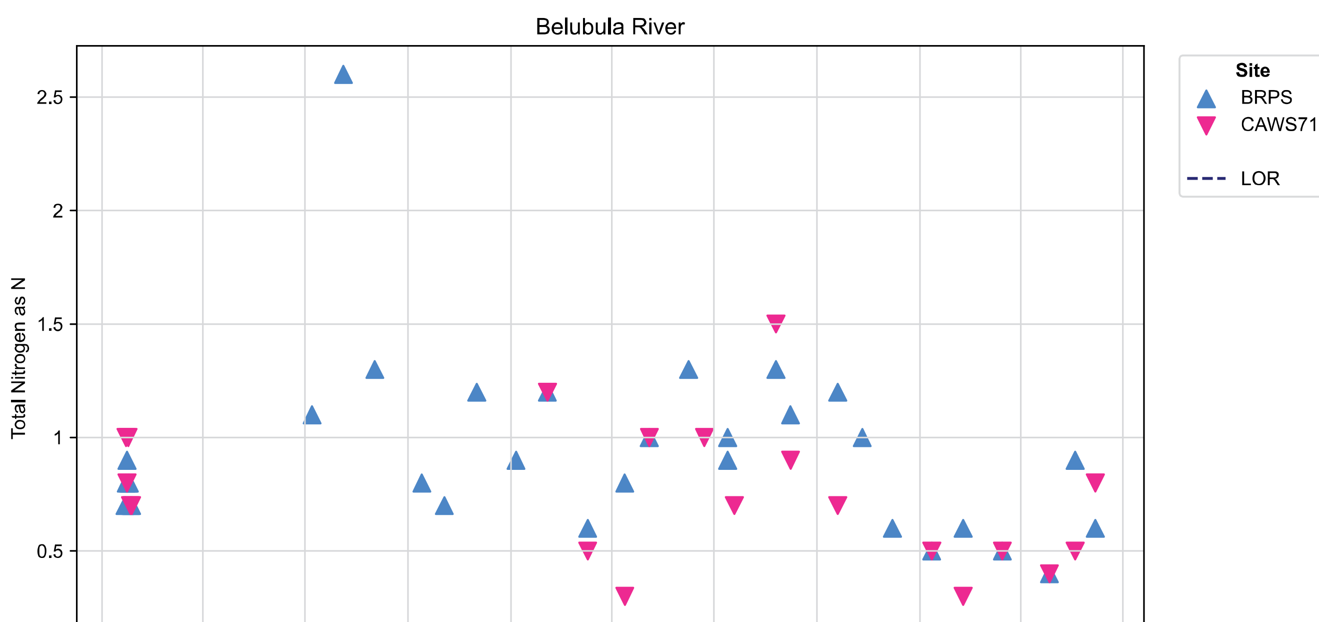
Belubula River
Total Nitrogen as N
2.5
2
1.5
1
0.5
Site
BRPS
CAWS71
LOR

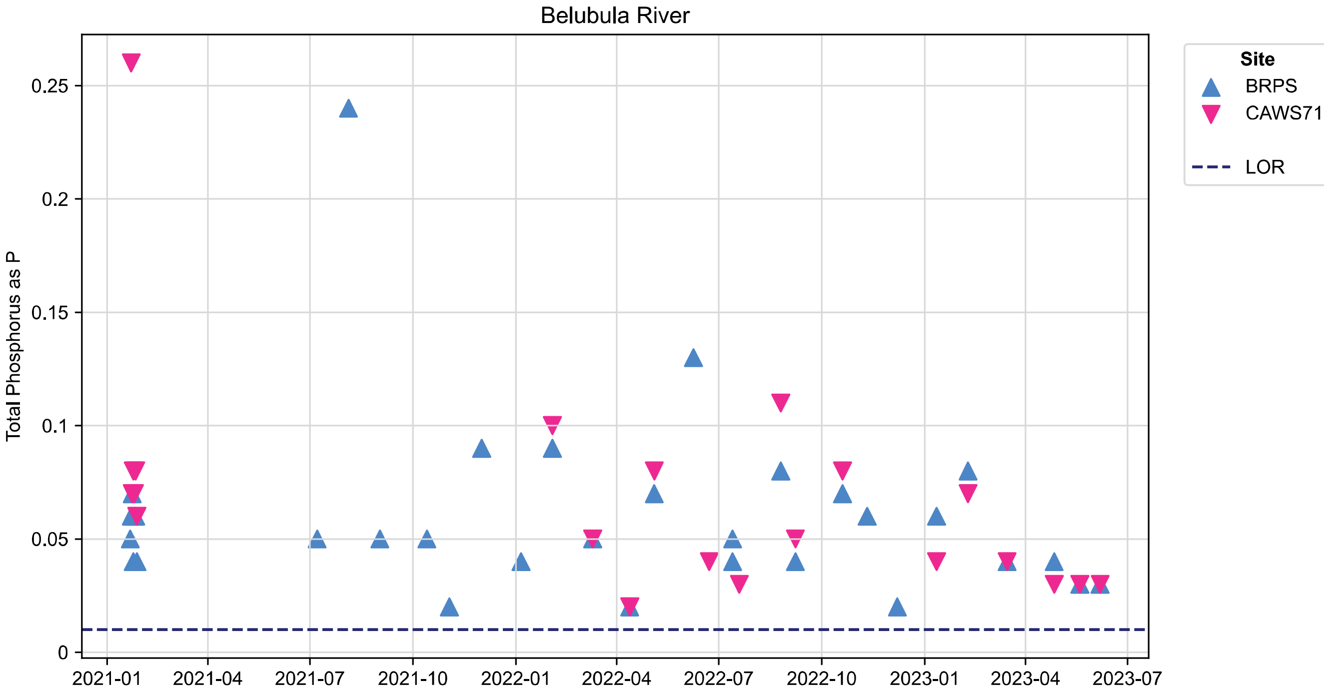
Belubula River
Total Phosphorus as P
0.25
0.2
0.15
0.1
0.05
0
2021-01
2021-04
2021-07
2021-10
2022-01
2022-04
2022-07
2022-10
2023-01
2023-04
2023-07
Site
BRPS
CAWS71
LOR

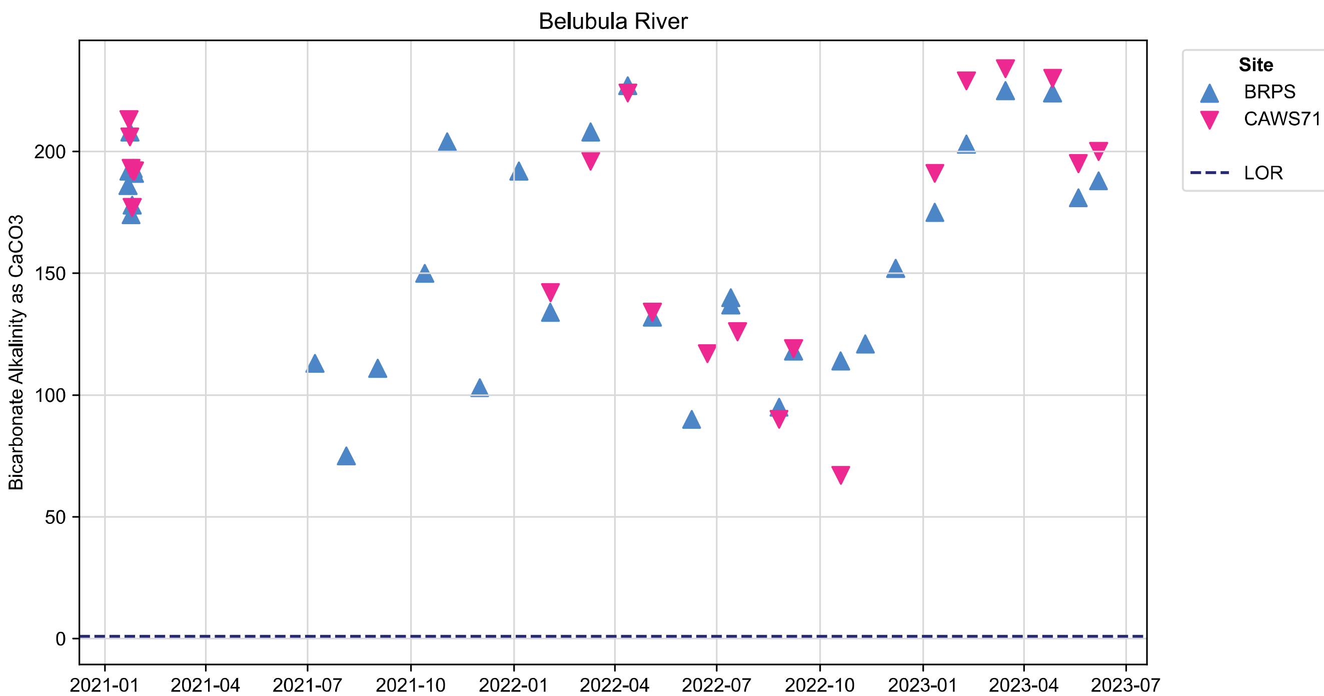
Belubula River
Bicarbonate Alkalinity as CaCO3
200
150
100
50
0
2021-01
2021-04
2021-07
2021-10
2022-01
2022-04
2022-07
2022-10
2023-01
2023-04
2023-07
Site
BRPS
CAWS71
LOR

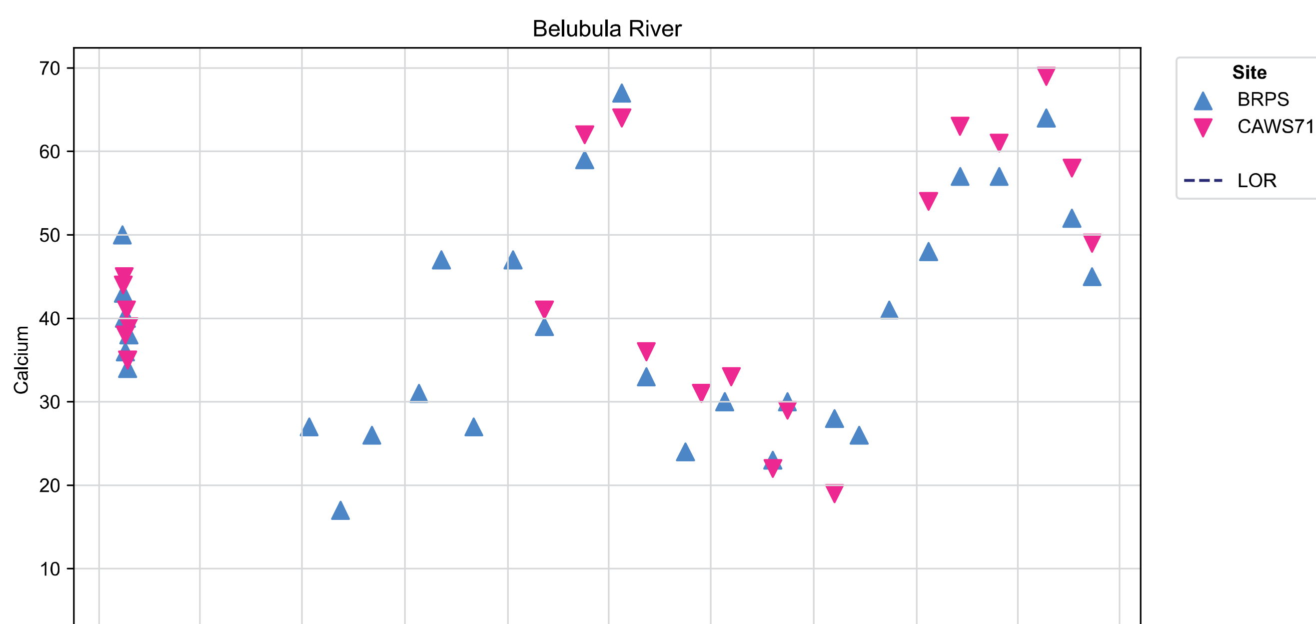
Belubula River
Calcium
70
60
50
40
30
20
10
Site
BRPS
CAWS71
LOR

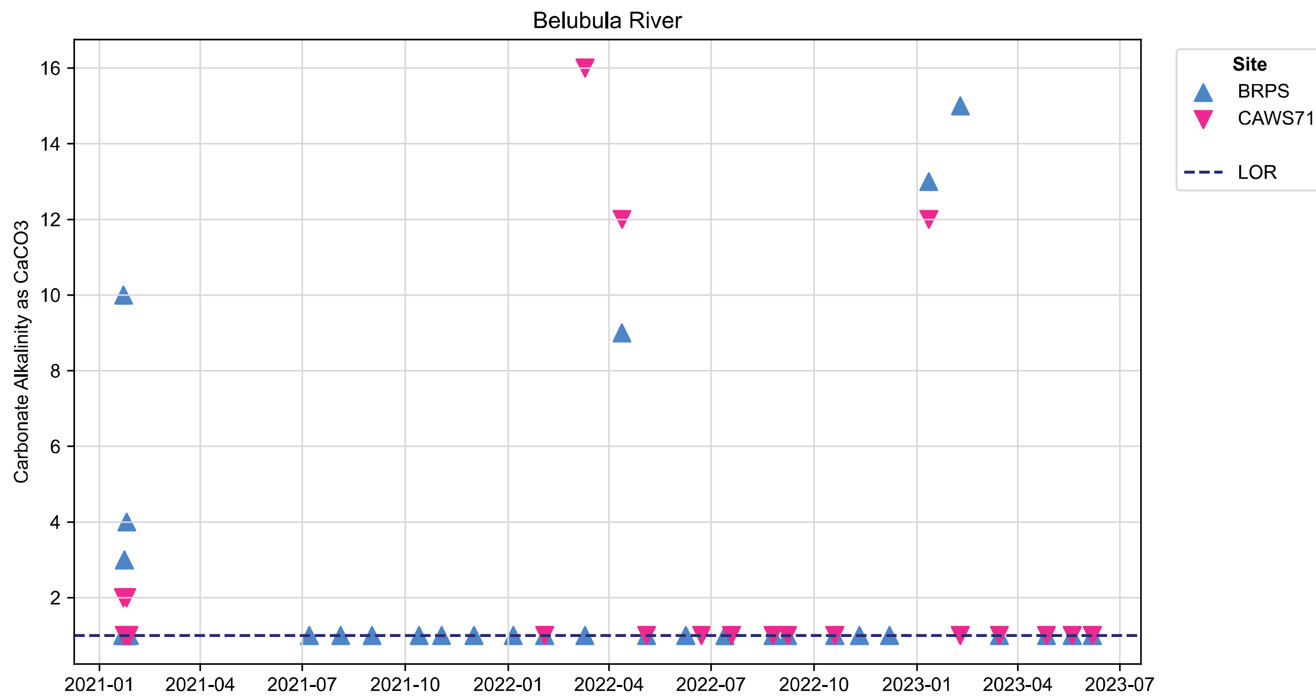

Belubula River
Carbonate Alkalinity as CaCO3
16
14
12
10
8
6
4
2
2021-01
2021-04
2021-07
2021-10
2022-01
2022-04
2022-07
2022-10
2023-01
2023-04
2023-07
Site
BRPS
CAWS71
LOR

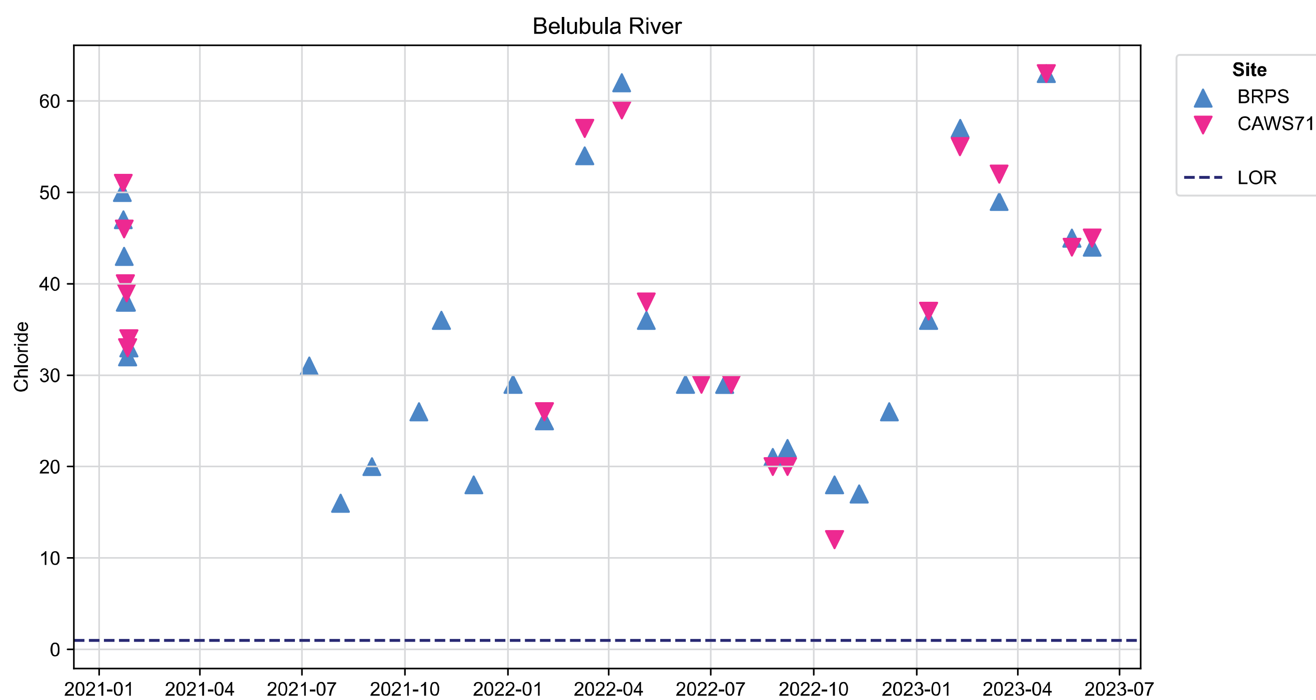

Belubula River
Chloride
60
50
40
30
20
10
0
2021-01
2021-04
2021-07
2021-10
2022-01
2022-04
2022-07
2022-10
2023-01
2023-04
2023-07
Site
BRPS
CAWS71
LOR

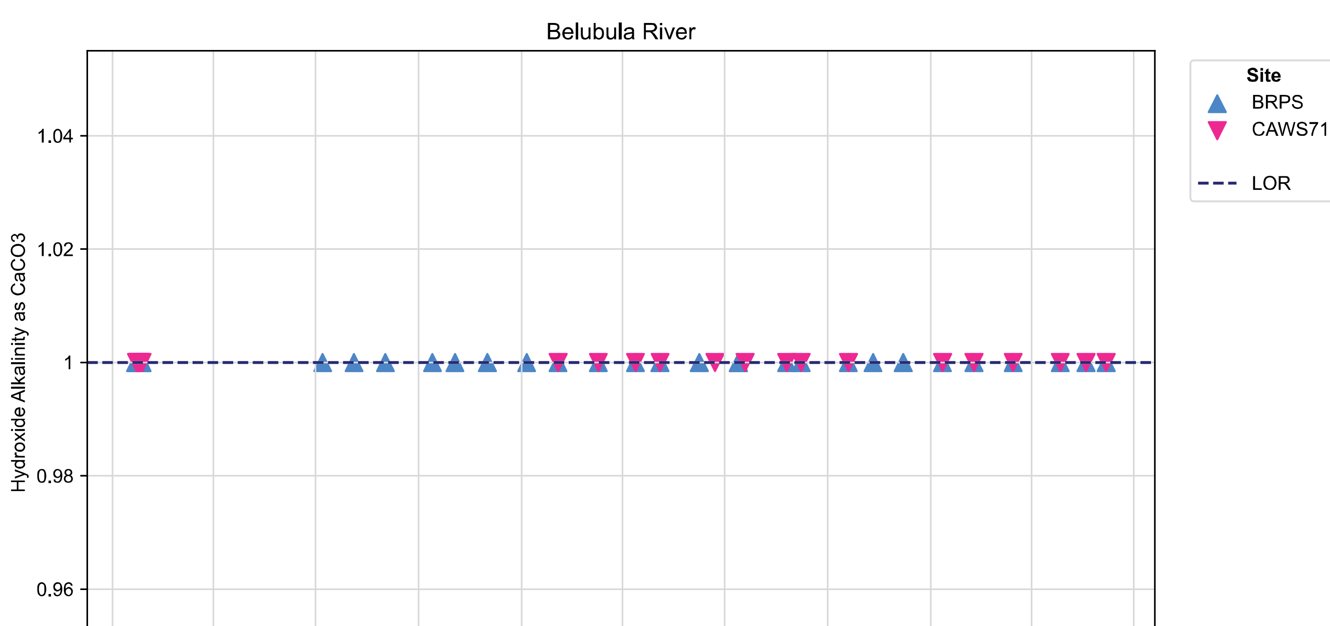

Belubula River
Hydroxide Alkalinity as CaCO3
1.04
1.02
1
0.98
0.96
Site
BRPS
CAWS71
LOR

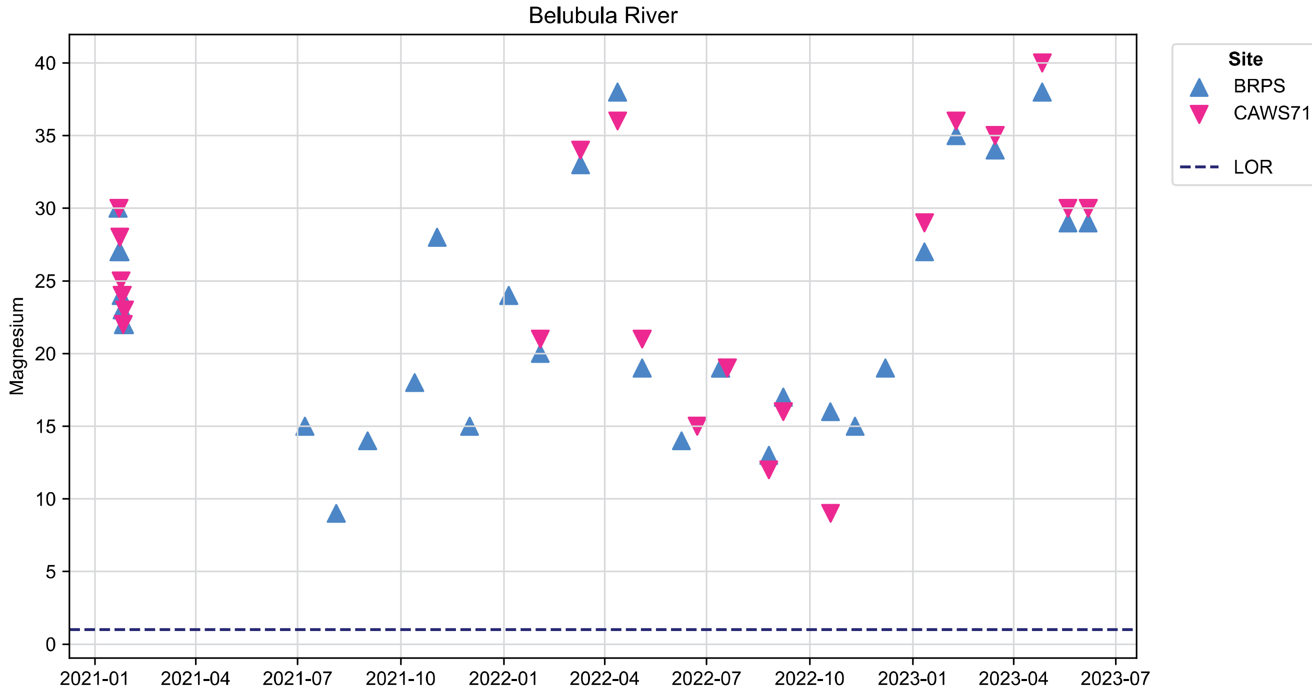
Belubula River
Magnesium
Site
BRPS
CAWS71
LOR
2021-01
2021-04
2021-07
2021-10
2022-01
2022-04
2022-07
2022-10
2023-01
2023-04
2023-07

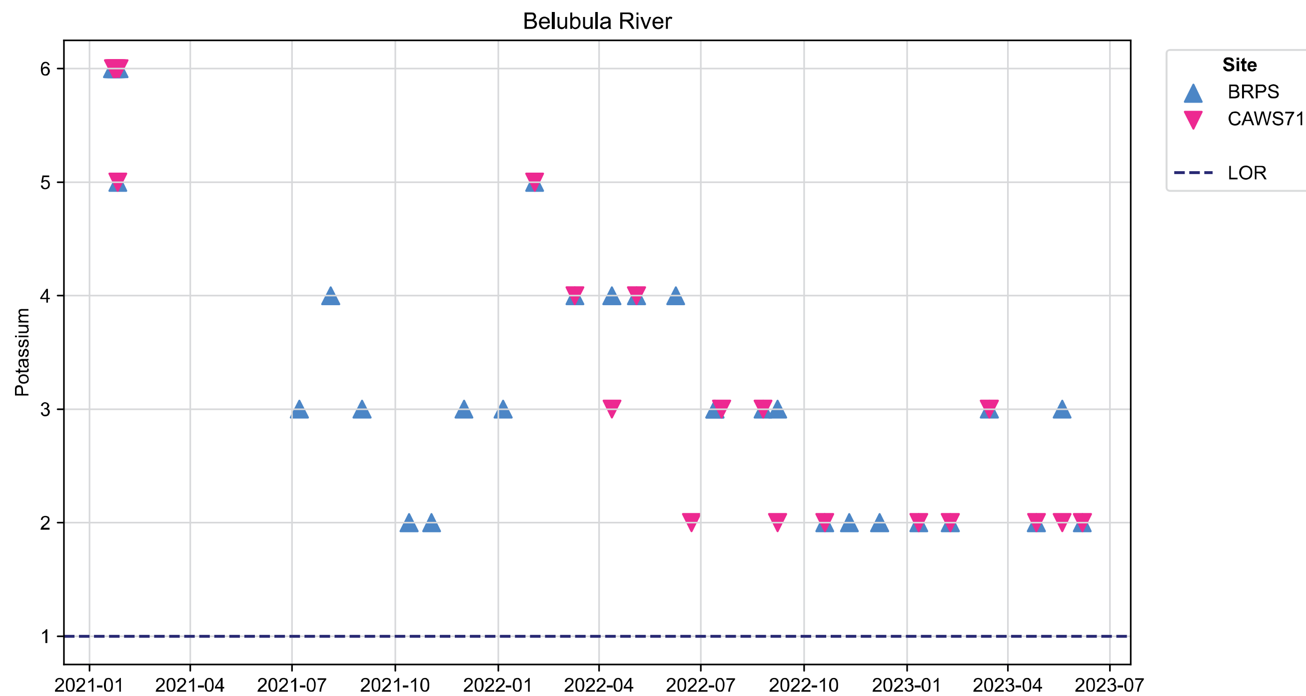
Belubula River
Potassium
Site
BRPS
CAWS71
LOR
2021-01
2021-04
2021-07
2021-10
2022-01
2022-04
2022-07
2022-10
2023-01
2023-04
2023-07

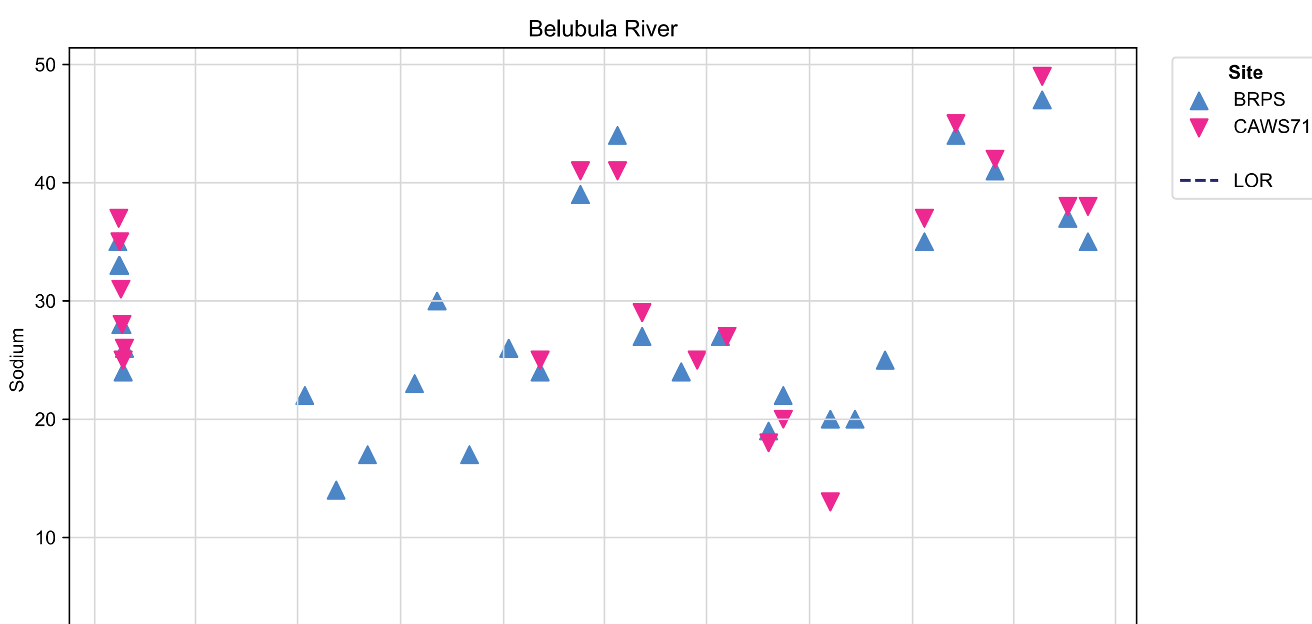
Belubula River
Sodium
Site
BRPS
CAWS71
LOR

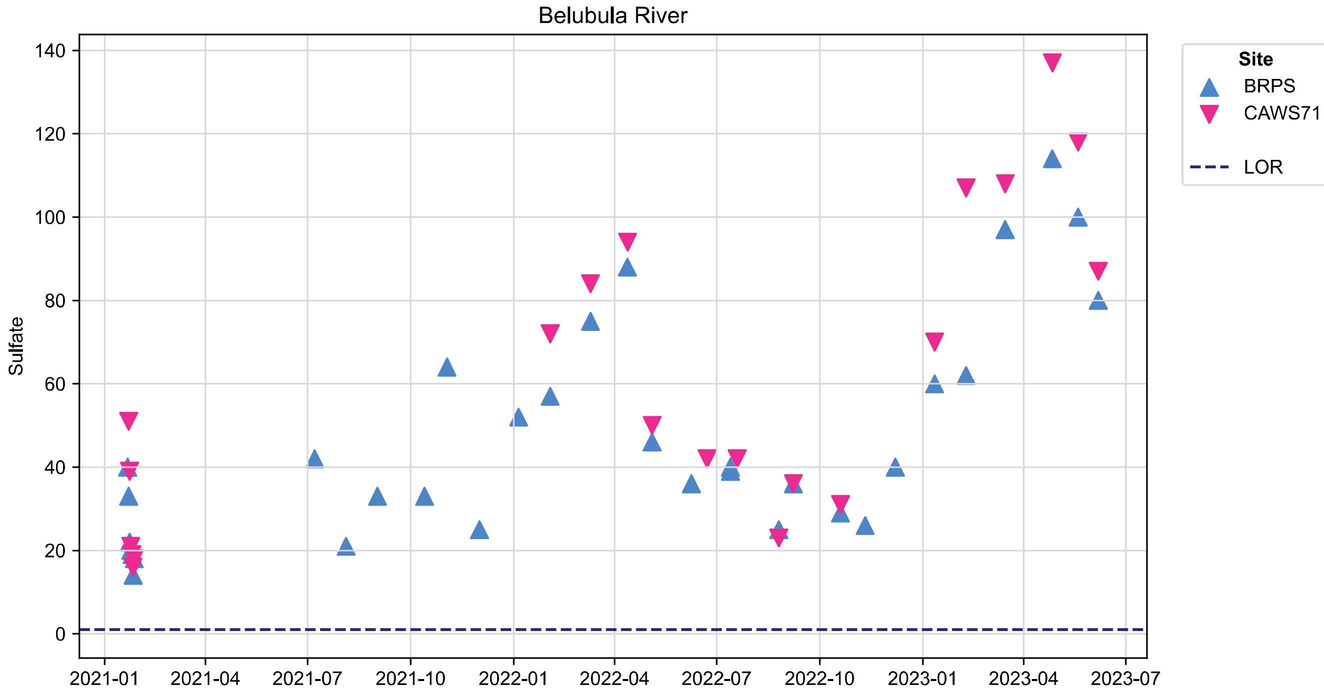

Belubula River
Sulfate
140
120
100
80
60
40
20
0
2021-01
2021-04
2021-07
2021-10
2022-01
2022-04
2022-07
2022-10
2023-01
2023-04
2023-07
Site
BRPS
CAWS71
LOR

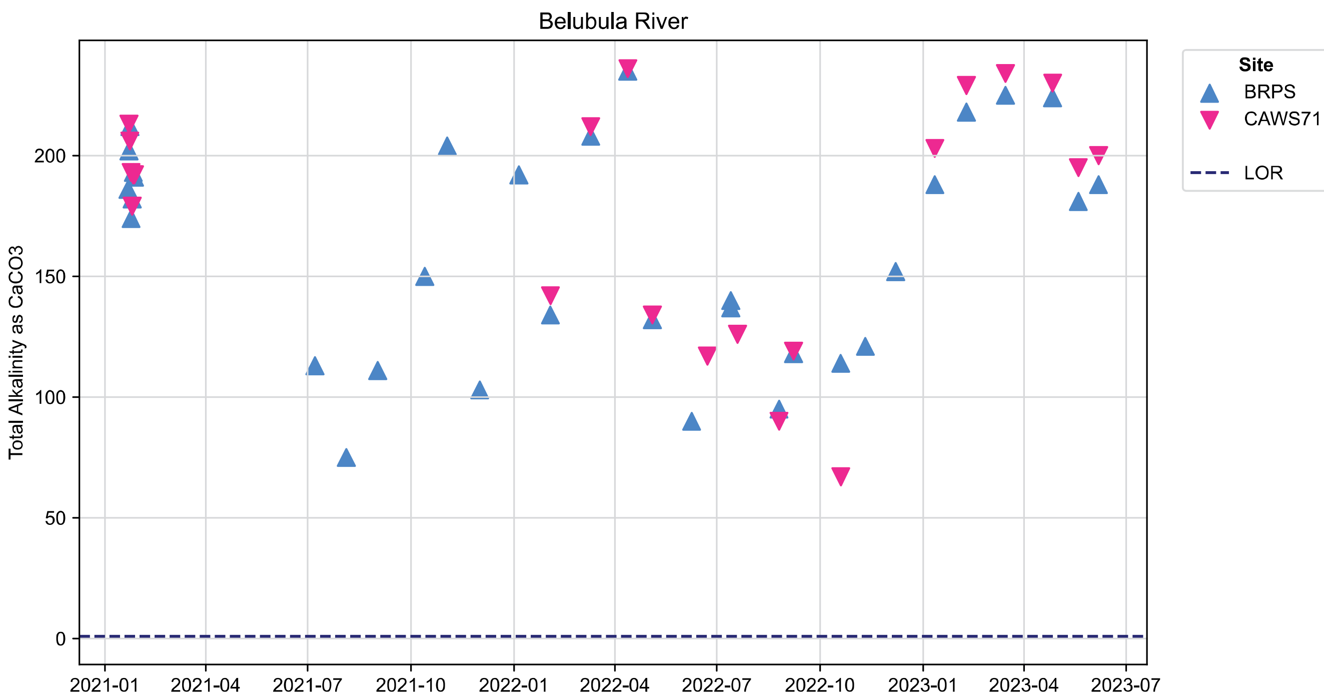

Belubula River
Total Alkalinity as CaCO3
200
150
100
50
0
2021-01
2021-04
2021-07
2021-10
2022-01
2022-04
2022-07
2022-10
2023-01
2023-04
2023-07
Site
BRPS
CAWS71
LOR

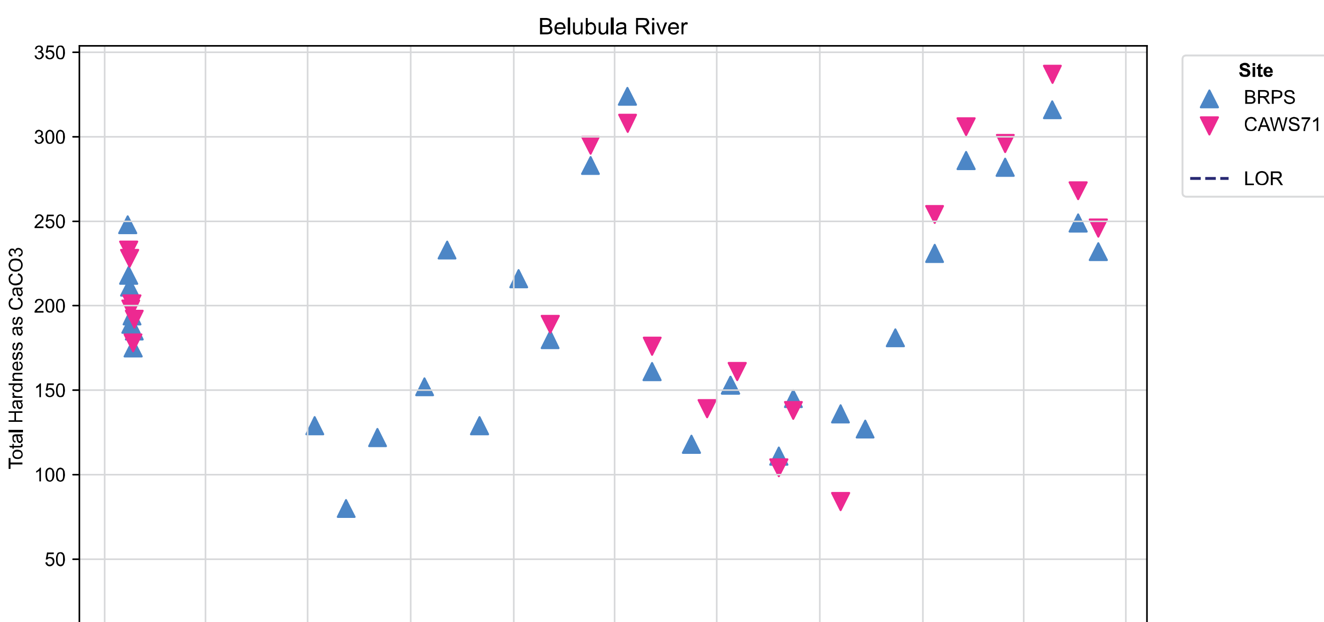

Belubula River
Total Hardness as CaCO3
350
300
250
200
150
100
50
Site
BRPS
CAWS71
LOR

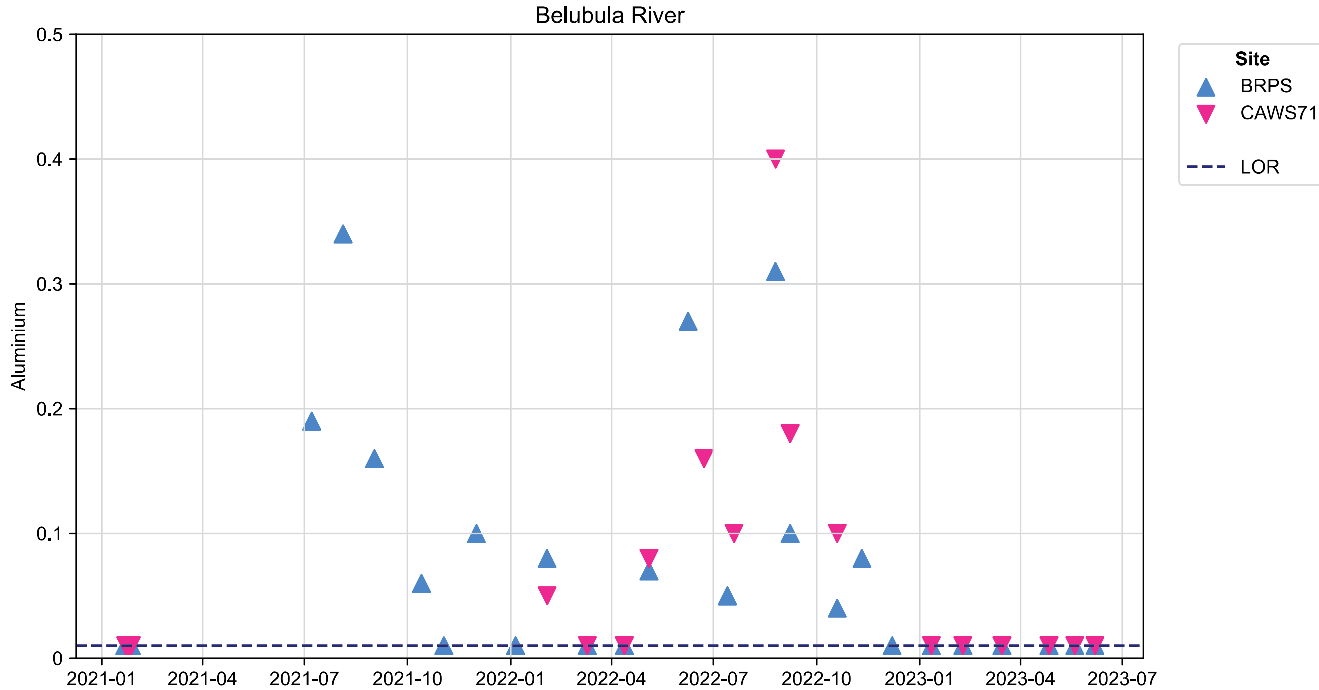
Belubula River
Aluminium
0.5
0.4
0.3
0.2
0.1
0
2021-01
2021-04
2021-07
2021-10
2022-01
2022-04
2022-07
2022-10
2023-01
2023-04
2023-07
Site
BRPS
CAWS71
LOR

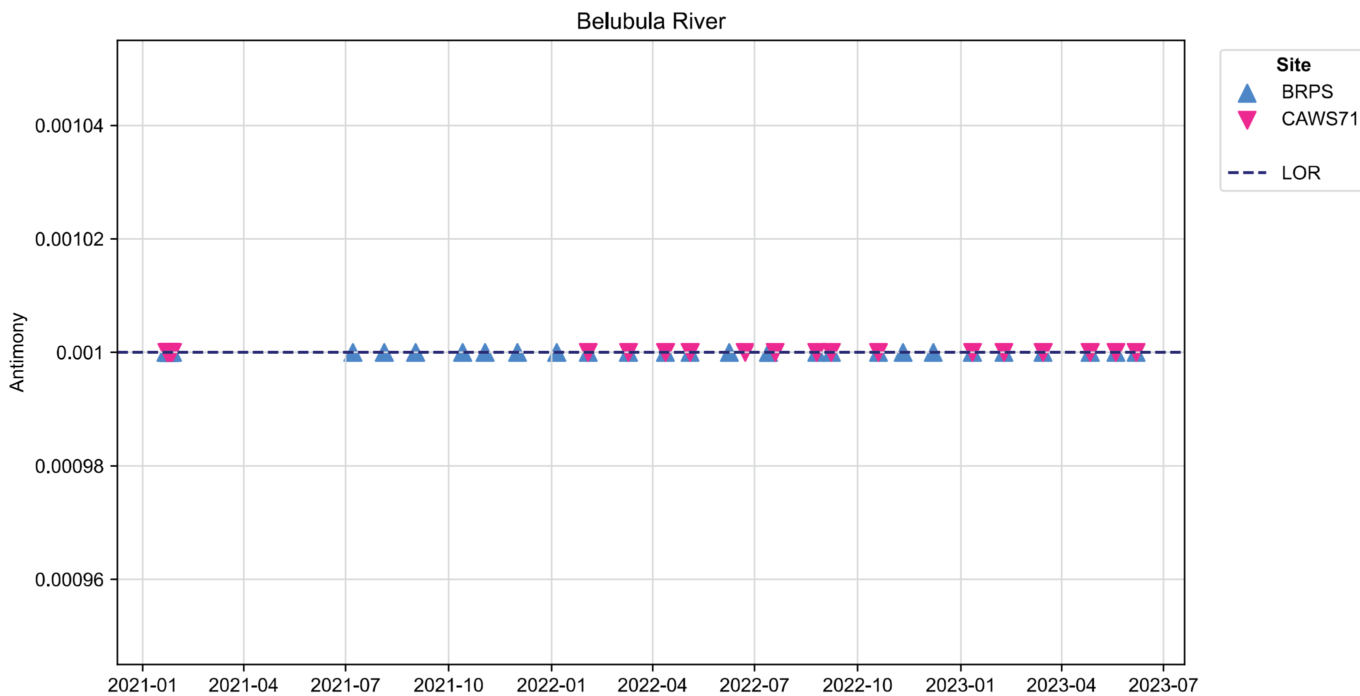
Belubula River
Antimony
0.00104
0.00102
0.001
0.00098
0.00096
2021-01
2021-04
2021-07
2021-10
2022-01
2022-04
2022-07
2022-10
2023-01
2023-04
2023-07
Site
BRPS
CAWS71
LOR

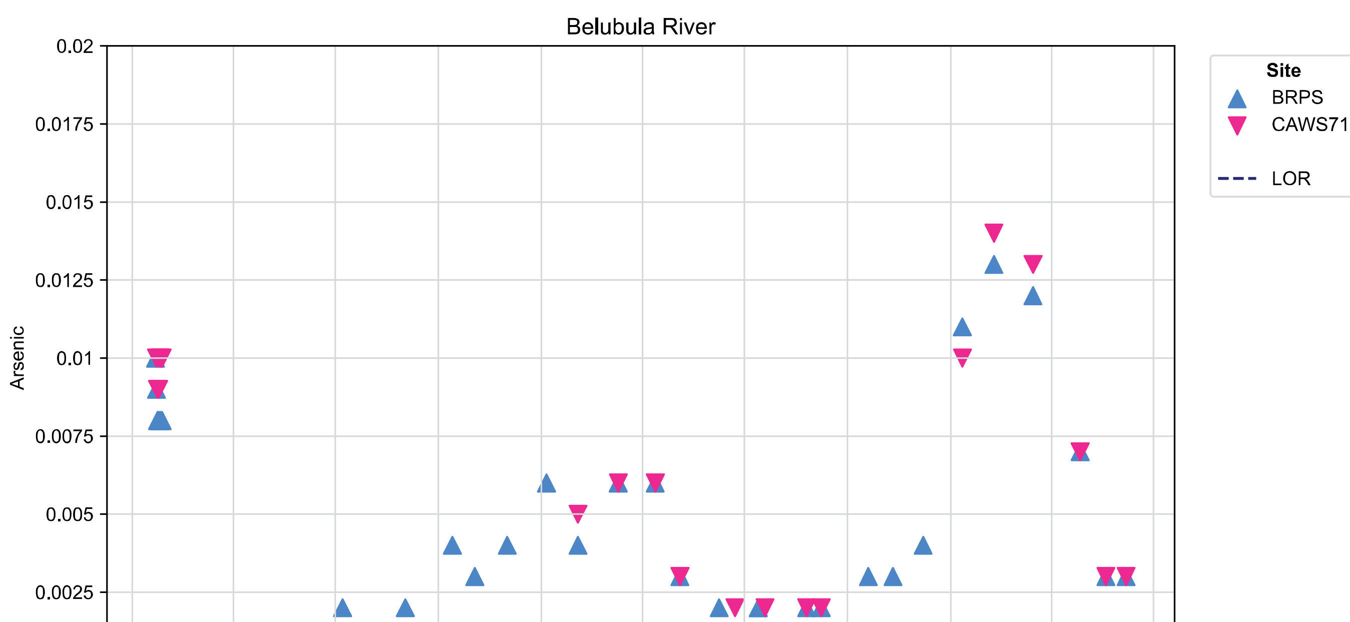
Belubula River
Arsenic
0.02
0.0175
0.015
0.0125
0.01
0.0075
0.005
0.0025
Site
BRPS
CAWS71
LOR

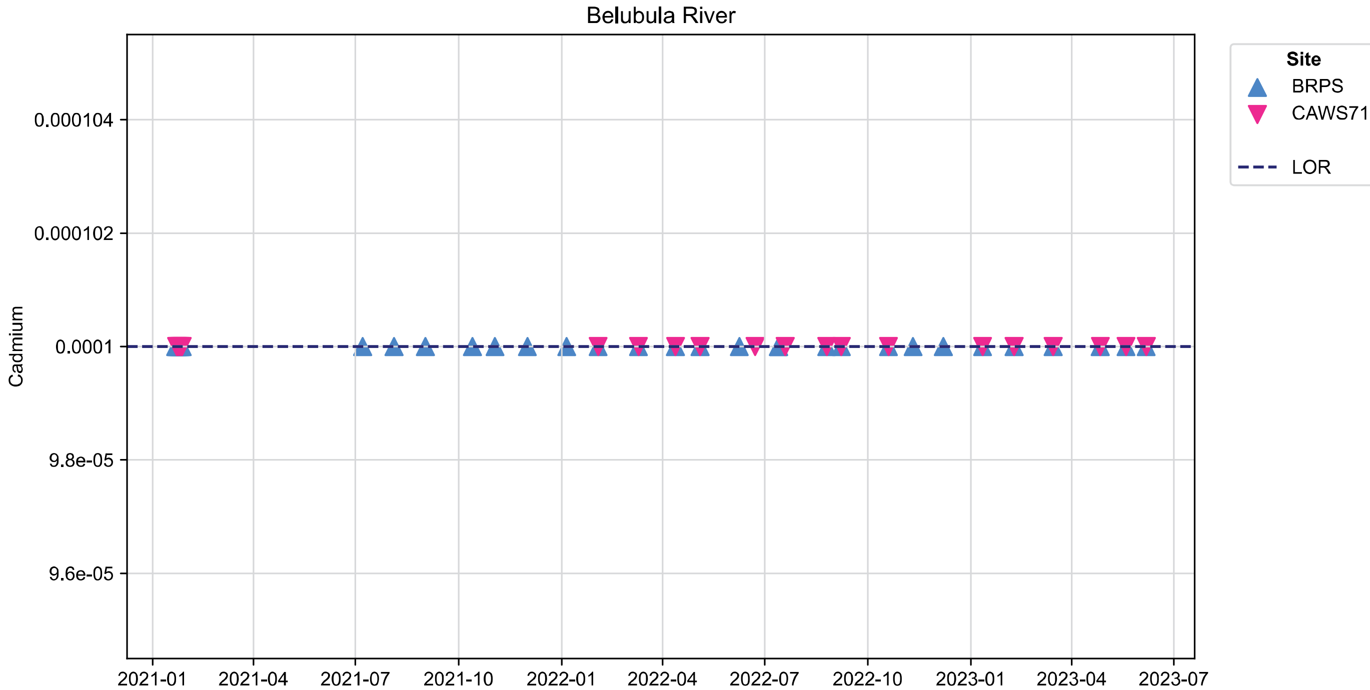
Belubula River
Cadmium
0.000104
0.000102
0.0001
9.8e-05
9.6e-05
2021-01
2021-04
2021-07
2021-10
2022-01
2022-04
2022-07
2022-10
2023-01
2023-04
2023-07
Site
BRPS
CAWS71
LOR

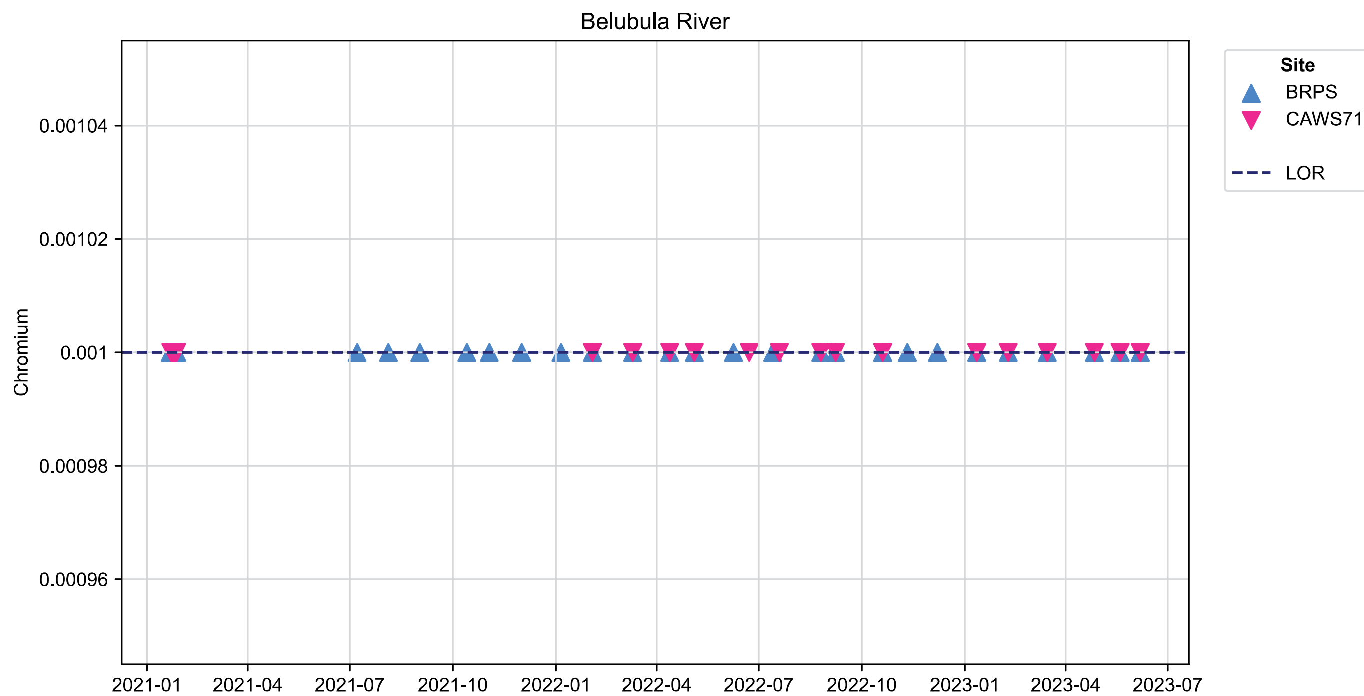
Belubula River
Chromium
0.00104
0.00102
0.001
0.00098
0.00096
2021-01
2021-04
2021-07
2021-10
2022-01
2022-04
2022-07
2022-10
2023-01
2023-04
2023-07
Site
BRPS
CAWS71
LOR

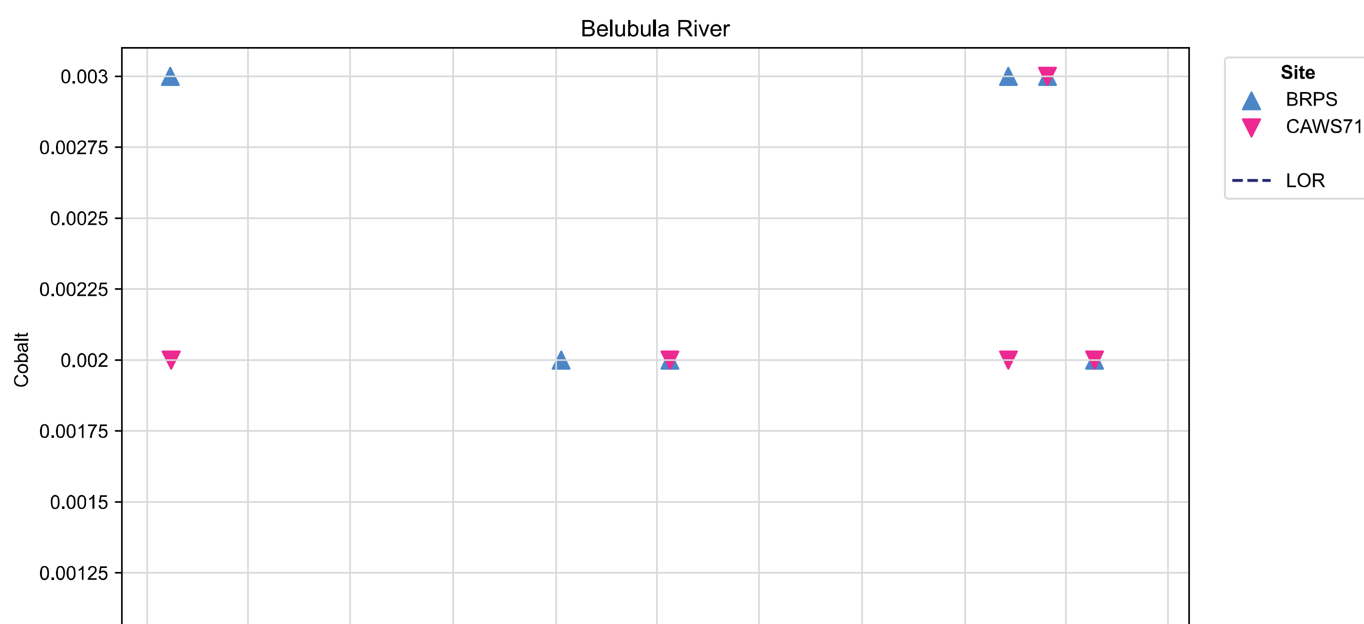
Belubula River
Cobalt
0.003
0.00275
0.0025
0.00225
0.002
0.00175
0.0015
0.00125
Site
BRPS
CAWS71
LOR

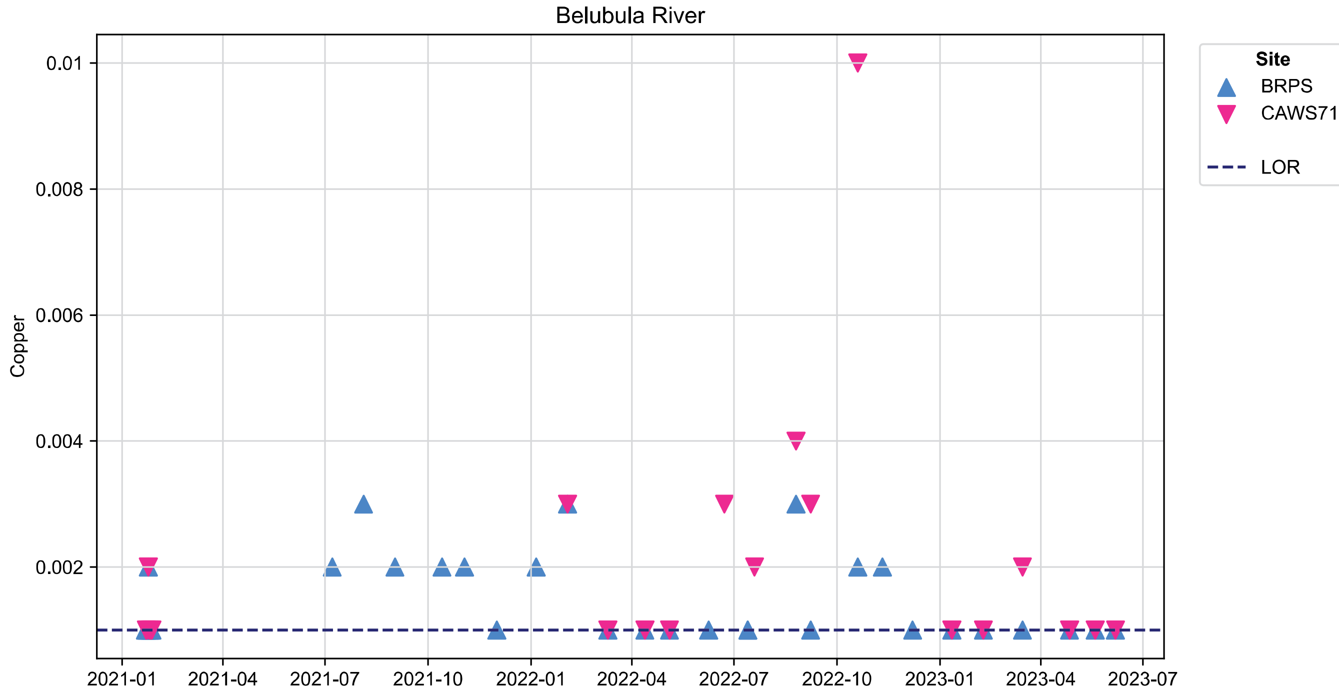
Belubula River
Copper
0.01
0.008
0.006
0.004
0.002
2021-01
2021-04
2021-07
2021-10
2022-01
2022-04
2022-07
2022-10
2023-01
2023-04
2023-07
Site
BRPS
CAWS71
LOR

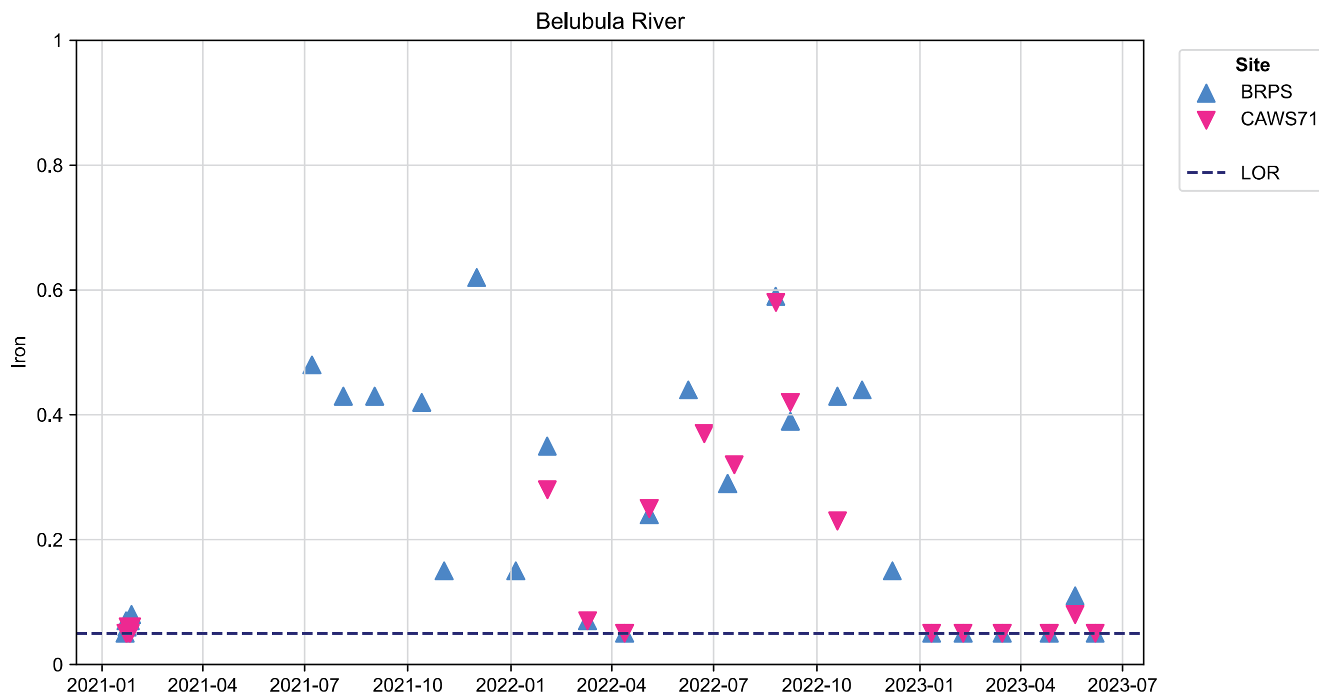
Belubula River
Iron
1
0.8
0.6
0.4
0.2
0
2021-01
2021-04
2021-07
2021-10
2022-01
2022-04
2022-07
2022-10
2023-01
2023-04
2023-07
Site
BRPS
CAWS71
LOR

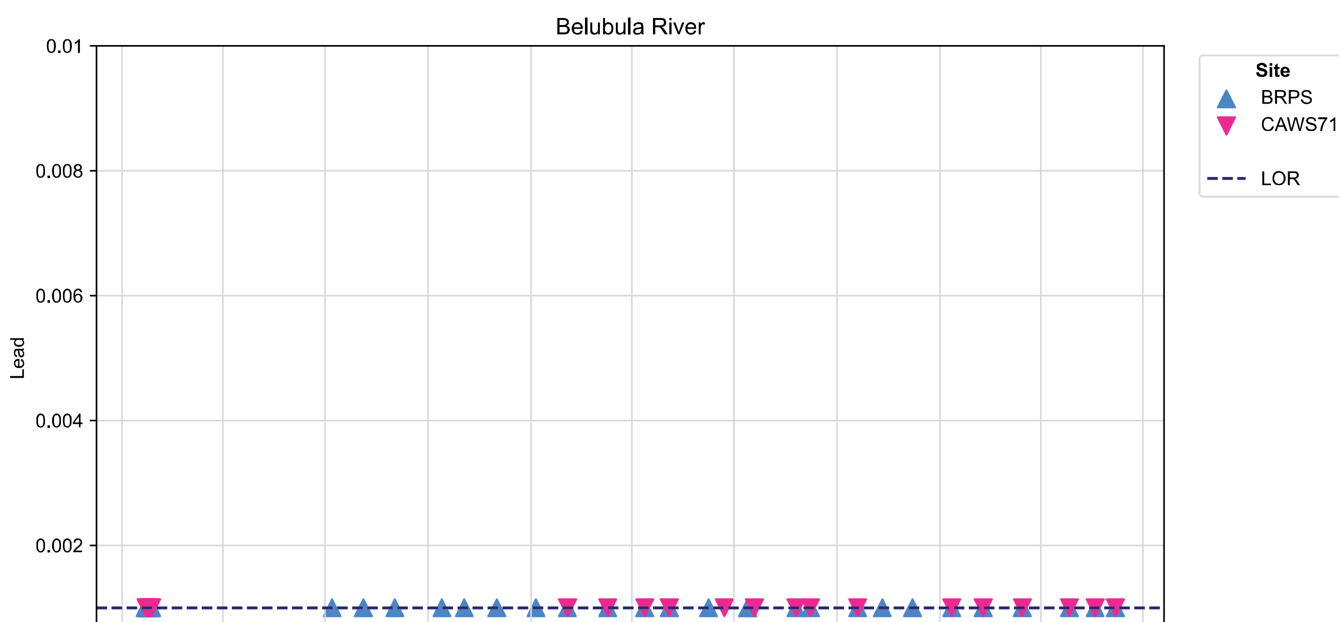
Belubula River
Lead
0.01
0.008
0.006
0.004
0.002
Site
BRPS
CAWS71
LOR

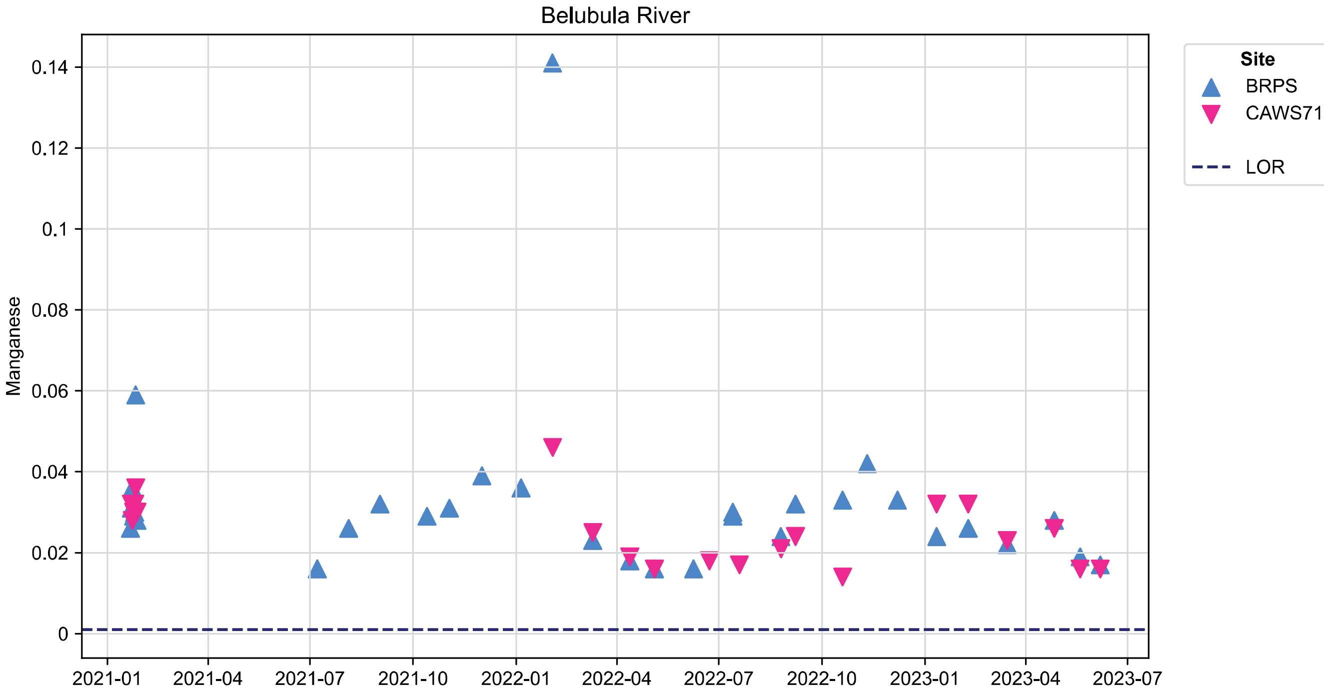
Belubula River
Manganese
0.14
0.12
0.1
0.08
0.06
0.04
0.02
0
2021-01
2021-04
2021-07
2021-10
2022-01
2022-04
2022-07
2022-10
2023-01
2023-04
2023-07
Site
BRPS
CAWS71
LOR

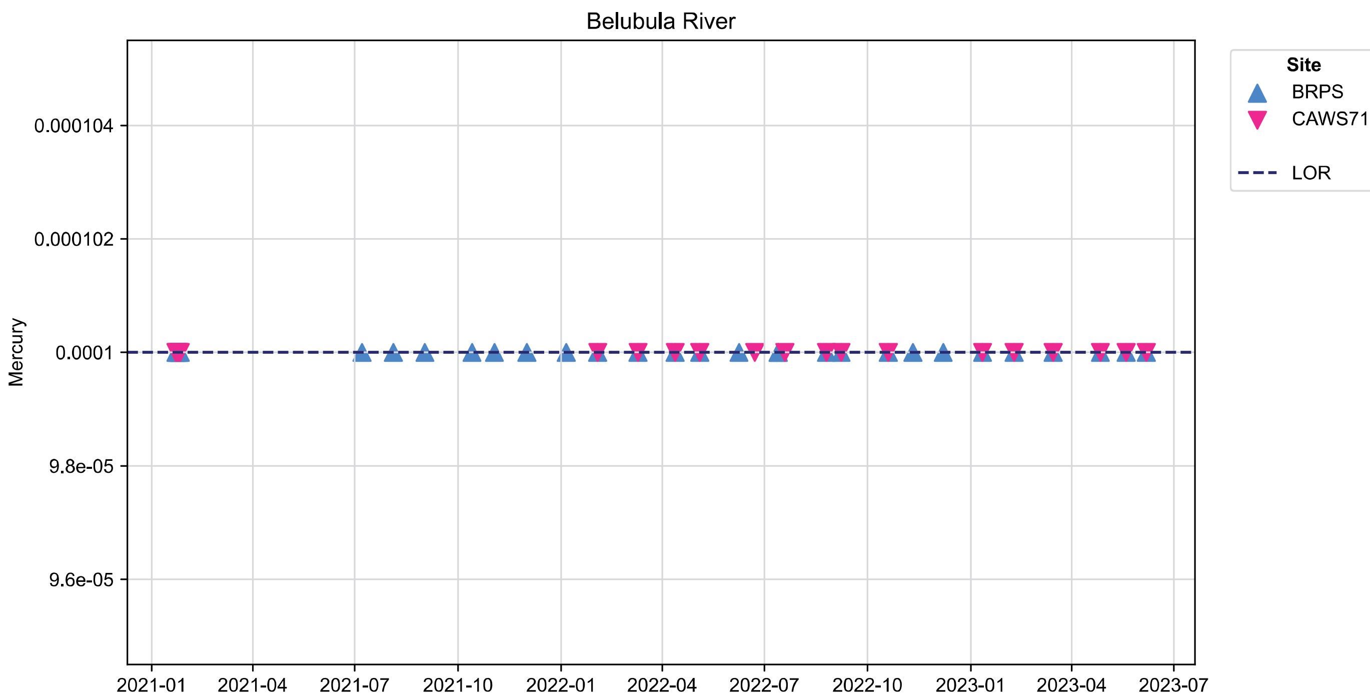
Belubula River
Mercury
0.000104
0.000102
0.0001
9.8e-05
9.6e-05
2021-01
2021-04
2021-07
2021-10
2022-01
2022-04
2022-07
2022-10
2023-01
2023-04
2023-07
Site
BRPS
CAWS71
LOR

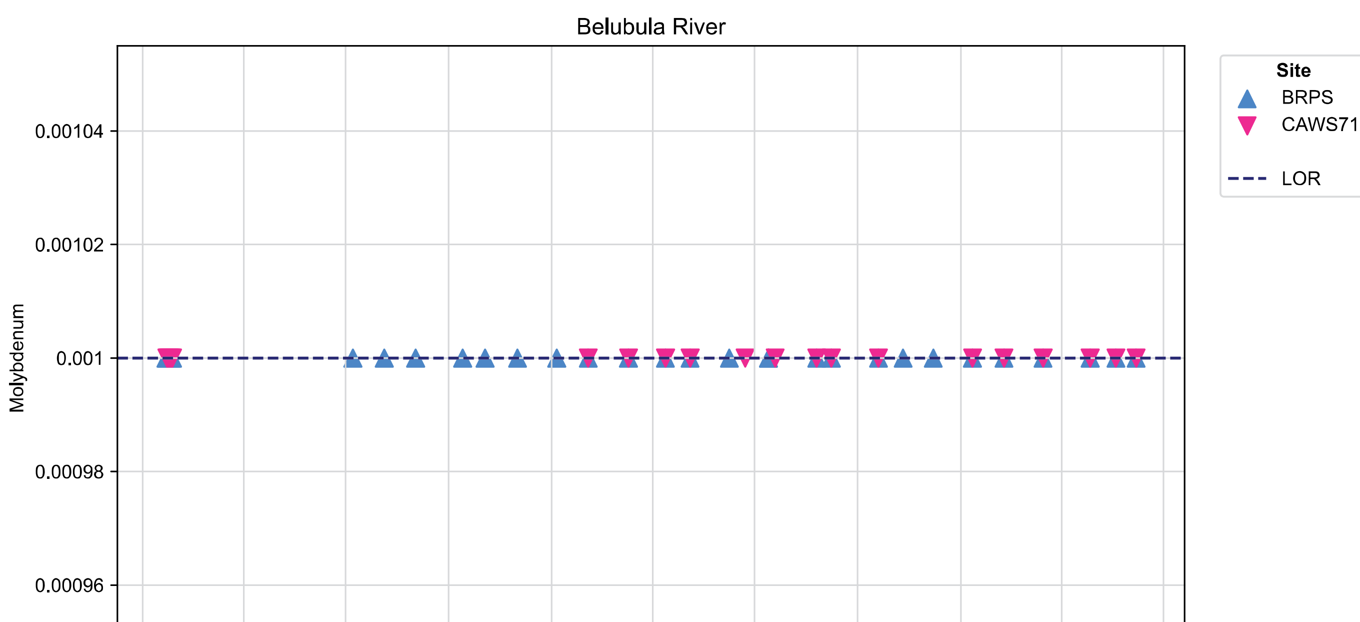
Belubula River
Molybdenum
0.00104
0.00102
0.001
0.00098
0.00096
Site
BRPS
CAWS71
LOR

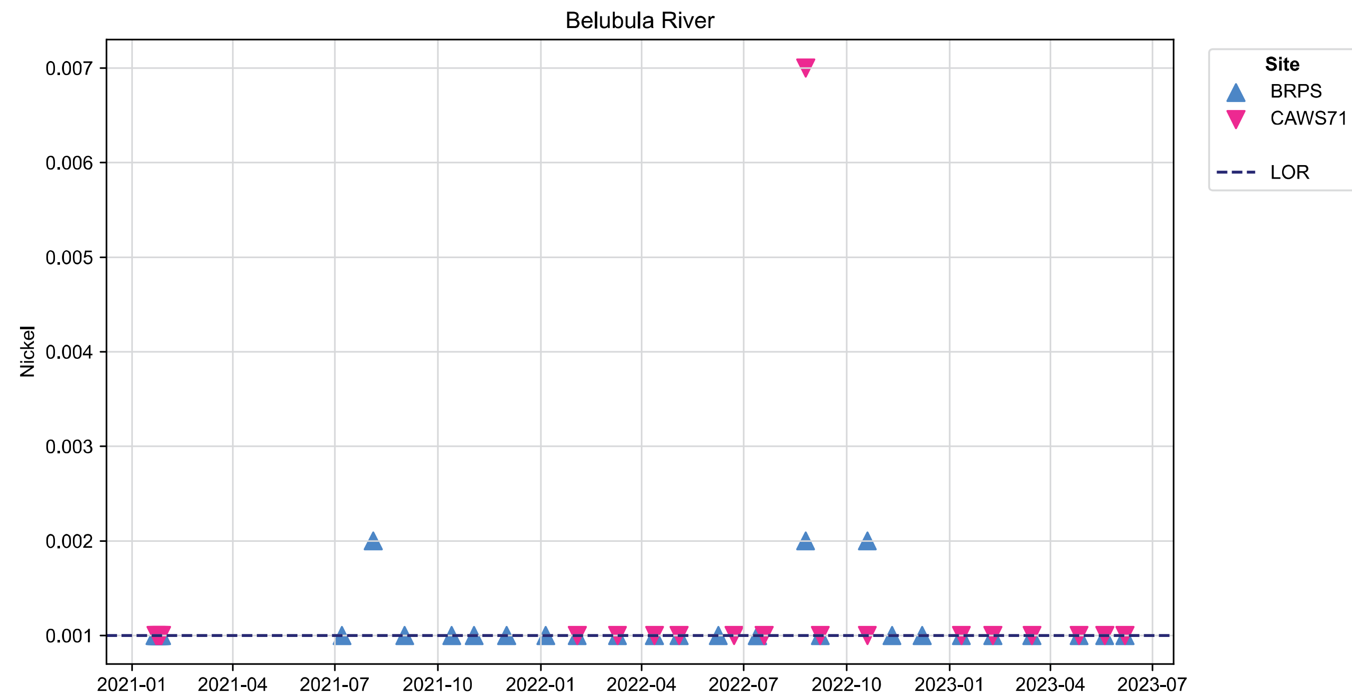
Belubula River
Nickel
0.007
0.006
0.005
0.004
0.003
0.002
0.001
2021-01
2021-04
2021-07
2021-10
2022-01
2022-04
2022-07
2022-10
2023-01
2023-04
2023-07
Site
BRPS
CAWS71
LOR

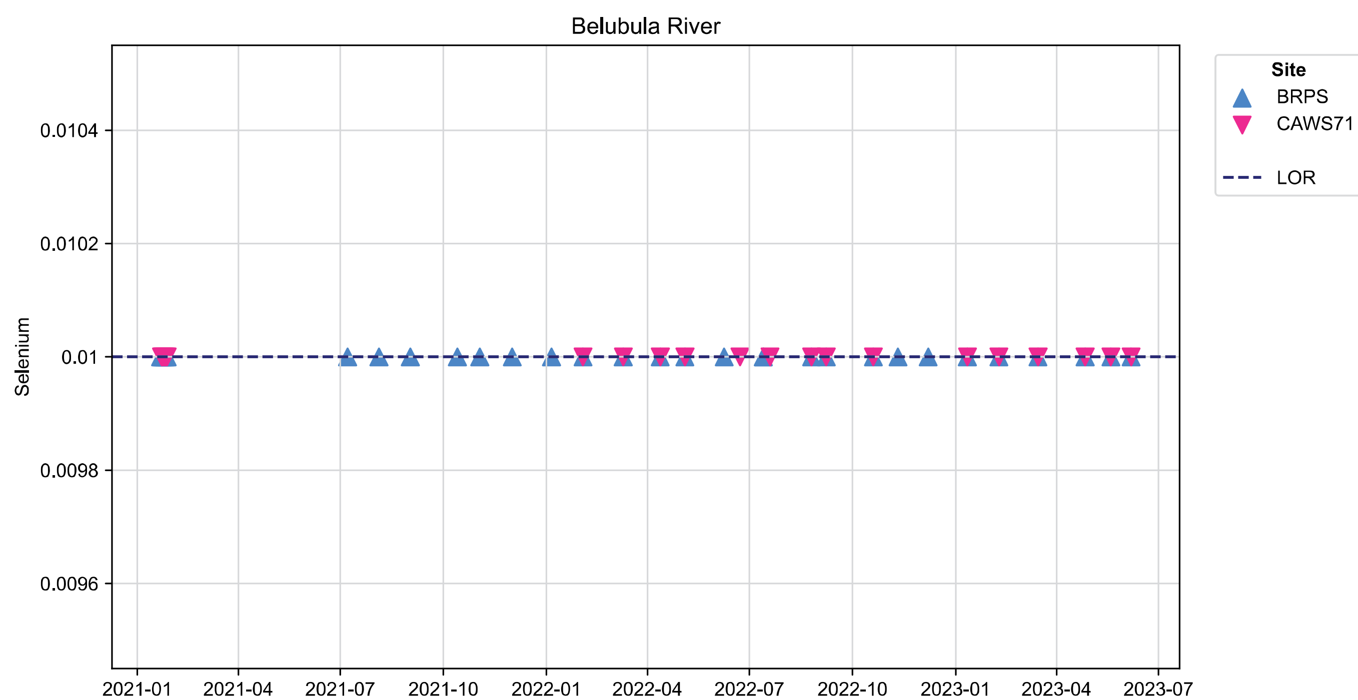
Belubula River
Selenium
0.0104
0.0102
0.01
0.0098
0.0096
2021-01
2021-04
2021-07
2021-10
2022-01
2022-04
2022-07
2022-10
2023-01
2023-04
2023-07
Site
BRPS
CAWS71
LOR

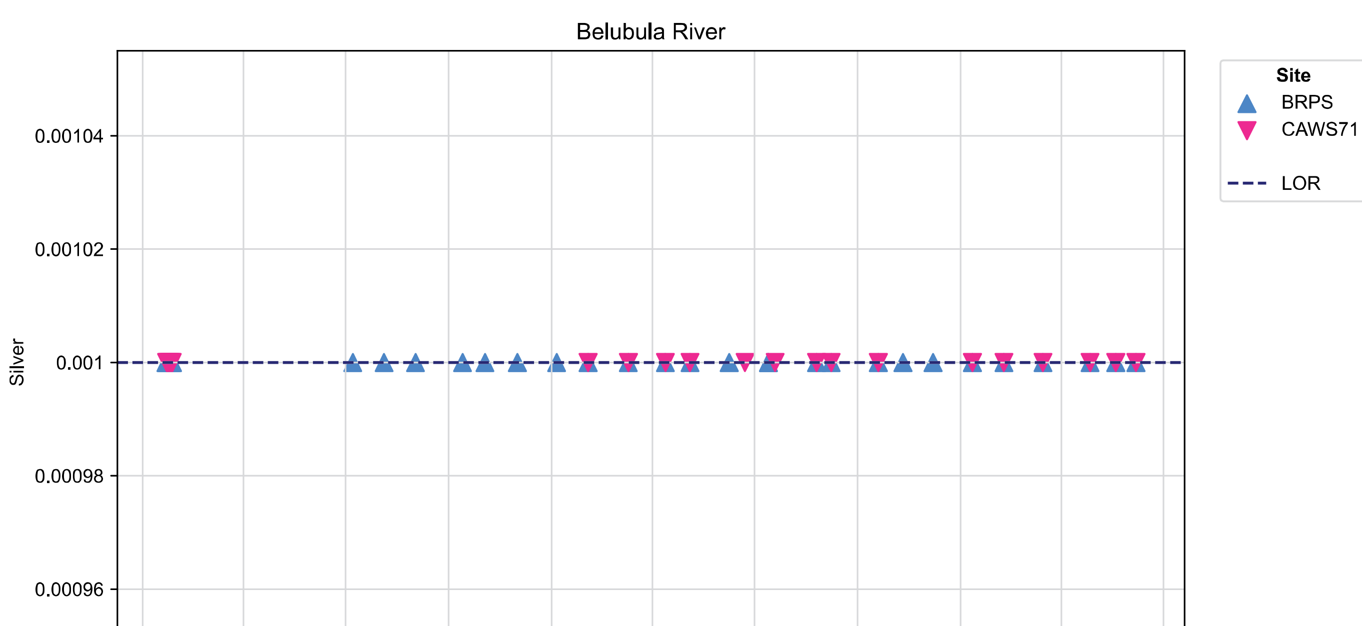
Belubula River
Silver
0.00104
0.00102
0.001
0.00098
0.00096
Site
BRPS
CAWS71
LOR

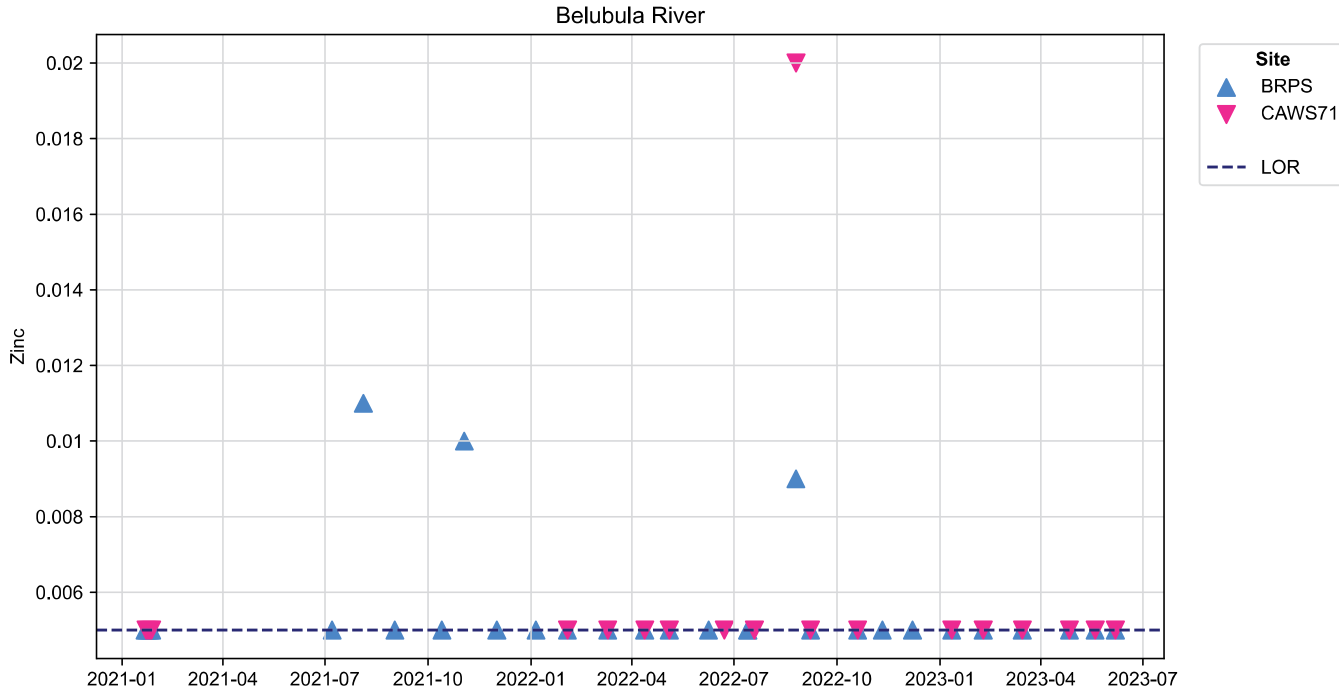

Belubula River
Zinc
0.02
0.018
0.016
0.014
0.012
0.01
0.008
0.006
2021-01
2021-04
2021-07
2021-10
2022-01
2022-04
2022-07
2022-10
2023-01
2023-04
2023-07
Site
BRPS
CAWS71
LOR

Project name	Cadia surface water assessment						
Document title	Report | Cadia surface water assessment - Belubula River						
Project number	12640002						
File name	12640002-REP_Cadia Belubula River surface water assessment.docx						
Status Code	Revision	Author	Reviewer		Approved for issue		
			Name	Signature	Name	Signature	Date
S4	0	T. Hopwood	S. Gray		S. Gray		10/05/24
S4	1	T. Hopwood	S. Gray		S. Gray		15/05/24
S4	2	T. Hopwood	S. Gray		S. Gray		24/05/24

GHD Pty Ltd | ABN 39 008 488 373
Contact: Tegan Hopwood, Senior Aquatic Ecologist | GHD

CCSN - Appendix 5i

Environmental Research 225 (2023) 115518

Contents lists available at ScienceDirect

Environmental Research

journal homepage: www.elsevier.com/locate/envres

Spatio-temporal trends in livestock exposure to per- and polyfluoroalkyl substances (PFAS) inform risk assessment and management measures

Antti T. Mikkonen[a,b,*], Jennifer Martin[b,f], Richard N. Upton[a], Andrew O. Barker[c], Carolyn M. Brumley[b,f], Mark P. Taylor[b], Lorraine Mackenzie[a,d], Michael S. Roberts[a,e]

[a] University of South Australia, Clinical and Health Sciences, Adelaide, South Australia, Australia
[b] Environment Protection Authority Victoria, Centre for Applied Sciences, Macleod, Victoria, Australia
[c] Senversa L6, 15 William St, Melbourne, Victoria, Australia
[d] Basil Hetzel Institute for Translational Health Research, The Queen Elizabeth Hospital, Woodville South, South Australia, Australia
[e] University of Queensland, Diamantina Institute, Queensland, Australia
[f] Arcadis L18, Queen & Collins Tower, 376–390 Collins Street, Melbourne, VIC, Australia

ARTICLE INFO

Handling Editor: Jose L Domingo

Keywords:
Perfluorooctane sulfonate (PFOS)
Perfluorohexane sulfonate (PFHxS)
Livestock
Dynamic exposure
Risk assessment
Risk management

ABSTRACT

The migration of per- and polyfluoroalkyl substances (PFAS) onto agricultural properties has resulted in the accumulation of PFAS in livestock. The environmental determinants of PFAS accumulation in livestock from the grazing environment are poorly understood, resulting in limited capacity to manage livestock exposure and subsequent transfer of PFAS through the food chain. Analytical- ($n = 978$ samples of soil, water, pasture, and serum matrices), farm management/practice- and livestock physiology data were collated and interrogated from environmental PFAS investigations across ten farms, from four agro-ecological regions of Victoria (Australia). Statistical analysis identified perfluorooctane sulfonate (PFOS) and perfluorohexane sulfonate (PFHxS) as key analytes of concern for livestock bioaccumulation. PFOS and PFHxS concentrations in livestock drinking water were positively correlated with serum concentrations while other intake pathways (pasture and soil) had weaker correlations. Seasonal trends in PFAS body burden (serum concentrations) were identified and suggested to be linked to seasonal grazing behaviours and physiological water requirements. The data showed for the first time that livestock exposure to PFAS is dynamic and with relatively short elimination half-lives, there is opportunity for exposure management. Meat from cattle, grazed on PFAS impacted sites, may exceed health-based guideline values for PFAS, especially for markets with low limits (like the European Commission Maximum Limits or EC MLs). This study found that sites with mean livestock drinking water concentrations as low as 0.003 μg PFOS/L may exceed the EC ML for PFOS in cattle meat. Risk assessment can be used to prioritise site cleanup and development of management plans to reduce PFAS body burden by considering timing of stock rotation and/or supplementation of primary exposure sources.

1. Introduction

Per- and polyfluoroalkyl substances (PFAS) are a group of synthetic compounds manufactured since the early 1940s (Buck et al., 2011). They have been used extensively across different industries with hundreds of documented use categories for some 1400 compounds (Glüge et al., 2020). The migration of these compounds onto agricultural properties has resulted in their accumulation of in livestock (Death et al., 2021).

Although the grouping "PFAS" consists of a large number of individual chemicals with distinct physical and chemical properties, most of the information published on health effects pertain to legacy PFAS of the perfluoroalkyl carboxylate- (PFCAs) and perfluoroalkane sulfonate groups (PFSAs) which include perfluorooctanoic acid (PFOA) and perfluorooctane sulfonate (PFOS) respectively (Fenton et al., 2020; ATSDR, 2018; EFSA, 2020). PFOS and PFOA have been the focus of much research due to their prolific historical use, their ubiquitous presence in the environment and rapidly growing associations with health effects (Rogers et al., 2021). One key historical source of PFAS to the environment (especially PFOS) is aqueous film forming foams (AFFF) which have been widely used to contain and control Class B fires (OECD, 2021). Firefighting and training activities with AFFF products have

* Corresponding author. University of South Australia, Clinical and Health Sciences, Adelaide, South Australia, Australia.
E-mail address: antti.mikkonen@epa.vic.gov.au (A.T. Mikkonen).

https://doi.org/10.1016/j.envres.2023.115518
Received 7 September 2022; Received in revised form 26 January 2023; Accepted 15 February 2023
Available online 24 February 2023

Table 1
Summary of data sources and grouping.

Region ID[a]	Site ID	Distance to PFAS source (km)[b]	Environmental and biomonitoring PFAS data (# sampling rounds)						Primary DW source[d]	Stock rotation[e]
			Surface water[c]	Drinking trough	Soil	Grass	Cattle	Sheep		
A	A1	0.50	×	✓(4)	✓(1)	✓(1)	✓(3)	✓(1)	T[f]	Limited
	A2	1.30	✓(2)	×	✓(1)	✓(1)	✓(1)	✓(1)	SW	Extensive
	A3	0.05	✓(3)	×	✓(1)	✓(1)	×	✓(1)	SW	Limited
	A4	2.40	✓(1)	×	×	×	×	✓(1)	SW	Extensive
B	B1	0.07	✓(3)	×	×	✓(1)	✓(4)	✓(1)	SW	Limited
C	C1	2.00	✓(2)	×	✓(1)	×	✓(1)	✓(1)	SW	Moderate
	C2	6.00	✓(1)	✓(1)	✓(1)	×	✓(1)	✓(1)	SW + T	Extensive
	C3	0.05	✓(1)	✓(2)	✓(1)	×	✓(1)	✓(1)	SW + T	Extensive
	C4	onsite	✓(2)	✓(1)	✓(1)	✓(1)	✓(1)	×	SW + T	Moderate
D	D1	0.14	✓(2)	×	×	×	✓(1)	×	SW	Moderate

[a] Agro-ecological regions (Agriculture Victoria): A = Central Victorian Southern Slopes (temperate climate with mean annual rainfall 500–800 mm), B = Victorian Volcanic Plains (temperate climate with mean annual rainfall 500–700 mm), C = Eastern Plains (temperate climate with mean annual rainfall 550–1120 mm), D = Northern Plains (temperate climate with mean annual rainfall 350–550 mm).

[b] Distance from source site to livestock grazing areas in Km approximated using google maps (measure distance) (Google. Google Maps Victoria Australia, 1895).

[c] Surface water made up of dams, drainage ditches and areas of inundation.

[d] T = trough; SW = surface water; DW = drinking water.

[e] Stock rotation refers to the availability of uncontaminated grazing pasture and drinking water sources and rotation between these sources. “Limited” refers to sites without access to unimpacted pastures or drinking sources, “Moderate” refers to sites with access to several paddocks and drinking water sources with varying levels of PFAS and “Extensive” refers to sites with PFAS impacts confined to few paddocks/drinking water sources (≤25%) and/or a structured rotation practice that involves defined periods without exposure.

[f] Stock trough supplied from a surface water collection dam.

resulted in highly-concentrated and sometimes large-scale (volumes in tons) PFAS releases to the environment (Dorrance et al., 2017; Field et al., 2017; EHP, 2014). Due in part to poor controls for AFFF containment and the mobility and persistence of many of the PFAS (many are not susceptible to biotic or abiotic degradation beyond the dead-end perfluoroalkyl acid transformation products) contained in AFFF, these PFAS releases can lead to far-reaching dispersal from the point of contamination and transfer into plants and animals (Death et al., 2021; Bräunig et al., 2017; Dauchy et al., 2019).

As evidence of PFAS transfer from the environment to food has increased, so too has research and environmental investigations into understanding uptake of PFAS into livestock (Death et al., 2021; Bräunig et al., 2017; Kowalczyk et al., 2012; Kowalczyk et al., 2013; Vestergren et al., 2013; Cardno LanePiper, 2014; Parliament of Victoria, 2016; Zafeiraki et al., 2016; Senversa, 2018; Golder, 2020; Drew et al., 2021a). The transfer of PFAS to edible tissues and milk in livestock creates exposure pathways for their consumers (Death et al., 2021; Dauchy, 2019; Costello and Lee, 2020), and in some countries, impacted farms have been subject to risk based interventions (USDA, 2021).

In Victoria, Australia, the major sources of PFAS release which have resulted in site investigations, has been attributed to the use of AFFF in fire training and firefighting scenarios (based on the experience of the Environment Protection Authority, EPA Victoria). It is noted that other sources with potential to impact agriculture exist, however, sites associated with AFFF use have been more widely investigated in Victoria to date and are thus the focus of this paper.

Environmental assessment of AFFF sites across the State, have shown PFAS migration (from the points of release) to neighboring properties, including farm/grazing land, and PFAS have been reported in livestock as a result (Cardno LanePiper, 2014; Parliament of Victoria, 2016; Senversa, 2018; Golder, 2020).

In 2019–20, approximately 1.8 million adult cattle and 300,000 calves, 3.1 million adult sheep and 10.4 million lambs were processed in Victoria (Agriculture Victoria, 2021). Based on the number of known PFAS source sites with proximity to farming land, the number of animals thought to be impacted by PFAS is considered very low, and consequently exposure of the wider community to PFAS through meat produce is expected to be very low. These observations also reflect the findings of the 27th Australian Total Diet Survey which found that the levels of PFAS in the general food supply are low and acceptable from a public health and safety perspective (FSANZ, 2021). The survey found that out of a suite of 30 analytes, PFOS was the only congener detected and from a total of 112 commonly consumed foods and beverages, PFOS was only detectable in 5 foods (the highest level found in mammalian offal at 0.63 μg/kg) (FSANZ, 2021). While the risk to the general population is considered low, the exposure pattern and market share dilution relevant to the general population may result in an underestimate of exposure to population subgroups that may have higher exposure to PFAS contaminated produce, such as subsistence farmers (enHealth, 2012; U.S. Environmental Protection Agency, 2019).

In Australia, there are no regulatory maximum limits for PFAS in food, with the guidance being that PFAS levels should be kept as low as reasonably achievable (FSANZ, 2021). Health-based guideline values, expressed as tolerable daily intakes, have been derived for the sum of PFOS and PFHxS (20 ng/kg bw/d) and for PFOA (160 ng/kg bw/d) to enable risk assessments for PFAS exposed populations and these were used to develop food produce trigger points (TPs) for investigation at localized contaminated sites in 2016 (FSANZ, 2021). More recently the European Commission released an amendment of Regulation (EC) No 1881/2006 which provides maximum levels (MLs) for perfluoroalkyl substances in some specific food groups including livestock meat and offal (EC, 2022). It is noted there are no exceedances of the MLs for livestock meat or offal from the recent Australian Total Diet Survey (FSANZ, 2021) which reinforces that risk to the general population is considered low and the focus of this paper is on management of localized settings.

Internationally, human health risk assessments for PFAS in meat produce have typically relied on a combination of monitoring (serum) and livestock exposure modelling methods to estimate secondary exposure to consumers. Although several authors have described the uptake, distribution and elimination of PFAS in cattle (Van Asselt et al., 2013; Numata et al., 2014; Drew et al., 2021), exposure pathways and how they relate to the levels of environmental contamination are not well understood.

EPA Victoria has observed several settings in which static approaches to modelling livestock exposure and accumulation of PFAS in serum has resulted in significant over-estimation compared to measured serum concentrations, and in at least one case, underestimation. Challenges in estimating PFAS transfer from the environment to livestock can have subsequent implications for the quality of advice to farmers on the management of livestock exposure. This has led to increased interest in developing understanding of PFAS impacts on livestock farms in a

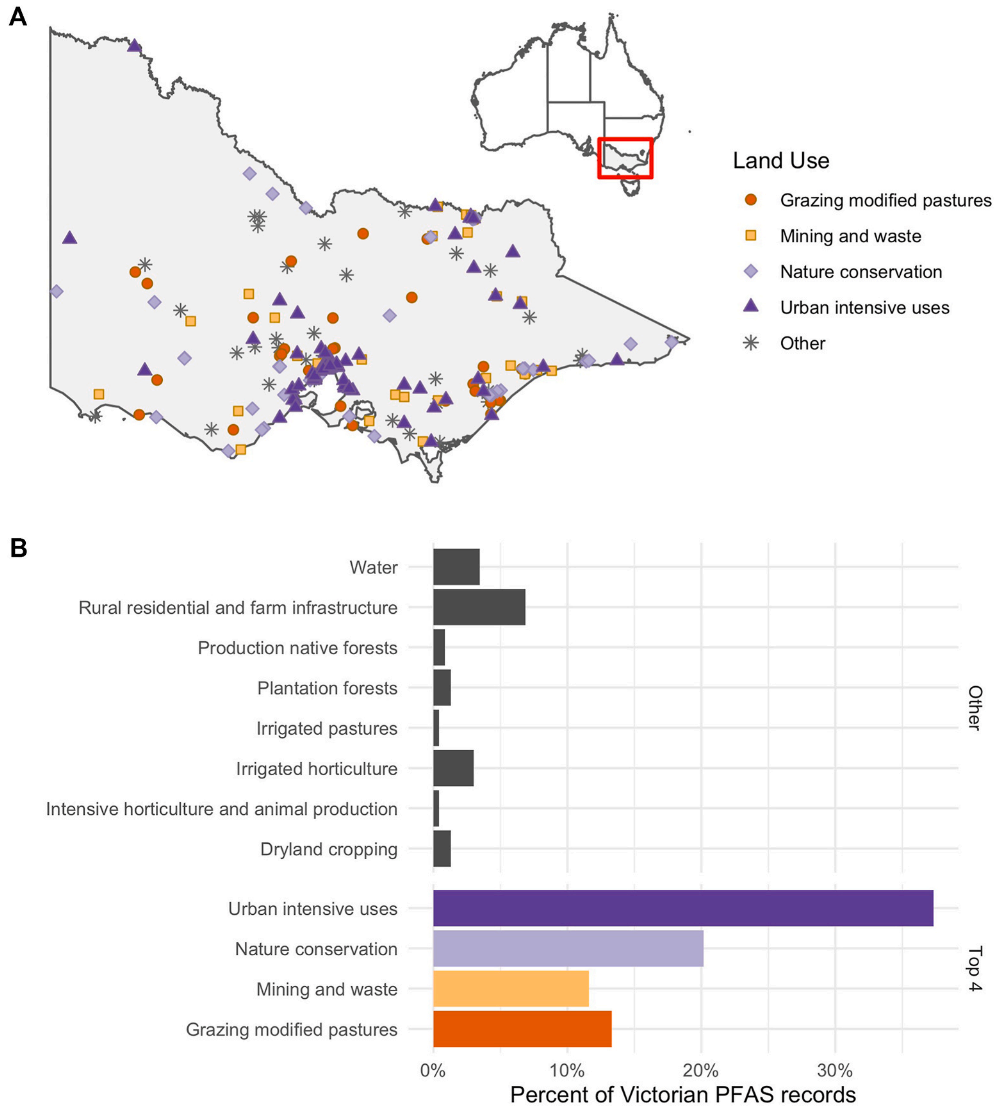

Fig. 1. Representation of known PFAS source sites and surrounding land uses in Victoria (Australia). A) Dots indicate approximate source site locations (Todd, 2021) with colours representing surrounding land-use based on open source datasets (Australian Bureau of Agricultural Resource Economics and Sciences (ABARES), 2021). B) Bar graph representation of surrounding land uses corresponding to each PFAS source site as a percentage of Victorian PFAS records.

wholistic way that can enable proportionate and practical advice to farmers on options to reduce PFAS body burden in their stock, support ongoing farming operations whilst also ensuring exposure to local and home-butchering consumers is kept as low as reasonably practical. The objectives of this study were.

(1) To evaluate which PFAS congeners are of most concern for bioaccumulation in livestock.
(2) To investigate livestock exposure pathways (for grazing livestock) and characterise the determinants of variability in livestock exposure to PFAS to aid risk assessment considerations.
(3) To assess if and how farming practices impact accumulation and what interventions can reduce the body burden of PFAS where livestock have been exposed.

To address these questions, data was compiled and analysed from environmental PFAS investigations undertaken at farms in Victoria, Australia. The anonymized dataset is available for download in supplementary materials. The farms are within four agro-ecological regions of Victoria (Australia) and include PFAS concentrations (for up to 28 analytes) in soil, water, pasture grasses and livestock serum for cattle and sheep, n = 978 all samples, Table 1.

2. Methods

2.1. Study methods

This study involved the following steps: (i) review of environmental investigation reports (for undisclosed agricultural sites) from the study areas to extract PFAS monitoring data for environmental media and livestock; (ii) collation, anonymisation and grouping of data within the study area; (iii) statistical assessment of PFAS concentrations; and (iv) regression analysis to determine the key PFAS exposure pathways for livestock (in the agricultural setting). The methods are further described in the following sections.

2.2. Study area

The study area encompassed PFAS impacted agricultural sites across Victoria, Australia. To keep sites confidential, Fig. 1 provides an overlay of known (reported in public forums) PFAS source sites in Victoria with agricultural land uses, however individual agricultural sites are not

Table 2
Summary of pooled analytical data.

Group[a]	Analyte	Acronym	Serum			Water			Soil			Grass		
			No[b]	Detect[c]	LOR[d]	No	Detect	LOR	No	Detect	LOR	No	Detect	LOR
		Units	#	%	ng/ml	#	%	ng/ml	#	%	ng/g	#	%	ng/g
PFSAs	Perfluorobutanesulfonic acid	PFBS	220	2.7	0.5–10	173	68.2	0.002–0.02	428	13.3	0.1–5	66	48.5	0.2–5
	Perfluoropentane sulfonic acid	PFPeS	117	3.4	1–10	147	69.4	0.002–0.02	315	11.1	0.1–5	57	35.1	0.2–1
	Perfluorohexane sulfonic acid	PFHxS	246	85	1–1	173	73.4	0.002–0.02	426	69.2	0.1–5	59	50.8	0.2–5
	Perfluoroheptane sulfonic acid	PFHpS	136	76	1–10	147	68	0.002–0.02	315	21.6	0.1–5	57	3.5	0–1
	Perfluorooctane sulfonic acid	PFOS	253	92.5	1–6	184	83.7	0.002–0.02	460	78	0.1–5	81	43.2	0.2–5
	Perfluorononane sulfonic acid	PFNS	117	0	1–10	127	11.8	0.0005–0.02	426	5.4	0.1–5	59	0	0.2–5
	Perfluorodecane sulfonic acid	PFDS	156	0	0.5–10	122	30.3	0.002–0.1	315	6	0.2–5	59	10.2	0–5
PFCAs	Perfluorobutanoic acid	PFBA	116	0	1–1	140	68.6	0.0005–0.02	317	18.9	0.1–5	59	42.4	0.2–5
	Perfluoropentanoic acid	PFPeA	145	0	1–10	173	67.1	0.002–0.02	428	36.7	0.1–5	81	38.3	0.2–20
	Perfluorohexanoic acid	PFHxA	184	0.5	0.5–10	143	73.4	0.002–0.02	428	26.6	0.1–5	81	16	0.2–10
	Perfluoroheptanoic acid	PFHpA	184	0.5	0.5–10	184	68.5	0.002–0.02	460	17.2	0.2–5	81	4.9	0.2–5
	Perfluorooctanoic acid	PFOA	184	0	0.5–50	146	51.4	0.0005–0.02	408	12.7	0.1–5	81	2.5	0.2–5
	Perfluorononanoic acid	PFNA	203	21.7	1–10	135	18.5	0.0005–0.05	408	4.2	0.1–5	81	0	0.2–5
	Perfluorodecanoic acid	PFDA	203	0	0.5–10	119	9.2	0.0005–0.05	408	1.7	0.1–5	81	0	0.2–5
	Perfluoroundecanoic acid	PFUnDA	184	0	0.5–10	119	8.4	0.0005–0.05	408	0.7	0.1–5	81	0	0.2–5
	Perfluorododecanoic acid	PFDoDA	184	0	0.5–10	119	8.4	0.0005–0.05	408	0.7	0.1–5	59	0	0.2–5
	Perfluorotridecanoic acid	PFTrDA	156	0	1–10	118	8.5	0.0005–0.5	408	0	0.1–5	59	0	0.5–5
	Perfluorotetradecanoic acid	PFTeDA	139	0	1–10	116	12.9	0.001–0.05	317	0.6	0.1–5	59	0	0.2–5
PFTSs	4:2 Fluorotelomer sulfonic acid	4:2 FTS	156	0	1–10	174	50.6	0.001–0.1	460	5.4	0.2–10	81	3.7	0.5–10
	6:2 Fluorotelomer sulfonic acid	6:2 FTS	184	0	1–20	122	9	0.001–0.5	324	2.5	0.1–5	66	0	0.5–5
	8:2 Fluorotelomer sulfonic acid	8:2 FTS	184	0	1–10	106	0	0.001–0.05	194	0	0.1–5	57	1.8	0.2–2
FASA	Perfluorooctane sulfonamide	PFOSA	156	0	0.5–10	121	21.5	0.0005–0.02	408	6.9	0.2–5	59	0	0.2–10
	N-Methyl perfluorooctane sulfonamide	N-MeFOSA	156	0	1–10	119	8.4	0.001–0.5	408	0	0.2–5	59	0	0.5–10
	N-Ethyl perfluorooctane sulfonamide	N-EtFOSA	110	0	1–10	106	0	0.0005–0.05	295	0.7	0.2–5	57	0	0–1
	N-Methyl perfluorooctane sulfonamidoacetic acid	N-MeFOSAA	156	0	1–10	117	8.5	0.001–0.5	406	0	0.2–5	57	5.3	0.5–2
	N-Ethyl perfluorooctane sulfonamidoacetic acid	N-EtFOSAA	156	0	1–10	119	8.4	0.001–0.05	347	0	0.2–5	59	0	0.5–10
	N-Methyl perfluorooctane sulfonamidoethanol	N-MeFOSE	156	0	1–10	121	1.7	0.0005–0.5	301	0.7	0.2–5	57	0	0.2–2
	N-Ethyl perfluorooctane sulfonamidoethanol	N-EtFOSE	156	0	1–10	119	8.4	0.001–0.5	406	0	0.2–5	57	0	0.5–2

[a] Analyte grouping: PFSAs = Perfluoroalkyl sulfonates, PFCAs = Perfluoroalkyl carboxylates, PFTSs = Fluorotelomer sulfonates, FASA = Perfluoroalkane sulfonamides and perfluoroalkane sulfonamido substances.
[b] No = number (#) of samples refers to the total number of results reported (>LOR and <LOR).
[c] Detect (%) refers to number of results above the LOR.
[d] LOR column displays the range in reported LORs for each analyte.

identified. All sites were impacted due to migration of PFAS from soils and water bodies at source sites through surface water migration and, surface run-off and erosion of sediments, into farm dams and water ways used to support stockwater. No farms in the study applied biosolids or used PFAS impacted water for irrigation of pasture.

2.3. Data collation

Ten agricultural sites with existing investigation reports that covered a number of land uses were identified from environmental investigations. These reports are available on EPA Victoria's website under environmental audits online tool and on the Australian Department of Defence website. Data were anonymized and collated. Victoria has varied agro-ecological zones (AEZ) with differing climate and agricultural systems (Williams et al., 2002) which can lead to differences in livestock rearing conditions and practices. As such, the sites were grouped by AEZ (A-D) and proximity to contaminant source sites. Table 1 provides an overview of data availability, grouping and livestock rearing practices relevant to contaminant exposure on livestock farms. The livestock in this assessment, were grazed on primarily non-irrigated and non-biosolids amended pastures. This meant that stockwater was the primary exposure pathway for livestock, with smaller contributions from soil and pasture, particularly in areas prone to inundation. At some sites livestock had access to drainage ditches, dams, and areas of inundation with vegetation, which made up varying proportions of accessible grazing land. Stock rotation was also considered, as this practice may provide information on the duration and continuity of exposure. Stock rotation potential was noted based on the availability of uncontaminated pasture and water resources within the operation (from limited to extensive), with only one farm with a structured rotation practice.

Data were collated from individual monitoring reports (for each site and sometimes over multiple monitoring periods) spanning approximately 5 years. All analytical work was undertaken by commercial laboratories with acceptable quality assurance and control measures (analysis of surrogate and matrix spike recoveries, blanks and duplicates provided with each analytical report). Throughout this period there were advances in analytical methods, changes in the limits of reporting (LOR) and chemicals added to the analytical suites. As such the number analytes monitored varies between reports as do LORs (LOR ranges provided). It is noted that there are significant differences in LORs for different matrices which reflect differences in guidelines for these matrices as well as difficulties with achieving ultra-low level reporting limits.

Differences in analytical and analyte extraction methods from different matrices exist between different laboratories, however, a proficiency study (NMI, 2018) demonstrated an acceptable interlaboratory consensus for results measuring spiked PFAS concentrations from soil, water and biological samples. In the proficiency study, laboratory performance (accuracy) was compared using standard (z) scores (how

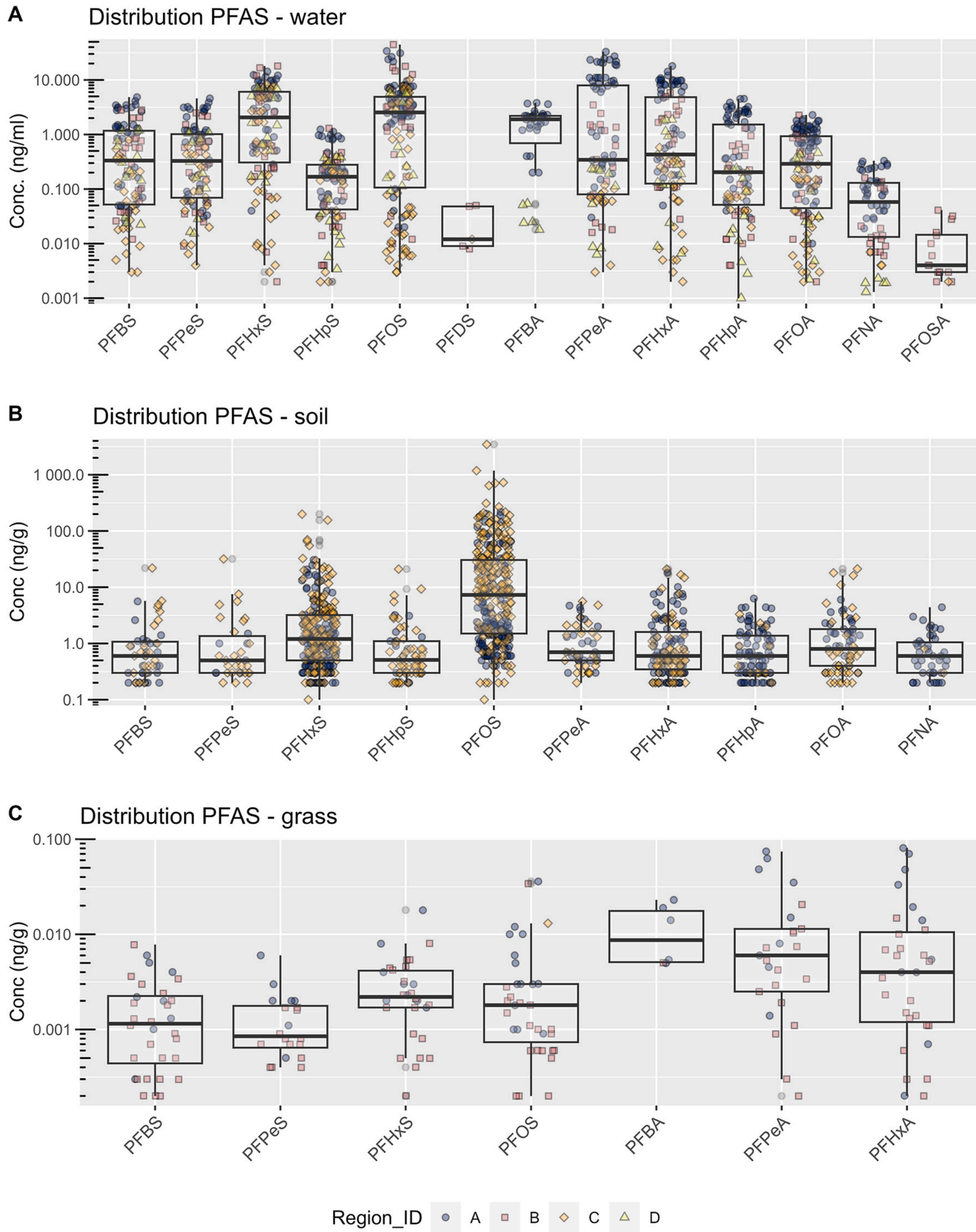

Fig. 2. Box plots (ggplot2 package in R) displaying environmental PFAS distribution in A: water; B: soil; C: pasture grasses for pooled data from 10 PFAS impacted sites across 4 agro-ecological regions in Victoria (A–D).

much the result differs from the assigned value) and En-scores (how closely the result agrees with the assigned value with consideration of uncertainty) which showed that 82% of the results were satisfactory allowing the data to be pooled (NMI, 2018).

The pooled dataset is comprised of a total of 142 cattle serum samples (from a mix of beef cattle breeds, age, and sex), 111 sheep serum samples (from a mix of breeds, age, and sex), 184 water samples (from dams, drainage ditches and areas of inundation and stock troughs), 81 pasture samples and 460 soil samples. It is noted that at most sites targeted environmental sampling was undertaken as the sites were too large for gridded random sampling; and the sampling was typically targeted to areas which livestock accessed. An overview of pooled analytical data, rates of detection and LOR ranges reported for each medium are shown in Table 2.

All analytes are reported as the sum (or total) of its isomers (i.e. sum of linear and branched isomers for each PFAS). Individual isomer reporting is not common in environmental site assessment reports as the individual isomers do not have any bearing on regulation, the perceived risk or how a site may be managed.

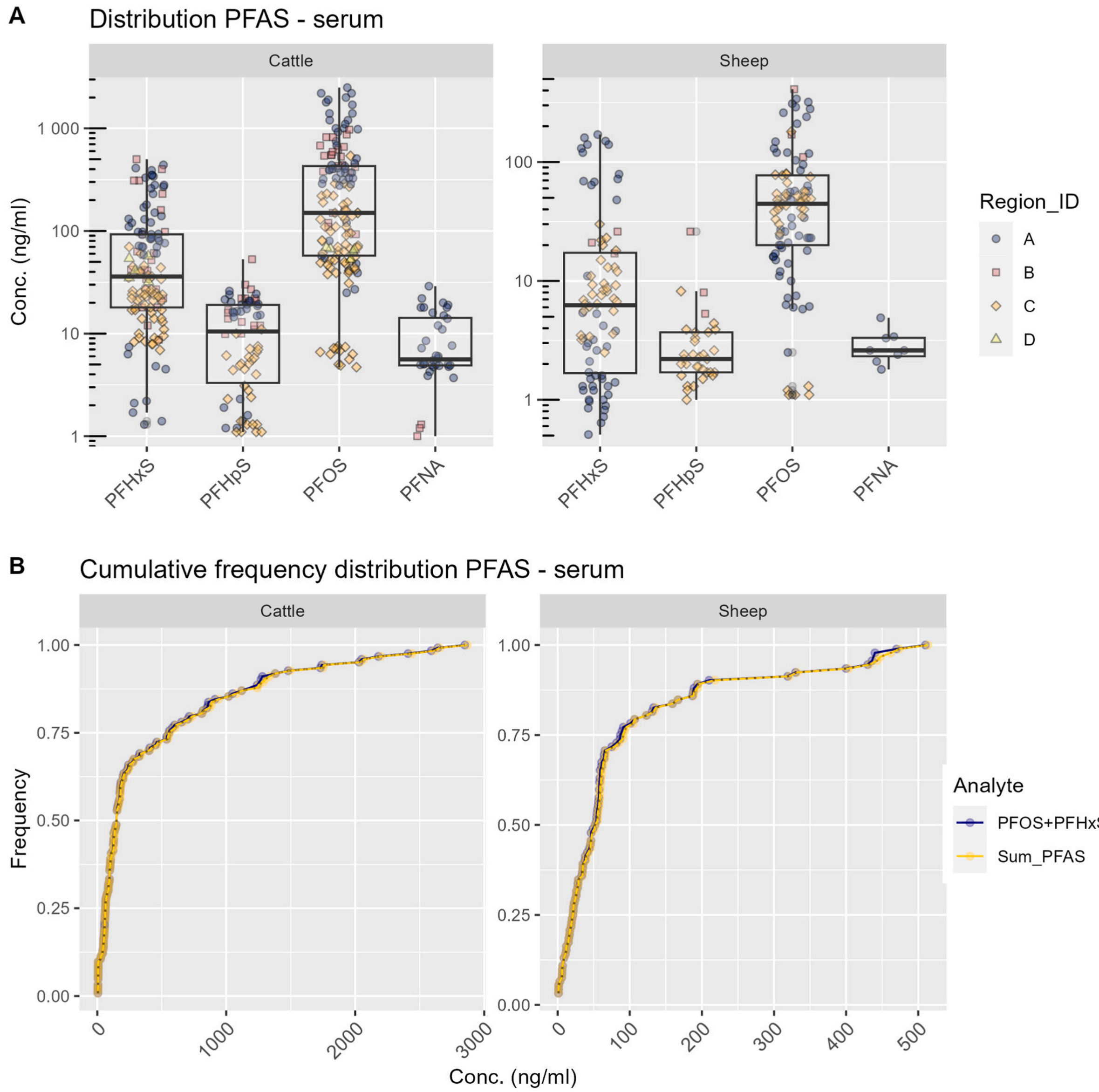

Fig. 3. PFAS distributions plotted (ggplot2 package) for cattle and sheep serum samples. A) Serum PFAS distribution shown for analytes detected in >10% of pooled samples; B) Cumulative frequency distributions shown for total PFAS and the sum of PFOS + PFHxS indicating that the predominant composition of total PFAS was made up of PFOS + PFHxS in both cattle and sheep.

2.4. Data analysis

Censored (or non-detect) results were managed using a substitution method which replaced censored results with a value equal to half-the-limit of reporting (LOR x 0.5). Based on previous studies, this substitution method is comparable to or more accurate than alternative censored data management methods when describing environmental data (Mikkonen et al., 2018). Spearman rank coefficients were then used (psych package (Revelle, 2021)) to test the strength of possible correlations between PFAS concentrations (median) in different environmental matrices and serum samples from each site.

For matrices that showed significant correlations ($p < 0.01$) sample pairing was undertaken to generate relevant spatio-temporal datasets for regression analysis. Surface water PFAS concentrations may be influenced by a number of variables and show temporal variability (Gallen et al., 2014; Lanza et al., 2017; Abunada et al., 2020). As such median annual PFAS concentrations in stock water were paired with median annual serum samples (for the same sampling year). In addition, the dataset used for regression analysis only included cattle with a minimum of 12 months exposure and sheep with a minimum of 6 months exposure (measured as time on-site and based on elimination half-lives for PFOS) to avoid biasing the dataset with serum levels resulting from short-term exposures. PFOS half-lives have been reported to vary depending on the physiological status of the animal and range between 74 and 120 days for cattle (Lupton et al., 2015; Drew et al., 2021b) and 17–74 days for sheep (Hagen et al., 2019). We determined that steady state could be achieved after regular exposure for more than four half-lives which is approximately 12–18 months for cattle (Ito, 2011; Gupta, 2016) and 1–6 months for sheep (Hagen et al., 2019).

The Shapiro-Wilk test, used to check for data distribution normality, indicated that serum PFAS concentrations were skewed to the right so the data were log transformed (log base 10) prior to performing linear regression analyses (ggplot2 (Wickham, 2016)). All analyses were conducted in R Core Team. R, 2019.

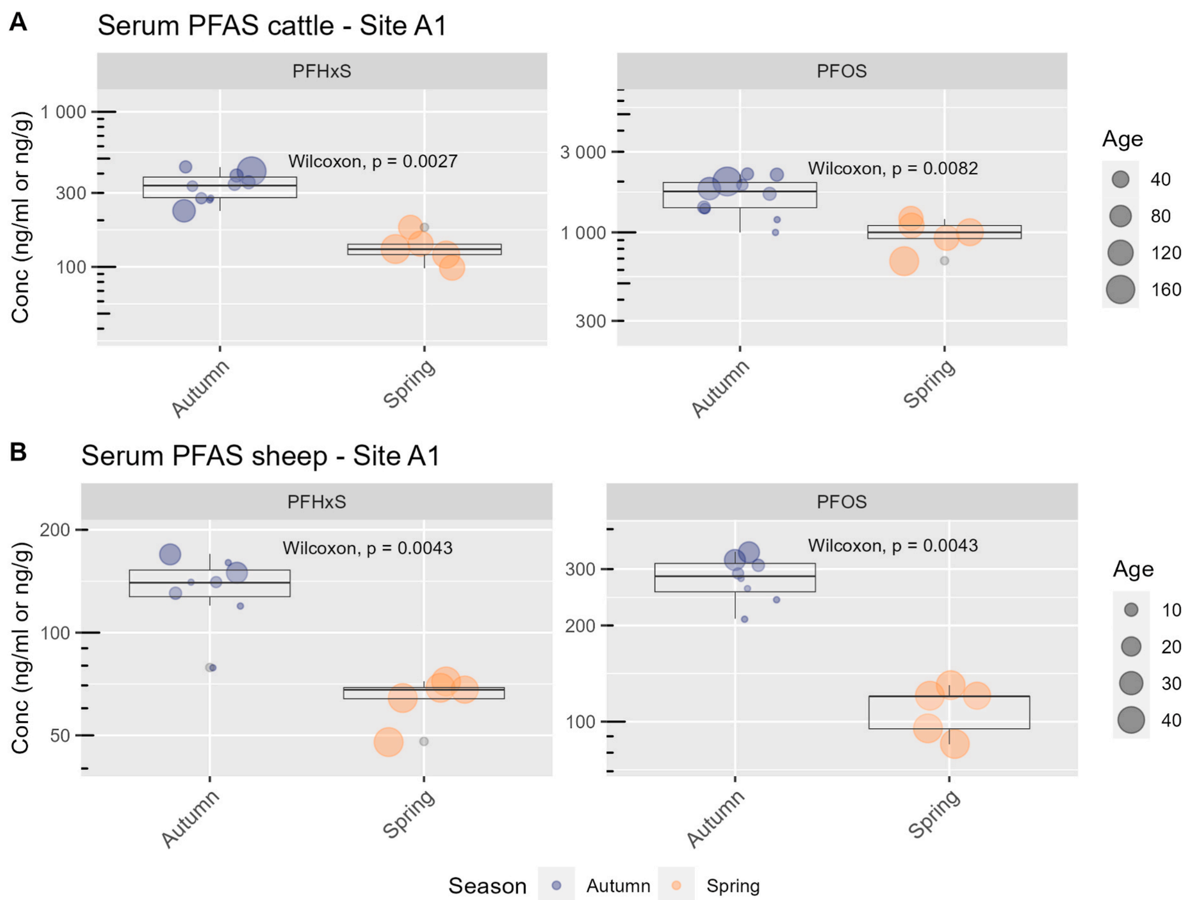

Fig. 4. Boxplots displaying seasonal distribution (ggplot2) of serum PFHxS and PFOS at Site A1 for A) cattle; and B) sheep. Size of the marker conveys age of the animals in months and the Wilcoxon signed-rank test was used to compare the serum concentration means.

3. Results and discussion

3.1. PFAS distribution

The number of PFAS compounds detected (at a rate >10% of samples) were greatest in water samples (16), > soil (10), > pasture (8) and > serum (4). The higher detection rate for PFAS in water is likely influenced by having significantly lower reporting limits while soil, grass and serum had comparable reporting limits. Four-to eight-carbon perfluoroalkyl sulfonates (PFSAs) and -carboxylates (PFCAs) were detected most frequently across environmental media (pasture-, water-, and soil samples) while detections for fluorotelomer sulfonates (PFTSs) and perfluoroalkane sulfonamides and perfluoroalkane sulfonamido substances (FASAs) were most commonly detected in water samples. The predominantly detected compounds (from each group PFSA, PFCA, PFTS and FASA) are consistent with our understanding from the environmental investigations and site histories therein, with AFFF being the primary source. Although the composition of PFAS within historic AFFF formulations varies (depending on manufacturer and the year of manufacture), a significant percentage of these products were made up of PFOS and related perfluoroalkyl sulfonates (PFSAs) like PFHxS (Field et al., 2017; Leeson et al., 2021). Another class of compounds used extensively in AFFF formulations were polyfluorinated fluorotelomer thioamido sulfonates (otherwise known as FtTAoS or the trade name Lodyne) which can be biodegraded (under aerobic conditions) to PFTSs and PFCAs (Field et al., 2017; Yi et al., 2018). Of the FASA compounds only PFOSA was detected at a rate >10% (in any media tested), which may also be found in AFFF foams (Harding-Marjanovic et al., 2016) and is a PFOS precursor (i.e. has potential to biotransform to PFOS (Mejia Avendaño and Liu, 2015; Kowalczyk et al., 2020)).

Individual PFAS from each group typically increased relative to one another with respect to region and matrix; for example, the presence of PFOS typically correlated with the presence of other sulfonate group compounds for a given matrix and region. PFAS concentrations (median) in water and soil showed similar trends with elevated PFTSs and PFSAs in comparison to PFCAs while this trend was reversed in pasture grasses, possibly due to biotransformation processes reported elsewhere (Costello and Lee, 2020; Zhao et al., 2019) and/or the PFAS physicochemical characteristics (like chain length, head group functionality and water solubility) affecting transfer from soil to plants (Wang et al., 2020). Overall soil and pasture grass PFAS concentrations showed high variability which is thought to be due to PFAS migration being driven by surface water flow and variation in sampling programs from site to site (Cardno LanePiper, 2014; Senversa, 2018; Golder, 2020). In most cases the highest soil and pasture PFAS concentrations were found along drainage lines, areas of inundation or proximity to surface water. Fig. 2 provides a summary of environmental PFAS distributions observed for each region (for analytes detected at a rate >10% of samples).

The number of PFAS compounds reported above detection limits in livestock serum was lower than the number detected in environmental samples. In environmental samples (water, soil, pasture grass), 27 of the 28 analytes were detected whereas in serum only 8 analytes were detected (Table 2). This is partly due to differences in LORs and partly due to toxicokinetic factors like excretion rate (or half-life). Where a compound is present in environmental media at a concentration below the serum LOR it will only be detected in serum when the excretion rate < intake rate. This has also been observed in other livestock studies where concentrations of perflouoroalkyl carboxylic acids and

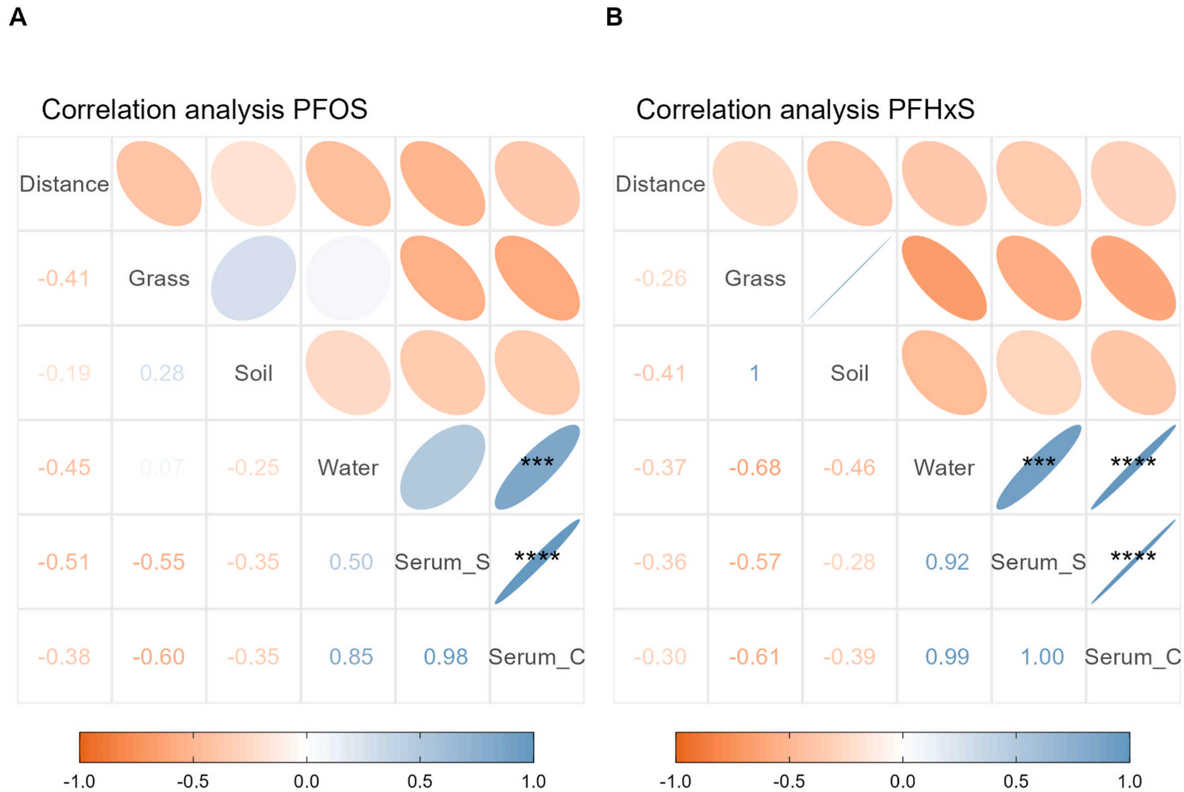

Fig. 5. Correlation analysis (using psych and ggplot2 packages) showing associations between environmental- and serum levels for A) PFOS; and B) PFHxS. The shape, angle and color signify the type (positive = blue, 45°; negative = orange, 135°) and strength of association, with flat elliptoid shape and intensity of color representing a strong correlation (R^2 values displayed on bottom half of plot). Significance denoted by * (* for $p < 0.1$, **for $p < 0.05$, *** for $p < 0.01$ and **** for $p < 0.001$). Serum_S denotes sheep serum samples and Serum_C denotes cattle serum.

perfluoroalkyl sulfonic acids with four or less carbons, were either not detected or detected in very low concentrations (Kowalczyk et al., 2013; Lupton et al., 2022). It is thus likely other PFAS are present in serum (to reflect intake media) however at levels < LOR in this case. Although fewer PFAS were found in serum, they were present more consistently with an overall detection rate >90% of samples (in sheep and cattle combined and 100% in cattle alone). PFASs are known to bioaccumulate to varying degrees (i.e. bioaccumulation increases with the carbon chain length (Xu, 2020) and similar trends have been reported previously for livestock exposed to contaminated feed or water sources (Bräunig et al., 2017; Kowalczyk et al., 2012; Drew et al., 2021a; Van Asselt et al., 2013). Four of the PFAS detected in serum (PFHxS, PFHpS, PFOS and PFNA) had levels higher than those reported in corresponding environmental samples. As shown in Fig. 3 (Panel B), on average PFOS and PFHxS made up >98% of total PFAS detected in serum and as such the lines appear overlaid. Further PFOS was found to account for on average > 70% of the total PFAS detected. PFNA was the only carboxylate compound found in serum while PFTS and FASA were not observed in any animal. This is despite higher overall concentrations of PFAS such as 6:2FTS, PFHxA, PFPeA compared to PFOS and PFHxS in water, indicating elimination half-lives are a driver behind the type and concentration of PFAS detected in serum, rather than the concentration in water itself. Although the precursor PFOSA was not detected in serum, it is considered unlikely that it would have been metabolized and contribute significantly to serum PFOS levels due to low environmental concentrations. Fig. 3 provides an overview of PFAS distribution in serum of cattle and sheep for analytes with >10% detection rate across pooled samples.

Livestock serum levels may also be influenced by season. Fig. 4 presents box plots of serum PFOS and PFHxS levels based on the time of year samples were collected (spring and autumn). The box plots are limited to one site as only site A1 had multiple rounds of serum collected at different times of the year for livestock comprising 52 serum samples total. After the second round of sampling mitigation measures were taken and as such the third round of samples are not comparable which left two years of (single point in time) serum results for cattle aged >6 months (n = 6 for spring and 10 autumn) and two years serum results for sheep aged >6 months (n = 6 spring) and n = 8 autumn)).

Fig. 4 shows that serum concentrations for PFOS and PFHxS, in both cattle and sheep, were significantly higher in autumn than in spring (approximately 6 months apart). Although the dataset is limited, this is not an unexpected result due to livestock consumption patterns. Previous publications have shown that as pasture moisture levels decrease throughout summer and autumn, livestock require more water to meet their daily water requirements (NRC, 2000; Lukas et al., 2008; Olkowski, 2009), which in turn increases the PFAS intake of the animals when the available stock water is contaminated with PFAS. Conversely, in winter and spring, when pasture moisture levels are typically higher, livestock require less drinking water often reaching very low to negligible water intake (NRC, 2000; Lukas et al., 2008) and subsequently serum levels are correspondingly lower as elimination rate exceeds intake during this time. Seasonal differences appear more pronounced in sheep likely due to the comparatively shorter half-lives and their capacity to meet daily water requirements from green pasture alone (NSW DPI, 2014).

3.2. Correlation analysis

Considering PFOS and PFHxS account for >98% of PFAS body burden in cattle and sheep, correlation analysis was undertaken for these compounds only. Fig. 5 provides a summary of associations between median environmental PFOS and PFHxS concentrations and serum concentrations.

The correlation plots showed a strong positive correlation between

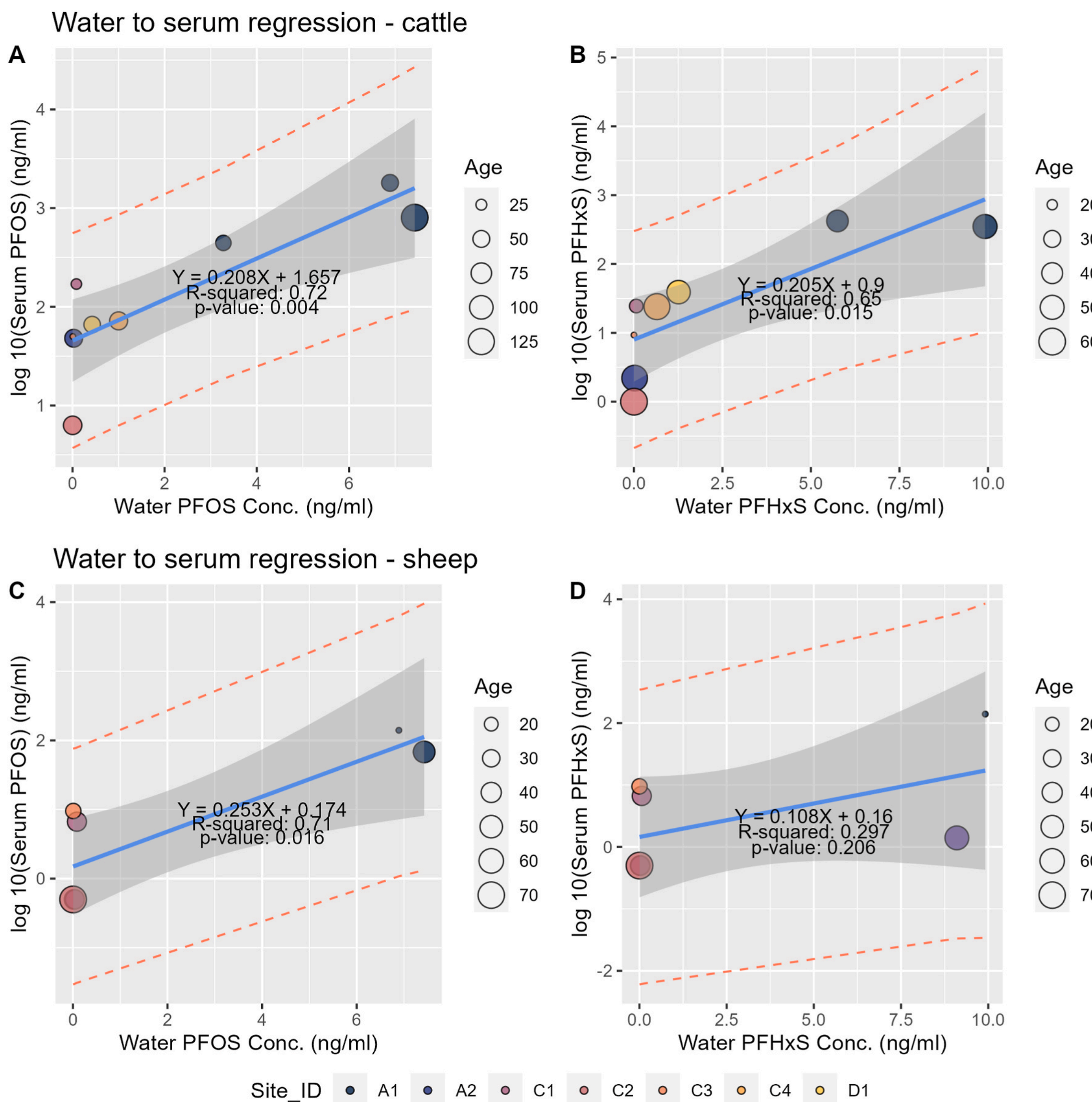

Fig. 6. Summary of PFAS-water to PFAS-serum regression analysis (plotted using ggplot2) for A) PFOS and B) PFHxS in cattle and C) PFOS and D) PFHxS in sheep. 95% confidence intervals (CI) presented using grey shading and the prediction intervals (for future observations) shown using dashed red lines. Size of the marker conveys median age of the animals in months. Statistical summary included in figure provides the slope, R^2 and p-value for the regression line.

water and serum PFHxS concentrations for both cattle (R^2 0.99, $p < 0.001$) and sheep (R^2 0.92, $p < 0.01$) and a moderately strong positive correlation for PFOS between water and cattle (R^2 0.85, $p < 0.01$). While sheep serum and water did show a positive correlation for PFOS this was not statistically significant. Interestingly serum PFOS and PFHxS concentrations showed an inverse correlation with pasture grass and soil concentrations. This is likely because the contributions of PFOS and PFHxS from soil and grass, when drinking water is elevated, are relatively small. Similar conclusions, regarding the relative exposure contributions, were made in a recent publication in which water to serum (cattle and sheep) transfer factors were estimated for PFAS (Drew et al., 2021a).

3.3. Regression analysis

Regression analysis was performed to investigate whether environmental data, gathered from multiple sites (with differing levels of contamination), could provide an adequate regression relationship for the extrapolation of serum concentrations for a given water concentration. Fig. 6 summarises the PFAS-water to PFAS-serum regression results for cattle and sheep.

Overall, the water to serum regression plots for cattle and sheep indicate a positive relationship between increasing serum- and stock water concentrations for both PFOS and PFHxS. Based on the R-squared values, the goodness-of-fit was better for PFOS, and the p-values indicate that the relationships are significant (assuming a 0.05 significance level) in cattle for both PFOS and PFHxS, and for PFOS in sheep. The 95% confidence intervals are wider for sheep, likely to be influenced by the relatively small number of paired water-serum samples as well as the range in serum concentrations observed, especially for PFHxS. In general, the regression relationships and reported concentrations indicate that PFOS and PFHxS bioaccumulation (from water) is lower in sheep than in cattle. This result is not unexpected, given the differences in half-lives between sheep and cattle and perhaps also their water consumption patterns. At very low PFAS water concentrations serum predictions are less reliable due to the influence of other pathways like soil and pasture intake that may contribute more to total exposure as exposure from water decreases. The reported regression relationships may also differ for sites with historical biosolids application/irrigation which could lead to accumulation of PFAS in soils and pastures and therefore

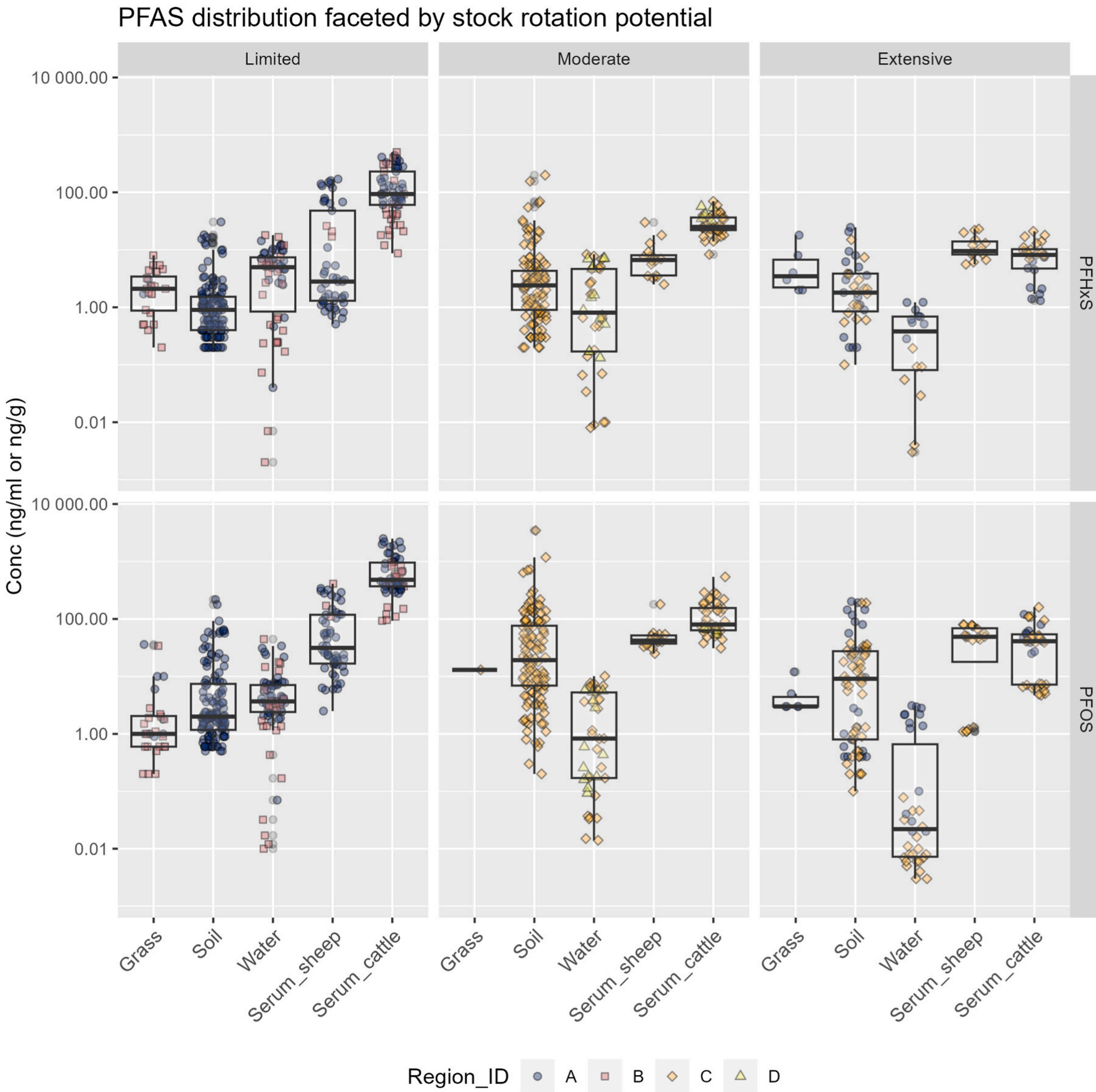

Fig. 7. Boxplots displaying concentration distribution of PFHxS and PFOS in the environment and livestock serum for all sites (faceted by limited, moderate or extensive stock rotation potential).

higher relative contributions. It is also possible that these regression relationships may not be relevant to sites with elevated concentrations of PFOS precursors where precursor biotransformation could lead to higher serum levels of PFOS than otherwise expected (Martin et al., 2010; Glaser et al., 2021).

3.4. Observations on variable livestock exposure

Understanding exposure pathways and trends can provide insights for risk assessment and livestock management. Based on this work, the primary exposure pathway for grazing livestock downgradient from AFFF contaminated sites (on pastures without history of biosolids treatment or irrigation with contaminated water) has been stock water. The role of stock rotation on accumulation of PFAS was assessed by comparing environmental and serum data from farms with “limited,” “moderate” or “extensive” stock rotation potential. Stock rotation refers to the availability of uncontaminated grazing pasture and drinking water sources and rotation between these sources. Sites with “Limited” stock rotation opportunities comprised farms with no unimpacted pasture or drinking sources. Sites with “Moderate” stock rotation opportunities were those with access to several paddocks and drinking water sources with varying levels of PFAS. Sites with “Extensive” stock rotation potential were those where PFAS impacts were confined to a few paddocks/drinking water sources (≤25%) and/or a structured rotation practice was in place that involved defined periods without exposure. Fig. 7 provides a summary of environmental and livestock PFAS distributions based on the level of stock rotation potential identified for each site.

Sites with limited stock rotation (or access to unimpacted water or pasture sources) typically had higher sample densities around the median for water than those with higher stock rotation potential which may be due to limited sources. In general, soil samples showed wider distribution ranges (spanning up to three orders of magnitude for PFHxS and four orders of magnitude for PFOS) than water which may be due to the heterogeneous nature of the contaminant distribution in soil (Zhang et al., 2019). As noted previously soil concentrations appear to have less influence, relative to water, on livestock serum levels. Overall, increasing stock rotation or availability of alternate water sources resulted in lower serum PFOS and PFHxS levels in both cattle and sheep. It was also observed that livestock distance from the source site does not correlate strongly with PFAS serum levels and may not be a good indicator of risk. This may be because overland flows (and their solutes and

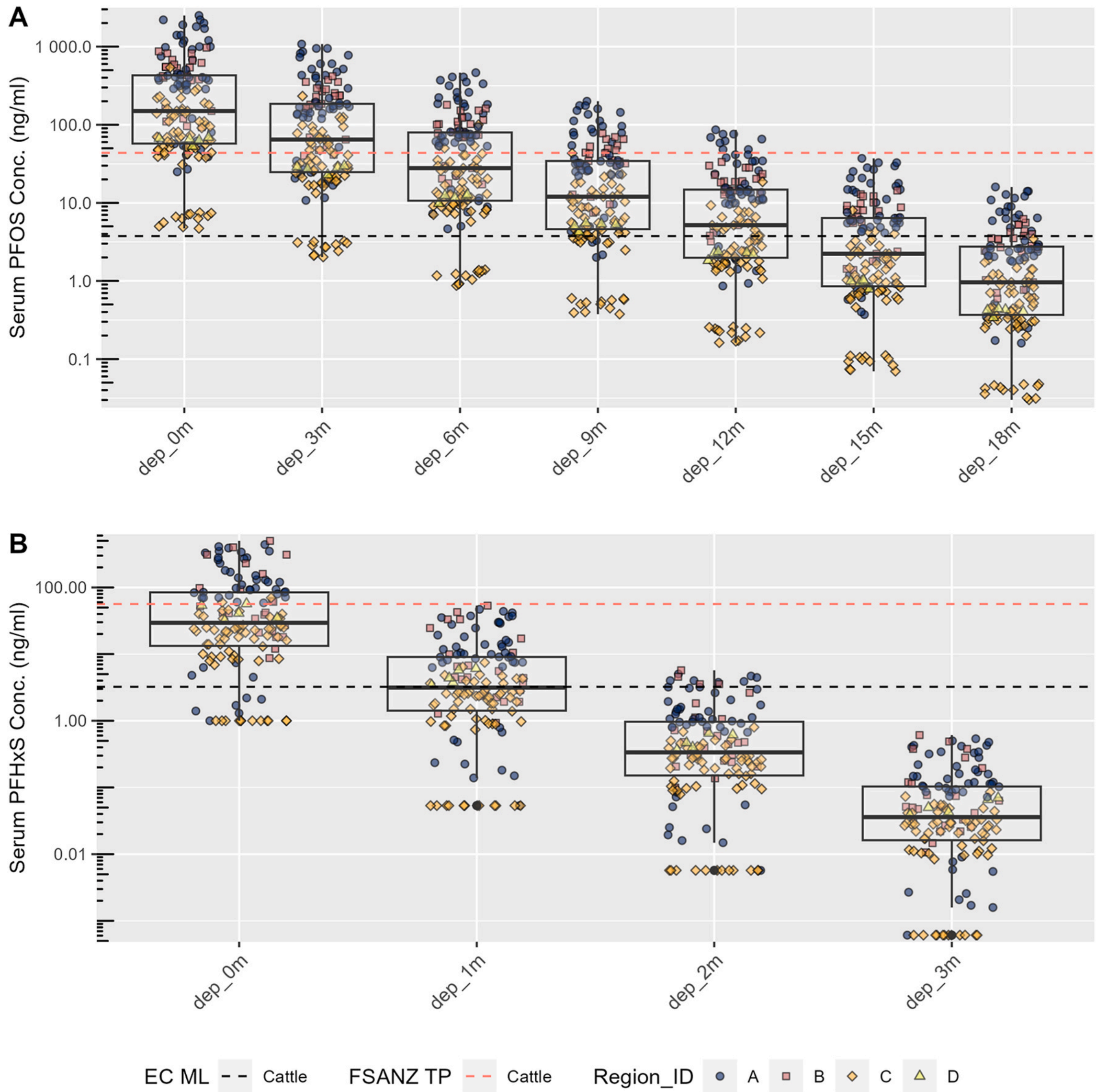

Fig. 8. Boxplots displaying measured and modelled serum A) PFOS; and B) PFHxS levels in cattle from PFAS impacted sites compared to acceptable serum concentrations over time. Time zero (dep_0 m) are measured serum concentrations and dep_1 m – dep_18 m are modelled serum estimates for cattle where exposure to PFAS has been prevented and depuration is occurring.

or suspended particle load) tend to follow topographic gradients or drainage lines (Hu et al., 2020) and proximity to the source is not related to how farm operations capture overland runoff and to what extent it may be utilised for livestock drinking. As such the availability of alternative water sources or stock rotation potential may be a more important determinant of body burden (serum conc.) than distance to a source site.

3.5. Implications for risk assessment and livestock management

A key outcome demonstrated by the analyses conducted within this study is that farm practices can have a significant influence on the level and extent of PFAS accumulation and may also support exposure reduction. To that end farm information coupled with environmental investigation data for PFAS, can provide a greater understanding of the need and level of detail required for risk assessment and management. While several PFAS may be identified in environmental media, the number and concentration of PFAS identified in livestock was significantly lower. While detection limits may preclude identification of certain PFAS (i.e. very low environmental concentrations and/or short half-life), they are unlikely to contribute significantly to the risk assessment or management measures for a contaminated site (given that the LORs are below relevant health-based criteria). The importance of livestock management is highlighted in Fig. 8 which provides a comparison of livestock serum levels from impacted sites to health-based criteria in the form of acceptable (or target) serum concentrations estimated based on the FSANZ TPs and the EC MLs over a depuration timeframe of 18 months (where dep_0 m is time zero). Depuration or clearance was modelled using an exponential decay function (Eq (1).) where C is the concentration at a given time, C0 is the concentration at time zero, Ke is the elimination rate (ln (2)/half-life) and t is time. The half-lives (PFOS 74 days; PFHxS 9.4 days) used in the decay estimates are based on cattle field trials conducted in Australia (Drew et al., 2021b, 2021c).

$$C\left(\frac{ng}{ml}\right) = C_0\left(\frac{ng}{ml}\right) \times \exp\hat{(}-Ke\left(d^{-1}\right) \times t(d)) \quad (1)$$

The acceptable serum concentrations were determined by converting tissue levels to serum levels using partition coefficients for meat (ML or TP/serum:tissue partition coefficient). The acceptable serum

Table 3
Risk assessment considerations for problem formulation.

Questions to consider	Example information	Purpose
What type of farm/ operation in question?	Intensive, large, artisan, hobby	Scale of operation may be important for exposure considerations, management measures and market share.
What livestock and purpose?	Cattle for food production	Sets the context for human health risk assessment.
What breed, age, sex?	Angus steers (3–4 months)	Age and sex may be an important consideration for physiological parameters (and exposure considerations).
Production systems	Pasture based grazing, supplementation, stock rotation	Gives context on stock exposure and any potential natural depuration times associated with the farming practice
Discharge intention	(weaners, yearlings, cull for age), selling for growing out, fattening, slaughter, breeding?	Gives context on the likely duration of time between exposure and end market.
Time of year of discharge?	Spring	Time of year influences exposure and should be considered especially when designing monitoring programs.
What is the expected finishing age for market?	12–18 months (yearlings)	Body burden is related to the exposure period.
Home consumption?	One animal per year	Gives indication of amount of produce realistically consumed in home setting.
What is the destination market?	Large abattoir or small-town market or home consumption	Market dilution considerations may apply for large markets, noting this informs risk management rather than risk assessment.
What are the surrounding land uses (and history) and pathways for PFAS contamination?	Former fire fighter training ground	Important for identifying contaminants of interest and contextualising migration pathways. Firefighting activities are linked to the use of AFFF which contain certain classes of PFAS depending on the products used. Some products also contain higher levels of precursors which may biodegrade to PFOS.
Are biosolids used onsite? If so, how many years?	Yes, between 1990 and 2000	PFAS composition and concentrations have changed over time which may be important for identifying chemicals of interest as well as an additional uptake pathway.
What is/are the source(s) of livestock drinking water?	Dams fed by surface water runoff	The number of sources and level of contamination and time spent at each is informative for livestock exposure as well as management options (rotation).
What levels of PFAS found in each drinking source?	PFOS at conc. ranging < LOR to 10 ng/ml	
How long do animals spend in the vicinity of each drinking source?	Weeks to months	
What are the dominant production systems in place?	Pasture based grazing (80% of intake) and supplementation with hay or silage from unimpacted source (20%)	Information about production systems is relevant for exposure estimation.
What levels of PFAS detected in soils and pasture?	PFOS at conc. ranging < LOR to 100 ng/g	

concentrations for the FSANZ TP of 3.5 ng PFOS + PFHxS/g (wet weight) were estimated as 43.75 ng/ml for PFOS and 56.5 ng/ml for PFHxS using serum:tissue partition coefficients of 0.08 [45] for PFOS and 0.062 for PFHxS (Drew et al., 2021c). The acceptable serum concentrations based on the EC MLs for cattle meat (0.3 ng/g for PFOS and 0.2 ng/g for PFHxS) were estimated to be 3.75 ng/ml for PFOS and 3.2 ng/ml for PFHxS.

This figure shows that without management, cattle grazed on PFAS impacted sites may exceed acceptable serum levels, especially for export markets with lower limits (like the EC MLs), however, most cattle can achieve acceptable serum levels (depending on the serum target) between 6 and 18 months for PFOS and within 1–3 months for PFHxS, following prevention of exposure. This is particularly relevant for livestock practices where animals go to feedlots prior to market. Depending on market specifications, some cattle spend a minimum of 100 days in a feedlot to be classed as grain fed, while feeder steers (long fed) and Wagyu can spend up to 300 days in a feedlot (DPI NSW, 2015). The estimated depuration timeframes can aid in prioritising sites for remedial intervention where the depuration timeframes are impracticable or exposure management is not possible.

It is noted that the livestock discussed here were either acquired for further research (Drew et al., 2021b) or managed by either moving to another site or by limiting access to PFAS contaminated resources such that serum levels reduced to acceptable levels (based on FSANZ non-regulatory trigger points for meat in Australia).

With regard to risk assessment and management, this work has highlighted environmental, seasonal and resource factors that have significant impact on the bioaccumulation of PFAS in animals. Although the trends highlighted in this work pertain to surface water contamination, the same principles apply for managing exposure via other sources like biosolids or contaminated groundwater. To develop a robust conceptual site model for site specific livestock risk assessment, certain parameters require consideration, presented here as a series of questions that should be considered during the problem formulation of the risk assessment (Table 3).

4. Conclusions

This study investigated trends in PFAS monitoring- and farm operational data with a focus on furthering our understanding of exposure pathways, determinants of variability in livestock PFAS body burdens and how these relate to risk assessment and management. The PFAS of most concern for risk assessment and management were PFOS and PFHxS. This study showed that PFOS and PFHxS body burden are positively correlated with water intake which, in turn, is influenced by climate, timing and season of sampling. Water intake levels can be as low as 1–8% of bodyweight (non-lactating cattle and sheep) in winter and spring months when pasture moisture is high and evaporative losses low compared to 10–20% of bodyweight (non-lactating cattle and sheep) in summer (NRC, 2000; Olkowski, 2009). These seasonal variables in water and feed intake can also influence PFAS body burden and result in seasonal body burden fluctuations. Due to this, estimates of PFAS body burden currently based on steady state kinetics may result in large discrepancies between actual measured and estimated concentrations depending on the timing of sampling. As such, dynamic exposure models are likely more suitable for modelling PFAS exposure in grazing livestock.

In addition, farming practices such as livestock rotation and timing (of rotation) may be critical for management of livestock on sites with PFAS contamination in order to reduce PFAS body burden prior to finishing livestock. For sites with limited cattle rotation potential supplementation of feed and water sources may also need to be considered whilst remediation options are devised. Biomonitoring data, along with estimated elimination timeframes (to meet health-based guidelines), can assist in prioritising remediation options where the timeframes are impracticable, or exposure management is not feasible or possible.

Author contribution statement

The manuscript was written through contributions of all authors. **Antti T. Mikkonen:** Conceptualization, Methodology, Formal analysis, Visualization, Writing – Original Draft **Jennifer Martin:** Investigation, Resources, Data Curation, Writing – Original Draft **Richard N. Upton:** Methodology, Validation, Supervision **Andrew O. Barker:** Software, Validation, Visualization **Carolyn M. Brumley:** Writing – Review and Editing **Mark P. Taylor:** Writing – Review and Editing **Lorraine Mackenzie:** Writing – Review and Editing, Supervision **Michael S. Roberts:** Writing – Review and Editing, Supervision.

Funding

This research did not receive any specific grant from funding agencies in the public, commercial, or not-for-profit sectors.

Declaration of competing interest

The authors declare the following financial interests/personal relationships which may be considered as potential competing interests: Antti Mikkonen reports a relationship with Nation Partners Pty Ltd that includes: employment. Carolyn Brumley reports a relationship with Nation Partners Pty Ltd that includes: employment. Jennifer Martin reports a relationship with Arcadis Australia Pacific that includes: employment. Antti Mikkonen reports a relationship with CDM Smith Pty Ltd that includes: employment.

Data availability

Attached as supplementary material

Acknowledgments

The authors would like to acknowledge Dr. David Champness from Agriculture Victoria and Effi Liden from the Victorian Department of Health for their comments on the manuscript. The authors thank the Environment Protection Authority Victoria for supporting this work through access to their facilities, administrative- and in-kind support. AM acknowledges the Australian Government, Department of Education, Skills and Employment Research Training Program scholarship that supported his PhD studies at UniSA, which includes this study. MSR was supported by an Australian National Health & Medical Research Council Research Fellowship (#1107356).

Appendix A. Supplementary data

Supplementary data to this article can be found online at https://doi.org/10.1016/j.envres.2023.115518.

References

Abunada, Z., Alazaiza, M.Y.D., Bashir, M.J.K., 2020. An overview of per- and polyfluoroalkyl substances (PFAS) in the environment: source, fate, risk and regulations. Water 12 (12), 3590. https://doi.org/10.3390/w12123590.

Agriculture Victoria, 2019. Prim. Prod. Landsc. Victoria. http://vro.agriculture.vic.gov.au/dpi/vro/vrosite.nsf/pages/prim_prod_lscapes.

Agriculture Victoria, 2021. Victorian Beef Industry Fast Facts. https://agriculture.vic.gov.au/__data/assets/pdf_file/0009/657126/Beef_Fast-Facts_March-2021.pdf.

ATSDR, 2018. Toxicological Profile for Perfluoroalkyls, Draft for Public Comment. U.S. Department of Health and Human Services, Public Health Service, Atlanta, GA.

Australian Bureau of Agricultural Resource Economics and Sciences (ABARES), 2021. In: Catchment Scale Land Use of Australia – Update December 2020. https://doi.org/10.25814/AQJW-RQ15.

Bräunig, J., Baduel, C., Heffernan, A., Rotander, A., Donaldson, E., Mueller, J.F., 2017. Fate and redistribution of perfluoroalkyl acids through AFFF-impacted groundwater. Sci. Total Environ. 596–597, 360–368. https://doi.org/10.1016/j.scitotenv.2017.04.095.

Buck, R.C., Franklin, J., Berger, U., Conder, J.M., Cousins, I.T., de Voogt, P., Jensen, A.A., Kannan, K., Mabury, S.A., van Leeuwen, S.P., 2011. Perfluoroalkyl and polyfluoroalkyl substances in the environment: terminology, classification, and origins. Integrated Environ. Assess. Manag. 7 (4), 513–541. https://doi.org/10.1002/ieam.258.

Cardno LanePiper, 2014. Human Health Risk Assessment - Fiskville Community Fiskville Training College 4549 Geelong-Ballan Rd. Fiskville Victoria. https://www.parliament.vic.gov.au/images/stories/committees/enrc/Fiskville_training_college/other_docs/05_-_2014_CPL_Human_Health_Risk_Assessment_-_Fiskville_Community.pdf.

Costello, M.C.S., Lee, L.S., 2020. Sources, fate, and plant uptake in agricultural systems of per- and polyfluoroalkyl substances. Curr. Pollut. Rep. https://doi.org/10.1007/s40726-020-00168-y.

Dauchy, X., 2019. Per- and polyfluoroalkyl substances (PFASs) in drinking water: current state of the science. Curr. Opin. Environ. Sci. Health 7, 8–12. https://doi.org/10.1016/j.coesh.2018.07.004.

Dauchy, X., Boiteux, V., Colin, A., Bach, C., Rosin, C., Munoz, J.-F., 2019. Poly- and perfluoroalkyl substances in runoff water and wastewater sampled at a firefighter training area. Arch. Environ. Contam. Toxicol. 76 (2), 206–215. https://doi.org/10.1007/s00244-018-0585-z.

Death, C., Bell, C., Champness, D., Milne, C., Reichman, S., Hagen, T., 2021. Per- and polyfluoroalkyl substances (PFAS) in livestock and game species: a review. Sci. Total Environ. 774, 144795 https://doi.org/10.1016/j.scitotenv.2020.144795.

Dorrance, L.R., Kellogg, S., Love, A.H., 2017. What you should know about per- and polyfluoroalkyl substances (PFAS) for environmental claims. Environ. Claims J. 29 (4), 290–304. https://doi.org/10.1080/10406026.2017.1377015.

DPI NSW, 2015. Market specifications for cattle. Primefact 621. https://www.dpi.nsw.gov.au/__data/assets/pdf_file/0005/148415/Market-specifications-for-cattle.pdf.

Drew, R., Hagen, T.G., Champness, D., 2021a. Accumulation of PFAS by livestock – determination of transfer factors from water to serum for cattle and sheep in Australia. Food Addit. Contam. 1–17. https://doi.org/10.1080/19440049.2021.1942562.

Drew, R., Hagen, T.G., Champness, D., Sellier, A., 2021b. Half-lives of several polyfluoroalkyl substances (PFAS) in cattle serum and tissues. Food Addit. Contam. 1–21 https://doi.org/10.1080/19440049.2021.1991004.

Drew, R., Hagen, T., Champness, D., Sellier, A., 2021c. PFAS Tissue Distribution in Cattle. Poster Presentation at IUTOX 15th International Congress of Toxicology.

EC, 2022. ANNEX to the Commission Regulation (EU) …/… Amending Regulation (EC) No 1881/2006 as Regards Maximum Levels of Perfluoroalkyl Substances in Certain Foodstuffs. https://members.wto.org/crnattachments/2022/SPS/EEC/22_4494_00_e.pdf.

EFSA, 2020. Risk to human health related to the presence of perfluoroalkyl substances in food. EFS2 18 (9). https://doi.org/10.2903/j.efsa.2020.6223.

EHP, 2014. Managing Firefighting Foam Policy Explanatory Notes accessed 2022-08-30. https://environment.des.qld.gov.au/__data/assets/pdf_file/0022/89140/firefighting-foam-policy-notes.pdf.

enHealth, 2012. Environmental Health Risk Assessment: Guidelines for Assessing Human Health Risks from Environmental Hazards.

Fenton, S.E., Ducatman, A., Boobis, A., DeWitt, J.C., Lau, C., Ng, C., Smith, J.S., Roberts, S.M., 2020. Per- and polyfluoroalkyl substance toxicity and human health review: current state of knowledge and strategies for informing future research. Environ. Toxicol. Chem. https://doi.org/10.1002/etc.4890 etc.4890.

Field, J.A., Higgins, C.P., Deeb, R., Conder, J.M., 2017. FAQs regarding PFASs associated with 15 AFFF use at U.S. Military sites. Catalyzing Rapid Information Transfer among Key 16 Stakeholders on Per- and Polyfluoroalkyl Substances (PFASs) at Contaminated Military 17 Sites. https://apps.dtic.mil/dtic/tr/fulltext/u2/1044126.pdf.

FSANZ, 2021. In: 27th Australian Total Diet Study Per- and Poly-Fluoroalkyl Substances accessed 2022-01-25). https://www.foodstandards.gov.au/publications/Documents/27th%20ATDS%20report.pdf.

Gallen, C., Baduel, C., Lai, F.Y., Thompson, K., Thompson, J., Warne, M., Mueller, J.F., 2014. Spatio-temporal assessment of perfluorinated compounds in the Brisbane river system, Australia: impact of a major flood event. Mar. Pollut. Bull. 85 (2), 597–605. https://doi.org/10.1016/j.marpolbul.2014.02.014.

Glaser, D., Lamoureux, E., Opdyke, D., LaRoe, S., Reidy, D., Connolly, J., 2021. The impact of precursors on aquatic exposure assessment for PFAS: insights from bioaccumulation modeling. Integrated Environ. Assess. Manag. 17 (4), 705–715. https://doi.org/10.1002/ieam.4414.

Glüge, J., Scheringer, M., Cousins, I.T., DeWitt, J.C., Goldenman, G., Herzke, D., Lohmann, R., Ng, C.A., Trier, X., Wang, Z., 2020. An overview of the uses of per- and polyfluoroalkyl substances (PFAS). Environ. Sci.: Process. Impacts 22 (12), 2345–2373. https://doi.org/10.1039/D0EM00291G.
Golder, 2020. Human Health and Ecological Risk Assessment Bandiana Military Area. https://www.defence.gov.au/Environment/PFAS/docs/Bandiana/Reports/202011BandianaHHERAMainReportFiguresTables.pdf.
Google. Google Maps Victoria Australia. https://www.google.com/maps/place/Victoria/@-36.4856423,140.9779425,6z/data=!3m1!4b1!4m5!3m4!1s0x6ad4314b7e18954f:0x5a4efce2be829534!8m2!3d-36.9847807!4d143.3906074.
Gupta, P.K., 2016. Principles and basic concepts of toxicokinetics. In: Fundamentals of Toxicology. Elsevier, pp. 87–107. https://doi.org/10.1016/B978-0-12-805426-0.00009-3.
Hagen, T., Drew, R., Champness, D., Ryan, J., 2019. PFAS clearance and distribution in sheep. Honolulu, Hawaii. In: IUTOX 15th International Congress of Toxicology; July 15-18. P366–0932.
Harding-Marjanovic, K.C., Yi, S., Weathers, T.S., Sharp, J.O., Sedlak, D.L., Alvarez-Cohen, L., 2016. Effects of aqueous film-forming foams (AFFFs) on trichloroethene (TCE) dechlorination by a dehalococcoides mccartyi -containing microbial community. Environ. Sci. Technol. 50 (7), 3352–3361. https://doi.org/10.1021/acs.est.5b04773.
Hu, L., Bao, W., Shi, P., Wang, J., Lu, M., 2020. Simulation of overland flow considering the influence of topographic depressions. Sci. Rep. 10 (1), 6128. https://doi.org/10.1038/s41598-020-63001-y.
Ito, S., 2011. Pharmacokinetics 101. Paediatr. Child Health 16 (9), 535–536. https://doi.org/10.1093/pch/16.9.535.
Kowalczyk, J., Ehlers, S., Fürst, P., Schafft, H., Lahrssen-Wiederholt, M., 2012. Transfer of perfluorooctanoic acid (PFOA) and perfluorooctane sulfonate (PFOS) from contaminated feed into milk and meat of sheep: pilot study. Arch. Environ. Contam. Toxicol. 63 (2), 288–298. https://doi.org/10.1007/s00244-012-9759-2.
Kowalczyk, J., Ehlers, S., Oberhausen, A., Tischer, M., Fürst, P., Schafft, H., Lahrssen-Wiederholt, M., 2013. Absorption, distribution, and milk secretion of the perfluoroalkyl acids PFBS, PFHxS, PFOS, and PFOA by dairy cows fed naturally contaminated feed. J. Agric. Food Chem. 61 (12), 2903–2912. https://doi.org/10.1021/jf304680j.
Kowalczyk, J., Göckener, B., Eichhorn, M., Kotthoff, M., Bücking, M., Schafft, H., Lahrssen-Wiederholt, M., Numata, J., 2020. Transfer of per- and polyfluoroalkyl substances (PFAS) from feed into the eggs of laying hens. Part 2: toxicokinetic results including the role of precursors. J. Agric. Food Chem. 68 (45), 12539–12548. https://doi.org/10.1021/acs.jafc.0c04485.
Lanza, H.A., Cochran, R.S., Mudge, J.F., Olson, A.D., Blackwell, B.R., Maul, J.D., Salice, C.J., Anderson, T.A., 2017. Temporal monitoring of perfluorooctane sulfonate accumulation in aquatic biota downstream of historical aqueous film forming foam use areas: variability of PFOS downstream of historic AFFF application. Environ. Toxicol. Chem. 36 (8), 2022–2029. https://doi.org/10.1002/etc.3726.
Leeson, A., Thompson, T., Stroo, H.F., Anderson, R.H., Speicher, J., Mills, M.A., Willey, J., Coyle, C., Ghosh, R., Lebrón, C., Patton, C., 2021. Identifying and managing aqueous film-forming foam-derived per- and polyfluoroalkyl substances in the environment. Environ. Toxicol. Chem. 40 (1), 24–36. https://doi.org/10.1002/etc.4894.
Lukas, J.M., Reneau, J.K., Linn, J.G., 2008. Water intake and dry matter intake changes as a feeding management tool and indicator of health and estrus status in dairy cows. J. Dairy Sci. 91 (9), 3385–3394. https://doi.org/10.3168/jds.2007-0926.
Lupton, S.J., Dearfield, K.L., Johnston, J.J., Wagner, S., Huwe, J.K., 2015. Perfluorooctane sulfonate plasma half-life determination and long-term tissue distribution in beef cattle (Bos taurus). J. Agric. Food Chem. 63 (51), 10988–10994. https://doi.org/10.1021/acs.jafc.5b04565.
Lupton, S.J., Smith, D.J., Scholljegerdes, E., Ivey, S., Young, W., Genualdi, S., DeJager, L., Snyder, A., Esteban, E., Johnston, J.J., 2022. Plasma and skin per- and polyfluoroalkyl substance (PFAS) levels in dairy cattle with lifetime exposures to PFAS-contaminated drinking water and feed. J. Agric. Food Chem. 70 (50), 15945–15954. https://doi.org/10.1021/acs.jafc.2c06620.
Martin, J.W., Asher, B.J., Beesoon, S., Benskin, J.P., Ross, M.S., 2010. PFOS or PreFOS? Are perfluorooctane sulfonate precursors (PreFOS) important determinants of human and environmental perfluorooctane sulfonate (PFOS) exposure? J. Environ. Monit. 12 (11), 1979. https://doi.org/10.1039/c0em00295j.
Mejia Avendaño, S., Liu, J., 2015. Production of PFOS from aerobic soil biotransformation of two perfluoroalkyl sulfonamide derivatives. Chemosphere 119, 1084–1090. https://doi.org/10.1016/j.chemosphere.2014.09.059.
Mikkonen, H.G., Clarke, B.O., Dasika, R., Wallis, C.J., Reichman, S.M., 2018. Evaluation of methods for managing censored results when calculating the geometric mean. Chemosphere 191, 412–416. https://doi.org/10.1016/j.chemosphere.2017.10.038.
NMI, 2018. Proficiency Test Report AQA 18-09 PFAS in Soil, Water, Fish and Prawn. https://www.industry.gov.au/sites/default/files/2019-06/aqa-18-09-pfas-in-water-soil-biota-proficiency-test-final-report.pdf.
NRC, 2000. Nutrient Requirements of Beef Cattle: Seventh Revised Edition: Update 2000. National Academies Press, Washington, D.C., p. 9791. https://doi.org/10.17226/9791
NSW DPI, 2014. Water requirements for sheep and cattle. In: Primefact, , third ed.vol. 326
Numata, J., Kowalczyk, J., Adolphs, J., Ehlers, S., Schafft, H., Fuerst, P., Müller-Graf, C., Lahrssen-Wiederholt, M., Greiner, M., 2014. Toxicokinetics of seven perfluoroalkyl sulfonic and carboxylic acids in pigs fed a contaminated Diet. J. Agric. Food Chem. 62 (28), 6861–6870. https://doi.org/10.1021/jf405827u.
OECD, 2021. Emission scenario document on the use of aqueous film-forming foams in firefighting. Ser. Emiss. Scenario Doc. 40 accessed 2022-08-30. https://www.oecd.org/officialdocuments/publicdisplaydocumentpdf/?cote=ENV/CBC/MONO(2021)5&doclanguage=en.
Olkowski, A.A., 2009. Canada; agriculture and agri-food Canada. In: University of Saskatchewan; Saskatchewan; Ministry of Agriculture. Livestock Water Quality: A Field Guide for Cattle, Horses, Poultry and Swine. Agriculture and Agri-Food Canada, Ottawa.
Parliament of Victoria, 2016. Inquiry into the CFA Training College at Fiskville, Final Report. https://www.parliament.vic.gov.au/file_uploads/ENRRDC_Fiskville_Inquiry_Final_Report_myHbwdGN.pdf.
R Core Team. R, 2019. A Language and Environment for Statistical Computing. https://www.R-project.org/.
Revelle, W., 2021. Psych: Procedures for Psychological, Psychometric, and Personality Research. Northwestern University, Evanston, Illinois.
Rogers, R.D., Reh, C.M., Breysse, P., 2021. Advancing per- and polyfluoroalkyl substances (PFAS) research: an overview of ATSDR and NCEH activities and recommendations. J. Expo. Sci. Environ. Epidemiol. 31 (6), 961–971. https://doi.org/10.1038/s41370-021-00316-6.
Senversa, 2018. Human Health and Ecological Risk Assessment RAAF Base East Sale – Per- and Poly-Fluoroalkyl Substances (PFAS) Investigations. https://www.defence.gov.au/Environment/PFAS/docs/EastSale/Reports/RAAFEastSaleFinalHHERAReportBody.pdf.
Todd, G., 2018. Aust. PFAS Chem. Map accessed 2021-05-16. https://pfas.australianmap.net/.
U.S. Environmental Protection Agency, 2019. Guidelines for Human Exposure Assessment. EPA/100/B-19/001.
USDA. Dairy Indemnity Payment Program Expanded to Assist with Livestock Losses Due to Contamination. U.S. Deaprtment of Agriculture News Releases. https://www.fsa.usda.gov/state-offices/Maine/news-releases/2021/dairy-indemnity-payment-program-expanded-to-assist-with-livestock-losses-due-to-contamination.
Van Asselt, E.D., Kowalczyk, J., Van Eijkeren, J.C.H., Zeilmaker, M.J., Ehlers, S., Fürst, P., Lahrssen-Wiederholt, M., Van Der Fels-Klerx, H.J., 2013. Transfer of perfluorooctane sulfonic acid (PFOS) from contaminated feed to dairy milk. Food Chem. 141 (2), 1489–1495.
Vestergren, R., Orata, F., Berger, U., Cousins, I.T., 2013. Bioaccumulation of perfluoroalkyl acids in dairy cows in a naturally contaminated environment. Environ. Sci. Pollut. Control Ser. 20 (11), 7959–7969. https://doi.org/10.1007/s11356-013-1722-x.
Wang, W., Rhodes, G., Ge, J., Yu, X., Li, H., 2020. Uptake and accumulation of per- and polyfluoroalkyl substances in plants. Chemosphere 261, 127584. https://doi.org/10.1016/j.chemosphere.2020.127584.
Wickham, H., 2016. Ggplot2: elegant graphics for data analysis. In: 2016.; Use R!, second ed. Springer International Publishing, Cham. https://doi.org/10.1007/978-3-319-24277-4. Imprint: Springer.
Williams, J., Hamblin, A.P., Hook, R.A., 2002. CSIRO (Australia); Division of Land and Water. Methodologies for Their Derivation and Key Issues in Resource Management. CSIRO Land and Water, Canberra.
Xu, Y., 2020. Serum half-lives for short- and long-chain perfluoroalkyl acids after ceasing exposure from drinking water contaminated by firefighting foam. Environ. Health Perspect. 12.
Yi, S., Harding-Marjanovic, K.C., Houtz, E.F., Gao, Y., Lawrence, J.E., Nichiporuk, R.V., Iavarone, A.T., Zhuang, W.-Q., Hansen, M., Field, J.A., Sedlak, D.L., Alvarez-Cohen, L., 2018. Biotransformation of AFFF component 6:2 fluorotelomer thioether amido sulfonate generates 6:2 fluorotelomer thioether carboxylate under sulfate-reducing conditions. Environ. Sci. Technol. Lett. 5 (5), 283–288. https://doi.org/10.1021/acs.estlett.8b00148.
Zafeiraki, E., Vassiliadou, I., Costopoulou, D., Leondiadis, L., Schafft, H.A., Hoogenboom, R.L.A.P., van Leeuwen, S.P.J., 2016. Perfluoroalkylated substances in edible livers of farm animals, including depuration behaviour in young sheep fed with contaminated grass. Chemosphere 156, 280–285. https://doi.org/10.1016/j.chemosphere.2016.05.003.
Zhang, Q., Yu, R., Fu, S., Wu, Z., Chen, H.Y.H., Liu, H., 2019. Spatial heterogeneity of heavy metal contamination in soils and plants in Hefei, China. Sci. Rep. 9 (1), 1049. https://doi.org/10.1038/s41598-018-36582-y.
Zhao, S., Liang, T., Zhu, L., Yang, L., Liu, T., Fu, J., Wang, B., Zhan, J., Liu, L., 2019. Fate of 6:2 fluorotelomer sulfonic acid in pumpkin (cucurbita maxima L.) based on hydroponic culture: uptake, translocation and biotransformation. Environ. Pollut. 252, 804–812. https://doi.org/10.1016/j.envpol.2019.06.020.